Sponge Diversity and Distribution in the Labrador Sea

Timothy S. Culwick

Supervisors: Katharine R. Hendry, Claire Goodwin, Jeremy Phillips, and Emily j. Rayfield

A dissertation submitted to the University of Bristol in accordance with the requirements for award of the degree of Doctor of Philosophy in the Faculty of Science School of Earth Sciences

School of Earth Sciences

August, 2021

Word Count: 39,432

Abstract

Sponges are an overlooked component of the benthic marine ecosystem, despite being known to perform important functional roles within the ocean. Understanding the distribution, density and population make up of sponge grounds as well as what drives these patterns is imperative to constraining the environmental, ecological and biogeochemical role sponges perform. This thesis uses three studies that take differing approaches the problem. These studies focus on the Labrador Sea, an area that is experiencing rapid temperature change due to global warming and is important for deep water formation.

Firstly, a mathematical modeling study aimed to constrain the role of fluid forcing in sponge distribution. This was done using clustering analysis combined with fluid flow finite element modeling. Clustering patterns were observed for sponges within each sponge ground and were statistically significant. Simulation of flow looking at wake interactions around simplified sponge shapes predict that sponges are changing the mean flow conditions when they are spaced at similar distances to those observed in the sponge grounds. Further simulations using topographic models of the sponge grounds show the generation of a boundary layer of slowed flow caused by sponge wake interactions. This boundary layer could potentially be beneficial for sponge development and its presence may have implications for assessing the impact of anthropogenic damage on sponge grounds. Damage to sponge grounds will change the distribution of sponges and therefore would change or reduce the boundary layer thickness, potential affecting recovery rates.

Secondly, a taxonomic study of sponge samples was carried out from three localities. Samples were collected by Remotely Operated Vehicle enabling the collection of delicate and encrusting sponges and the effective sampling of steep bedrock habitats. Twelve new species are described: *Halicnemia flavospina* sp.nov., *Paratimea marionae* sp.nov., A*sbestopluma (Asbestopluma) frutex* sp.nov., *Lissodendoryx (Acanthodoryx) magnasigma* sp.nov., *Fibulia textilitesta* sp.nov., *Hymedesmia (Hymedesmia) caerulea* sp.nov., *Hymedesmia (Hymedesmia*) *alba* sp.nov., *Sceptrella matia* sp.nov., *Clathria (Axosuberites) radix* sp.nov., *Stelodoryx groenlandica* sp.nov., *Stelodoryx rictus* sp.nov., and *Plakina jactus* sp.nov. New information on distribution, *in situ* images and spicule measurements are provided for *Hymedesmia (Hymedesmia) crux* (Schmidt, 1875) and *Phakellia robusta* Bowerbank, 1866. In total 68 sponge species were recorded by this survey, 13 of which had not previously been recorded in the Labrador Sea. These results significantly increase our understanding of the sponge biodiversity of the west Greenland shelf and knowledge of how this differs from that seen around Orphan Knoll.

Thirdly a biogeographic study using principal component analysis on sponge species data and *in situ* environmental data to identify sponge assemblages, and investigate the drivers of their distribution. We show that – within the sponge specimens assessed in this study – there are two distinct assemblages defined by the physical oceanographic conditions they inhabit. We suggest that these parameters, notably temperature, depth, and oxygen concentration, are the primary controlling factors for sponge distribution in the Labrador Sea. Within these sponge assemblages we show that there is a strong secondary grouping based on local ocean nutrient concentrations, which have not been considered in previous studies due to the unavailability of data at suitable granularity. These finding have implications for modelling the distribution of sponges in the Labrador Sea, and provide new insights into the vulnerability of these assemblages to climate change relevant for conservation strategies.

The most pertinent conclusion of these studies and this thesis is how little we understand of these organisms and how vulnerable they are to anthropogenic damage.

Acknowledgments

This Ph.D. was funded by the European Research Council (ERC Starting Grant 678371 ICY-LAB) as part of the Isotope CYcling in the Labrador Sea project.

My supervisors have been brilliant, and I am very grateful for their help and guidance during my PhD. They have all been continuously supportive and encouraging over the last four years making the whole process infinitely easier and more fun. Thank you to Kate for the discussion, encouragement, and patience with my writing; to Claire for the time spent helping guide me through the nuances of sponge taxonomy; to Jeremy for the support and assistance with the flow modelling; and to Emily Rayfield for her logistical support.

I would like to thank Mark Woodhouse and Kerry-Louise Howell for their discussion and assistance with the flow modelling. Paco Cardenas, Alexander Plotkin, Joana Xavier and Toufiek Samaai for their helpful discussion and assistance regarding aspects of sponge taxonomy. The organisers of the 5th International Workshop on Taxonomy of Atlanto-Mediterranean Deep Sea and Cave Sponges, Marseille, for the introduction to sponge taxonomy. The organisers of the 2019 SpoNGES conference for the opportunity to present my research as well as the sponge research community in general for their openness, support and encouragement. Michelle Taylor who was responsible for the biological collection on the DY081 Cruise. Many thanks to the Master and crew of the RRS discovery with a particular thanks to the ROV pilots David Turner, Allan Davies, David Edge, Russell Locke, Ella Richards, Josue Viera Rivero and Andrew Webb. I would also like to that the staff of the Taxonomy and Biodiversity labs at the Huntsman Marine Science Centre for making me feel welcome and included during the time I spent in St Andrews.

I am very gratefully for the support of my fellow Ph.D. students and research colleagues who have helped make this experience so enjoyable and who I sorely missed during the department closure. With particular thanks to Nick Hayes, Anna Williams, Bob Myhill and David Edwards for their weekly support and commiseration during our Dungeons and Dragons sessions.

Finally, this would have all been impossible without my incredibly supportive and infinitely encouraging wife Marion. Even if she still insists "there is only one sponge" despite my best attempts to persuade her otherwise.

Author's declaration

I declare that the work in this dissertation was carried out in accordance with the requirements of the University's Regulations and Code of Practice for Research Degree Programs and that it has not been submitted for any other academic award. Except where indicated by specific reference in the text, the work is the candidate's own work. Work done in collaboration with, or with the assistance of, others, is indicated as such. Any views expressed in the dissertation are those of the author.

Timothy S. Culwick Date 26/08/2021

Table of Contents

List of Figures

1. Chapter 1. Introduction

1.1. Motivations

1.1.1. The ecological importance of sponges

Sponges (phylum Porifera Grant, 1836) are overlooked and understudied both as an organism and as a important component of the benthic marine ecosystem. They are some of the most diverse and varied of the aquatic invertebrates with about 10,000 species described worldwide (van Soest *et al.*, 2021). They are known to perform several functional roles within the ocean, primarily as reef building organisms both in shallow and deep-sea environments (Miller *et al.*, 2012; Knudby, Kenchington and Murillo, 2013; Roberts *et al.*, 2018). These sponge grounds support areas of high biodiversity, forming biogenic habitats and acting as nurseries for fish and invertebrate species (Klitgaard, 1995; Chu and Leys, 2010; Hogg, Tendal and Conway, 2010; Kenchington, Power and Koen-Alonso, 2013; Lehnert and Stone, 2016; Maldonado *et al.*, 2017). The high biodiversity in and around these sponge grounds is not only of an ecological interest, as they act as nurseries for many commercial fish stocks (Klitgaard, 1995; Freese and WIng, 2003).

This study was initially motivated by the lack of understanding in to the role that sponges may play in nutrient availability (Hendry, 2017). It has been suggested that sponges can influence primary production in the ocean by controlling nutrient availability (Bell, 2008; Maldonado, Ribes and van Duyl, 2012; Murillo *et al.*, 2012; Kutti, Bannister and Fosså, 2013; Maldonado, 2016). In particular, there is a strong link between the biogeochemical cycles of carbon and silicon due to the uptake of silicic acid by diatoms, with sponges potentially influencing the concentrations of silicic acid (Maldonado *et al.*, 2005, 2011; Tréguer *et al.*, 2017). Diatoms are key organisms for fixation of carbon in the ocean, accounting for 40% of marine primary production as part of the biological pump and as producers of particulate carbon which is exported to depth (Tréguer and De La Rocha, 2013; Tréguer *et al.*, 2017). With Individuals able to filter large volumes of water (Ludeman, Reidenbach and Leys, 2017), sponges may be a major driver of nutrient fluxes within the pelagic system, especially given previous estimates of the predicted density and ranges sponge grounds (Knudby, Kenchington and Murillo, 2013). However the concentration and distribution of sponge grounds is

poorly understood (Howell *et al.*, 2016) and without knowing an accurate picture of distribution and population makeup their effect on the environment is effectively unknown (McIntyre *et al.*, 2016).

Despite performing key ecosystem services, sponges and sponge grounds are critically understudied, following the trend that sessile benthic organisms are overlooked in biodiversity studies (Archambault *et al.*, 2010; Kenchington, Link, *et al.*, 2011; Piepenburg *et al.*, 2011; Darnis *et al.*, 2012; Roy, Iken and Archambault, 2015). This is particularly the case with sponges due to the extreme challenges associated with species identification from images alone and therefore then need for specimen collection (Hooper and van Soest, 2002; Leys *et al.*, 2004). In addition, the drivers of sponge ground distribution are poorly understood and have been attributed to a wide range of factors from silicic acid concentration (Beazley *et al.*, 2015; Howell *et al.*, 2016) temperature, depth (Rice, Thurston and New, 1990; Bett, 2001; Murillo *et al.*, 2012), to particulate carbon availability (Barthel, Tendal and Thiel, 1996; Howell *et al.*, 2016). This complexity, and general lack of diversity and density mapping, makes predicting sponge ground occurrence difficult without localized biodiversity studies (Klitgaard and Tendal, 2004; Knudby, Kenchington and Murillo, 2013; Cathalot *et al.*, 2015; Howell *et al.*, 2016; Murillo *et al.*, 2016; Kazanidis *et al.*, 2019).

1.1.2. Sponges in the Labrador Sea

The Arctic is experiencing some of the biggest changes in temperature rising twice as fast as the global average driven by anthropogenic increases in greenhouse gases, with projected further warming (Fyfe, Gillett and Zwiers, 2013; Najafi, Zwiers and Gillett, 2015; Notz and Stroeve, 2016; Meredith *et al.*, 2019; Overland *et al.*, 2019). The mechanisms behind this amplified Arctic warming is not clear but include reduced albedo (due to land and sea ice loss), increased atmospheric water vapor, northward transport of heat and reduced heat loss to space compared to subtropics. (Serreze, Barrett and Stroeve, 2012; Pithan and Mauritsen, 2014; Goosse *et al.*, 2018; Stuecker *et al.*, 2018). Sea Ice in the Arctic has dramatically declined over the past 15 years, with winter sea ice maxima at record low levels (Overland *et al.*, 2019).

Alongside this, the Greenland Ice Sheet (GIS) has lost significant mass and this rate is likely to increase (Shepherd *et al.*, 2012; Schrama, Wouters and Rietbroek, 2014; Velicogna, Sutterley and Broeke, 2014; Bamber *et al.*, 2018; King *et al.*, 2018; Sandberg Sørensen *et al.*, 2018). These changes are not only worrying locally but global due to sea level change and the influence on meltwater on ocean buoyancy and deepwater formation (Meredith *et al.*, 2019). The GIS melting has a massive

impact of sea level change constituting a over half of the total global sea level change between 2012 and 2016 (Bamber *et al.*, 2018; Meredith *et al.*, 2019). However, it is the potential impact of large scale release of freshwater on ocean circulation by modulation or inhibition of the deep water formations for the Atlantic Meridional Overturning Circulation (AMOC) that is of greatest consequence. There has been a decrease of 50% in dense water mass formation in the Labrador Sea suggesting a link between increased freshwater fluxes from the Fram Strait, Davis Strait and GIS melting, and suppressed North Atlantic Deep Water formation (Yang *et al.*, 2016). Climate modeling of ocean circulation shows the melting of the GIS will impact AMOC by a 5-10% weakening by 2100 (Collins *et al.*, 2019). This predicted weakening of the AMOC has global consequences including increased flooding, methane release, drought (Lynch-Stieglitz, 2017), carbon drawdown (Kostov, Armour and Marshall, 2014; Romanou *et al.*, 2017), and sea level rise (McCarthy *et al.*, 2015; Palter *et al.*, 2017; Collins *et al.*, 2019).

Meltwater off the Greenland ice sheet is thought to be a significant source of silica and iron (Bhatia *et al.*, 2013; Hawkings *et al.*, 2014, 2017; Meire *et al.*, 2016) and so its presence has the potential to increase primary production in fjords (Juul-Pedersen *et al.*, 2015; Cape *et al.*, 2018; Kanna *et al.*, 2018). However, glacial retreat may reduce upwelling as a source of nutrients therefore reducing summer productivity in Greenland fjord ecosystems (Meire *et al.*, 2017; Hopwood *et al.*, 2018). Nutrient cycling in the region is critically understudied in general including what influence increase in primary production in fjords may have to nutrient availably further out to sea (Pedulli *et al.*, 2014; Bourgeois *et al.*, 2016).

This thesis is part of the Isotope CYcling in the Labrador Sea project (ICY-LAB) which aims to address the lack of understanding around nutrient and isotope cycling in the Labrador Sea, with the aim to capture the whole biogeochemical system from Coastal Greenland to the open Labrador Sea (Hendry, 2017). The DY081 Discovery cruise focused on the influence of meltwater on nutrient cycling within the Labrador Sea using the silicon cycle as a model system, due to its importance to carbon uptake via diatoms (Hendry, 2017; Tréguer *et al.*, 2017). The role and importance of sponges within the silicon cycle in Labrador Sea is unknown due to their concentration and distribution being poorly constrained (Howell *et al.*, 2016; McIntyre *et al.*, 2016). I will be using sponge sampling and environmental data collection form the DY081 Discovery cruise to attempting to identify sponge species and sponge grounds, and to predict there distribution and density within the Labrador Sea(Figure 1.1).

The lack of data around sponge grounds and sponge species is compounded in the Labrador Sea due to the remote deep nature of the sponge grounds (Archambault *et al.*, 2010), with an order of

magnitude fewer species recorded in the area when compared to diversity at similar latitudes globally (Sarà *et al.*, 1992; Ackers *et al.*, 2007; Picton and Goodwin, 2007a; Downey *et al.*, 2012; van Soest *et al.*, 2012; Lehnert and Stone, 2016). The waters off South Western Greenland stand out within the region as being particularly understudied, with the last large taxonomic study before this thesis from 1933 (Brøndsted, 1933b). This lack of knowledge of both location and extent of the sponge grounds – and the species that are contained within them – is of concern given the rapid climate change in recent decades and the importance of the region for global ocean circulation.

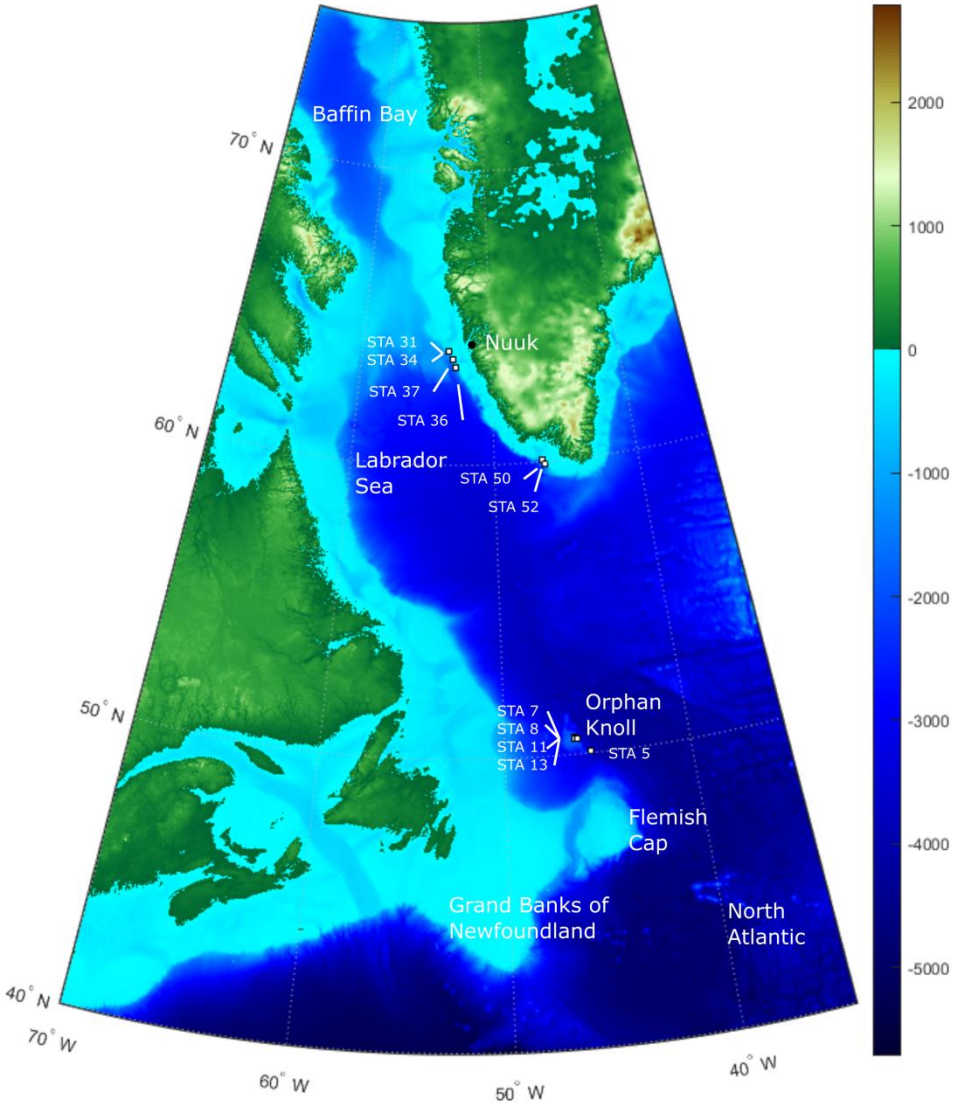

Figure 1-1. Overview map showing points of interest in the Labrador Sea and surrounding area overlain with the position of the sample collection stations (STA): STA 5, STA 7, STA 8, STA 11, STA 13, STA 31, STA 34, STA 36, STA 37, STA 50, and STA52 from the DY081 Cruise in the Labrador Sea. Bathymetry used is from ETOPO1 model from https://www.ngdc.noaa.gov/mgg/global/

1.2. Scientific background

The following section contains a brief literature review to provide a foundation understanding of the research topics covered in this thesis. It will summarise key findings of previous studies in the field and frame the gaps in knowledge that I will address. Additional scientific background will be included in the analytical research chapters **(Chapters 2-4)**.

1.2.1. Marine sponges

Sponges (Porifera Grant, 1836) are an ancient animal group with a body fossil record back to the Cambrian and potentially Precambrian (Zumberge *et al.*, 2018). They comprise of a multicellular body, containing several varying cell types with differing functions. These cells are grouped into specific functional regions in a sponges body. However the only true tissue is the epithelioum, clearly shown in Homoscleromorphs (Leys and Riesgo, 2012). A sponges body plan is essentually a piping system designed to process as much water as possible. This body plan looks deceptively simple, lacking a nervous system and a conventional digestive and circulation systems (Hooper and van Soest, 2002). Despite this relatively simple body plan, the group is highly diverse and are a globally important member of the benthic fauna (Bell and Barnes, 2000b; Bell, 2008; Bell, Mcgrath, *et al.*, 2015). They have been found in all ocean basins and at apparently all depths from shallow tidal waters to abyssal depths as well as in fresh lakes and rivers (Rapp, Janussen and Tendal, 2011; Lim, de Voogd and Tan, 2012; Hestetun, Rapp and Pomponi, 2019). Sponges are very effective filter feeders: an Individual sponge is able to filter large volumes of water, which can be up to 900 times their body volume per hour, using a combination of active pumping and ambient flow (depending on species) through complex canal-like structures (Ludeman, Reidenbach and Leys, 2017)(Figure1.2). They are not limited to this method of feeding with different subgroup evolving other survival strategies include symbiotic photosynthesis (Achlatis *et al.*, 2019) and carnivorous modes of life (Brusca and Brusca, 2003; Hestetun *et al.*, 2015)(Figure 1.3 c).

The majority of deep-marine sponges have a skeleton formed of spicules of silica (SiO_2) that support the mesohyl, canal system and cells, although some form skeletons of calcite, aragonite or spongin structures (Hooper and van Soest, 2002). Spicule and skeleton morphology is the primary means of classification (Hooper and van Soest, 2002), although in more recent studies this is often supported by molecular work (Xavier *et al.*, 2010; Cárdenas *et al.*, 2011). This is due to the flexibility of body

morphology species can exhibit, and convergent evolution producing sponges with essentially identical morphology from radically differing families or even classes (Hooper and van Soest, 2002; Leys *et al.*, 2004). This plasticity is one of the biggest potential reasons for the lack of work carried out on these organisms, and their reputation for being difficult to identify, particularly from images (Hooper and van Soest, 2002; Leys *et al.*, 2004). Therefore specimen collection is required for species identification, and is usually necessary for family and genus level identification with a few genera (i.e *Geodia* Lamarck, 1815(Figure1.3.)) being the exception (Howell *et al.*, 2016).

The Porifera Grant, 1836 (sponges) are split in to four classes; Hexactinellida Schmidt, 1870, Demospongiae Sollas, 1885, Calcarea Bowerbank, 1862 and Homoscleromorpha Bergquist, 1978 (Figure 1.3). Hexactinellida have a silica skeleton, which may be made up of fused or individual spicules and never with spongin fibers, there body form is leuconoid (Figure 1.2.), also the bulk of the body is syncytia for most species (Hooper and van Soest, 2002). They are most commonly found in deep water at high latitudes – but not exclusively –with some species present in tropical shallow waters (van Soest *et al.*, 2021). Calcarea have a skeleton made of calcite without spongin fibers, often creating a massive exoskeleton, they produce body form of asconoid, syconoid, leuconoid or solenoid (Figure 1.2.) (Hooper and van Soest, 2002). They are distributed globally but are usually limited to shallow tropical waters (van Soest *et al.*, 2021). Demospongia and Homoscleromorpha both have silica skeletons with spongin fibers present in many species, with a leuconoid body form(Figure 1.2.), the two classes being separated phylogenetically (Hooper and van Soest, 2002). Demospongia is the largest class of sponges and contains the majority of species and are found in all environments from which sponges have been described (van Soest *et al.*, 2021). Homoscleromorpha is a very small class with only two families with the majority of known species described in shallow water caves in the Mediterranean (van Soest *et al.*, 2021). This narrow class distribution is probably due to sampling and study bias.

Sponges have very slow growth rate, particularly in the deep sea. Hexactinellida sponges have a growth rate of ~2.2 cm per year for small sponges to less than 0.5cm for larger sponges (Prado *et al.*, 2021). However, there regeneration rates can be up to 20 times higher (Leys and Lauzon, 1998). These rates of growth and regeneration are resource intensive and so are dependent on optimal conditions (Henry and Hart, 2005), so in areas of low nutrient availably these rates can be reduced significantly. They also appear to have variable growth rates that decrease as their body size get large (Prado *et al.*, 2021). This poses a problem for age estimation, which is usually based on size. Sponge ages are poorly constrained but there is consensus that are very long lived, with age ranges

varying from an estimates of approximately 200 years old (Prado *et al.*, 2021) to radiocarbon dating putting some individuals at more than 400 years old (Fallon *et al.*, 2010).

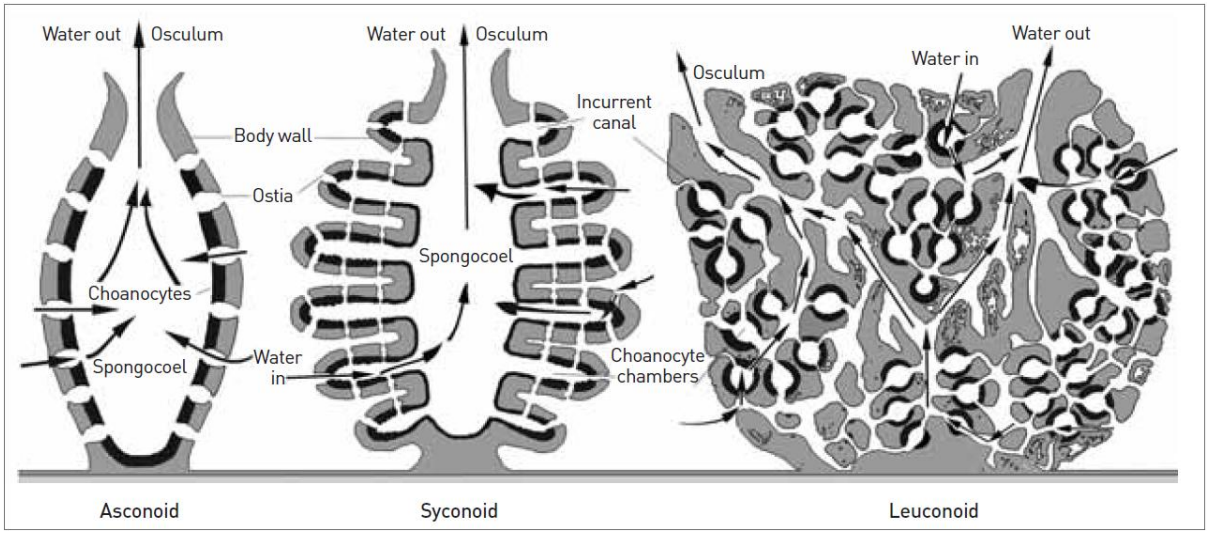

Figure 1-2. Diagram showing patterns of fluid flow through three different sponge body structures: asconoid (a simple vase or tube shape); syconoid (with a pleated body wall); and leuconoid (with a network of chambers). Figure 3.1 from "Deep-sea Sponge Grounds : Reservoirs of Biodiversity" (Hogg, Tendal and Conway, 2010)

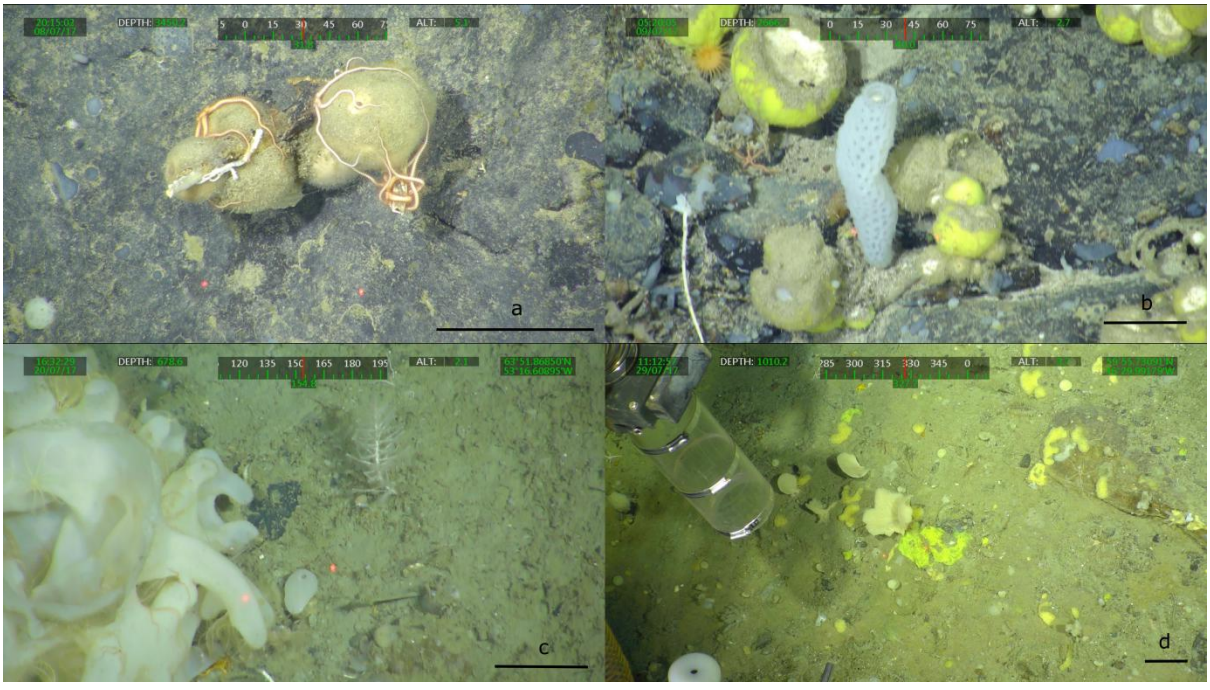

Figure 1-3. Examples sponges of some common species collected, from the DY081 Discovery cruise. Scale 10 cm a) *Geodia barretti* (Bowerbank, 1858) b) *Euplectella* Owen, 1841 (white cylinder) c) *Cladorhiza abyssicola* (Sars, 1872) (erect and branching) d) *Phakellia robusta* Bowerbank, 1866(fans).

1.2.2. Sponge Habitats

Under certain geological, hydrological and biological conditions, sponges can become exceptionally successfully forming large aggregations. These sponge aggregations will often form the bases of unique structural habitats, the nature of which depends on location, substrate and the dominating species (Rice, Thurston and New, 1990; Barthel, Tendal and Thiel, 1996; Bett, 2001; Murillo *et al.*, 2012; Beazley *et al.*, 2015; Howell *et al.*, 2016). These aggregations have been observed globally and at essentially all depths with ranges from hundreds of KM^2 to a hundred of M^2 (Miller *et al.*, 2012; Beazley *et al.*, 2013; Knudby, Kenchington and Murillo, 2013; Maldonado *et al.*, 2017).

The terminology of these sponge habitats is in its early stages, with confusion and overlap between catch all terms and those that are precisely defined based on a singular habitat.

Klitgaard & Tendal (2004) were some of the first people to study sponge grounds, with Klitgaard et al. (1997) first loosely defining an "ostur" as ‘‘a restricted area where large-sized sponges are strikingly common’’ (Klitgaard et al., 1997). These are described around the Faroes Islands where sponges can make up more than 90% of biomass from a catch aside from benthic fish. They refine this definition further into two types of "ostur" from the northeast Atlantic. "Firstly a boreal ‘‘ostur’’ which is dominated by *Geodia barretti, Geodia macandrewi, Geodia atlantica, Isops phlegraei, Stryphnus ponderosus* and *Stelletta normani*, and occurs around the Faroe Islands, Norway, Sweden, parts of the western Barents Sea and south of Iceland. Secondly a cold water ‘‘ostur’’ characterized by the same genera but represented by different species, viz. *Geodia mesotriaena, Isops phlegraei pyriformis* and *Stelletta rhaphidiophora*, which is found north of Iceland, in most of the Denmark Strait, off East Greenland and north of Spitzbergen " (Klitgaard & Tendal, 2004).

This has developed further with OSPAR defining "sponge aggregations as "Deep-sea sponge aggregations occur on both soft and hard substrates and are principally composed of Hexactinellids and Demosponges. Hexactinellids have been reported at densities of 4-5m2 and ‘massive’ growth forms of demosponges have been reported at densities of 0.5-1/m2 "(OSPAR commission, 2008, 2010). The FAO in defining the Vulnerable marine ecosystem habitat of "Deep-sea sponge aggregations" (FAO, 2009) splits this down further into: " Other sponge aggregations" primarily Geodiidae, Ancorinidae, Pachastrellidae , " Hard-bottom sponge gardens" Containing Axinellidae, Mycalidae, Polymastiidae, Tetillidae, and "Glass sponge communities".

In the current literature, sponge grounds (Hogg et al. 2010; Murillo et al. 2016, 2018) and sponge aggregations (OSPAR, 2010) are used interchangeably.

In this thesis I will be following the FAO term using four terms to describe sponge habitats:

1. "Sponge Aggregations" are habitats with a high numbers of sponges present, encompass sponge gardens and sponge grounds (FAO, 2009).
2. "Sponge grounds" Habitats where sponges dominate. In N Atlantic typically astrophorids are the most common species and can constitute up to 90% of the biomass (Hogg et al. 2010; Murillo et al. 2016, 2018).
3. "Sponge gardens" lower densities than sponge grounds and on hard substrate. Typically dominated by Axinellidae, Mycalidae, Polymastiidae and Tetillidae (FAO, 2009).
4. "Sponge reefs" are habitats where sponges form massive reef frameworks by biohermal growth, with the only example being found of the western coast of Canada (Cook and Conway, 2008; Conway *et al.*, 2017).

There are a large number of very diverse sponge habitats all of which are associated with specific depths, oceanographic conditions and species contributions.

The most easily accessible for study are coral reef aggregations, of which there are two distinct regions, those of the Atlantic Ocean and those of the Indo-Pacific (Wilkinson and Cheshire, 1989; Maldonado *et al.*, 2017). In both cases they form on continental or island coasts with greatest concentrations at depth of 20m. Typically They form in areas where average sea surface temperature is above 21C, salinity between 30 and 40, with low levels of sedimentations and often high levels of particulate organic carbon (POC). Sponges in these habitat often are associated with photosynthetic symbionts (Maldonado *et al.*, 2017).

A second shallow water sponge habitat occuring at similar latitudes to the coral reef aggregates is that of mangrove aggregations. These occur in the intertidal regions associated with mangroves. This habitat can occur at greater ranges in temperature and salinity than that of the coral reef aggregates though is limited to areas with lower tidal ranges as sponges in general have a limited tolerance to exposure (Rützler, Macintyre and Smith, 1990).

There are more varied and diverse sponge habitats occurring in the deep sea. The most wide spread and diverse is that of deep-sea sponge grounds, these range from *Geodia* dominated sponge grounds on the northern Norwegian shelf (Kutti, Bannister and Fosså, 2013) to hexactinellid dominated sponge grounds on the Porcupine Seablight (Rice, Thurston and New, 1990). These sponge grounds are seen globally in temperate latitudes usually at depths ranging from 150-1700 m across a range of substrates. The species compositions and density varies depending on topography and local environmental conditions. Demosponge dominated sponge grounds are well known from within the 40-75N latitude band in the North Atlantic often associated with elevated levels of primary production and dissolved nutrients in the surface ocean and at depths of 150-1700m with rocky or coarse sand substrates type (Howell, Billett and Tyler, 2002; Howell, 2010; Howell *et al.*,

2016). Dense hexactinellid dominated sponge grounds are more often associated with depths of 800-1350m and muddy substrates covered with spicule mats (Leys and Lauzon, 1998). Sponge grounds are not limited to temperate latitudes and are observed at tropical and Arctic latitudes but are less common and dense. This is also true for depth with low density field of scattered haxactinellids seen over large areas of the abyssal plains (Xavier, Tojeira and Van Soest, 2015)

Hexactinellids also form sponge reefs, these are found on the western continental shelf of Canada in depths of 90-240m (Cook and Conway, 2008; Conway *et al.*, 2017). These are massive reef frameworks formed by biohermal growth as young sponges attach to the skeleton of dead sponges. It appears very specific environmental and geographic conditions are necessary for their formations, including long term stability of the deep seas, high silicate availability combined with just the right amount of organic rich marine sown and suspected sediment to sediment the gaps and interstices in the reefs surface but not smother the living sponges(Tompkins-Macdonald and Leys, 2008).

The Southern Ocean has its own distinct set of Antarctic Sponge Aggregations with distinct traits separating them from other sponge habitats. There is strong endemism (approx 60%) and surprising taxonomic homogeneity along the coast line of Antarctica but with high levels of taxonomic diversity across a range of environments and depth(Downey *et al.*, 2012; Downey, Fuchs and Janussen, 2018). This general pattern appear to be modified by local environment but the specifics of deep sea Antarctic environment are poorly known.

This gives an idea of the breadth and depth in the variability of sponge habitats. Other example are lithistid aggregations (Schuster *et al.*, 2021) and deep sea carnivorous sponge aggregations (Baums *et al.*, 2020). All of these habitats are constrained by a combination of factors including oceanographic conditions, topography and food availability. If we can accurately predict the environmental conditions associated with each habitat we should be able to map their constraints, there by, improving our knowledge of their distribution.

1.2.3. Sponge functional roles

Sponges are known to perform several functional roles within the ocean, firstly stemming from their ability to form structural habitats and secondly due to the impressive amount of seawater they can filter. They have been observed forming aggregations, creating structural habitats both in shallow and deep-sea environments (Miller *et al.*, 2012; Beazley *et al.*, 2013; Knudby, Kenchington and Murillo, 2013; Maldonado *et al.*, 2017). These sponge grounds are areas of very high biodiversity

(Klitgaard, 1995; Chu and Leys, 2010; Hogg, Tendal and Conway, 2010; Kenchington, Power and Koen-Alonso, 2013; Lehnert and Stone, 2016; Maldonado *et al.*, 2017). They are associated with very high microbial biodiversity with some sponges constituting of up to 40% by volume of microbial associates (Osinga *et al.*, 2001) leading to an considerable increase in bacterial biomass estimates where sponges are present (Hentschel *et al.*, 2002). For a long time it has been known that sponge grounds are significant hotspots for invertebrate diversity, with 242 species related to deep-sea sponge grounds in 1995 (Klitgaard, 1995) with a more recent study recording 162 species associated with sponge grounds on the Sackville Spur (Barrio Froján *et al.*, 2012). However, a more up-to-date comprehensive estimate of species associated with sponge grounds in the North Atlantic is missing and requires further study. The high invertebrate biodiversity is due to the creation of microhabitats by the sponges, including within their canal systems, inside their body structures (McClintock *et al.*, 2005; Buhl-Mortensen *et al.*, 2010), within accumulated sediment and organic detritus around them feeding phyla Nematoda, Polycheta and Sipuncula (Klitgaard, 1995), and spicule mats forming hard substrates for other organisms (e.g. echinoids and bivalves)(Bett and Rice, 1992). Beyond invertebrates they are known to be important for many fish species, providing nurseries for spawning, area to feed and acting as refuges from predators (Klitgaard, 1995; Freese and WIng, 2003).

Sponges also play a role in benthic-pelagic coupling and biogeochemical processing within the ocean. In addition to their high filtration rates (Ludeman et al., 2017), sponges can obtain very high biomass within sponge grounds, for example, the Norwegian shelf is characterized by an average sponge biomass of 1.4 kg m^{-2} and up to 45 kg m^{-2} (Maldonado *et al.*, 2017). The volume processed when scaled up using the predicted density and ranges of sponge grounds in the deep ocean (Knudby, Kenchington and Murillo, 2013) is such that they have the potential to be major drivers within the pelagic system (Bell, 2008; Maldonado, Ribes and van Duyl, 2012; Murillo *et al.*, 2012; Kutti, Bannister and Fosså, 2013; Maldonado, 2016). The two main nutrient cycles that have been look at with regard to sponges are the carbon (C) cycle and the silica (Si) cycle.

Silicon is important as it is a key nutrient for diatom in the surface ocean (Nelson and Dortch, 1996; Thamatrakoln and Hildebrand, 2008) and can be a limiting nutrient in some regions of the Arctic (Krause *et al.*, 2018, 2019). Diatoms are key organisms for fixation of carbon in the global ocean accounting for 40% of marine primary production as part of the biological pump, they are also major producers of particulate carbon which falls as marine snow removing it from the surface ocean (Tréguer and De La Rocha, 2013; Tréguer *et al.*, 2017). This rate of carbon transfer is modulated by the Si/C ratio of diatom cells, the thickness of the shells and their life strategies (Tréguer *et al.*,

2017). The role of silicic acid as both a key nutrient and in some Arctic regions a limiting nutrient, for diatoms, link the biogeochemical cycles of carbon and silicon. This means that changes in the Si cycle have the potential to affect global climate (Friedlingstein *et al.*, 2006). The extent of which sponges influence the Si cycle by changing concentrations of silicic acid is poorly constrained and is one on the unknown within this system (Maldonado *et al.*, 2005, 2011; Tréguer *et al.*, 2017).

The deposition of Si within a sponge in the formation of siliceous spicules is one of the major limiting factors of their growth. Sponges are often not included in models of the Si cycle or their effect deemed negligible, with authors sighting diatoms to be essentially entirely responsible for global Si cycling e.g. (Greenwood, Truesdale and Rendell, 2001; Rickert, Schlüter and Wallmann, 2002). However, work done on the dissolution rates comparing diatoms frustules and sponge spicules (Kamatani, 1971; Maldonado *et al.*, 2005) show much shower rates in spicule dissolution. Combined with the long lifespan of sponges and how spicules may be a significant component of sediments in reefs (RUtzler and Macintyre, 1978), their impact on the global Si cycle could be greater than generally thought.

Significant carbon and nitrogen cycling by sponges has also be documented, with estimates for a single *Geodia* Lamarck, 1815, sponge of the Norwegian shelf estimated at 200 mg C m^{-2} d^{-1} (Kutti, Bannister and Fosså, 2013). When scaled up to the population on the Norwegian shelf, for example, this equates to approximately 250 million m^3 of water filtered and 60 tonnes of carbon consumed in a single day (Kutti, Bannister and Fosså, 2013). Further studies investigating community respiration rates suggest that sponge grounds in the area are responsible for 36% of benthic respiration and 5% of primary production (Cathalot *et al.*, 2015).

The major challenge with modeling the impact of sponges on both the C and Si cycles relates to the difficulties in estimating density and distribution of sponges. Without knowing an accurate picture of distribution and population makeup, their effect on the environment is unknown (McIntyre *et al.*, 2016). However, there is good evidence that they have the potential to be a major influence for primary production by controlling nutrient availability (Bell, 2008; Maldonado, Ribes and van Duyl, 2012; Murillo *et al.*, 2012; Kutti, Bannister and Fosså, 2013; Maldonado, 2016).

1.2.4. Effects of flow on distribution

Previous work carried out on the effects of flow on sponge morphology, and how it effects sponge species distribution, has been observational and predominantly in shallow environments (Palumbi,

1986; Bell and Barnes, 2000a; Bell, McGrath, *et al.*, 2015). The modern focus on sponge morphology and flow interaction has surrounded the effect of sediment smothering on sponge grounds (Pineda, Duckworth and Webster, 2016; Schönberg, 2016; Strehlow *et al.*, 2017). Within the literature there is observational evidence that sponge morphology is driven by environmental energy levels in the shallow marine system (Bell and Barnes, 2000b) and observations of distinct assemblages forming within different deep-sea environments (Berman *et al.*, 2013; Hajdu *et al.*, 2017). Bell and Barnes (2000) observed that sponge body form and density (sponge m^{-2}) changed depending on the flow conditions to which the specimens were subjected. The study showed that the density of sponges increased with depth where moderate current flow was observed, but not when subject to turbulent flow. Their observations of how morphology changed depending on current followed the logical expectation that as current speed increased there was a loss of delicate forms resulting in only massive and encrusting forms in high energy sites. Berman *et al* (2013) suggested that there is some correlation between maximum wind gust speed and morphological changes in sponge assemblages and related this to strong swells within shallow water damaging sponges and increasing turbidity and sedimentation. There is also a correlation of sponge ground distribution with topography, internal waves and current speeds, which control flow conditions at the seafloor (Klitgaard and Tendal, 2004; Howell *et al.*, 2016). Kiltgaard and Tendal (2004) showed that the sponge grounds are most often found in highly irregular topography where special hydrographic conditions are thought to be found, such as current acceleration and the breaking of internal wave features. It would follow that these factors would also effect the distribution of sponges at a smaller scale and that the sponges themselves could potentially try and optimize their localized conditions (Kutti, Bannister and Fosså, 2013). This is seen in other organisms throughout nature, with examples ranging from marine corals (Chindapol *et al.*, 2013; Cresswell *et al.*, 2017) to terrestrial trees (Holtmeier and Broll, 2017). These organisms can be seen to cluster to slow the average flow around themselves, in order to increase particulate dropout or purely for protection from high flow velocities, or are spaced so there is a maximum distance between individuals to receive the largest proportion of unprocessed flow available.

So there is precedent to suspect that, in the deep-sea, fluid flow may impact sponge distribution and density, although many drivers operating in shallow water (wave damage, water opacity and light levels) will not be applicable. However, in deeper environments observational data on localized fluid flow and how it interacts with sponges are very limited due to the inherent problems of conducting science at depth. These difficulties revolve around cost of such research, the requirement of specialized equipment, and limited field of view of remotely operated vehicles (Howell, Bullimore and Foster, 2014; Henry and Roberts, 2014a, 2014b). Empirical analysis of sponge distribution within

sponge grounds in the deep-sea is limited with previous studies looking at species occurrence only (Henry and Roberts, 2014a) or are purely non-empirical observational studies. For example, sponge density within sponge grounds has been looked at in the Faroe-Shetland channel with benthic trawler activity and substrate (sand, gravel, cobble, etc.) being significant drivers (Kazanidis *et al.*, 2019).

Computational models have been used to quantitatively predict and interpolate limited observational data. However, for sponges there has been is little or no modeling carried out of the flow around the structure or the stresses that they induce, with the only associated studies investigating the effect of increased spicule number on the resistance to wave force (Palumbi, 1986). Therefore it presents itself as a potentially useful tool to help predict sponge distribution and density within deep-sea sponge grounds (Klitgaard and Tendal, 2004; Cathalot *et al.*, 2015; Kazanidis *et al.*, 2019). Being able to create a mathematic simulation of current conditions in the deep sea would allow us to test the hypothesis that sponge distribution is rated to the prevailing current. If this supposition is true then it could explain patterns observed within sponge grounds and may be a starting point in making robust predictions of large-scale distribution in the future. The model could also be used to provide a more detailed picture of small-scale flow patterns in and around the sponges themselves that would be impossible to produce in the field. These types of measurements would also be extremely challenging in shallow water as any current measuring apparatus would also interact with any flow. As such, these simulations have the potential to increase our understanding of how sponges react to and potentially influence their local habitat in a wide range of environments.

1.2.5. Biodiversity of the Labrador Sea

Biodiversity within the Labrador Sea is understudied compared with areas of a similar latitude globally (Darnis *et al.*, 2012). This is not limited to sponges and is consistent with the common trend that deeper and more remote habitats are less well constrained than shallower counterparts (Archambault *et al.*, 2010). In the Labrador Sea a complete picture of fish species has only recently been described (Mecklenburg, Møller and Steinke, 2011; Coad and Reist, 2019), which is surprising given the high level of fishing activity in the area. This lack of data is compounded for benthic organisms, which are consistently overlooked in biodiversity studies in general (Archambault *et al.*, 2010; Kenchington, Link, *et al.*, 2011; Piepenburg *et al.*, 2011; Darnis *et al.*, 2012; Roy, Iken and Archambault, 2015). For sponges in particular, there is an order of magnitude fewer species

described in the Labrador Sea than compared to the reported diversity elsewhere at similar latitudes (Sarà *et al.*, 1992; Ackers *et al.*, 2007; Picton and Goodwin, 2007a; Downey *et al.*, 2012; van Soest *et al.*, 2012; Lehnert and Stone, 2016). This difference can be seen clearly when comparing very similar *Geodia* Lamarck, 1815, dominated sponge grounds from the Labrador Sea to those of the North East Atlantic, which have up to 50 other associated sponge species (Klitgaard and Tendal, 2004).

This apparent lack of sponge diversity in the Labrador Sea is probably due the limited number of sample collection studies performed in the area. Most of the recent work on biodiversity has been focused around trying to identify areas for increased environmental protection, particularly the identification of Vulnerable Marine Ecosystems (VME) off Canada (Hogg, Tendal and Conway, 2010; Kenchington *et al.*, 2015; Howell *et al.*, 2016) (ICES, 2009)(Figure 1.4.). The identification of VMEs is usually done though positive identification of indicator taxa (ICES, 2009). For this region most of the studies have been looking for the presence of Tetractinellida Marshall, 1876 (e.g. *Geodia* Lamarck, 1815*, Stelletta* Schmidt, 1862, and *Craniella* Schmidt, 1870) (Beazley *et al.*, 2013; Howell *et al.*, 2016; McIntyre *et al.*, 2016) (Figure 1.4.) as well as some Hexactinellida Schmidt, 1870 (e.g. *Pheronema* Leidy, 1868 and *Vazella* Gray, 1870) (Kenchington *et al.*, 2010; McIntyre *et al.*, 2016) . This is due to these groups being identifiable from Remotely Operated Vehicle (ROV) and towed camera footage (Beazley *et al.*, 2015; McIntyre *et al.*, 2016). This is important given the vast area that has not been sampled, combined with the cost and time it takes to effectively collect specimens from an area. This work using remote imaging techniques has been backed up along the Canadian margin with specimen data from trawl studies (Kenchington, Murillo-Perez, *et al.*, 2011; Murillo *et al.*, 2012, 2018; Knudby, Kenchington and Murillo, 2013), and has been used to model distribution of sponge grounds by looking at environmental parameters (Knudby, Kenchington and Murillo, 2013; Howell *et al.*, 2016; Murillo *et al.*, 2016)(Figure 1.4.).

The problem of relying on remote imaging techniques lies in the challenge of identifying sponges to a reasonable taxonomic level from images alone (Hooper and van Soest, 2002; Leys *et al.*, 2004), with specimen collection usually required to identify a sponge accurately even to family let alone species. Although surveys based on image analysis are very useful in determining location of sponge grounds, they are unable to describe the true biodiversity of an area.

Previous studies of biodiversity in the Labrador Sea are particularly limited for the West Greenland shelf. The earliest study of species in the areas reported 14 sponge species and described 7 new species from Baffin Bay, the Davis Strait and West Greenland shelf (Fristedt, 1887). Lambe (1900) continued this work reporting 21 species from the Canadian east coast, and a further 15 from the Davis Strait, describing 11 new species in total. (Lundbeck, 1902) described 15 sponge species from

the West Greenland shelf, and the last large taxonomic study of the Labrador Sea that included the West Greenland shelf was conducted in 1933 (Brøndsted, 1933b). This collated earlier work with a total of 112 sponge species being listed for the South West Greenland shelf as well as reporting 36 species and describing three new species (Brøndsted, 1933b).

Work has continue beyond this for the Canadian east coast with description of new species being described in taxonomic review papers, notably for families Tetillidae Sollas, 1886 (Cárdenas, Rapp, Best, *et al.*, 2013), Cladorhizidae Dendy, 1922 (Hestetun, Tompkins-Macdonald and Rapp, 2017a) and Polymastiidae Gray, 1867 (Plotkin, Gerasimova and Rapp, 2018) and genus *Geodia* Lamarck, 1815 (Cárdenas, Rapp, Klitgaard, *et al.*, 2013). A technical report on sponge biodiversity from trawl surveys from 2010-2014 conducted in Baffin Bay, Davis Strait and Hudson Strait recorded over 100 sponges taxa with the majority coming from order Poecilosclerida Topsent, 1928 (Baker *et al.*, 2018).

Murillo *et al* 2018 conducted a comprehensive study on sponge taxa from the Eastern Canadian Arctic using specimens from trawl surveys, including describing two new species. They identified 93 taxa broken into five sponge assemblages with unique environmental conditions, four of which have been observed elsewhere. Two of these assemblages are defined by *Geodia* Lamarck, 1815 species broken into Boreal species and coldwater or Arctic species (Klitgaard and Tendal, 2004; Cárdenas, Rapp, Best, *et al.*, 2013). The third assemblage was indentified by presence of both *Chondrocladia* Thomson, 1873 and

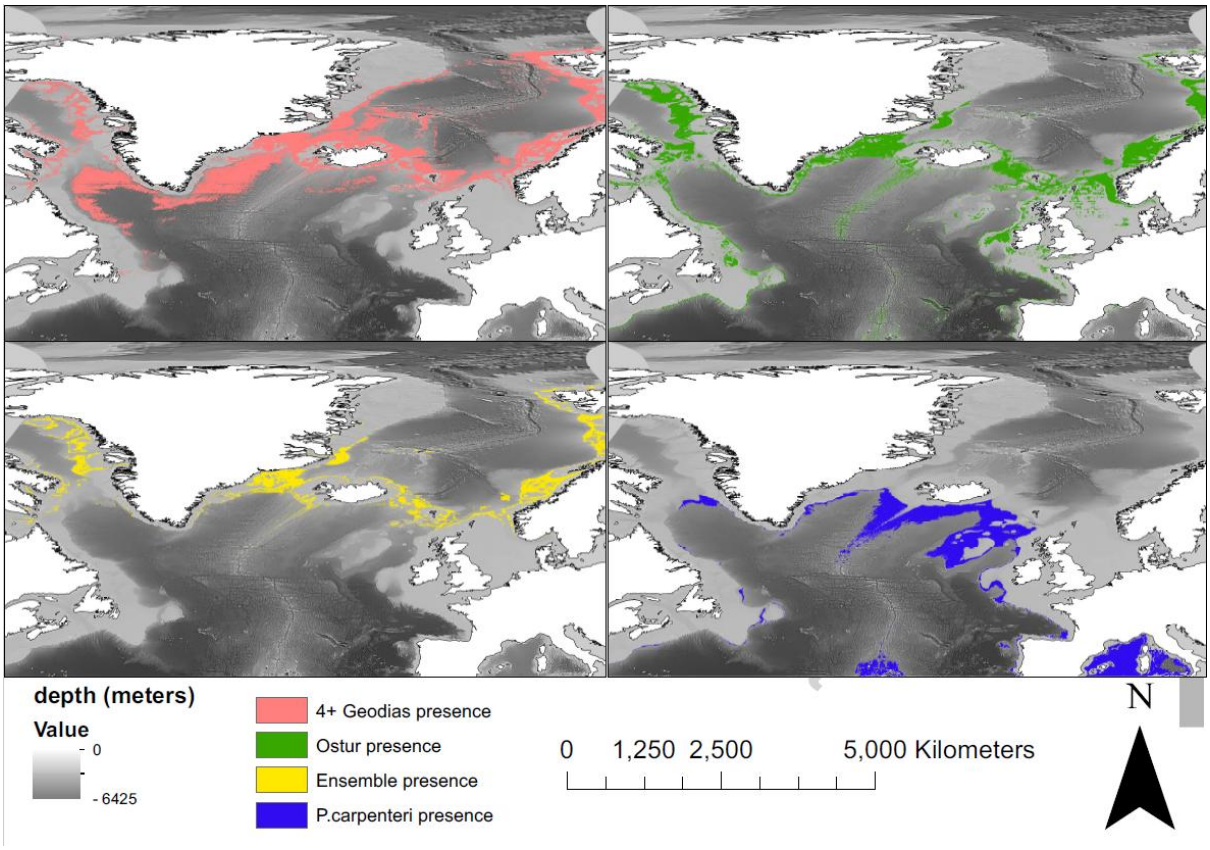

Figure 1-4. Predicted distribution maps for: a) areas with at least 4 *Geodia* Lamarck, 1815 species, b) ostur habitats, c) ostur habitat with the presence of at least 4 *Geodia* Lamarck, 1815 species, and d) *Pheronema carpenteri* (Thomson, 1869). Map projected in WGS 1984. Figure 2 from "The distribution of deep-sea sponge aggregations in the North Atlantic and implications for their effective spatial management" (Howell *et al.*, 2016).

Bathydorus Schulze, 1886, the forth by species assosacted with *Mycale (Mycale) lingu* (Bowerbank, 1866), and the fifth being very weakly described due to difficulties with species identification. Further south, Murillo *et al* 2012 looked at the Grand Banks of Newfoundland, Flemish Pass and Flemish Cap recording 30 species dominated by *Geodia* Lamarck, 1815 species. Recently work done on the Orphan Seamount described a new species of *Tedania* Gray, 1867 (Ríos *et al.*, 2021) (Appendix A) and a comprehensive pictorial guide for the area has recently been published (Wudrick *et al.*, 2020).

There are large holes in our understanding of the biodiversity of the Labrador Sea, particularly off Greenland. There is also an interesting question as to whether there could be a missing component of diversity comprising small, delicate and encrusting sponges species, given that the majority of samples that have been collected in the region has been done using trawling.

1.2.6. Labrador Sea Oceanography

The Labrador sea is an area with highly complex oceanography that is an important area of deep water formation for the Atlantic Meridional Overturning Circulation (Yang *et al.*, 2016). It is part of a larger circulation system including Baffin Bay, Davis Straits and the Labrador Sea. There are five major water masses in the effecting the Labrador Sea, three on the western Greenland shelf : Baffin Bay Polar Water (BBPW), Southwest Greenland Coastal Water, (CW) and Subpolar Mode Water (SPMW), and two on the East coast of Canada : Labrador Sea Water (LSW) and North Atlantic Deep Water (NADW) (Talley and McCartney, 1982; Lavender, Davis and Owens, 2000; Yeager and Jochum, 2009; Talley *et al.*, 2011; Rysgaard *et al.*, 2020) (Figure 1-5,1-6,1-7,1-8,1-9,1-10,1-11). The interaction of theses water masses shape dictate the characteristics of the environmental conditions experienced at the sea floor.

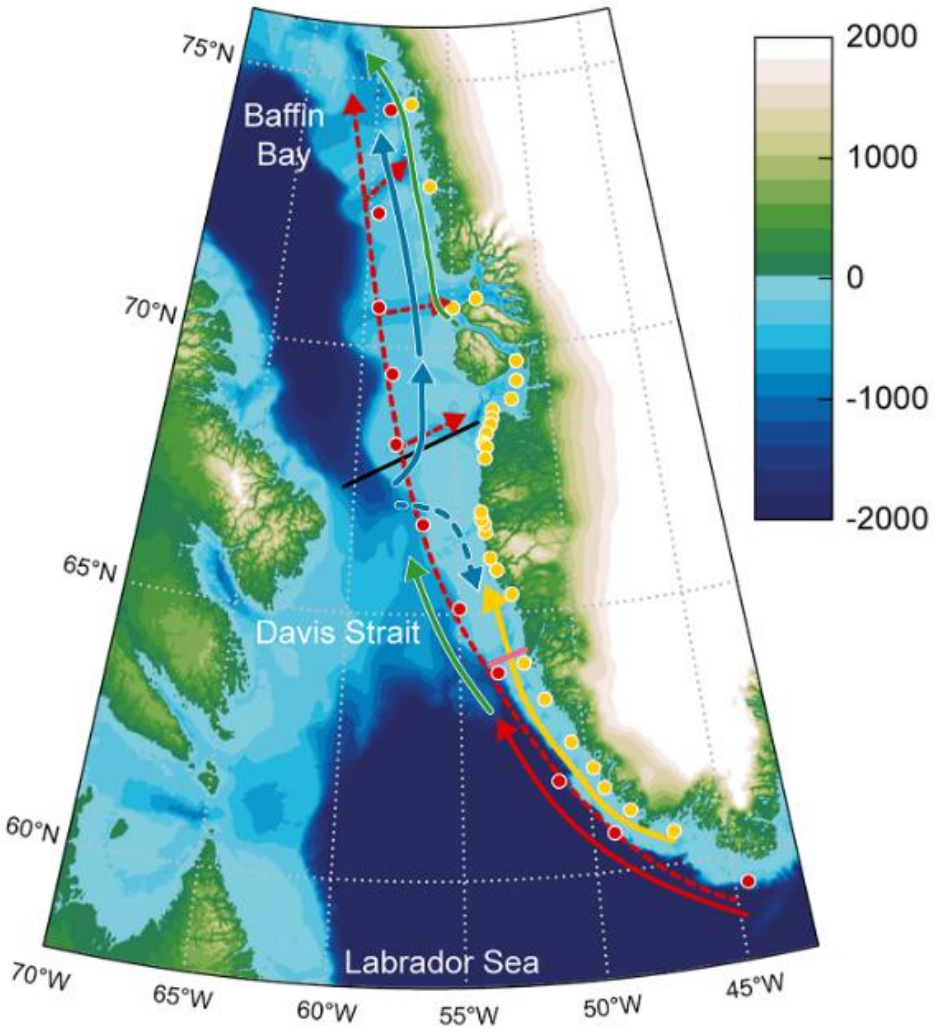

Figure 1-5. Study area showing Baffin Bay, Davis Strait, and the northern Labrador Sea between Canada and Greenland. Contours are in meters. Red dots show sampling stations on the continental slope, and yellow dots show sampling stations along the coast section during early summer 2016. Red lines show the distribution of warm upper Subpolar ModeWater (uSPMW) associated with the West Greenland Current. Dotted red lines show distribution of deep Subpolar ModeWater (dSPMW). Blue lines show the distribution of cold Baffin Bay Polar Water (BBPW). Broken blue line shows the southward transport of BBPW. Yellow line shows the distribution of Southwest Greenland Coastal Water (CW). Greenlines show the distribution of “diluted water”, see text for explanation. The black near horizontal line separates the northern and southern parts. Pink line shows the location of the Fyllas Banke section at 64°N. The suggested circulation system in 2016 is indicated by arrowheads representative of early summer. Figure 1 from " An Updated View on Water Masses on the pan-WestGreenland Continental Shelf and Their Linkto Proglacial Fjords" (Rysgaard *et al.*, 2020)

The SPMW is subdivided into the upper Subpolar Mode Water (uSPMW) and deep Subpolar Mode Water (dSPMW) (Lin *et al.*, 2018, Rysgaard *et al.*, 2020). The dSPMW has temperature of 4 °C and salinity of 34.7 the uSPMW is warmer and more saline with temperatures of 6 °C and salinity of 35. The uSPMW is found at the top of the water column and the dSPMW is found below it (Lin *et al.*, 2018, Rysgaard *et al.*, 2020). The CW is a shallow water mass on the west Greenland shelf that rounds Cape Farewell as the tail end of the Greenland Coastal Current (Lin et al., 2018). It has very low temperature 0°C and salinity 33. These water masses flow north up the Greenland shelf undergoing gradual modification of the uSPMW, dSPMW and CW due to water mass mixing (Rysgaard *et al.*, 2020) and influx of melt water from West Greenland (Luo *et al.*, 2016; Hendry *et al.*, 2019). This northward progression is halted close to the Davis Strait by the BBPW with only a heavily modified dSPMW being seen to enter Baffin Bay (Figure 1-5). The CTD plots of depth, temperature, salinity and oxygen concentration for the two Greenland sites sampled by the DY081 cruise (Figure 1-8,1-9,1-10,1-11) highlight the presence of the uSPMW, dSPMW and CW in both localities with no evidence of the cold and very saline Baffin Bay Polar Water (BBPW) dominating the Northern Greenland Shelf (Knudby, Kenchington and Murillo, 2013; Rysgaard *et al.*, 2020).

The western Labrador Sea along the coast of Canada is primarily influenced by the southern progression of LSW. This continues until around Orphan Knoll where it encounters Atlantic waters close to Newfoundland and Orphan Knoll. The LSW has temperature of temperature 3.5 °C and salinity 35, this is quite similar to those of the NADW (Talley and McCartney, 1982; Lavender, Davis and Owens, 2000; Yeager and Jochum, 2009; Talley *et al.*, 2011; Rysgaard *et al.*, 2020). However, there is a significant difference in oxygen levels with oxygen concentrations of LSW around 290 Mm/L and NADW at 270 Mm/L (Talley and McCartney, 1982; Lavender, Davis and Owens, 2000; Yeager and Jochum, 2009; Talley *et al.*, 2011) . The CTD sensor data from the study site at Orphan Knoll from the DY081 cruise show clearly the sharp deviation in the oxygen level between LSW and NADW (Figure 1-6,1-7).

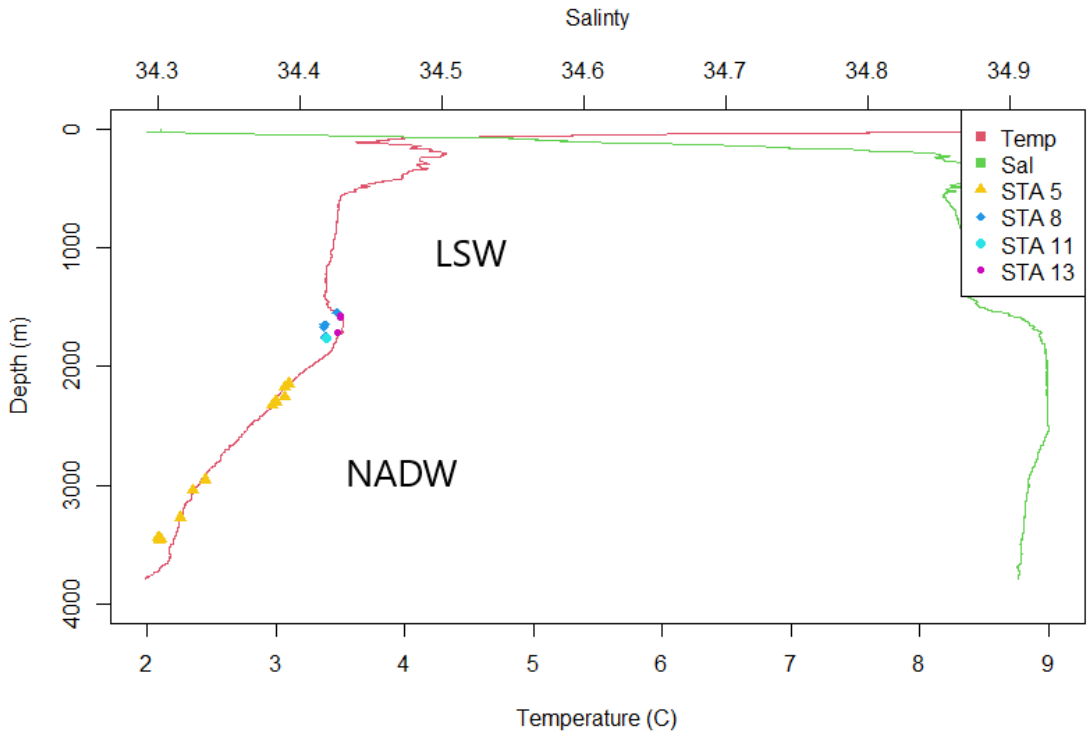

Figure 1-6. CTD depth, temperature, salinity profile from DY081 CTD001 at Orphan Knoll. With Labrador Sea Water (LSW) North Atlantic Deep Water (NADW) labeled.

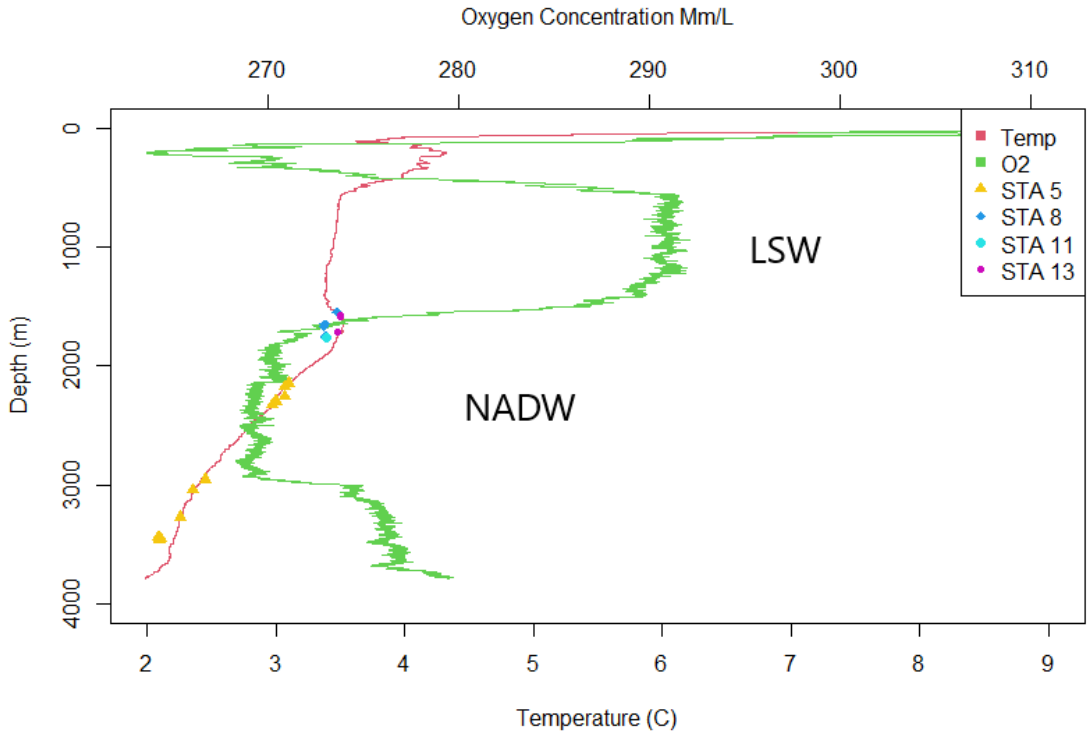

Figure 1-7. CTD depth, temperature, oxygen concentrations profile from DY081 CTD001 at Orphan Knoll. With Labrador Sea Water (LSW) North Atlantic Deep Water (NADW) labeled.

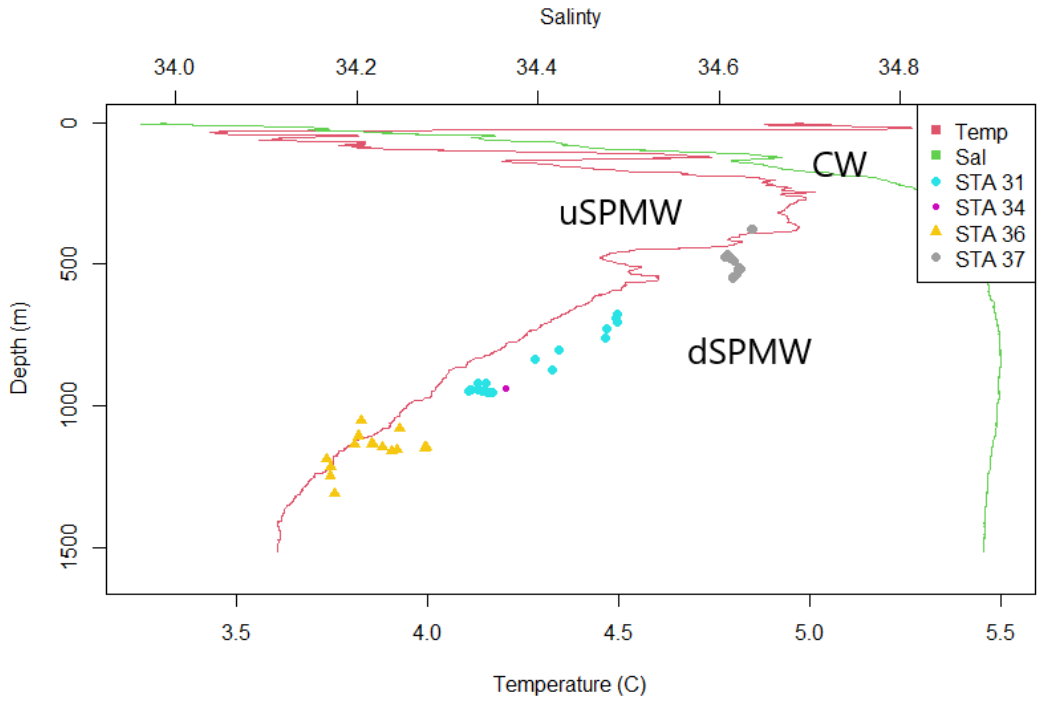

Figure 1-8. CTD depth, temperature, salinity profile from DY081 CTD013 at Nuuk. With upper Subpolar Mode Water (uSPMW), deep Subpolar Mode Water (dSPMW) and South Greenland Coastal Waters (CW) labeled.

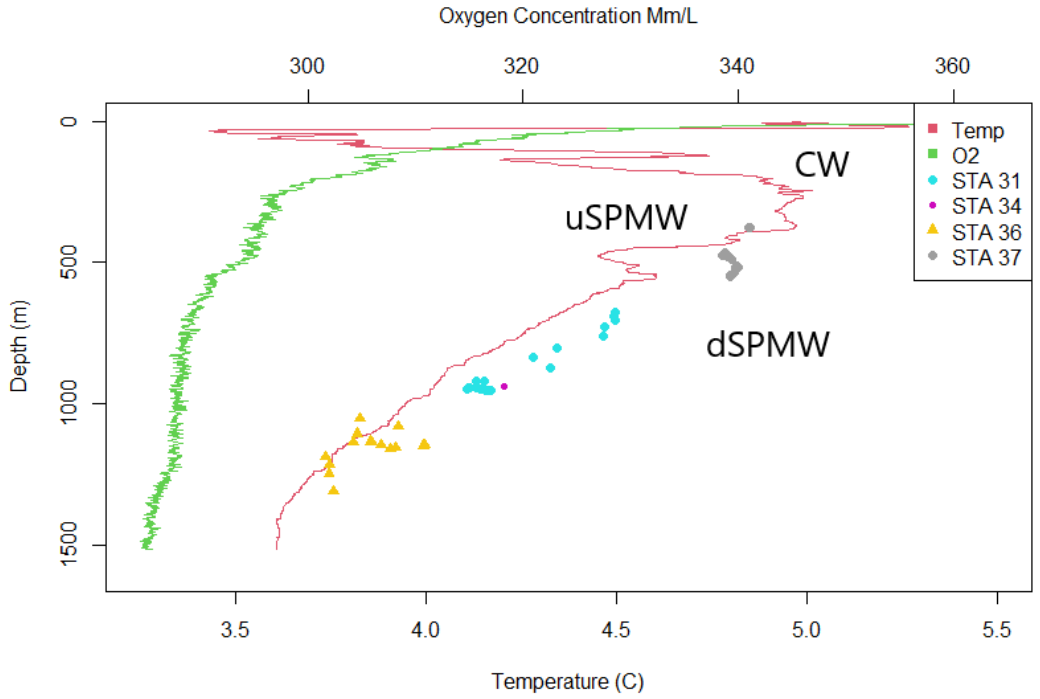

Figure 1-9. CTD depth, temperature, oxygen concentrations profile from DY081 CTD013 at Nuuk. With upper Subpolar Mode Water (uSPMW), deep Subpolar Mode Water (dSPMW) and South Greenland Coastal Waters (CW) labeled.

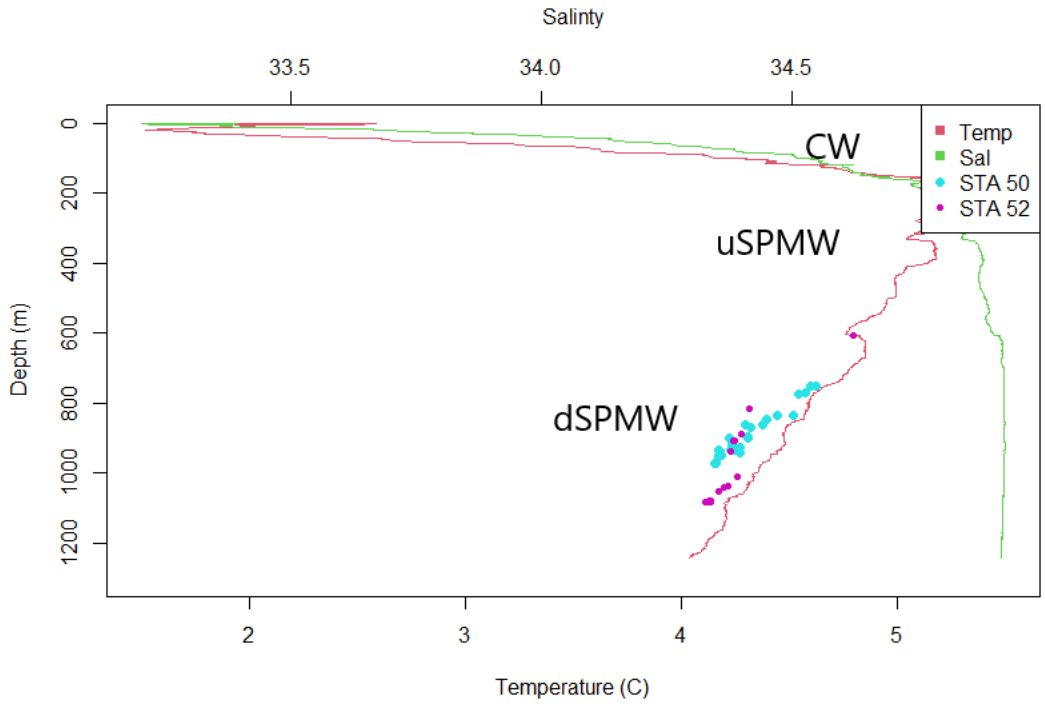

Figure 1-10. CTD depth, temperature, salinity profile from DY081 CTD020 at South West Greenland. With upper Subpolar Mode Water (uSPMW), deep Subpolar Mode Water (dSPMW) and South Greenland Coastal Waters (CW) labeled.

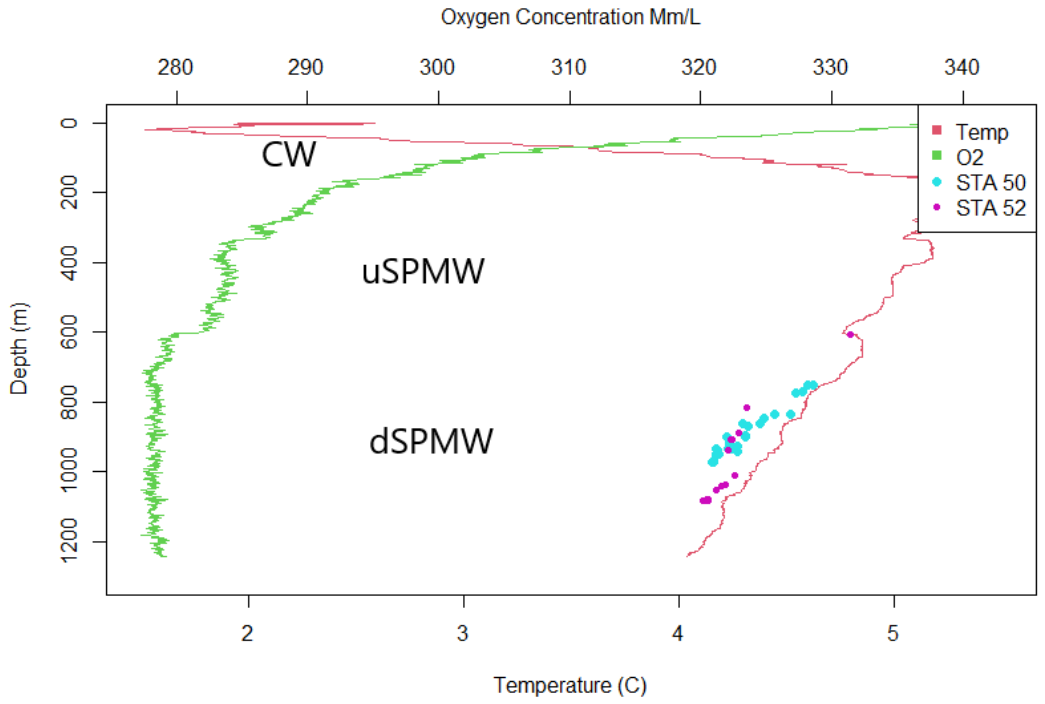

Figure 1-11. CTD depth, temperature, oxygen concentrations profile from DY081 CTD020 at South West With upper Subpolar Mode Water (uSPMW), deep Subpolar Mode Water (dSPMW) and South Greenland Coastal Waters (CW) labeled Greenland.

1.2.7. Drivers of sponge distribution

Sponge distribution has been attributed to a number of factors with the weight of these appearing to vary depending on the sponge species and assemblage (Howell *et al.*, 2016). The factors that appear to be the most important in driving diversity are silicic acid concentration (Beazley *et al.*, 2015; Howell *et al.*, 2016), temperature, depth (Rice, Thurston and New, 1990; Bett, 2001; Murillo *et al.*, 2012) and particulate carbon availability (Barthel, Tendal and Thiel, 1996; Howell *et al.*, 2016). Howell 2016 used a Maximum Entropy Model and presence data to look at the drivers of distribution for two deep-sea sponge aggregations with the North Atlantic. Dissolved silicate (i.e. silicic acid) was to be the primary factor explaining the distribution for the three boreal *Geodia* Lamarck, 1815 species and second most import for another one with all species look at showing variability explained by silica. Temperature, depth and dissolved organic carbon (DOC) were the primary drivers of other species in the study, particularly for those from cold waters, although depth was suggest to probably be a proxy for unmeasured correlating factors including temperature, current speed, water mass structure, food availability and sediment type (Howell, Billett and Tyler, 2002; Howell, 2010; Howell *et al.*, 2016). Temperature and depth in other studies are shown to be the diving factors of distribution for sponges on the Flemish Cap, Flemish Pass and Grand Banks of Newfoundland, but other factors must also be at play given the absence of sponges in the area at similar temperatures and depth to known sponge grounds (Murillo *et al.*, 2012). Flow conditions around sponge driven by internal waves, topography and bottom currents have also been suggested to play a role in sponge ground distribution (Klitgaard and Tendal, 2004; Kutti, Bannister and Fosså, 2013; Howell *et al.*, 2016), with Kiltgaard and Tendal (2004) linking sponge ground location to areas of irregular topography theorizing that these areas would have special hydrographic conditions such as current acceleration and breaking internal waves.

This work on the factors that affect sponge distribution has been extended using modeling efforts, in an attempt to extrapolate distribution of sponge grounds based on environmental parameters (Knudby, Kenchington and Murillo, 2013; Howell *et al.*, 2016; Murillo *et al.*, 2016). Knudby *et al* 2013 used environmental data that were selected based on their consistent availability within the Labrador Sea and a general notion of relevance, derived from large scale studies of the area. These data were then narrowed down based on coverage and the removal of correlated variables, and compared to a presence/ absence/ abundance of species, to construct models of distribution (Knudby, Kenchington and Murillo, 2013). There have been questions regarding the reliability of this

model, as they rely on a very basic understanding of ecology in the area and the environmental drivers of species distribution (Howell *et al.*, 2016). Howell *et al* (2016) made predictive maps of 7 species of deep-sea sponges as well as the distribution of two deep-sea sponge aggregations assuming silicic acid concentration, temperature and depth were the main drivers of their distribution. These mapped out mainly around the base of continental slopes and nearby deep seafloor (Howell *et al.*, 2016) (Figure 1.4.). Whilst Howell *et al.* (2016) is the most comprehensive study of distribution in the North Atlantic, the approach predominantly used data from the Eastern North Atlantic and was focused on a limited number of species (Figure 1.4.).

Sponges there appear to be linked with water mass and current structure particularly in the genus *Geodia* Lamarck, 1815,(Hogg, Tendal and Conway, 2010; Maldonado *et al.*, 2017). Roberts *et al.* (2021) mapped *Geodia* species in the North Atlantic and Nordic Sea tracking water masses based on potential temperature and salinity curves. They demonstrated sponges were particularly associated with the turning points of theses curves. Further they were able to show links between Arctic *Geodia* (*Geodia parva* Hansen, 1885*, Geodia hentscheli* Cárdenas *et al.*, 2010) and Arctic intermediate and wee water masses in the Nordic sea and dense overflows in the North Atlantic. These were separate and different to Boreal *Geodia* (*Geodia barretti* Bowerbank, 1858, *Geodia macandrewii* Bowerbank, 1858, *Geodia phlegraei* Sollas, 1880) which were associated with Upper and Intermediate waters in the Northeast Atlantic and Upper Atlantic derived water in the Nordic sea. They suggest that physical constrains of the water masses impact on larval distribution and that sponges have evolved specific tolerance for condition within them. Water column stratification may also benefit sponges filtering feeding due to associated phenomenon for example density current neopholoid layers and internal waves. The link between sponge distribution and water masses has been suggested previously by Klitgaard & Tendal (2004), with observations of hydrological conditions in the Northeast Atlantic pointing to specific water masses as well as sponge grounds appearing of follow branches of the North Atlantic Drift. This idea was explored further for *Geodia* species in the North Atlantic finding sites were typically boreal and arctic sponges occurred together in areas of potential mixing between water masses (Cárdenas, Rapp, Klitgaard, *et al.*, 2013). Water masses have also attributed to the distribution of *Geodia* in the Sackville Spur off Newfoundland (Beazley *et al.,* 2015). Looking at the drivers of distribution for the Labrador Sea and testing the accuracy of the prediction would be invaluable to understand the system and confirming or not the presence of the sponge grounds.

1.2.8. Anthropogenic risks

Human induced destruction of sponges and sponge habitats is a major concern given the important functional role they perform in the ocean (Klitgaard and Tendal, 2004; Miller *et al.*, 2012; Murillo *et al.*, 2012; Knudby, Kenchington and Murillo, 2013; Maldonado, 2016; Roberts *et al.*, 2018; Hawkes *et al.*, 2019). These risks can be split into two main categories: direct destruction and environmental change. These risks are potentially more harmful for sponges than many other benthic organisms as they slow growing and long lived (Lindholm, Auster and Valentine, 2004; Howell, 2010; Kenchington, Murillo-Perez, *et al.*, 2011; Bell, McGrath, *et al.*, 2015; Grant *et al.*, 2018, 2019; Prado *et al.*, 2021) .

The largest contributor by far to the direct destruction component is bottom-fishing. Destruction though interaction with fishing gear can be classified into three types: blunt impacts, line shear and hooking (Ewing and Kilpatrick, 2013; Clark *et al.*, 2016). Blunt interaction results in the dislodgment or crushing of individuals, particular erect forms of sponges (Koslow *et al.*, 2001; HallSpencer, Allain and Foss, 2002; Althaus *et al.*, 2009; Rooper *et al.*, 2011; Clark *et al.*, 2019; Durán Muñoz *et al.*, 2020). Sponges can also be hooked, tangled and sheared off with long-lines (Orejas *et al.*, 2009; Sampaio *et al.*, 2012; Bo *et al.*, 2014; Durán Muñoz *et al.*, 2020). In addition, ground gear can gouge into soft substrate and these scars can remain for many years. For example, bottom-water fishing scars in waters off New Zealand remained for at least 15 years after fishing stopped (Clark *et al.*, 2009). To compound this damage, bottom-water fishing destruction leaves behind rubble that can effectively eliminate habitat for commercially important fish (Wassenberg, Dews and Cook, 2002) resulting in the collapse of fish stocks and leading to trawlers moving onto areas where there are intact sponges.

A secondary more indirect effect of trawling – as well as oil, gas and mining activities – is the effect of sediment suspension (Clark *et al.*, 2016; Vad *et al.*, 2018), with trawl gear creating plumes of particles typically 2-4 m high and around 130m wide (Palanques, Guillén and Puig, 2001; Durrieu De Madron *et al.*, 2005; Bradshaw *et al.*, 2012). In the deep sea these disperse slowly and effect large areas (Bluhm, 2001; Rolinski, Segschneider and Sündermann, 2001). This sediment is known to smother and kill sponges particularly the flat, funnel-shaped, encrusting and small sponges (Pineda, Duckworth and Webster, 2016; Schönberg, 2016; Strehlow *et al.*, 2017). This is one of the primary reasons for loss in biodiversity when there is an increase in the industrial and commercial exploitation of the deep waters, and given this is increasing dramatically within the Labrador Sea it is of particular concern (Eriksson *et al.*, 2010; Hewitt and Thrush, 2010; Love *et al.*, 2013).

Potentially the greatest long term threat to sponges is that of climate change, in particular ocean warming. Ocean acidification that also comes with climate change appears to have little apparent effects on sponges with no strong correlation between change in pH and loss of sponges (Bell *et al.*, 2018). Ocean warming in contrast has a negative effect on sponges is general (Bell *et al.*, 2018) with mass mortality events for sponges have been reported due to periods of abnormally high sea temperatures (1 - 3 ^{o}C above seasonal mean sea temperature) (Vicente, 1990; Vacelet, Boury-Esnault and Harmelin, 1994; Cerrano *et al.*, 2000; Garrabou *et al.*, 2009; Cebrian *et al.*, 2011; Camillo *et al.*, 2013; Rubio-Portillo *et al.*, 2016). Laboratory studies have shown the tolerance to temperature appears to vary depending on species (Massaro *et al.*, 2012). However, this work has only looked at shallow water species which are subject to greater temperature fluctuation than seen in the deep sea, so this may not hold true for species at depth. Given the comparatively stable temperatures at depth, you would expect deep-sea species to be more sensitive to temperature change than shallow water counterparts. Given that temperature is one of the stronger drivers of sponge distribution, it would be reasonable to assume that North Atlantic sponge ground distribution, and sponge diversity, are potentially sensitive to ocean warming (Howell *et al.*, 2016).

1.3. Thesis aims

The aim of this thesis was to endeavor to understand the distribution, density and biodiversity of sponge species and sponge grounds within the Labrador Sea. Using mathematical modeling, taxonomic identification of species and statistical analysis of oceanographic variables I looked at the controls of distribution within sponge grounds, identified species from these sponge grounds and explored the drivers of their distribution. This work will contribute to our understanding of the role of sponges within the Labrador Sea by identifying sponge grounds and drivers of their distribution, as well as helping to quantify the effects of anthropogenic damage to these organisms.

This thesis is presented across five chapters. In the introduction **(Chapter 1)**, I explain the motivations around this research and provide the relevant scientific background. In the next three chapters **(Chapters 2-4, described below)**, I represent the original research of this thesis: the first two present published work conducted as part of this thesis and the third written as a publication-style chapter. They are written to be read either individually or sequentially **(Chapters 2-4)**. In the Concluding Remarks **(Chapter 5)**, I summarise the key findings of the thesis and discuss potential directions for future works.

1.3.1. Quantifying the effect of flow on sponge distribution

Patterns of sponge distribution and density in the deep-sea have been ascribed to several factors in large scale biogeographic studies. These include the influence of factors that control flow condition on the seafloor including current speeds internal waves and topography (Klitgaard and Tendal, 2004; Howell *et al.*, 2016). These factors potentially also contribute at smaller scales and sponge distribution could be optimized to improve their localized conditions (Kutti, Bannister and Fosså, 2013). These patterns are seen in other organisms, either individuals create maximum distance from each other to increase the potential for unprocessed flow, or clustering together to slow the flow for protection from damage or potentially increasing particle dropout (Chindapol *et al.*, 2013; Cresswell *et al.*, 2017). However, these small scale processes have not been quantified before in deep-sea sponges.

In Chapter 2, I will investigate if there are patterns of density and distribution at small spatial scales and weather these patterns link to the prevailing flow conditions. I will be basing this study around differing four sponge grounds in the Labrador Sea. Using clustering analysis, I will quantify patterns of distribution at each site before moving on to create a mathematical flow model to analyze the fluid flow around these sponges in the study areas. I will discuss the possible explanations and implications of the results, and their potential impacts on our understanding of the role and sensitivity of sponge grounds in the deep sea.

1.3.2. Describing the sponge biodiversity

The Labrador Sea's biodiversity is critically understudied compared with other areas of a similar latitude (Darnis *et al.*, 2012). This is particularly bad around the South Western shelf of Greenland where there has been no sample collections since 1933 (Brøndsted, 1933b). Most of the studies from the Labrador Sea that have collected sponge samples have done so using trawl collection method potentially missing smaller, delicate and encrusting sponges.

In Chapter 3, I will increase the amount of information on the sponge biodiversity of the Labrador Sea, particularly in areas will little modern biodiversity data, by describing collections from three areas: Orphan Knoll, Nuuk and South West Greenland. These sponge samples were collected by ROV on the DY081 Discovery cruise, allowing the collection of small, delicate and encrusting sponges, in order to capture some of the missing biodiversity in the region.

1.3.3. Investigating the biogeography of sponge grounds

Identifying the factors that are driving sponge distribution is fundamental to understand their extent, importance and function within the global ocean. By understanding the environmental factors that influence the distribution of the sponge species and sponge grounds, we can improve our understanding of the organisms themselves as well as capture the parameters required to predict their total distribution and function (Knudby, Kenchington and Murillo, 2013; Howell *et al.*, 2016; Murillo *et al.*, 2016).

In Chapter 4, I aim to increase the understanding of the environmental drivers of distribution for the sponge grounds samples on the DY081 cruse in the Labrador Sea, with the aim of using these results to identify areas where we would expect sponge assemblages and the species they contain to occur in the Labrador Sea.. The samples were collected from three contrasting ocean environments driven by the influence of differing water mass interactions (Talley and McCartney, 1982; Lavender, Davis and Owens, 2000; Yeager and Jochum, 2009), providing the potential to determine the key differences between assemblages, and the underlying driving mechanisms behind these differences.

The sponge specimens were collected by ROV on the DY081 Discovery Cruise (**Chapter 3**) and combined with environmental variables measured by sensors on the ROV or using co-located water samples. I will conduct a principle component analysis study draw out the principle drivers of distribution from this combined data set. Such a localized environmental data set will giving us a more nuanced idea of conditions around the sponges at these localities. I discuss the implications and possible explanations of the results, and how these sponge grounds might be impacted in the future.

2. Chapter 2. Sponge density and distribution constrained by fluid forcing in the deep sea

Culwick, T., Phillips, J., Goodwin, C. E., Rayfield, E. J., & Hendry, K. R. (2020). Sponge Density and Distribution Constrained by Fluid Forcing in the Deep Sea. Frontiers in Marine Science, 7, 395.

Author contributions and declaration:

T.Culwick., J.Phillips. and K.R.Hendry. conceived the study. T.Culwick carried out the study. T.Culwick wrote the paper and prepared figures. All authors analysed the data, revised drafts of the paper and gave final approval for the publication

2.1. Abstract

Understanding the distribution and density of sponge grounds in the deep sea is key to appreciating the ecological importance, vulnerability, and role in ocean biogeochemistry of these important habitats. A novel combination of clustering analysis and fluid flow finite element modelling was used to study the distribution of four sponge grounds from the Labrador Sea, which were chosen for their distinct assemblages of sponges. Significant small-scale clustering patterns of sponges were found within each sponge ground, measured using the Ripley K function. A new approach using finite element modelling of fluid flow was then applied to understand the drivers of the observed sponge distribution, with detailed numerical experiments providing insights into the flow patterns that could not be obtained from field measurements. Simulations using idealised sponge shapes suggested that sponge wakes could interact and influence the mean flow conditions at the spacings observed within the sponge grounds. Simulations of flow over models of multiple individuals constructed using topographic models of the sponge grounds, showed that these interacting wakes generated a boundary layer of slowed flow, which may be beneficial to sponge development. The boundary layer may be acting as a protective layer, affecting larval recruitment, increasing particle fall out and increasing the effective radius of pumping. This observation has important implications for the impact of anthropogenic damage on sponge grounds, which changes the sponge distribution and may reduce the boundary layer thickness, affecting potential recovery rates. This study illustrates the power of incorporating mathematical modelling with field observations in the deep sea to increase our understanding of anthropogenic and climate change impacts on sponge ground ecosystem structure and function.

2.2. Introduction

Sponges (phylum Porifera Grant, 1836) are an often overlooked as important components of benthic marine ecosystems. They are known to perform several functional roles notably as reef building organisms in both the shallow and deep-sea (Miller *et al.*, 2012; Knudby, Kenchington and Murillo, 2013; Roberts *et al.*, 2018). Sponge grounds support areas of high biodiversity (Klitgaard and Tendal, 2004; Murillo *et al.*, 2012; Hawkes *et al.*, 2019), act as nurseries for many fish species (Klitgaard, 1995; Freese and WIng, 2003) and can influence primary production by controlling nutrient availability (Bell, 2008; Maldonado, Ribes and van Duyl, 2012; Murillo *et al.*, 2012; Kutti, Bannister and Fosså, 2013; Maldonado, 2016). This ecological importance is complimented by their economic potential from bioengineering (Wu, Wu and Wang, 2019) and novel chemicals for pharmaceutical applications (Koopmans, Martens and Wijffels, 2009; Anjum *et al.*, 2016). However, despite their ecological and socioeconomic importance, sponges are vulnerable to anthropogenic stressors such as trawl fishing (Kenchington *et al.*, 2014; Pusceddu *et al.*, 2014; Victorero *et al.*, 2018) and oil and gas activities (Vad *et al.*, 2018). Sponge ground locations and densities need to be known, in order to quantify their distribution and function, and – ultimately – protect the critical habitats that they form. In the deep-sea, observational data are very limited due to the difficulties in conducting science at depth, such as the cost and limited field-of-view of remotely operated vehicles (Howell, Bullimore and Foster, 2014; Henry and Roberts, 2014a, 2014b). Computational models can be used to interpolate and quantitatively predict sponge distribution, helping to circumvent the challenges involved in understanding the factors that control sponge distribution. The large (basin) scale distribution of sponge grounds in the North Atlantic has been studied. However, sponge distribution and density within deep-sea sponge grounds has been understudied and remains poorly constrained (Klitgaard and Tendal, 2004; Cathalot *et al.*, 2015; Kazanidis *et al.*, 2019).

Studies on sponge density and distribution in shallow water environments have been carried out using standard ecology survey techniques, with multiple studies across environments and latitudes. (Wilkinson and Evans, 1989; Roberts and Davis, 1996; Xavier and van Soest, 2012). However, the major drivers of these distribution patterns such as wave damage, water opacity and light levels do not operate in the deep-sea. Empirical analysis of localised distribution in deep-sea sponge grounds is very limited with most data being purely observational or on species occurrence only (Henry and Roberts, 2014a). Studies of sponge density have been carried out in the Faroe-Shetland Channel where fisheries pressure and substrate type (sand, gravel, cobble) were statistically significant factors (Kazanidis *et al.*, 2019). However, a host of other chemical oceanographic variables (silicic

acid, temperature, etc.) also exhibited strong controls over sponge density (Kazanidis *et al.*, 2019). The influence of multiple forcing mechanisms results in significant challenges in scaling-up from a small number of observational data points to whole-basin sponge ground densities using oceanographic variables (Howell *et al.*, 2016). Creating mathematical simulations of current conditions in the deep sea allows us to explore whether the observed distribution of sponges is related to prevailing currents. This in turn provides possible explanation of the patterns seen which could be scaled up to infer large-scale distributions. The simulations of the observed sponge grounds also allow a more detailed investigation of the small-scale flow patterns that would not be possible to measure the field, with the potential to increase our understanding of this important and understudied habitat.

Patterns of deep-sea sponge distribution and density have been attributed to several factors in large scale biogeographic studies. The primary drivers of sponge distribution are thought to be silicic acid concentration (Beazley *et al.*, 2015; Howell *et al.*, 2016) temperature, depth (Rice, Thurston and New, 1990; Bett, 2001; Murillo *et al.*, 2012) and particulate carbon availability (Barthel, Tendal and Thiel, 1996; Howell *et al.*, 2016), in addition to topography, internal waves and current speeds which control flow conditions at the seafloor (Klitgaard and Tendal, 2004; Howell *et al.*, 2016). It would be logical to assume these factors would also play a role at the smaller scale and that sponge distribution would potentially be optimised to improve their localised conditions (Kutti, Bannister and Fosså, 2013). The arrangement of organisms can affect the flow around individuals, either spacing themselves the maximum distance from each other to receive the greatest unprocessed flow potential, or clustering to slow the flow for potentially greater particle dropout or protection from damage. These patterns in distribution are seen abundantly in nature such as in corals (Chindapol *et al.*, 2013; Cresswell *et al.*, 2017) and terrestrially in trees (Holtmeier and Broll, 2017).

Fluid flow around sponges in the deep sea are predominatly driven by tidal currents and so topography will dictate areas of high or low average bottom water flow rates. Thermohaline currents will play a part, particularly at greater depths but the velocity of these flows is very low compared to those due to tidal forcing (Rahmstorf, 2003). Most sponge grounds in the Labrador Sea are found on the slopes of topographic highs within the ocean (Beazley *et al.*, 2015; Howell *et al.*, 2016), these are areas where you would expect a high influence of tidal currents (King, Zhang and Swinney, 2010) and these are the areas where high bottom water flow rates are observed (Klitgaard and Tendal, 2004; Howell *et al.*, 2016).

Here, we will investigate whether the patterns of density and distribution at small spatial scales in four different sponge grounds in the Labrador Sea are linked to the prevailing flow conditions, and

will explore possible explanations for the patterns observed. With particular focus on the cumulative effect on flow that the arrangement of multiple individuals produces, within a particular environment. We discuss the implications and possible explanations of our results, as well as their potential impacts on the greater understanding of the role and sensitivity of sponge grounds in the deep-sea.

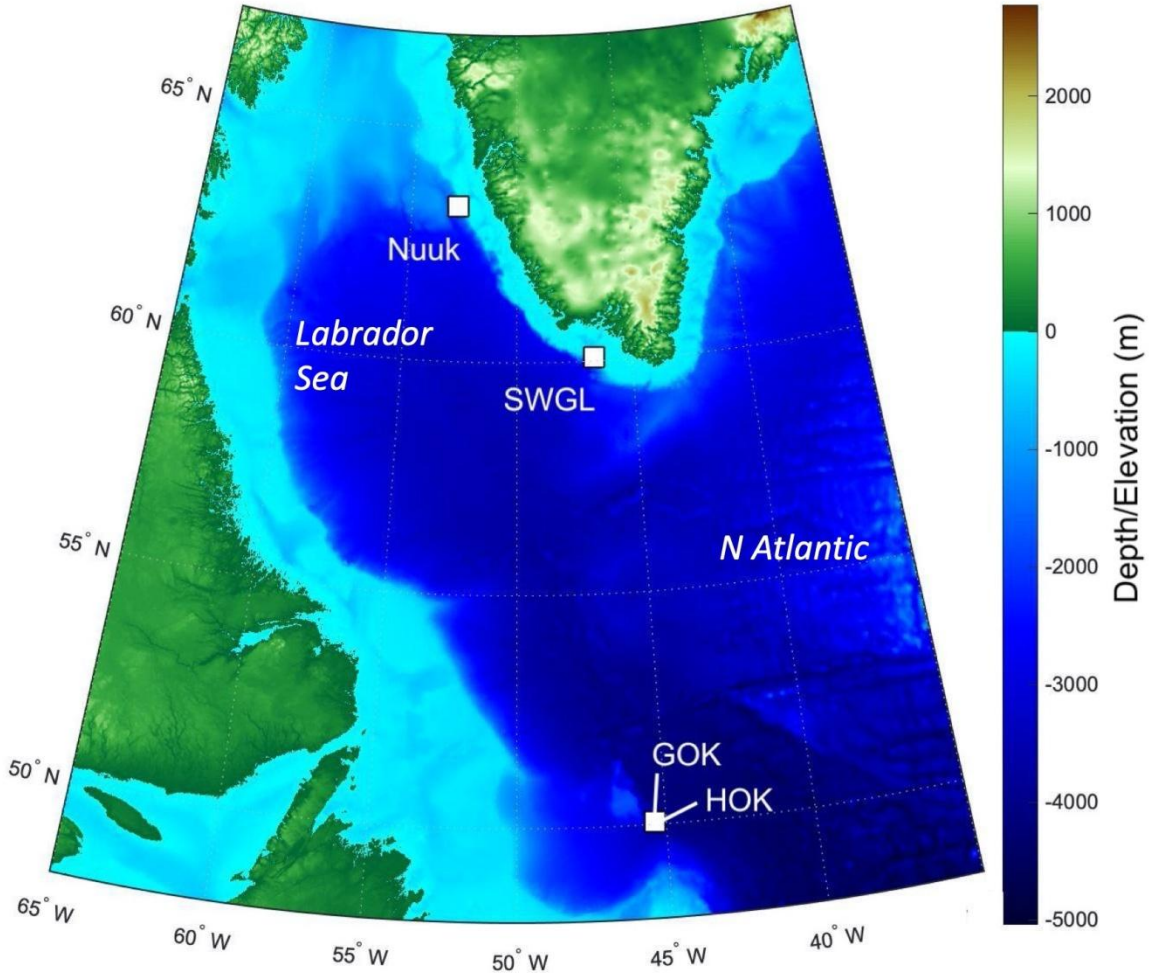

Figure 2-1. Overview map showing the position and depth of the four localities Nuuk, Southwest Greenland (SWGL), *Geodia* Lamarck, 1815 dominated sponge ground at Orphan Knoll (GOK), and hexactinellid dominated sponge ground at Orphan Knoll (HOK) from the DY081 Cruise in the Labra Labrador Sea. Bathymetry used is from ETOPO1 model from https://www.ngdc.noaa.gov/mgg/global/

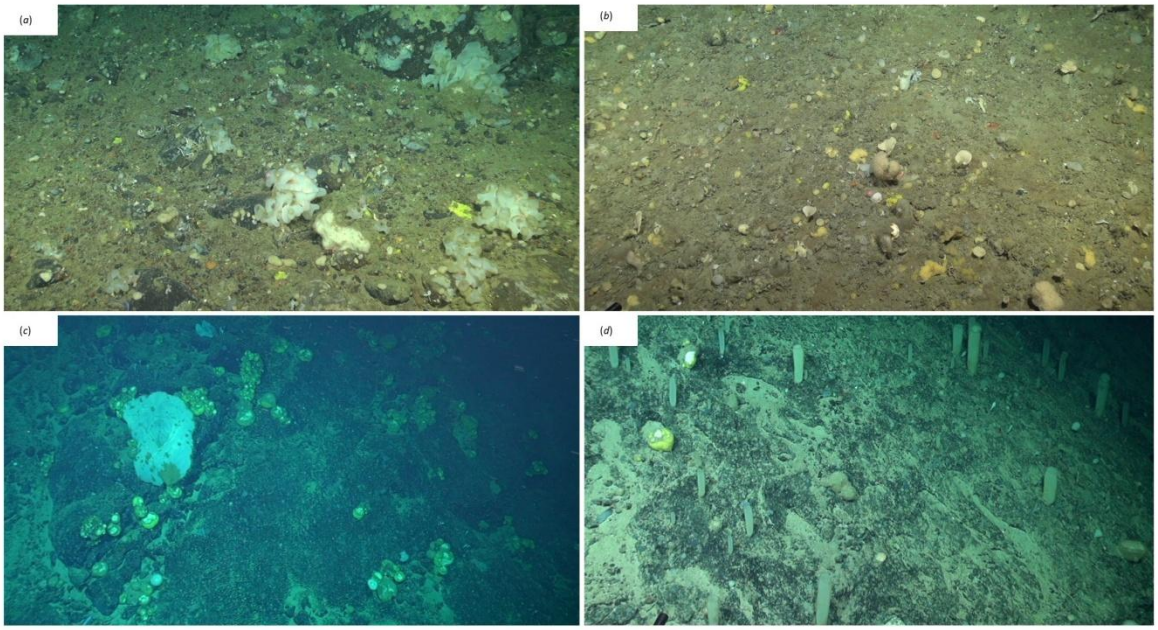

Figure 2-2. ROV Image of the four study areas from the DY081 Cruise (a) Nuuk (b) SWGL (c) GOK (d) HOK. Red laser scale makers are 10cm apart.

2.3. Methods

2.3.1. Sponge ground imaging

Sponge ground images were recorded on the DY081 RRS *Discovery* cruise summer 2017 at three locations: Orphan Knoll, Nuuk and Southwest Greenland (SWGL) (

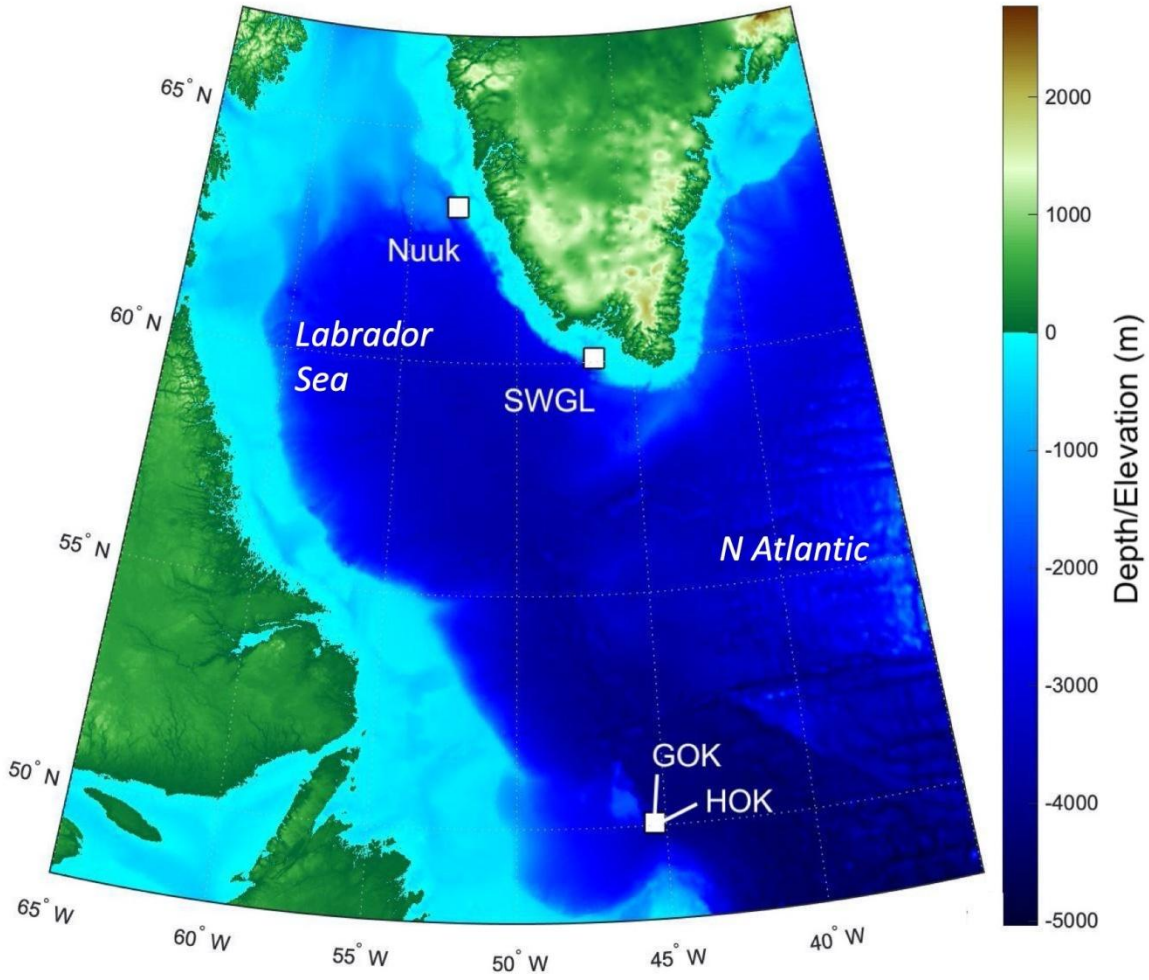

Figure 2-1) each chosen due to their differing water mass interactions. High-definition video was recorded via Remotely Operated Vehicle (UK National Marine Facilities ROV *Isis*) using a fixed view Scorpio camera. Images were recorded from a typical height of 1 m above the sea floor, with the field of view varying in width between 1 and 3 m. Lasers were attached to the Scorpio camera at 10 cm spacing so scale could be accurately resolved from images. The study areas were randomly selected within each location. A single study area was chosen for Nuuk (Figure 2-1,2 (*a*)) and SWGL Localities (Figure. 2-1,2(*b*)), which were uniform in depth and have no dominant species. Two study

areas were assigned at Orphan Knoll, due to the presence of two distinct sponge grounds at separate depths characterised by different dominant groups. These are i) a *Geodia* Lamarck, 1815 dominated sponge ground (GOK; Figure. 2-1,2(*c*)), and ii) a hexactinellid dominated sponge ground (HOK; Figure. 2-1,2(*d*)) at greater depth. Still images were the taken from the video at 2 second intervals which was sufficient to ensure that typically 30 individual, overlapping images were available to create a digital surface model of between 3 and 5 m in length.

2.3.2. Digital surface model

Surface mesh models were created from sets of images for each study area using photogrammetry. Agisoft PhotoScan software was used to align the images and create a 3D surface mesh using structure-form-motion algorithms (Westoby *et al.*, 2012); the SGM algorithm (Hirschmüller, 2005) and scale invariant feature transform (SIFT) operator (Lowe, 2004). A scaled 3D surface mesh was exported as a .stl file and a 2D point cloud map of sponge locations exported as a point pattern dataset. The 3D surface mesh was converted using AutoCAD Software to AutoCAD Drawing format to use as a solid boundary in COMSOL Multiphysics flow modelling simulations.

2.3.3. Clustering analysis

A point pattern map for each locality was input into RStudio, such that each point represents the position of an individual sponge. Multi-Distance Spatial cluster analysis was carried out using Ripleys K functions (Ripley, 1976, 1977, 1981). The K- function is defined by:

$$\mathrm{K}(d) = \lambda^{-1} \sum_{i \neq j} \frac{I(d_{ij} < t)}{n}$$

Where d_{ij} is the Euclidean distance between ith and jth points in a data set of n points, t is the search radius, λ is the average density of points (generally estimated as n/A, where A is the area which contains all the points) and I is the indicator function (1 if its operand is true, otherwise 0). $\mathrm{K}(d)$ approximates πt^2 if the points are homogenous with the region. This radial spatial analysis can become unrepresentative when applied close to the edges of the domain, because of the truncation of information at the edge. We used periodic boundary conditions (such that an edge of the domain is joined to its opposite edge and analysis treats this as a continuous surface) to eliminate the edge

effect, which may have been significant given the narrow transects. Upper and lower bounds of confidence of statistical significance were produced using Monte Carlo simulations. Monte Carlo simulations randomly generate a distribution of points equal to the number of input points. Multiple simulations were run and used to ensure clustering patterns were not due to random variation (at the 95% confidence level).

2.3.4. Fluid flow finite element analysis

We modelled the flow around idealised sponge shapes and around the 3D surface models of the sponge ground study areas using the finite-element package Comsol Multiphysics 5.1. The dimensions of the idealised sponge shapes were based on average sponge sizes of *Geodia* Lamarck, 1815 and *Euplectella* Owen, 1841 species collected on the DY081 Cruise. The idealized shapes chosen were a truncated sphere (simulating *Geodia* Lamarck, 1815 species) and truncated ellipsoid (simulating *Eupectella* species). These shapes were purposely kept very simple to reduce computations run times and meshing difficulties enabling effecting model testing. A preliminary study was conducted comparing the effect of using idealized structures to increasingly realistic structures based on a *Geodia* Lamarck, 1815 species using an single flow speed (0.5 m/s). This showed small increase in structural complexity leading to large increases in computational run times and insignificant differences in the flow field produced, when compared to the idealized shape. The flow through sponges was considered, however the small size of the ostia and therefore the volumes of fluid flow though each one spread out across the sponge would have little impact of the wake of the sponge. The outflow from the sponges could not be modeled in this study.

This prelimany work was extended to include the effect s of surface roughness of these idealised shapes on the flow fields. The results of this study saw the increased thickness of the turbulent boundary layer around the object with increased roughness however this increase in thickness was proportionaly insignificant compared to the size of the object itself.

The flow field was described using the Reynolds-averaged Navier-Stokes equations (RANS equations) coupled with the K-epsilon (K-ε) Turbulence model (Hanjalić and Launder, 1972). The flow was computed using the 3D surface meshes generated from photogrammetry, with a no-slip basal boundary condition, open boundaries (zero viscous stress condition) for those perpendicular to flow, downstream and upper boundaries, and a uniform inflow velocity at the upstream end. Initial flow conditions within the model area for the simulation calculations was set as a steady flow equal in

velocity to that of the inflow. Surface models were orientated so the simulated flow matched the observed current direction over the sea floor recorded at the time of the ROV survey.

A mesh was created using free tetrahedral elements for the geometries using the finite element mesher by Comsol. A coarse mesh was used to enable an efficient exploration of model parameter space, with some simulations being run at finer mesh resolution to ensure grid scale independence for the simulation results. This method of meshing was one of the limiting factors in this study. The the 3D surface models all had a number of very small polygons hidden in their structure which the Comsol mesher could not resolve at very finer mesh resolutions. This resulted in the coarseness of the mesh necessary, to be much greater than originally planned, as well as preculding the inclusion of more detailed 3D models.

The inbuilt material properties for water were used with fixed solid geometry for the idealised simulations. In all cases three-dimensional, incompressible (constant density) flow of water was simulated with idealised structures and sea floor reconstructions were held stationary. The sea floor reconstructions allowed us to take into account some elements of the varying sediment surfaces in the differing study areas. Rocky surfaces with protuberant verticality were captured by the photogrametry however the distinction between finer sediments for example sand and fine silt was not. However varying the surface roughness of the sea floor model had little effect on the boundary layer when compared to that caused by undulations in the sea floor.

Inlet and initial flow speed were varied between 0.1 m/s and 1 m/s in 0.1 m/s intervals (Reynolds numbers for all simulation fall between approximately 1.53×10^5 and 7.5×10^6). The volumetric flowrate used was matched to the mean bottom flow rates observed using the sonde on the DY081 RRS *Discovery* cruise (Hendry, 2017) and the range based on year-round observations from Orphan Knoll (Greenan *et al.*, 2010). A stationary solver was used to compute the steady-state flow patterns and a Turbulent flow k-ε model was used to solve the RANS equations and conservation of mass.

An initial simulation of three-dimensional flow around a sphere was used to benchmark the main Comsol simulations. The benchmarking method laid out in Nita and Allaire (2017) was used with drag coefficients for the flow around the sphere being in the range of 0.46-0.5 to verify the robustness of the numerical method used. Results were visualised as two-dimensional cross sections of flow velocity magnitude and wake length, and diameters were plotted against height and diameter for the idealised simulations.

2.4. Results

2.4.1. Clustering analysis

All study areas exhibited non-random ($p<0.05$) sponge distribution patterns, with variation in the presentation of distribution between sites (Figure. 2-3). The SWGL (Figure. 2-3(*d*)) and GOK (Figure. 2-3(*c*)) sites exhibited similar patterns of distribution. Individual sponges cluster together at distances of 0.1-1.2 m and the distribution becomes more uniform at distances greater than 1.4 m indicating that they form dense, sparse clusters. The HOK (Figure. 2-3(*a*)) site shows a very strong clustering pattern within the study area, although there is a random distribution at distances less than 0.25 m. The Nuuk (Figure. 2-3(*b*)) study site in contrast exhibits a consistent non-random but weak dispersion patterning.

2.4.2. Models of flow around idealised sponge morphologies

We initially used two simplified shapes to represent sponge morphology: a sphere and an ellipsoid. For both the spherical structure (Figure. 2-4) and the ellipsoidal structure (Figure. 2-5) the same patterns of wake (downstream regions of reduced flow velocity) are produced. There is a direct correlation between structure height and length of the initial wake, as well as the diameter of the wake and diameter of the structure (Figure. 2-6). Wake length and diameter are mostly unaffected by flow speed with the changes of flow speeds within the wake being directly proportional to the changes to the ambient flow speed (Figure. 2-6). The length of the effective slowing due to the wake is approximately ten times the height of the structure, which is similar to wake lengths of submerged hemispherical objects (Shamloo, Rajaratnam and Katopodis, 2001). Beyond this wake region the near-wall flow velocities are similar to those upstream. A second feature of both models is the presence of an area of lower velocity upstream and around the sides of the sponge structure caused by flow separation, which increases in size at high velocities (Figure. 2-4,2-5). These initial tests indicate that, for the sponge spacings (up to $1.4/m^2$) and heights (up to 0.5 m) in the four study areas, we expect the wakes of the sponges to be interacting and influencing the flow conditions.

2.4.3. Models of flow at the study area

For each of the study areas we ran simulations with sponges *in situ* and removed to look at the effect of multiple individuals on the flow. Individual sponges created wakes that were significantly

deeper than the boundary layer resulting from flow over the sea floor topography, even when surface roughness was changed to simulate varying sediment types. The structures in the Nuuk study area (Figure. 2-7) produced a boundary layer of similar height to that of the seafloor topography boundary layer but with a significantly slower velocity, which appears reduced by approximately 50% from the same point within the boundary layer. The area of wake influence from each sponge structure extends horizontally in a narrow cone pattern but the distance between each structure is such that a coherent and continuous boundary layer is produced, with properties set by the sponge height and spacing. Both SWGL (Figure. 2-8) and HOK (Figure. 2-9) sites show similar flow patterns as the Nuuk site but with slightly thinner boundary layers. Both SWGL and HOK have clusters of sponge structures sitting within small depressions causing the sheltering effect of the topography to make a greater contribution to the overall flow pattern. The GOK site (Figure. 2-10) differs due to the prominence of a single large sponge >0.5 m in diameter and height. The flow patterns around the large sponge result in a significantly sheltered area where smaller sponges are clustering. There are other small clusters of medium sized sponges causing localised areas of low flow. However, an extensive coherent boundary layer is not observed.

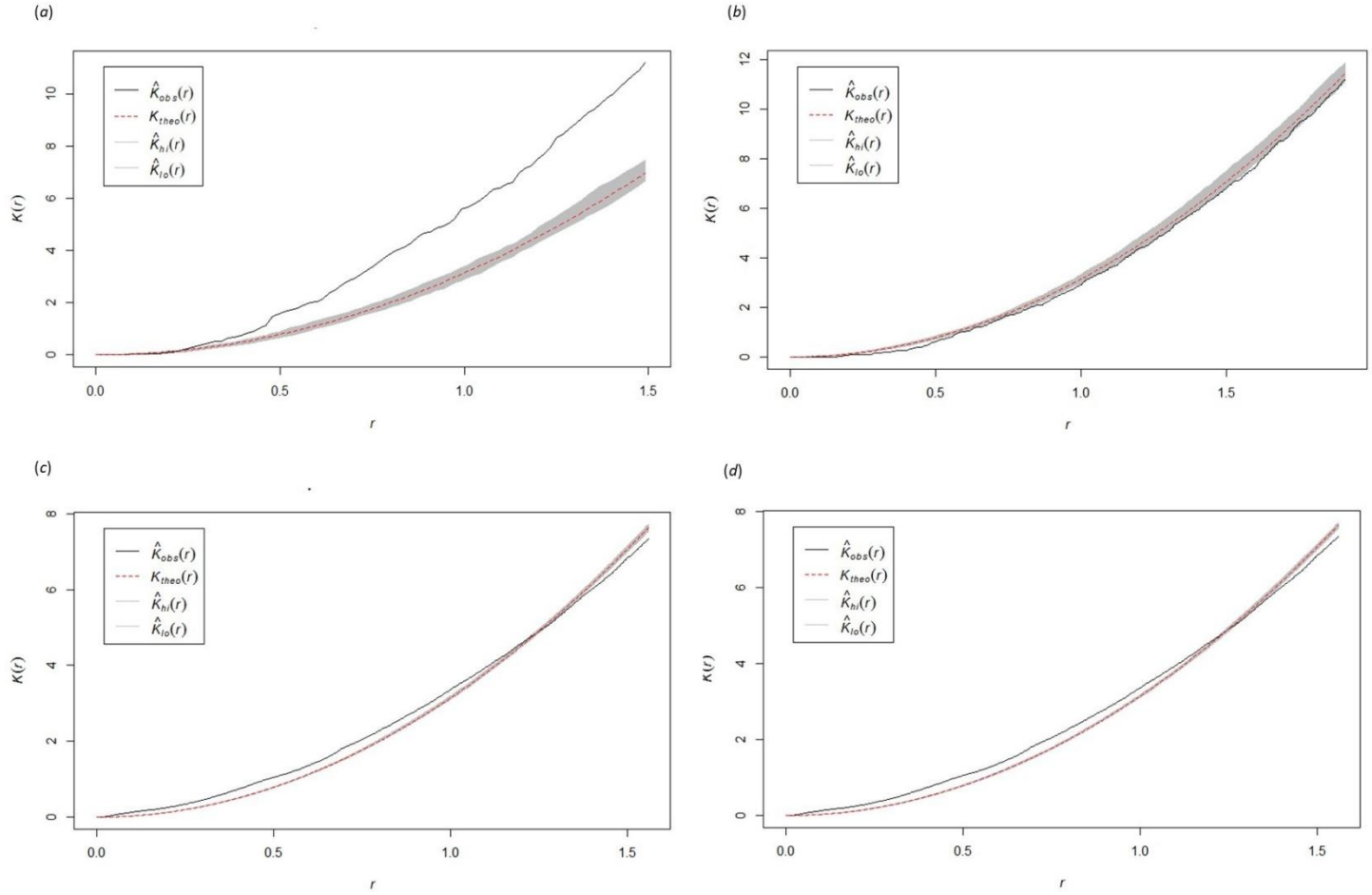

Figure 2-3 Plots of the Ripley K function clustering analysis (K) for the four study areas (a) HOK study area (b) Nuuk study area (c) GOK study area (d) SWGL study area. Observed value for K (Kobs(r)) theoretical random distribution value for K ($K_{theo}(r)$) <95% confidence limit of random distribution between upper confidence bound ($K_{Hi}(r)$) and lower confidence bound ($K_{lo}(r)$).

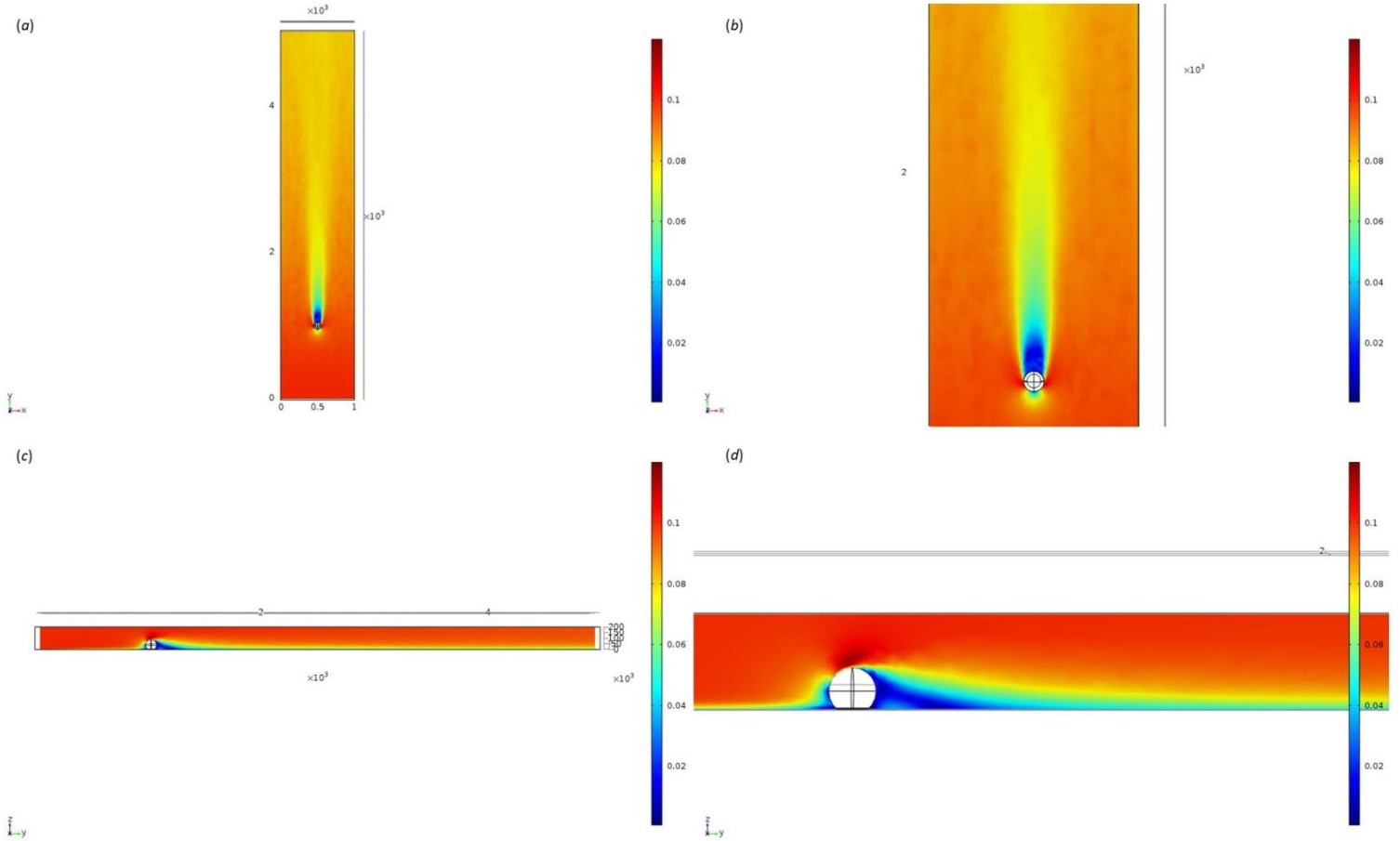

Figure 2-4. Results of the fluid flow finite element analysis simulation for an idealised sphere, visualised as two-dimensional plots (horizontal (a),(b) and vertical (c),(d) cross sections) of flow velocity magnitude (false-colour scales m/s). Scale in mm with a ambient flow of 0.1m/s along the y axis. (*b*) and (*d*) zoom in on the wake close to the sphere.

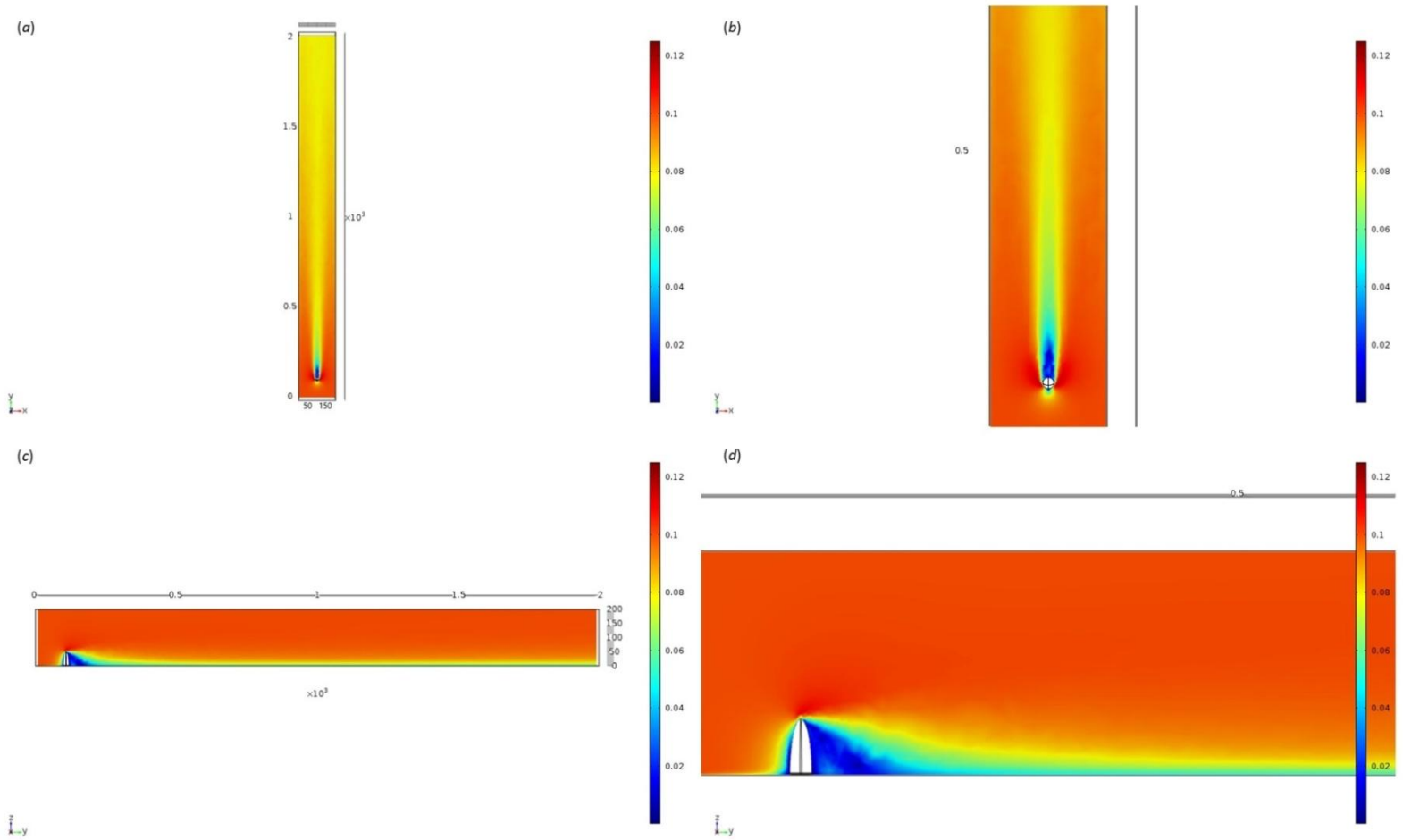

Figure 2-5. Results of the fluid flow finite element analysis simulation for an idealised ellipsoid, visualised as two-dimensional plots (horizontal (a),(b) and vertical (c),(d) cross sections) of flow velocity magnitude (false-colour scales m/s). Scale in mm with with ambient flow of 0.1m/s along the y axis. (*b*) and (*d*) zoom in on the wake close to the ellipsoid.

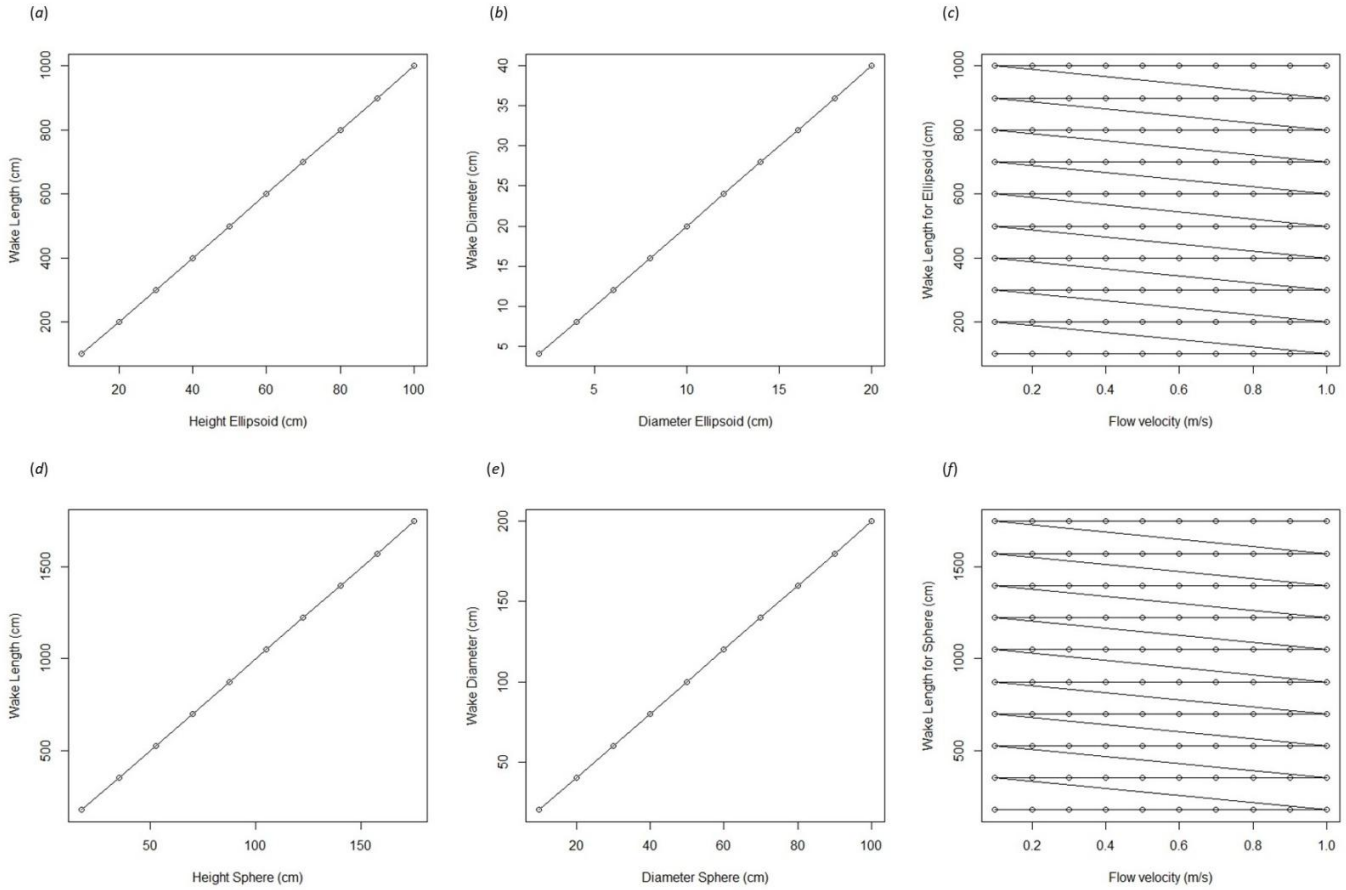

Figure 2-6. Plots of wake dimension, object dimension and flow speed taken from fluid flow finite element analysis simulation for an idealised sphere and ellipsoid. (a) Wake length (cm) plotted against ellipsoid hight (cm). (b) Wake diameter (cm) plotted against ellipsoid diameter (cm). (*c*) Wake length for all ellipsoid simulations (cm) plotted against corresponding flow velocity (m/s). (*d*) Wake length (cm) plotted against sphere hight (cm). (*e*) Wake diameter (cm) plotted against sphere diameter (cm). (*f*) Wake length for all sphere simulations (cm) plotted against corresponding flow velocity (m/s).

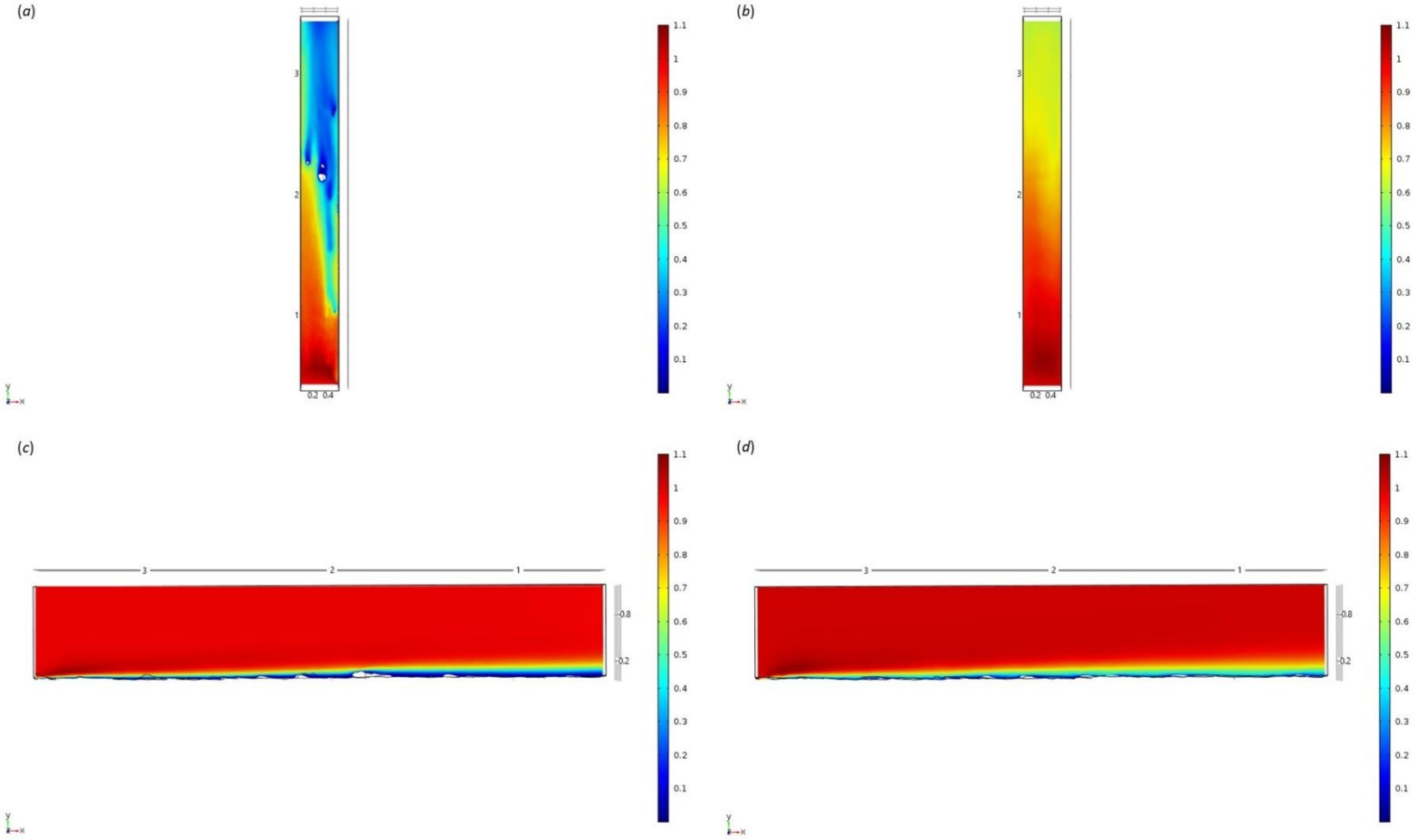

Figure 2-7. Results of the fluid flow finite element analysis simulation for surface models for Nuuk Study area visualised as two-dimensional plots (horizontal and vertical cross sections) of flow velocity magnitude (false-colour scales m/s). (a,c) Surface model w with sponges present (*b,d*) surface model with sponge structures removed. Scale in m with ambient flow of 1m/s along the y axis.

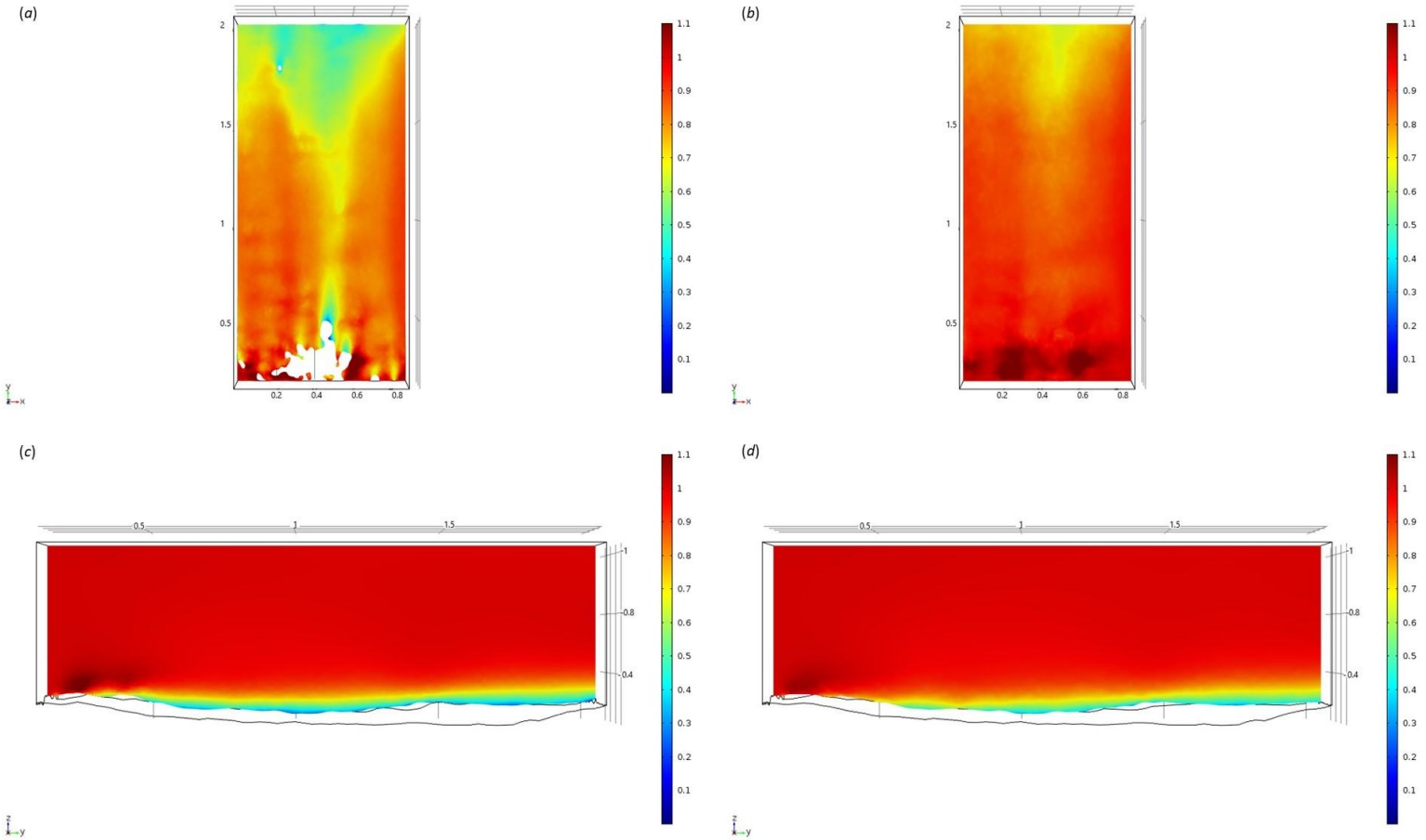

Figure 2-8. Results of the fluid flow finite element analysis simulation for surface models for SWGL Study area visualised as two-dimensional plots (horizontal and vertical cross sections) of flow velocity magnitude (false-colour scales m/s). (*a,c*) Surface model with sponges present (*b,d*) surface model with sponge structures removed. Scale in m with ambient flow of 1m/s along the y axis.

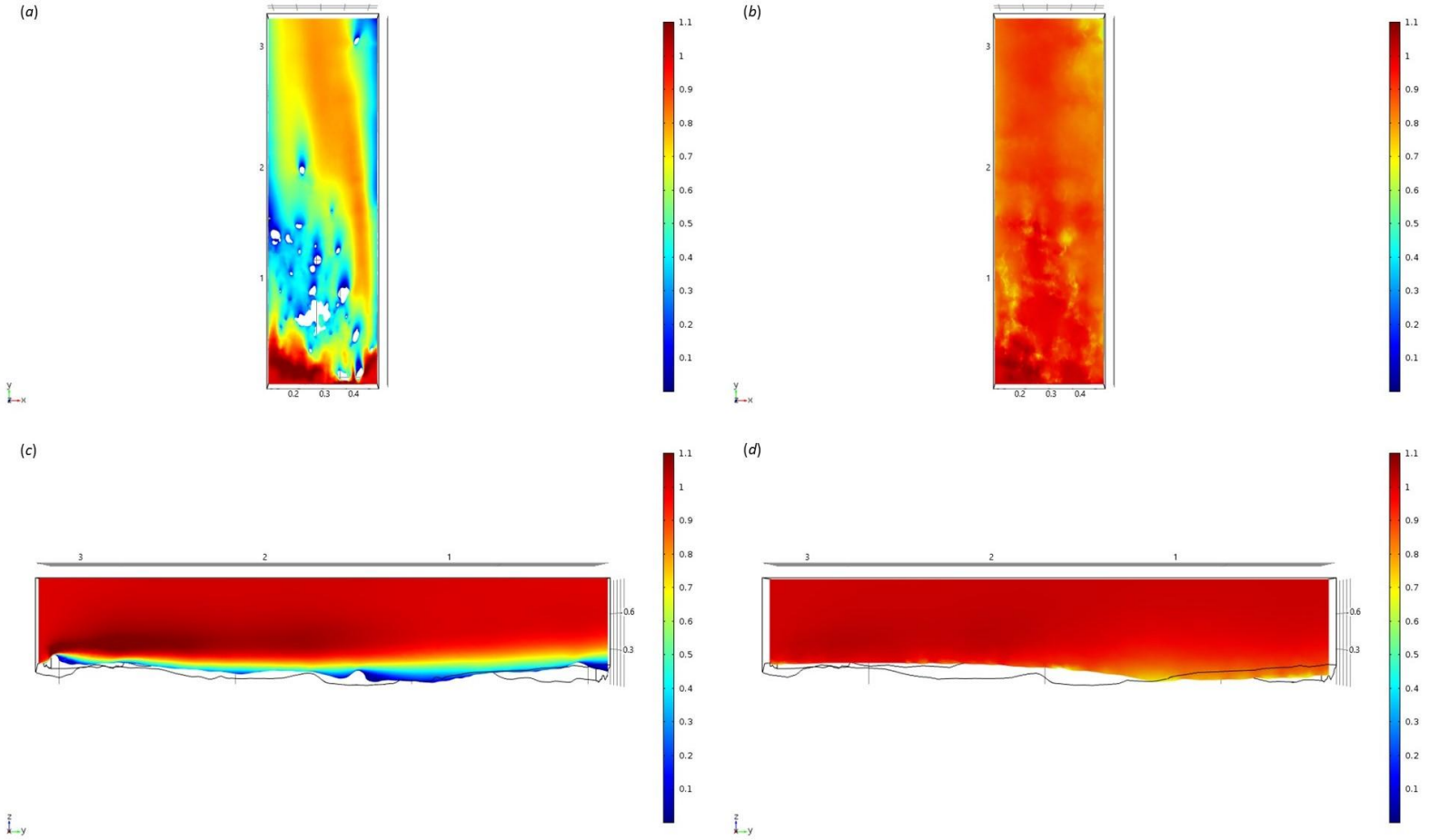

Figure 2-9. Results of the fluid flow finite element analysis simulation for surface models for HOK Study area visualised as two-dimensional plots (horizontal and vertical cross sections) of flow velocity magnitude (false-colour scales m/s). (*a,c*) Surface model with sponges present (*b,d*) surface model with sponge structures removed. Scale in m with ambient flow of 1m/s along the y axis.

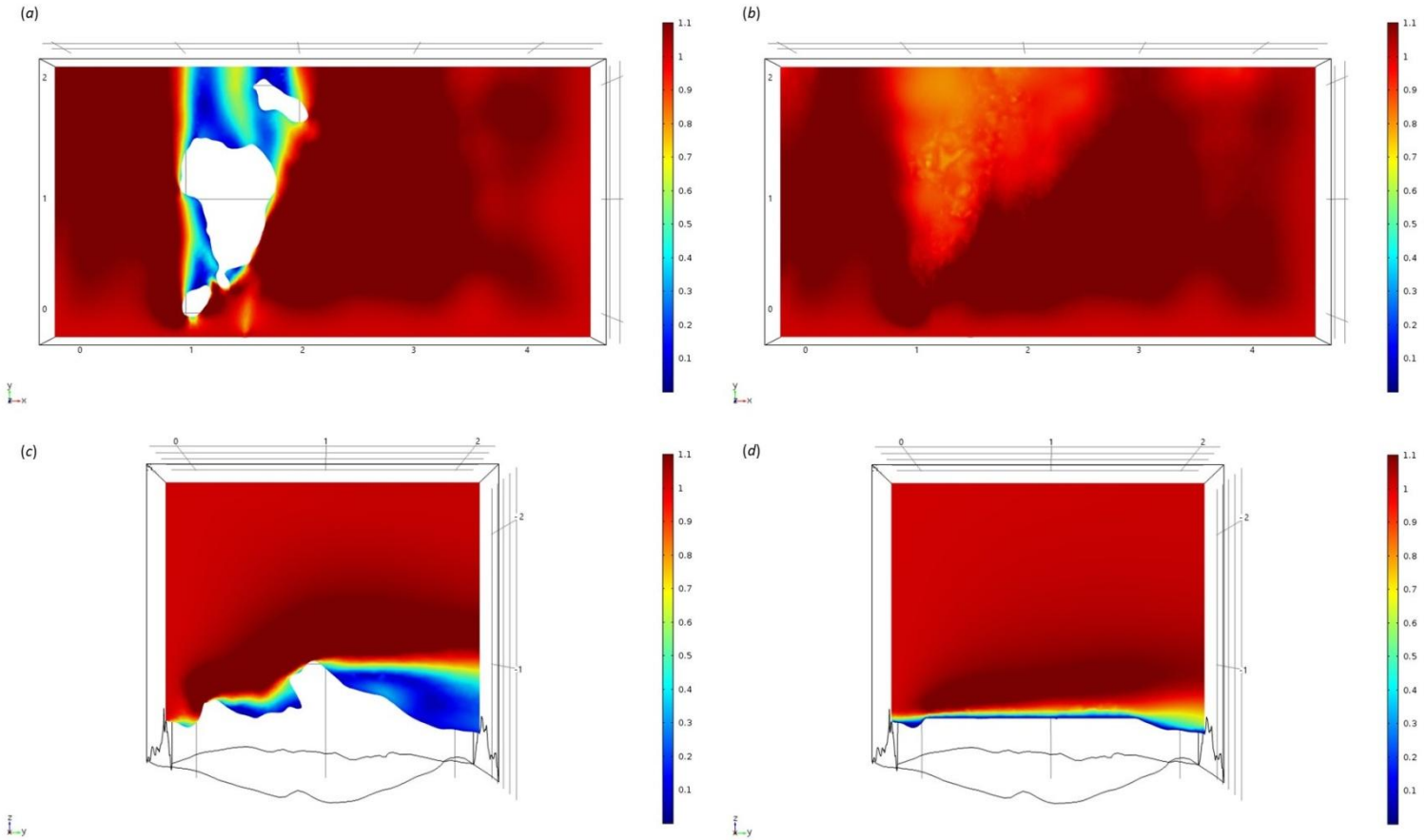

Figure 2-10. Results of the fluid flow finite element analysis simulation for surface models for GOK Study area visualised as two-dimensional plots (horizontal and vertical cross sections) of flow velocity magnitude (false-colour scales m/s). (*a,c*) Surface model with sponges present (*b,d*) surface model with sponge structures removed. Scale in m with ambient flow of 1m/s along the y axis.

2.5. Discussion

2.5.1. Do sponges cluster?

Patterns of distributions within sponge grounds have been noted before, but there has not been an analysis to date of the clustering patterns themselves (Kutti, Bannister and Fosså, 2013; McIntyre *et al.*, 2016). Clustering analysis gives a more robust approach to studying these patterns, by removing observational bias and allowing robust statistical tests to be performed to validate observations and hypotheses (Baddeley *et al.*, 2014). As the sponge grounds chosen as study sites are defined by distinct assemblages of sponges, it is interesting but not surprising that different functional groups follow distinct clustering patterns. The ability to scale up the distributions described here are limited due to the small study area. Their size is limited by the diameter of the areas surveyed by the ROV (Hendry, 2017; Hendry *et al.*, 2019). However, our flow-modelling method could be extended to a broader geographical area, and combined with localised environmental data and predictions, to make inferences about environmental driving factors for sponge distribution in sponge grounds on wider spatial and temporal scales. Uniquely, a modelling approach also allows us to simulate a great range of environmental conditions and therefore can be used as a predictive tool for both potential hypotheses and expected optimal conditions.

2.5.2. Why are sponges clustering?

The variability and the driving factors behind these distributions could be wide-ranging, from dispersion of gametes (Abelson and Denny, 1997) to food availability (Robertson, Hamel and Mercier, 2017). One factor that can be studied within limited geographical areas is localised flow around the sponges. Is this driving distribution patterns in deep-sea sponge grounds? This new application of modelling techniques to localised flow around sponge allows us to address such questions, previously not possible from observational approaches, especially in deep-sea environments.

We need to quantify the pattern of flow around a single structure to understand how fluid flow could be affecting the distribution of individuals within a sponge ground. The creation of both idealised single organism models and study area models give us a better understanding of this flow. The idealised models give us the predicted size and length of the wake given average heights of the sponges. In our study areas the length of the wake is greater than the spacing between individuals in

the sponge grounds, so the wake effect of other sponges is predicted to influence organism structures. The wake length-scales found in this study suggest that sponges that appear isolated may be influenced by the wake of other individuals to a greater extent than previously expected.

At first glace

Along with an increae in the number indevidules the flow has interacted with prior to arriving at any paricual sponge reducing of nutrients will be much lower if they have already been filtered out by a privious orgnisum. Therefor staying in a clear unfiltered flow would inishally apppear to be advantagous particually in the generally nutreint poor waters of the deep sea.

When the flow around the sponge structures within each study area is modelled and compared with the same seafloor surface without these structures, a significantly thickened boundary layer is observed as predicted by the idealised models (Figure. 2-4,2-5). This slowing effect is due to the overlapping of the wakes of each individual sponge to create a relatively uniform area of slowed flow. This has not been observed before and highlight the importance of studying the collective effect of multiple individuals and sets this study apart from others looking at the fluid flow interactions with sponges. Directly linking the slowed boundary layer as the driver behind patterns of distribution is difficult and would require many more and varied study sites. However, the observation of this slowed boundary layer and its potential effect as a factor in sponge distribution is important in its own right. Are the sponges distributing themselves to benefit from the slowed flow in this layer and, if so, what advantage does it provide?

2.5.3. Advantages of manipulating the boundary layer

The effects of flow on an individual sponge organism broadly fall into three categories: gamete dispersion (Abelson and Denny, 1997), nutrient supply (Kahn, Chu and Leys, 2018) and mechanical forcing (Palumbi, 1986). The presence of a slowed boundary layer whose thickness is governed by the velocity of the flow and roughness of the surface, has the effect of reducing any mechanical forcing. This lowering in the forces applied to a sponge will reduce the likelihood of damage or attachment failure due to high flow. Average flow velocities in deep sea sponge grounds are low in our study sites (~0.1 m/s) (Hendry, 2017; Hendry *et al.*, 2019) so this protective effect is likely negligible. However, records of much higher flow velocities during storm events > 1 m/s are recorded the depths of these study areas (Greenan *et al.*, 2010). The high mechanical forcing at these velocities would mean the slowed boundary layer would offer significant protection for both

sponges and other organisms associated with sponge grounds (Klitgaard, 1995; Freese and WIng, 2003; Miller *et al.*, 2012).

The consequences of high flow rates are difficult to quantify in this model. This is both in respect to the deformation and failure of the sponge structures and the knock on effect of this deformation on the flow fields. This difficulty is due to the problems encountered when trying to quantify the material properties of sponge structures. At low flow rates treating sponge structures as ridged, as in this model, closely reflects the small amount of flexure seen in the sponges are these study sites and lets us study their effect on the flow. However, at high flow rates sponges are known to bend and deform to a great extent therefore invalidating the result based on the ridged structure in our model. To add deformation to our model we would need to understand the plastic tensile properties of our structures or at least have an approximation of them. This may inevitably be a species by species approximation as the complexity and plasticity of sponge structural morphology differs wildly. Within a sponge some of the mechanical properties that would dictate their tensile properties would include, the density and arrangement of spicules, the amount of collagen present, thickness of cortex compared to body size, and the structure of the internal canal system. Trying to tease out the importance of these factors to the flexibility and strength of a sponge would be a worthwhile avenue to research in its own right. For the purpose of this modeling then conducting tensile testing on a number of sponges to create an approximation of the tensile properties would be a great leap forward in the realism and would much better model the deep-sea environment.

The most obvious impact of a reduced flow around the sponge on nutrient supply appears to be deleterious: reduced flow would result in a reduced supply of particulate and dissolved organic and inorganic (e.g. dissolved silicon) nutrients to the organism. Along with reduced flow rate being within this boundary layer equates to being within the wake of other organisms increasing the likelihood of the fluid being filtered by a previous organism reducing the potential nutrient availability further. Given this it would logically seem that in the deep sea where nutrients levels are low an organism being in a strong clear flow would be beneficial.

However, flow speed, sponge density and nutrient supply may be a more nuanced association due to particulate fallout rate and the active pumping effect of the sponges themselves. The slowing of the boundary layer may result in a greater proportion of the particulates carried by the flow above to be deposited around the sponges. The flow above the boundary layer is not slowed so the vertical supply of particulates to the sponges may increase even if the flow acting on the sponges themselves is reduced.

The reduction in flow speed at the sea floor due to the boundary layer could potentially lead to an increase in larvae deposition and recruitment (Abelson and Denny, 1997). The deposition and retention of larvae in the sponge ground should increase with lower flow speeds, and larvae attachment rates should also increase due to reduced flow stress (Mariani *et al.*, 2006; Guillas *et al.*, 2019). An increase in larvae deposition and retention impacts the recruitment of new individuals within the sponge grounds and should increase its ability to grow and recover from damage. On the other hand area already with high numbers of sponges will have a higher level of competition for resources and space compared with an uncolonized or low sponge density area of the sea floor.

Imposing a sediment flux into the model to look at the particulate dropout and distribution would be an interesting next step in the development of this research. It would enable us to get a better idea if clustering effect food availability and larvae recruitment and if so, by how much.

The importance of ambient flow rate compared to pumping rates for sponges is challenging to determine (Leys *et al.*, 2011; Ludeman, Reidenbach and Leys, 2017). Sponges appear to stop pumping at higher flows but whether this is to protect the canal system from being clogged and damaged (Ludeman, Reidenbach and Leys, 2017; Strehlow *et al.*, 2017), because it is unnecessary for flow though the sponge (Leys *et al.*, 2011), or due to another underlying mechanism, is currently unclear. Regardless, the presence of a slowed boundary layer is influential for each of these mechanisms. A slowed boundary layer may be advantageous as the sponge may be able to pump for longer before it must shut down for protection, or disadvantageous due to higher energy expenditure.

A noticeable feature of the idealized model is the boundary effect of the structures themselves (Figure. 2-4,2-5). A future avenue of exploration would be to investigate how this impacts the potential radius of intake around the sponge due to pumping as well as the effect of the outflow from the sponge on this boundary layer. At what point does the pumping rate become negligible compared to the dividing flow and increased turbulence around the structure, effectively isolating it from the surrounding flow? Does this result in a slower rate of flow becoming advantageous, as the pumping rate with lower turbulence would be more effective and could draw in particulates that would otherwise be lost to the current? Modeling would be particularly useful in investigating the behavior of particles and turbulent currents around sponges, both of which are challenging to measure or observe *in situ* because of interference from any recording device on the flow.

Regardless of the mechanism by which a slowed boundary layer is created, its presence has additional and important consequences for other organisms associated with sponge grounds (Freese

and WIng, 2003; Miller *et al.*, 2012). It also has a potential corollaries for conserving sponge grounds under threat of damage by anthropogenic activities. Removal of the sponge structures (e.g. by trawling) would result in the boundary layer velocities not being reduced as much, which – if this feature is beneficial – will have implications for any future recruitment of larvae and recovery of sponges, and so the sponge ground habitat itself.

2.6. Conclusions

This study shows that there are significant small-scale patterns in distribution of sponges within sponge grounds in the Labrador Sea. Further, we have developed a new approach to studying the drivers of these observed patterns using fluid flow modeling. The models produced allowed detailed quantitative experiments to be conducted, including modeling the effects created by the interactions of multiple individuals, producing data that would be impossible to obtain from field observations alone. By applying these models to sponge structures taken from four study areas in the North Atlantic, we identified a slowed boundary layer caused by sponge aggregations that may account for some of the distribution patterns. This slowed boundary layer may be acting as a protective layer, increasing larval recruitment or promoting increased particulate organic matter uptake due to increases in both particulate fallout from flow and effective radius of pumping. These observations increase the importance of protecting sponge grounds from anthropogenic damage as the removal of this slowed layer coupled with the relatively slow growth rates of sponges in the deep-sea and decreased larval recruitment could result in the inability of sponge ground to recover once damaged. This study highlights the importance of coupling mathematical modeling with field observations in the deep sea to provide a much greater understanding of anthropogenic and climate change impacts on sponge ground ecosystem structure and function, and biogeochemical cycling by sponges.

3. Sponge Biodiversity of the Labrador Sea

Culwick, T., Goodwin, C. E., & Hendry, K. R.

Author Contributions and declaration:

This chapter is presented as a manuscript for publication (not yet submitted) and has received contributions from other authors.

T.Culwick, C.E.Goodwin and K.R.Hendry conceived the study. T.Culwick carried out the study. T.Culwick analyzed of the data, wrote the paper and prepared figures. All authors reviewed the data and revised drafts of the paper.

3.1. Abstract

The diversity of sponges in the Labrador Sea is largely unknown, in particular in the region off the west coast of Greenland. Sponge samples were collected by Remotely Operated Vehicle (ROV) from 11 sampling stations from three localities. The use of the ROV sampling techniques enabled collection of delicate and encrusting sponges and the effective sampling of steep bedrock habitats. Twelve new species are described: *Halicnemia flavospina* sp.nov., *Paratimea marionae* sp.nov., A*sbestopluma (Asbestopluma) frutex* sp.nov., *Lissodendoryx (Acanthodoryx) magnasigma* sp.nov., *Fibulia textilitesta* sp.nov., *Hymedesmia (Hymedesmia) caerulea* sp.nov., *Hymedesmia (Hymedesmia*) *alba* sp.nov., *Sceptrella matia* sp.nov., *Clathria (Axosuberites) radix* sp.nov., *Stelodoryx groenlandica* sp.nov., *Stelodoryx rictus* sp.nov., and *Plakina jactus* sp.nov. New information on distribution, *in situ* images and spicule measurements are provided for *Hymedesmia (Hymedesmia) crux* (Schmidt, 1875) and *Phakellia robusta* Bowerbank, 1866. In total 68 sponge species were recorded by this survey, 13 of which had not previously recorded in the Labrador Sea. This significantly increases the number of sponge species described from the Eastern Labrador Sea. The species assemblages resemble that of the Faroese sponge grounds. We suggest the low sponge species diversity of the Western Atlantic is due to sampling bias. These results significantly increase our understanding of the sponge biodiversity of the west Greenland shelf and knowledge of how this differs from that seen around Orphan Knoll.

Keywords: Sponges (Porifera), Biodiversity, Sponge grounds, Labrador Sea, Greenland, Taxonomy

3.2. Introduction

Introduction

The Labrador Sea's biodiversity is critically understudied compared with other areas of a similar latitude (Darnis *et al.*, 2012). Even a complete picture of fish species in the region has only recently been known (Mecklenburg, Møller and Steinke, 2011; Coad and Reist, 2019). This lack of data is potentially unsurprising given the common trend seen in ecological studies that the more remote and deep an area is the less it is studied (Archambault *et al.*, 2010). Sessile benthic organisms are consistently overlooked in biodiversity studies (Archambault *et al.*, 2010; Kenchington, Link, *et al.*, 2011; Piepenburg *et al.*, 2011; Darnis *et al.*, 2012; Roy, Iken and Archambault, 2015). Sponges in the Labrador Sea are particularly understudied, with an order of magnitude fewer species recorded than expected when looking at diversity at similar latitudes globally (Sarà *et al.*, 1992; Ackers *et al.*, 2007; Picton and Goodwin, 2007a; Downey *et al.*, 2012; van Soest *et al.*, 2012; Lehnert and Stone, 2016). This knowledge gap is critical given the important ecological role played by sponges in forming biogenic habitats and acting as protective nurseries for fish and invertebrate species (Klitgaard, 1995; Chu and Leys, 2010; Hogg, Tendal and Conway, 2010; Kenchington, Power and Koen-Alonso, 2013; Lehnert and Stone, 2016; Maldonado *et al.*, 2017). Deep-sea sponge aggregations are recognized as threatened habitat OSPAR (OSPAR commission, 2008, 2010) and included on their list of threatened and/or declining species and habitats. As well as the Food and Agriculture Organization of the United Nations (FAO) recognizing them and Vulnerable Marine Ecosystems (Hogg, Tendal and Conway, 2010; Kenchington *et al.*, 2015) (FAO, 2009; ICES, 2009).The increase in industrial and commercial exploitation of the deep waters of the Labrador seen is of particular concern, given that there is good evidence that an increase in these activities leads to a loss in biodiversity (Eriksson *et al.*, 2010; Hewitt and Thrush, 2010; Love *et al.*, 2013) and damage caused to sponge grounds could be permanent (Lindholm, Auster and Valentine, 2004; Howell, 2010; Kenchington, Murillo-Perez, *et al.*, 2011; Bell, McGrath, *et al.*, 2015; Grant *et al.*, 2018, 2019; Culwick *et al.*, 2020).

The majority of recent work on sponges in this area has focused on the distribution of indicator taxa for Vulnerable Marine Ecosystem (VME) designation (Hogg, Tendal and Conway, 2010; Kenchington *et al.*, 2015) (ICES, 2009). Most of this has focused on groups that are identifiable from Remotely Operated Vehicle (ROV) and towed camera footage (Beazley *et al.*, 2015; McIntyre *et al.*, 2016) : predominantly the Tetractinellida Marshall, 1876 (e.g. *Geodia* Lamarck, 1815 *, Stelletta* Schmidt,

1862, and *Craniella* Schmidt, 1870) (Beazley *et al.*, 2013; McIntyre *et al.*, 2016) and Hexactinellida Schmidt, 1870 (e.g. *Pheronema* Leidy, 1868 and *Vazella* Gray, 1870 (Kenchington *et al.*, 2010; McIntyre *et al.*, 2016). These data, backed up with specimens data from trawl studies (Kenchington, Murillo-Perez, *et al.*, 2011; Murillo *et al.*, 2012, 2018; Knudby, Kenchington and Murillo, 2013), have been used to model the distribution of sponges grounds using environmental parameters (Knudby, Kenchington and Murillo, 2013; Murillo *et al.*, 2016).

Sponges are notoriously difficult to identify from images (Hooper and van Soest, 2002; Leys *et al.*, 2004) and specimen collection is nearly always required to determine species accurately. Spicule and skeleton morphology is still the primary means of classification (Hooper and van Soest, 2002), in more recent studies this is often supported by molecular work (Xavier *et al.*, 2010; Cárdenas *et al.*, 2011). While surveys based on image analysis are undeniably useful in determining locations of sponge grounds, they are unable to document the true biodiversity of these areas. This has resulted in an underrepresentation of species abundance in the Labrador Sea. Similar *Geodia* Lamarck, 1815 dominated sponge grounds of the North East Atlantic, which have been studied from collected specimens, have up to 50 other sponge species associated with them (Klitgaard and Tendal, 2004).

Given the ecological importance of sponge grounds for habitat formation (Bett and Rice, 1992; Klitgaard, 1995; Klitgaard and Tendal, 2004; Buhl-Mortensen *et al.*, 2010) as well as their role in benthic-pelagic coupling (Dayton *et al.*, 1974; Kahn *et al.*, 2015), understanding the true extent of species diversity in an area is vitally important in assessing the levels of marine management needed.

Limited previous studies have used collections to investigate sponge biodiversity in this area. (Fristedt, 1887) reported 14 sponge species and described 7 new species from Baffin Bay, the Davis Strait and west Greenland shelf. (Lambe, 1900) reported 21 species from the Canadian east coast, and a further 15 from the Davis Strait describing 11 new species. (Lundbeck, 1902) described 15 sponge species from the west Greenland shelf. The final large taxonomic study that includes the west Greenland shelf was done by (Brøndsted, 1933b) who reported 36 species and described three new species. This study also collated earlier work, listing 112 sponge species in total for the west Greenland shelf (Brøndsted, 1933b). More work has been carried out on the eastern Canadian coastal shelf with new species being described in taxonomic review papers of the families Tetillidae Sollas, 1886 (Cárdenas, Rapp, Best, *et al.*, 2013), Cladorhizidae Dendy, 1922 (Hestetun, Tompkins-Macdonald and Rapp, 2017b) and Polymastiidae Gray, 1867 (Plotkin, Gerasimova and Rapp, 2018) and genus *Geodia* Lamarck, 1815 (Cárdenas, Rapp, Klitgaard, *et al.*, 2013). A technical report on sponge biodiversity from trawl surveys from Baffin Bay, Davis Strait and Hudson Strait collected

between 2010-2014 recorded over 100 sponge taxa (Tompkins *et al.*, 2017). Murillo *et al* (2018), recorded 93 different species collected from Hudson Strait, Ungava Bay, Western Davis Strait and Western Baffin Bay broken down into five assemblages, including adding two new species. Recently work done on the Orphan Knoll seamount described a new species of *Tedania* (Ríos *et al.*, 2021).

In this study we aimed to gain additional information on the sponge biodiversity of the Labrador Sea by sampling three areas: Orphan Knoll, Nuuk and Southwest Greenland (Figure 3-1; Table I). These represent three differing ocean environments driven by the influence of differing water mass interactions (Talley and McCartney, 1982; Lavender, Davis and Owens, 2000; Yeager and Jochum, 2009).

3.3. Material and methods

3.3.1. Study Site

Samples were collected on RRS Discovery cruise DY0781 as part of the Isotope cycling in the Labrador Sea (ICY-LAB) project, the aims of the of project are "to understand nutrient and isotope cycling in the climatically critical but understudied regions of the Labrador Sea and Greenland fjords, and the impact of the cryosphere, biosphere, and hydrosphere on the biogeochemistry of the region and the global oceans." (Hendry, 2017). Sponge sampling was undertaken to investigate the biogeography of siliceous organisms in the Labrador Sea.

Samples were collected from 11 stations at three study sites within the Labrador Sea located at Orphan Knoll Seamount, off the coast of Nuuk, and off Southwest Greenland. Each study site contained several sample collection stations (Figure 3-1; Table I). Study sites were chosen to sample three different oceanographic environments resulting from differing dominant water masses that on either side of the Labrador Sea (Hendry, 2017). The Southwest Greenland shelf is influenced by two main water masses, the Subpolar Mode Water and the South Greenland Coastal Waters. These water masses are modified as they move North along the Greenland shelf due to mixing and the influx of melt water runoff from the Greenland Ice sheet. These modifications continue until they encounter the Baffin Bay Polar Water. (Talley and McCartney, 1982; Lavender, Davis and Owens, 2000; Yeager and Jochum, 2009; Rysgaard *et al.*, 2020). The Southwest Greenland study site sits close to where these water masses first interact. In contrast, the Nuuk study site which is close to a melt water fed fiord with potentially more modified water masses. The Eastern Canadian coast is

dominated by the Labrador Sea Water, with the coast south of Newfoundland being dominated by the North Atlantic Deep Water. Orphan Knoll sits in the Fluctuation zone between these two water masses (Talley and McCartney, 1982; Lavender, Davis and Owens, 2000; Yeager and Jochum, 2009; Rysgaard *et al.*, 2020). The sample collection depth range of the study sites varies with the Nuuk and Southwest Greenland sites sampling only on the shelf (589-1281 m), whereas samples were collected from deeper water (1527- 3550 m) at Orphan Knoll), where stations were positioned down the flank of seamounts (Figure 3-1; Table I).

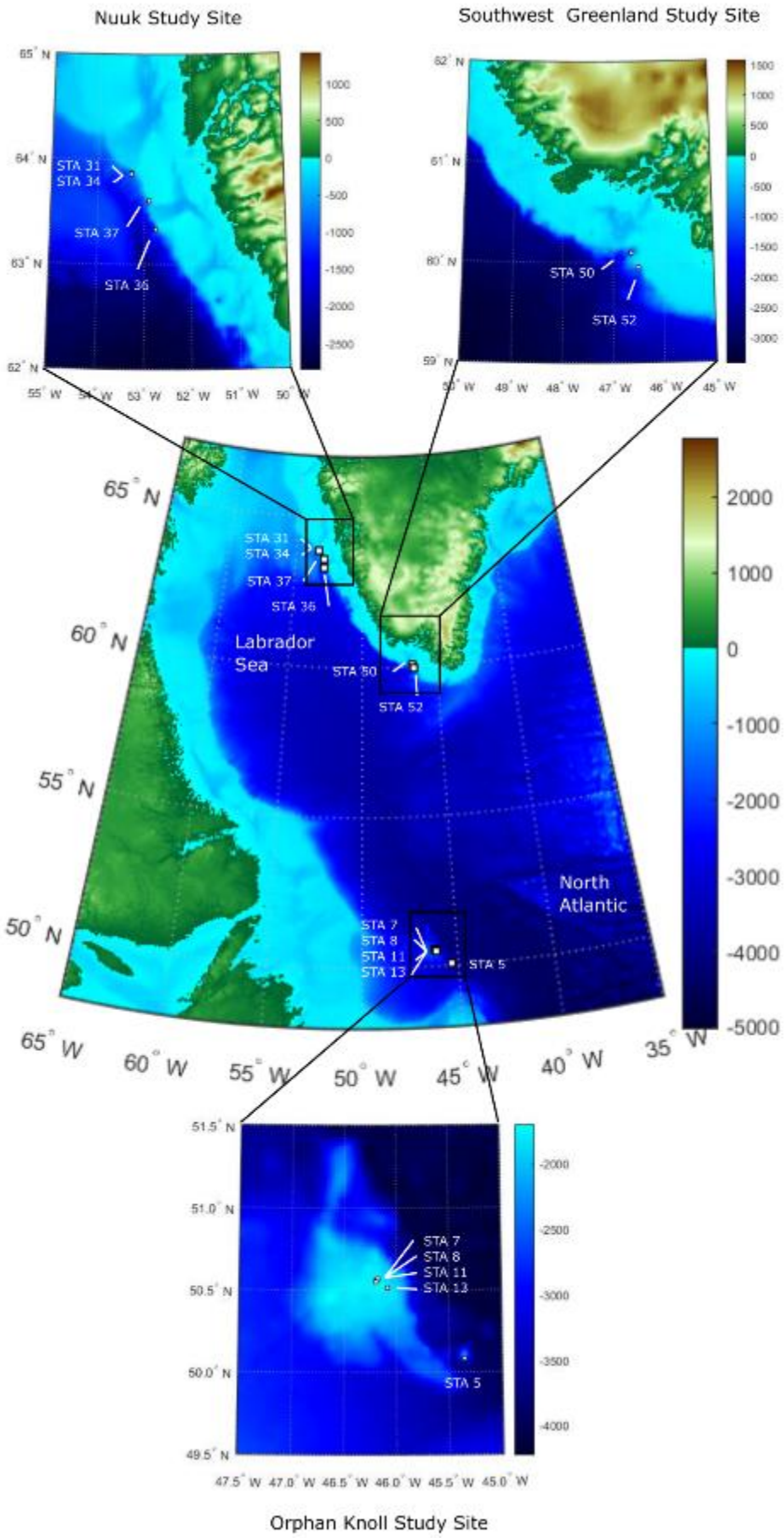
Nuuk Study Site
Southwest Greenland Study Site
STA 31
STA 34
STA 37
STA 36
STA 50
STA 52
Labrador Sea
North Atlantic
STA 7
STA 8
STA 11
STA 13
STA 5
Orphan Knoll Study Site

Figure 3-1. Overview map showing the position of the three study sites and sample collection stations (STA): STA 5, STA 7, STA 8, STA 11, STA 13, STA 31, STA 34, STA 36, STA 37, STA 50, and STA52 from the DY081 Cruise in the Labrador Sea. Bathymetry used is from ETOPO1 model from https://www.ngdc.noaa.gov/mgg/global/

Table I. Sample collection station list. ROV = Remotely Operated vehicle.

Site	Station	Gear	Start Time (GMT)	Start Lat (DD)	Start lon (DD)	Start Depth (m)	End Depth (m)
Orphan Knoll	5	ROV327	16:19:00	50.04158	-45.3794	3550.8	1941
Orphan Knoll	7	ROV328	07:50:00	50.55481	-46.19323	1669.2	1576.7
Orphan Knoll	8	ROV329	20:48:00	50.55182	-46.19227	1792	1527
Orphan Knoll	11	ROV330	23:23:00	50.55118	-46.19071	1825.5	1717
Orphan Knoll	13	ROV331	16:15:00	50.50629	-46.0825	1848	1586
Nuuk	31	ROV333	03:49:00	63.86612	-53.28869	970	805
Nuuk	34	ROV334	07:00:00	63.86511	-53.28258	807	683
Nuuk	36	ROV335	03:38:00	63.33217	-52.7771	1281	898
Nuuk	37	ROV336	10:51:00	63.60375	-52.91897	515	345.9
SW. Greenland	50	ROV338	18:46:00	60.09	-46.62533	603.5	1064
SW. Greenland	52	ROV339	07:04:00	59.94672	-46.5481	1148	589

3.3.2. Sampling methodology

Samples were collected using the UK National Marine Facilities Remotely Operated Vehicle (ROV), *Isis*. Either the manipulator arms or a suction system were used for sponge collection. Sponges to be sampled were selected by scientists viewing live ROV footage, with the aim being to sample as many different species as possible on each ROV dive. Time, depth, location, and a physical description (colour, size, etc) and *in situ* images were recorded for each sample at collection. Upon recovery of the ROV, the sponge samples were transferred to buckets and taken into the onboard temperature-controlled wet lab for processing. Here each sponge sample was photographed and labeled. All specimens were subsampled for genetic analysis (preserved in 95% ethanol) and either frozen at -20^{o}C or preserved in 95% ethanol.

3.3.3. Laboratory methodology

Sponges were identified from spicule preparations and tissue sections. Specimens were identified to the lowest possible taxonomic level. For spicule preparations, to isolate the spicules, sponge tissue was digested in bleach (15% Sodium Hypochlorite). Spicules were then washed twice with water and once in 95% ethanol, allowing the spicules to settle out of the washing solution for ~45 min between each change. A few drops of the final ethanol solution were placed on a slide, and then this was placed on a heat plate, evaporating the alcohol, and leaving the spicules behind. The spicules were mounted in Canada balsam and covered with a glass coverslip. A thick tissue section (0.2 mm) was cut by hand using a scalpel and mounted using Canada balsam. Spicule measurements were made using an Olympus BX43 microscope, with thirty spicules measured per spicule type. Optical microscopy digital photographs were taken to aid identification, using the combination of the Olympus BX43 microscope with a SC50 camera. Where higher resolution observations of spicules were required, the isolated spicules were mounted on aluminium stubs and gold-coated to a thickness of 10 nm. These were then examined and imaged through a Hitachi S3500 scanning electron microscope (SEM). The World Porifera Database, was used as the taxonomic authority and for reference to known species distributions (van Soest *et al.*, 2021).

3.4. Results

3.4.1. Specimen collections

In total, 213 sponge specimens were collected and identified of which 174 are of class Demospongiae Sollas, 1885, 38 were Hexactinellida Schmidt, 1870, and one Homoscleromorpha Bergquist, 1978. Through taxonomic identification, 141 Demospongiae were identified to species, 22 were identified to genus, and fifteen identified to higher taxonomic levels. The single Homoscleromorpha was identified as a new species. These specimens represent 68 sponge taxa with 12 previously not described from the Labrador Sea and 13 new to science (Table II).

Table II. Species recorded from cruise DY081 associated with location and sample collection station.

Location	Nuuk				Nuuk Total	Orphan Knoll			Orphan Knoll Total	SWGL			SWGL Total	Grand Total
Station	31	34	36	37		5	8	13		49	50	52		
Ancorina Schmidt, 1862			**1**		**1**									**1**
sp.6			1		1									1
Aplysilla Schulze, 1878	**1**				**1**									**1**
sp.7	1				1									1
Asbestopluma (Asbestopluma) Topsent, 1901	**6**	**1**	**1**		**8**									**8**
frutex sp. nov.			1		1									1
pennatula (Schmidt, 1875)	5	1			6									6
ruetzleri Hestetun, 2017	1				1									1
Axinella Schmidt, 1862	**2**				**2**							**2**	**2**	**4**
artica (Vosmaer,1885)	2				2							2	2	4
Biemna Gray, 1867			**1**		**1**						**1**	**1**	**2**	**3**
dautzenberghi Topsent, 1890			1		1									1
variantia (Bowerbank, 1858)											1	1	2	2
Cladorhiza Sars, 1872	**2**				**2**	**1**			**1**		**1**		**1**	**4**
abyssicola Sars,1872	2				2									2
corticocancellata Carter, 1876											1		1	1
gelida Lundbeck, 1905						1			1					1
Clathria (Axosuberites) Topsent, 1893b	**1**				**1**						**2**		**2**	**3**
radix sp. nov.	1				1						2		2	3
Clathria (Clathria) Schmidt, 1862	**1**				**1**									**1**
barleei (Bowerbank, 1866)	1				1									1
Coelosphaera (Coelosphaera) Thomson, 1873						**2**			**2**					**2**
tubifex Thomson, 1873						2			2					2
Coelosphaera (Histiodermion) Topsent, 1927			**1**		**1**									**1**
dividuum (Topsent, 1927)			1		1									1

Location	Nuuk				Nuuk Total	Orphan Knoll			Orphan Knoll Total	SWGL			SWGL Total	Grand Total
Station	31	34	36	37		5	8	13		49	50	52		
Craniella Schmidt, 1870	**3**				**3**									**3**
cranium (Müller, 1776)	1				1									1
zetlandica (Carter, 1872)	2				2									2
Dendoricella Lundbeck, 1905			**1**		**1**						**1**		**1**	**2**
flabelliformis (Hansen, 1885)			1		1						1		1	2
Esperiopsis Carter, 1882				**1**	**1**									**1**
villosa (Carter, 1874)				1	1									1
Fibulia Carter, 1886						**1**			**1**					**1**
textilitesta sp. nov.						1			1					1
Geodia Lamarck, 1815	**1**		**1**		**2**	**19**			**19**		**1**		**1**	**22**
barretti Bowerbank, 1858	1		1		2	11			11		1		1	14
macandrewi Bowerbank, 1858						3			3					3
parva Hansen, 1885						2			2					2
phlegraei (Sollas, 1880)						3			3					3
Halichondia (Halichondia) Fleming, 1828				**1**	**1**			**1**	**1**					**2**
sp.10				1	1			1	1					2
Haliclona (Gellius) Gray, 1867	**1**		**1**		**2**									**2**
sp.1	1		1		2									2
Haliclona (Haliclona) Grant, 1836			**1**	**2**	**3**							**2**	**2**	**5**
urceolus (Rathke & Vahl, 1806)			1	2	3							2	2	5
Halicnemia Bowerbank, 1864										**2**	**1**	**1**	**4**	**4**
flavospina sp. nov.											1	1	2	2
wagini Morozov, 2018										2			2	2
Hamacantha (Vomerula) Schmidt, 1880			**1**		**1**						**1**		**1**	**2**
papillata Vosmaer, 1885			1		1						1		1	2
Hemigellius Burton, 1932				**1**	**1**									**1**
arcofer (Vosmaer, 1885)				1	1									1

Location	Nuuk				Nuuk Total	Orphan Knoll			Orphan Knoll Total	SWGL			SWGL Total	Grand Total
Station	31	34	36	37		5	8	13		49	50	52		
Hymedesmia Bowerbank, 1864										**1**			**1**	**1**
sp.3										1			1	1
Hymedesmia (Hymedesmia) Bowerbank, 1864	**1**		**3**		**4**						**1**		**1**	**5**
crux (Schmidt, 1875)			1		1									1
caerulea sp. nov.	1		1		2						1		1	3
alba sp. nov.			1		1									1
Iophon Gray, 1867	**1**			**4**	**5**						**1**	**1**	**2**	**7**
sp.2	1			4	5						1	1	2	7
Lissodendoryx (Ectyodoryx) Lundbeck, 1909				**1**	**1**						**1**		**1**	**2**
diversichela Lundbeck, 1905				1	1									1
loyningi (Burton, 1934)											1		1	1
Lissodendoryx (Acanthodoryx) Lévi, 1961											**1**	**1**	**2**	**2**
magnasigma sp. nov.											1	1	2	2
Melonanchora Carter, 1874	**1**				**1**							**1**	**1**	**2**
elliptica Carter, 1874	1				1							1	1	2
Mycale (Mycale) Gray, 1867				**2**	**2**						**1**		**1**	**3**
lingua (Bowerbank, 1866)				2	2						1		1	3
Myxilla (Myxilla) Schmidt, 1862						**1**			**1**		**2**		**2**	**3**
sp.4						1			1		2		2	3
Paratimea Hallmann, 1916								**2**	**2**			**1**	**1**	**3**
marionae sp. nov.								2	2			1	1	3
Petrosia (Petrosia) Vosmaer, 1885	**1**		**1**		**2**						**4**	**4**	**8**	**10**
crassa (Carter, 1876)	1		1		2						4	4	8	10
Phakellia Bowerbank, 1862	**1**				**1**						**8**	**1**	**9**	**10**
cf. *robusta* Bowerbank, 1866	1				1						8	1	9	10
Phorbas Duchassaing de Fonbressin and Michelotti, 1864										**1**			**1**	**1**
sp.5										1			1	1

Location	Nuuk				Nuuk Total	Orphan Knoll			Orphan Knoll Total	SWGL			SWGL Total	Grand Total
Station	31	34	36	37		5	8	13		49	50	52		
Plakina Schulze, 1880											**1**		**1**	**1**
jactus sp. nov.											1		1	1
Plicatellopsis Burton, 1932											**1**		**1**	**1**
sp.8											1		1	1
Polymastia Bowerbank, 1862				**4**	**4**						**2**	**3**	**5**	**9**
andrica de Laudenfels, 1949				2	2									2
thielei Koltun, 1964											1	2	3	3
uberrima (Schmidt, 1870)				2	2						1	1	2	4
Rhizaxinella Keller, 1880										**1**		**1**	**2**	**2**
sp.9										1		1	2	2
Septrella Schmidt, 1870											**2**		**2**	**2**
matia sp. nov.											2		2	2
Spinularia Gray, 1867							**1**		**1**					**1**
njordi (Plotkin, 2018)							1		1					1
Stelodoryx Topsent, 1904						**4**			**4**		**1**		**1**	**5**
rictus sp. nov.						4			4					4
groenlandica sp. nov.											1		1	1
Stryphnus Sollas, 1886			**1**		**1**	**1**			**1**		**1**		**1**	**3**
fortis (Vosmaer, 1885)			1		1	1			1		1		1	3
Stylocordyla				**1**	**1**						**2**	**1**	**3**	**4**
borealis (Loven, 1868)				1	1						2	1	3	4
Tedania (Tedaniopsis) Dendy, 1924						**1**			**1**					**1**
rappi Ríos, 2021						1			1					1
Thenea Gray, 1867	**4**				**4**									**4**
valdiviae Lendenfeld, 1907	4				4									4
Topsentia Berg, 1899							**1**		**1**					**1**
sp.11							1		1					1

Location	Nuuk				Nuuk Total	Orphan Knoll			Orphan Knoll Total	SWGL			SWGL Total	Grand Total
Station	31	34	36	37		5	8	13		49	50	52		
Weberella Vosmaer, 1885				**1**	**1**									**1**
bursa Vosmaer, 1885				1	1									1
			1		**1**		**1**		**1**		**2**	**1**	**3**	**5**
Porifera			1		1		1		1		2	1	3	5
Grand Total	**27**	**1**	**15**	**18**	**61**	**30**	**3**	**3**	**36**	**5**	**39**	**21**	**65**	**162**

3.4.2. Taxonomy

Class Demospongiae Sollas, 1885

Order Bubarida Morrow & Cárdenas, 2015

Family Bubaridae Topsent, 1894

Genus *Phakellia* Bowerbank, 1862

Phakellia* cf. *robusta Bowerbank, 1866

(Figure 3-2; Table II, III)

Material: Sample in 95% ethanol, tissue section and spicule preparation on slides. DY081 315. Station 50, Southwest Greenland (60°5.4820'N, 46°38.2250'W); depth 932 m; collected 28th July 2017. DY081 326. Station 50, Southwest Greenland (60°5.4970'N, 46°38.2530'W); depth 932 m; collected 28th July 2017. DY081 327. Station 50, Southwest Greenland (60°5.3550'N, 46°38.2590'W); depth 938 m; collected 28th July 2017. DY081 1133. Station 50, Southwest Greenland (60°5.4100'N, 46°38.2310'W); depth 932 m; collected 28th July 2017. DY081 1376. Station 50, Southwest Greenland (60°5.5590'N, 46°38.2740'W); depth 948 m; collected 28th July 2017. DY081 1378. Station 50, Southwest Greenland (60°5.2100'N, 46°38.2420'W); depth 751 m; collected 28th July 2017. DY081 1407. Station 50, Southwest Greenland (60°5.3740'N, 46°-'W); depth 972 m; collected 28th July 2017. DY081 1409. Station 50, Southwest Greenland (60°5.4100'N, 46°38.2310'W); depth 932 m; collected 28th July 2017. DY081 1412. Station 52, Southwest Greenland (59°55.7320'N, 46°39.9930'W); depth 1008 m; collected 29th July 2017. DY081 872. Station 31, Nuuk (63°52.0020'N, 53°17.1960'W); depth 951 m; collected 20th July 2017.

Comparative material: *Phakellia robusta* Bowerbank,1866, Prob-Nw-ST6-66, Norway, Korsfjorden 59º 52.3700'N, 5º 32.9939'E, 29–213m *Phakellia ventilabrum* (Linnaeus, 1767, *),* BMNH1910.1.1.2687 Southern Norway, Pven-CS-DR2.2 Pven-CS-DR1-02, Cantabrian Sea 43º 43.703'N, 5º 50.480'W, 240m, *Phakellia hirondellei* Topsent, 1892, Phiron-CS-DR10-458 Cantabrian Sea, 44º06.080'N, 4º38.300'W, 541m

Description: Fan-shaped to cup-shaped, elevated on a short pedicle. Surface slightly hispid, oscula simple, dispersed. Sponges range from 10-(16)-25 cm wide by 5-(11)-16 cm high with a thickness of 0.4-(0.56)-0.8 cm, pedicle approximately 0.8-(1)-1.5 cm in diameter. The morphology changes between specimens from narrow funnel-shaped though to horizontal plates and flat upright fans;

the smaller specimens are funnel-shaped, with larger specimens generally being flatter (Figure 3-2). Colour in life off white, light brown in alcohol.

Skeleton: Choanosome: plumoreticulate with both primary and secondary tracts. The primary tracts are formed by styles and sinuous oxea. Tracts echinated by styles and oxea and connected by secondary tract of styles and very sinuous oxea.

Spicules: Table III.

Table III. Spicule dimensions of *Phakellia* cf. *robusta* compared to *Phakellia robusta* Bowerbank,1866, *Phakellia ventilabrum* (Linnaeus, 1767*)* and *Phakellia hirondellei* Topsent, 1892

	Styles µm	**Strongyles µm (rare)**	**Sinuous Oxea i µm**	**Sinuous Oxea ii µm**
***Phakellia robusta* Bowerbank,1866** measurements from type specimen	915-(1006)-1310 x 20 332-(554)-788 x 21	770-(979)-1280 x 24	690-(860)-1253 x 26	246-(412)-525 x 24
Phakellia robusta Bowerbank,1866 Prob-Nw-ST6-66: (Taboada *et al.*, 2022)	905-(1027)-1320 x 17 337-(557)-790 x 23	771-(978)-1286 x 25	675-(929)-1297 x 28	234-(406)-539 x 23-25
Phakellia ventilabrum* (Linnaeus, 1767*) measurements from type specimen	221-(265)-380 x 7	420-528-659 x 7	none	none
Phakellia ventilabrum (Linnaeus, 1767*)* Pven-CS-DR1-02: (Taboada *et al.*, 2022)	227–(272)–345 x 6.5–(7.4)–8.5	457–(721)–848 x 5.9–(6.8)–8.3	none	none
***Phakellia hirondellei* Topsent, 1892** measurements from Phiron-CS-DR10-458: (Taboada *et al.*, 2022)	191- (482)-1104 x 5.6 -(12)-17.9	1175-(1342)-1543 x 12-(13)-14	336-(697)-1551 x 62- (13)-22.3	144-(240)-472 x 3.7-(8)-12.5
Phakellia* cf. *robusta				
DY081 326, 932 m	1322-(1544)-1677 x 15-(20)-24	690-(1126)-1563 x 12-(13)-15 n=6	789-(1179)-1640 x 10-(18.2)-23	203-(321)-260 x 12-(12.5)-13
DY081 327, 938 m	835-(1232)-1570 x 9-(19.7)-24	758-(957)-1327 x 14-19.6-25 n=7	863-(1133)-1466 x 11-(18.6)-23	478-(669)-797 x 17-(19.25)-20
DY081 1412, 1008 m	832-(1206)-1411 x 14-(17.5)-21	none	1095-(1328)-1674 x 12-(18.1)-21	740-(849)-938 x 19-(19.8)-20
DY081 1378, 751 m	1033-(1167)-1301 x 19-20	1163-(1455)-1748 x 13-15 n=4	1472 x 17	none
DY081 1133, 932 m	1943 x 17	1830-(2321)-2964 x13-(18)-21 n=8	713-(815)-947 x 11-(18)-20	none
DY081 1407, 972 m	1247-(2022)-3000 x 16-(20)-24	1171-(1672)-2589 x 12-(14)-19 n=5	655-(673)-692 x 12-(15)-19	490-(547)-560 x 10-(16)-19
DY081 1409, 932 m	1354-(1452)-1804 x 14-(17)-21	709 n=1	463-(526)-590 x 11-(13)-15	608-(711)-815 x 12-(17)-21

Distribution: Recorded from the shelf off the coast of Nuuk and the Southern tip of Greenland in the Labrador Sea, recorded depth 932-1008 m.

Remarks: The type locality of *P. robusta* is the Shetland Islands in the North Sea. The species is widely distributed in the Northeast Atlantic from northern Norway to northern Africa and is also found in the Mediterranean Sea (Topsent, 1925; Maldonado, 1992; D'Onghia *et al.*, 2015). There are recent records of *P. robusta* from Newfoundland (Fuller, 2011) and Iceland (Broad, 2019), so its presence in the Labrador Sea is not unexpected.

These specimens are very similar to *Phakellia robusta* recorded from the northeast Atlantic. They share the same fan-shaped external morphology. Their spicule component contains thick styles and two categories of oxea in a similar size range. However, the styles and oxea in our specimens are slightly bigger than recorded in other specimens (Table III). Rare strongyles were present in our specimens, these have also been noted from specimens from Iceland and Norway (Broad, 2019; Table III) and by Taboada 2022. However, those recorded in our specimen can be considerably larger (Table III). These could be a modification of one of the other spicule types.

Phakellia ventilabrum (Linnaeus, 1767) has previously described from the Labrador Sea (Lundbeck, 1909) and has a similar external morphology to the specimens seen here. However, its sinuous megascleres are predominantly strongyles (420-(721)-848 x 6-(7)-8 µm) and only occasional anisoxeas with one end blunt, compared with oxea in these specimens. *P. ventilabrum* also has much thinner and smaller styles (227-(272)-345 x 7-(7)-9 µm) than the styles seen in these specimens. There is some debate whether *P. ventilabrum* and *P. robusta* constitute separate species (Van Soest et al. 2001). There is also a further species, *P. hirondellei* Topsent, 1892 described from deep-water which Boury-Esnault et al. (1994) maintain is different and is backed up by recent genetic studies (Taboada *et al.*, 2022), it is predominantly a Mediterranean species.

The position of *Phakellia* within Axinellida Axinellidae Carter, 1875 has also been challenged based on genetic analysis of 28S rRNA (Morrow *et al.*, 2012). Based on this analysis *Phakellia* falls within Bubarida Morrow and Cárdenas, 2015, family Bubaridae Topsent, 1894. This has been backed up by a further genetic study looking at *Phakellia* hybridization (Taboada *et al.*, 2022). This hybridization between *P. hirondellei* and *P.robusta* adds another level of nuance to the position of these new specimens; they may well be a hybridization between *P.robusta* and another *Phakellia* species, potentially *P. hirondellei*.

Genetic sequencing of these samples would be an incredibly valuable tool in confirming their potential hybrid status and place in the genus.

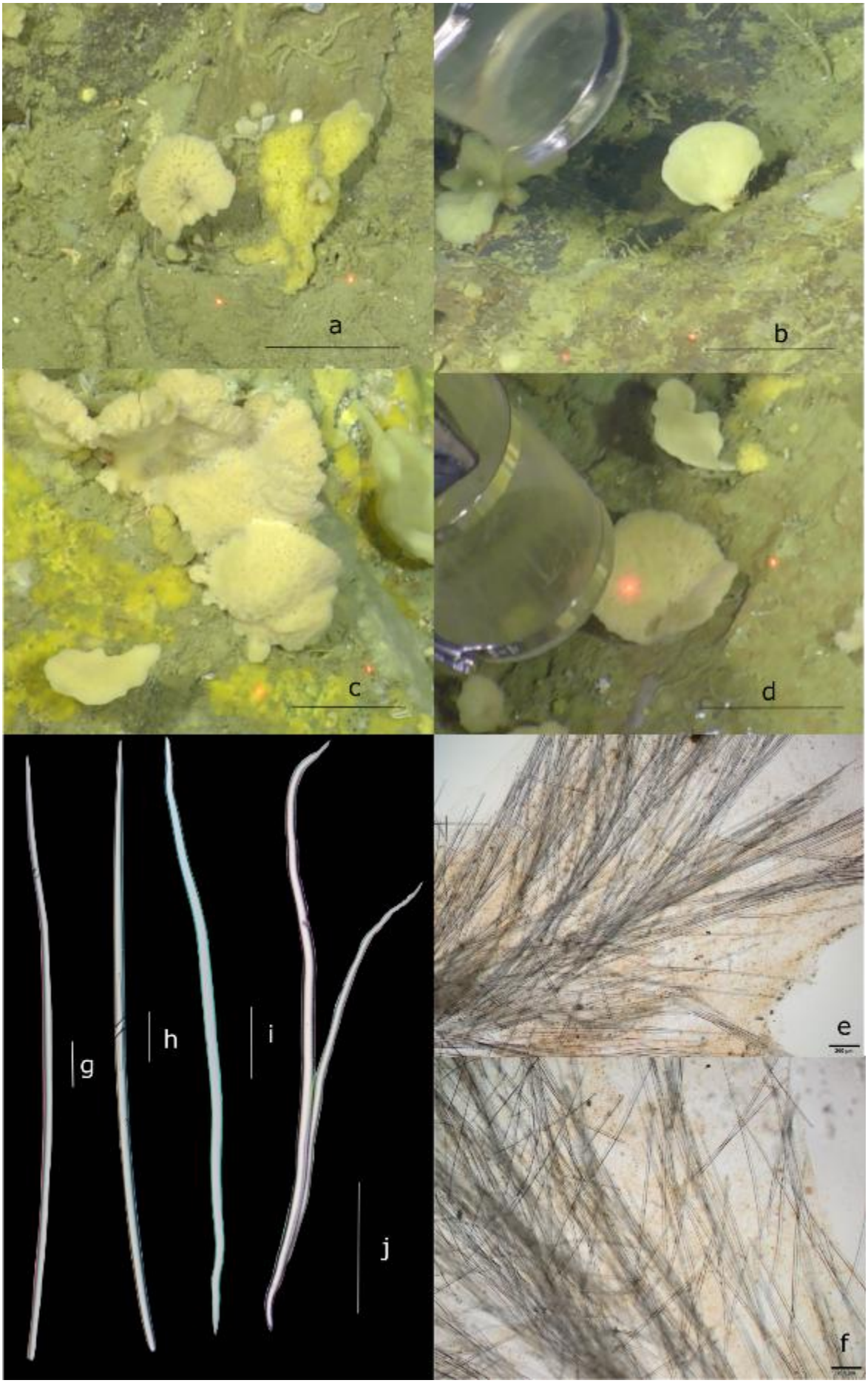
a
b
c
d
g
h
i
j
e
f

Figure 3-2. *Phakellia* cf. *robusta* Bowerbank, 1866 a) *In situ* appearance specimen DY081 327, scale bar 10 cm; b) *In situ* appearance specimen DY081 872, scale bar 10 cm; c) *In situ* appearance specimen DY081 1378, scale bar 10 cm; d) *In situ* appearance specimen DY081 326, scale bar 10 cm; e) skeleton DY081 315, scale bar 200 µm; f) skeleton DY081 326, scale bar 200 µm; spicules DY081 872 g) style, scale bar 100 µm, d) style, scale bar 100 µm, e) oxea, scale bar 100 µm, f) oxea, scale bar 200 µm.

Family Stelligeridae Lendenfeld, 1898

Genus *Halicnemia* Bowerbank, 1864

***Halicnemia flavospina* sp. nov.**

(Figure 3-3; Table II)

Type material: **Holotype:** Sample in 95% ethanol, tissue section, and spicule preparation on slides. DY081 1218. Station 52, Southwest Greenland (60°5.380'N, 46°38.232'W); depth 929 m; collected 29th July 2017.

Paratypes: Sample in 95% ethanol, tissue section, and spicule preparation on slides. DY081 1109. Station 50, Southwest Greenland (59°55.732'N, 46°29.993'W); depth 1008 m; collected 28th July 2017.

Diagnosis: Encrusting, conulose *Halicnemia*. Megascleres tylostyles and centrotylote oxeas; microscleres three categories of acanthostrongyles.

Description: Encrusting with strongly conulose surface, Sponge 10 cm by 3 cm with a thickness of 0.8 cm. Colour in life yellow, yellow brown in alcohol,

Etymology: From the Latin *flavo* meaning yellow and *spina,* a thorn or spine. Referring to its distinctive yellow spined surface.

Skeleton: Choanosome: A basal layer of scattered tylostyles arranged paratangential to the substrate, centrotylote oxeas forming columns 200 µm wide around the tylostyles.. Ectosome: A paratangential crust of acathostrongyles which is pierced by longer protruding tylostyle.

Spicules:

1. **Tylostyles,** 6706 x 46 -53 µm. Pronounced basal swelling 73 µm wide, straight and smooth with a blunt point (Holotype single unbroken tylostyle). 6695 x 43-54 µm (Paratype single unbroken tylostyle
2. **Centrotylote oxea,** 1661-(1757)-1929 x 19-(20)-21. Large, smooth, slight central bend tips are occasionally split (Holotype). 1647-(1794)-1944 x 19-(20)-21 µm (Paratype).
3. **Acanthostrongyles 1,** 217-(248)-350 x 13-(14)-16 µm. Verticillately spined with very slight flexure (Holotype). 141-(209)-334 x 12-(14)-15 µm (Paratype).
4. **Acanthostrongyles 2**, 76-(90)-124 x 5-(8)-10 µm. straight verticillately spined (Holotype). 76-(89)-100 x 5-8-10 µm (Paratype).
5. **Acanthostrongyles 2**, 42-(55)-65 x 4-(6)-8 µm. straight irregularly verticillately spined. (Holotype). 45-(57)-64 x 3-(5)-6 µm (Paratype).

Distribution: Recorded from the shelf off the coast of the Sothern tip of Greenland in the Labrador Sea, recorded depth 929-1008 m.

Remarks: Currently, there are six species of *Halicnemia* in the North Atlantic (van Soest *et al.*, 2021). *H. patera* Bowerbank, 1864, *H. gallica* (Topsent, 1893a), *H. arcuata* (Higgin, 1877), and *H. caledoniensis* Morrow et al., 2019 differ in possessing sharp pointed acanthoxeas that lack the verticillate spines seen on the acanthostrongyles in this species. *H. wagini* Morozov et al., 2018, has acanthostrongles (32-146 µm) which are not as large as those seen here, as well as a category of slightly larger acanthoxea (72-208 µm). The centrotylote oxea of *H. wagini* (826-1692 µm) are also considerably smaller than those described in this species. *H. verticillata* (Bowerbank, 1866) is probably the closest species, as it has very similar looking and similarly sized (50-400 µm) acanthostrongyles to those seen here. However, the centrotylote oxea of *H. verticillata* are only half as long as those found in this species (600-800 µm).

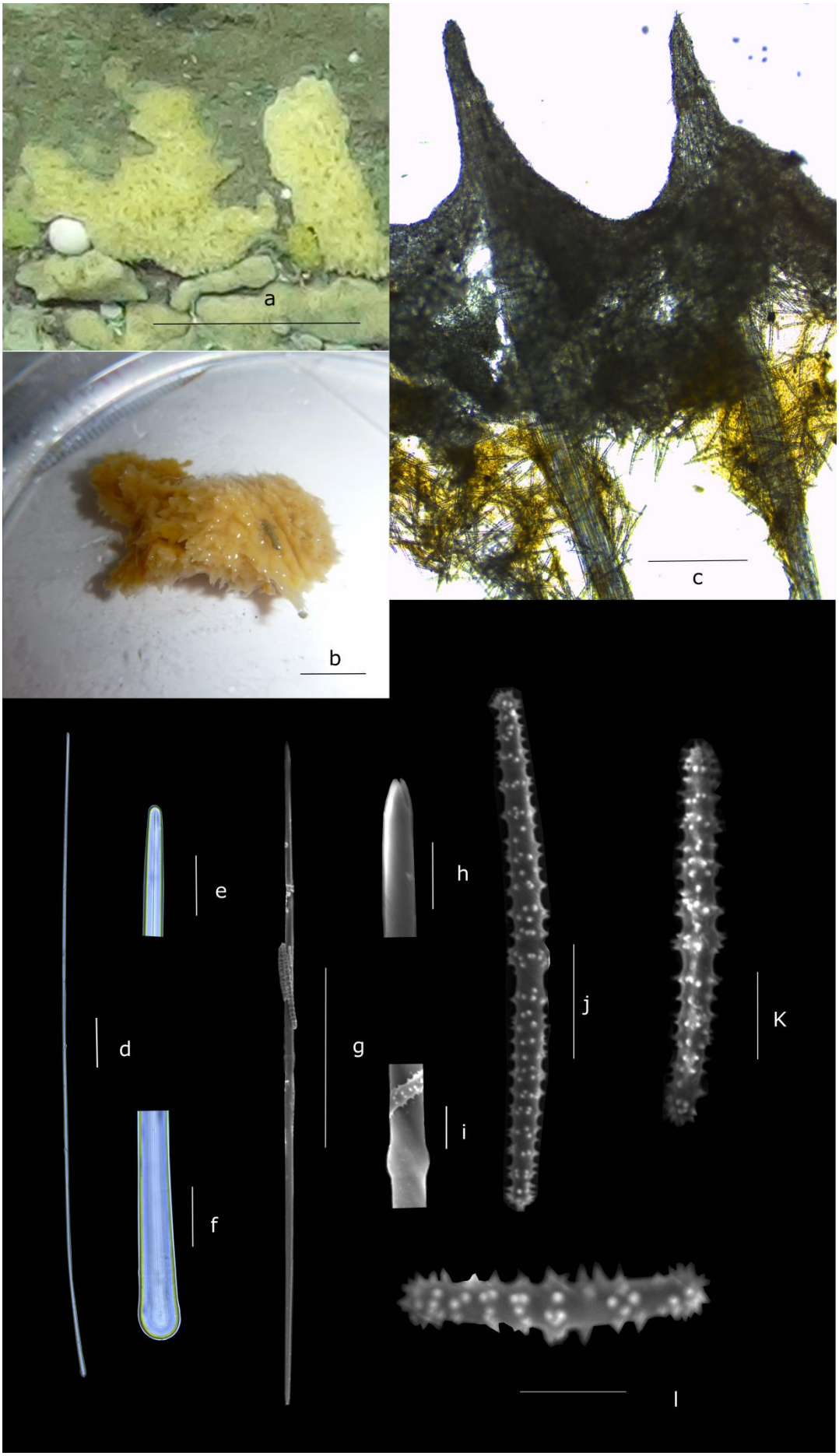
a
b
c
d
e
f
g
h
i
j
K
l

Figure 3-3. *Halicnemia flavospina* sp. nov. a) *In situ* appearance specimen DY081 1218, scale bar 10cm; b) surface appearances specimen DY081 1218, scale bar 1 cm; c) Skeleton DY081 1218, ectosome to top, scale bar 500 µm; spicules DY081 1218 d) tylostyle, scale bar 500 µm, e) point of tylostyle, scale bar 100 µm, f) head of tylostyle, scale bar 100 µm, g) centrotylote oxea, scale bar 500 µm, h) point of centrotylote oxea, scale bar 25 µm, i) central swelling of centrotylote oxea, scale bar 25 µm,, j) acanthostrongyle 1, scale bar 50 µm, k acanthostrongyle 2, scale bar 25µm, l) acanthostrongyle 3, scale bar 20 µm.

Genus *Paratimea* Hallmann, 1916

***Paratimea marionae* sp. nov.**

(Figure 3-4; Table II, IV)

Type material: **Holotype:** Sample in 95% ethanol, tissue section, and spicule preparation on slides. DY081 1394. Station 52, Southwest Greenland (59°55.709'N, 46°29.961'W); depth 1048 m; collected 29th July 2017.

Paratypes: Sample in 95% ethanol, tissue section and spicule preparation on slides. DY081 369. Station 13, Orphan knoll (50°30.790'N, 46°5.204'W); depth 1580 m; collected 13th July 2017. DY081 330. Station 13, Orphan knoll (50°30.794'N, 46°5.193'W); depth 1569 m; collected 13th July 2017.

Diagnosis: Thickly encrusting *Paratimea* with a conulose hispid surface. Megascleres oxeas; microscleres oxea and oxyasters.

Description: Thickly encrusting with a conulose and rough hispid surface, firm consistency. Seven obvious large ocules slightly elevated from surface. Sponge 10 cm wide, 15 cm long and 8 cm high. Colour white, light brown in alcohol.

Skeleton: Choanosome: hymedesmioid skeleton architecture with ascending tracts of oxea, oxyasters scattered throughout. Ectosome: a crust of tightly packed oxyasters with large choanosomal oxea protruding though the surface and surrounded by bouquets of thin oxea pulling the oxyaster crust into conules.

Spicules:

1. **Oxea 1,**1326-(1699)-2312 x 26-(30)-37 µm. Straight and smooth, occasionally with a slight central bend.
2. **Oxea 2,** 876-(975)-1156 x 9-(16)-23µm. Thin straight and smooth.
3. **Oxyasters,** 38-(60)-75 µm wide. smooth with small centrum 12-(14)-16 µm wide and between 6-17 rays.

Table IV. Spicule dimensions of *Paratimea marionae* sp. nov. and *Paratimea hoffmannae* Morrow et al., 2019

	Oxea 1 µm	**Oxea 2 µm**	**Oxyasters µm**
***Paratimea hoffmannae* Morrow & Cárdenas, 2019**	2056-(2187)-2250 x 25-(26)-28	rare, occasionally centrotylote 353-(446)-520 x 3-(4)-5	42-(60)-81
***Paratimea marionae* sp. nov.**			
DY081 1394 (Holotype)	1326-(1699)-2312 x 25-(29)-31	876-(975)-1156 x 9-(16)-23	38-(60)-75
DY081 369 (Paratype)	1289 -(1667)-2229 x 27-(29)-32	880-(1056)-1107 X 8.9-(15)-20	42-(63)-76
DY081 330 (Paratype)	styles 1281-(1721)-2363 x 19-(28)-30	877-(983)-1149 x 9-(16)-22	36-(59)-77

Distribution: Recorded from the shelf off the coast of the Southern tip of Greenland and the seamount of Orphan knoll in the Labrador Sea, recorded depth 1048-1580 m.

Etomology: This species is named after Marion Wyllie in recognition of her support of TC during his PhD research.

Remarks: There are currently nine species of *Paratimea* in the North Atlantic (van Soest *et al.*, 2021). *Paratimea aurantiaca* Morrow et al., 2019, *P. azorica* (Topsent, 1904) , *P. constellata* (Topsent, 1893c), *P .dentata* Morrow et al., 2019, and *P. loennbergi* (Alander, 1942) all have tylostyles as their only megascleres, differentiating them from this species, Their euasters are also considerably smaller than described here. *P. duplex* (Topsent, 1927) has both oxea (2000-2600 µm) and oxyasters (50-100 µm) slightly larger than those from this species. It also has subtylostyles (1600-1800 µm) as megascleres which are absent here. *P. arbuscula* (Topsent, 1928) has small centrotylote oxea (560-1000 µm) and small oxyasters (15-60 µm) with no centrum, the oxea described here are much bigger with no central swelling; its oxyasters are also bigger and have a small centrum. *P. hoffmannae* Morrow et al., 2019*,* and *P. lalori* Morrow et al., 2019 are the closest species to this one, with oxyasters of a similar size and oxea as megascleres. *P. hoffmannae* can be

differentiated by its large oxea (2000-2250 µm), which overlap slightly with the largest seen here. However, the average size of the megasclere oxea of this species is approximately 500 µm smaller than the smallest described for *P. hoffmannae*. The rare accessory spicules (353-(446)-520 x 3-(4)-5 µm) of *P. hoffmannae* are also considerably smaller and thinner than the common accessory oxea in this species. *P. lalori* again has very similar oxyasters, but its oxea (1439-2020 µm) are bigger than those seen here. The clear distinguishing feature is the common accessory oxea with conspicuous centrotylote swellings (278-422 µm) of *P. lalori* which are entirely absent from this species.

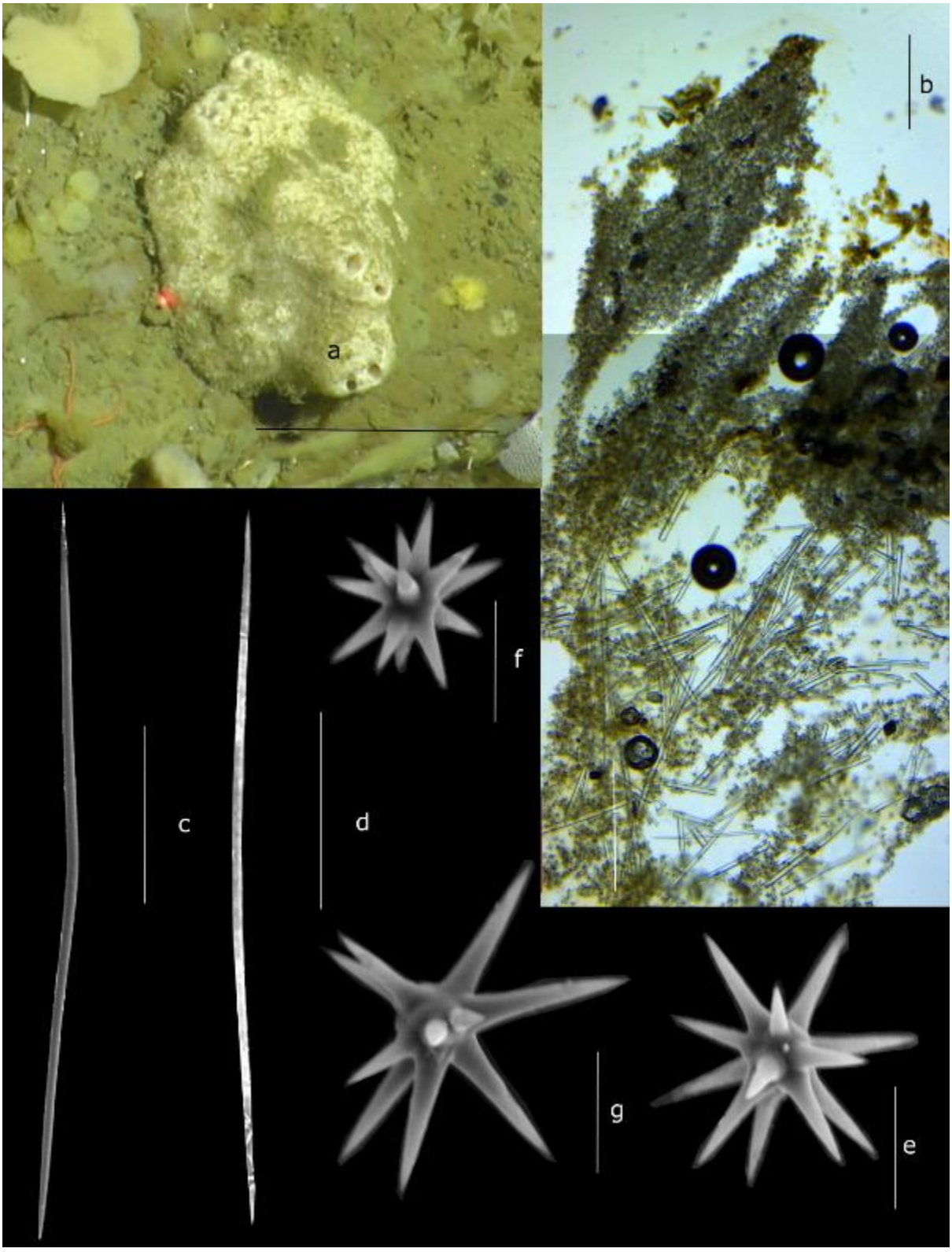

Figure 3-4. *Paratimea marionae* sp. nov. a) *In situ* appearance specimen DY081 1394, scale bar 10 cm; b) Skeleton DY081 1394, ectosome to top, scale bar 500 µm; spicules DY081 1394 c) oxea 1, scale bar 500 µm, d) oxea 2, scale bar 250 µm, e, f, g) Oxyasters, scale bar 25 µm.

Order Poecilosclerida Topsent, 1928

Family Cladorhizidae Dendy, 1922

Genus *Asbestopluma* Topsent, 1901

Subgenus *Asbestopluma (Asbestopluma)* Topsent, 1901

***Asbestopluma (Asbestopluma) frutex* sp. nov.**

(Figure 3-5; Table II)

Type material: **Holotype:** Sample in 95% ethanol, tissue section, and spicule preparation on slides. DY081 855. Station 36, Nuuk (63°19.9630'N, 52°45.9630'W); depth 1135 m; collected 22nd July 2017.

Diagnosis: Erect, shrub-like, branched *Asbestopluma* with multiple filaments. Megascleres mycalostyles, subtylostyles, and acanthotyostyles; microscleres one type of palmate to arcuate anisochela 49-50 µm, one type of palmate anisochela 10-13 µm and sigmancistras 26-29 µm.

Appearance: Erect sponge with irregularly branching hard but flexible, stems forming a roughly hemispherical shrub-like structure reaching 15 cm in diameter. Colour of the lower part brown; upper part slightly yellow, fading to white at branch ends. Branches have filaments projecting in all directions from the stem. Filaments typically 2 mm long. Sponge connected to substrate with a structure comprised of several branching root-like processes anchoring it to the sediment.

Skeleton: Branches cored by fibres 100 µm thick composed of longitudinally arranged mycalostyles. Lower stems have an ectosomal layer of acanthotylostyles. The filaments are 50-150 µm thick and composed of subtylostyles originating from the coring fibres of the branches.

Spicules:

1. **Mycalostyles**, 398-(449)-489 x 5-(6)-7 µm, straight or very slightly curved, fusiform.
2. **Subtylostyles**, 268-(287)-323 x 4-(5)-7 µm, straight, with an elongated, slightly offset tyle, characteristic for the genus, slightly fusiform. Found in filamentous upper part of the stem.
3. **Acanthotylostyles**, 197-(205)-216 x 2-(3)-5 µm, curved, found in the lower section of the stem.
4. **Arcuate anisochelae**, 49-50 µm with a straight shaft, a central tooth and lateral alae covering about 50% of the length of the spicule. The lower end of the shaft has two rudimentary dorsal processes and two flat frontal alae, about 15% of the total chelae length. Found in filamentous upper part of the stem.

5. **Palmate anisochelae**, 10-(11)-13 µm. Uncommon, with a curved shaft, a central tooth and lateral alae covering approximately 65% of the total spicule length and the lower end with two rudimentary dorsal processes with two leaf-shaped teeth up to 20% of the total spicule length.
6. **Sigmancistras**, 26-(27)-29 µm. Twisted around 90^{o}. Have a flattened internal margin. Numerous throughout the sponge.

Distribution: Type specimen recorded from the shelf off the coast of Nuuk in the Labrador Sea, recorded depth 1135 m.

Etymology: the name derives from *frutex* (Latin), meaning shrub or bush, and refers to the external morphology of the species.

Remarks: Four species of *Asbestopluma (Asbestopluma)* are currently known from the Boreal North Atlantic and Arctic (Hestetun, Tompkins-Macdonald and Rapp, 2017b). The majority of these species consist of single stems. *A. furcata* Lundbeck, 1905 is branched but in a regular dichotomous pattern with long branches which is distinct from the squat bushy habit of our specimen.

In terms of spicules, the majority of species in the region have much larger larger mycalostyles: *A. (A.) ruetzleri* Hestetun et al., 2016 (581-918 µm), *A. (A.) bihamatifera* (Carter, 1876) (653-935 µm) and *A. (A.) pennatula* (Schmidt, 1875) (500-1010 µm). The smallest mycalostyles of *A. (A.) furcata* are similar in size (333-968 µm), but the size range is much broader, in addition *A. (A.) furcata* has smaller acanthotylostyles (44-107 µm), and sigmancistras (12.1-22.7 µm) and its smaller anisochelae are different in morphology.

Worldwide there are 32 species of *Asbestopluma (Asbestompluma)* considered valid (van Soest *et al.*, 2021). However, there are only ten that exhibit a branching habit, all other species comprise of a single stem or pedunculate habit. Comparing the branching species to this specimen, three lack a second large category of anisochela: (*A. (A.) sarsensis* Goodwin et al., 2017*, (A. (A.) rickettsi* Lundsten et al., 2014, and *A. (A.) monticola* Lundsten et al., 2014. Three more, *A. (A.) jamescooki* Hestetun et al., 2017*, A. (A.) ramuscula* Hestetun et al., 2017, and *A. (A.) gemmae* Goodwin et al., 2017*,* lack acanthotylostyles, and also have much longer mycalostyles *(A. (A.) jamescooki* (466-(652)-820 µm), *A. (A.) ramuscula* (351-(567)-742 µm), *A. (A.) gemmae,* largest category is (1000-1202 µm). *A. (A.) bitrichela* Lopes et al., 2011, and *A. (A.) desmophora* Kelly & Vacelet, 2011, have desmas in addition to acathostyles. *A. (A.) unguiferata* Hestetun et al., 2017 has very distinct smaller slender chelae (20-21-24 µm) with long sharp upper alae and three sharp bottom alae, it also has smaller acanthotylostyles (54-65-79 µm) and sigmancistras (11-13-16 µm) and larger mycalostyles (445-(588)-718 µm). *A. (A.) magnifica* Lopes et al., 2011, has two categories of styles (I =554-995 µm,

II=205-268 µm) of which the largest is bigger than the single type of subtylostle in this species; it also has smaller arcuate chelae (30-38 µm) and bigger palmate chelae (13-18 µm) and sigmancistras (25-40 µm). *A. (A.) quadriserialis* Tendal, 1973, can be distinguished by its two size classes of sigmancistras (I=75-125 µm II=28-38 µm).

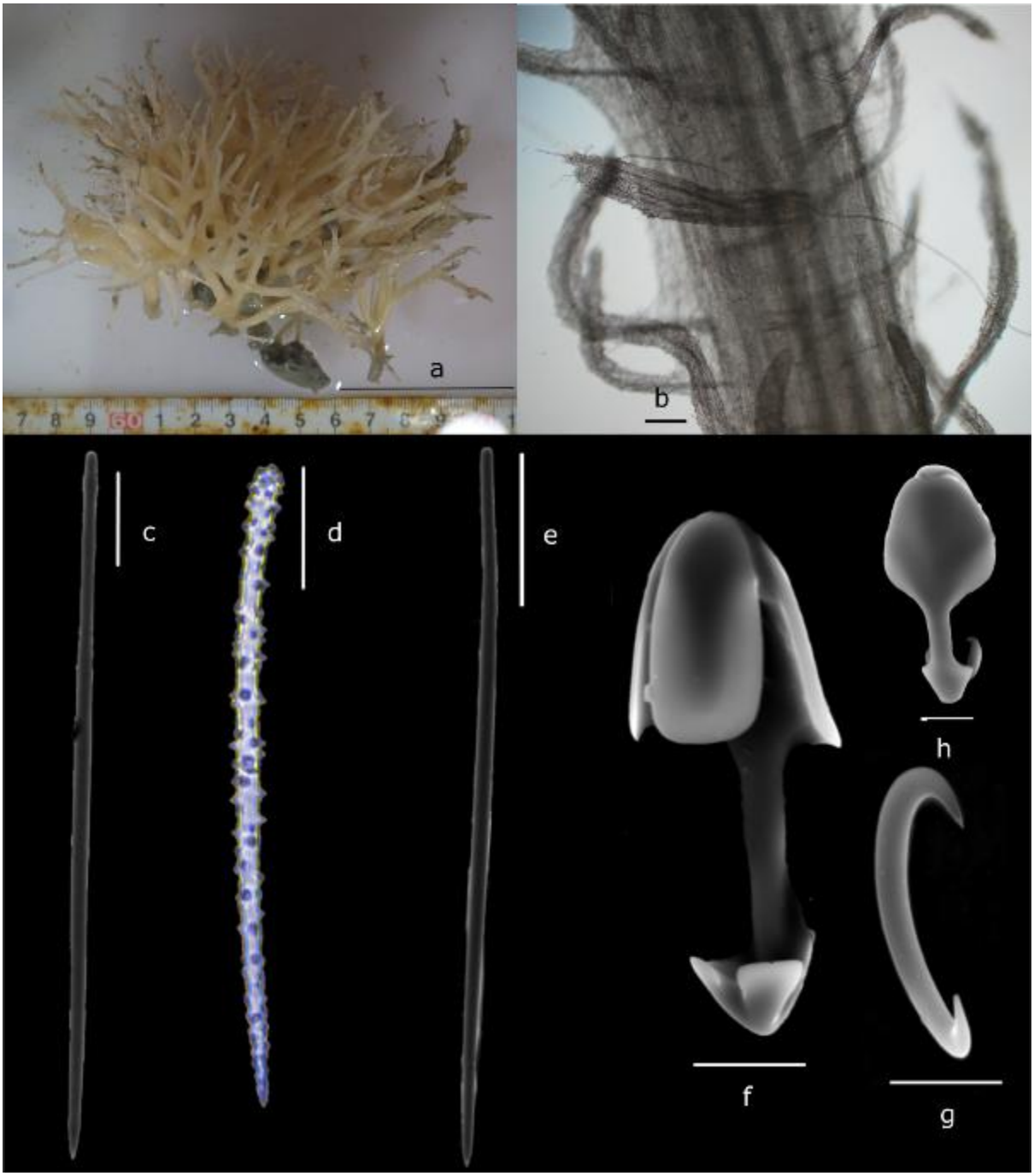

Figure 3-5. *Asbestopluma (Asbestopluma) frutex sp. nov.* a) *A*ppearance specimen DY081 855, scale bar 5 cm; b) Skeleton DY081 855, extremity to top, scale bar 200µm; Spicules DY081 855 c) mycolostyle, scale bar 100 µm, d) subtylostyle, scale bar 50 µm, e) acanthotylostyle, scale bar 50 µm,

f) arcuate anisochelae, scale bar 10 µm, g) palmate anisochelae, scale bar 10 µm. h) sigmancistras, scale bar 10 µm.

Family Coelosphaeridae Dendy, 1922

Genus *Lissodendoryx* Topsent, 1892

Subgenus *Lissodendoryx (Acanthodoryx)* Lévi, 1961

***Lissodendoryx (Acanthodoryx) magnasigma* sp. nov.**

(Figure 3-6; Table II)

Type material: **Holotype:** Sample in 95% ethanol, tissue section and spicule preparation on slides. DY081 1411. Station 50, Southwest Greenland (60°5.4100'N, 46°38.2310'W); depth 934 m; collected 28th July 2017.

Diagnosis: Massive, irregular *Lissodendoryx* , that when broken forms hair like strands. Megascleres tornotes and styles; microscleres three categories of arcuate isochela and large sigmas.

Description: Massive and irregular with no visible oscula. The holotypeis 5 cm in diameter and connected to the substrate by a mass of loose hair-like root systems. Colour in life white to yellow, white in alcohol, the root system is dark brown.

Skeleton: Choanosome: Plumoreticulate. Styles forming multispicular strands (4-12 spicules thick) and plumose tracts. Occasionally anastomosing, without distinct reticulation, microscleres present throughout. Ectosome: Tangentially strewn tornotes and microscleres

Spicules:

1. **Ectosomal tornotes,** 560-(571)-584 x 13-(16)-17 µm. Smooth.
2. **Styles,** 593-(712)-824 x 18-(19)-23 µm. Smooth.
3. **Arcuate isochela 1,** 33-(35)-38 µm long, alae one quarter of total length, slight curve in centre of shaft
4. **Arcuate isochela 2**, 18-(20)-21 µm long, alae one quarter of total length, slight curve in centre of shaft.
5. **Sigma 1**, 174-(185)-195 µm long, very large and robust.
6. **Sigma 2**, 77-(79)-88 µm long, smaller and thinner.
7. **Sigma 3,** 19-(22)-23 µm

Distribution: Recorded from the shelf off the coast of the Sothern tip of Greenland in the Labrador Sea, recorded depth 931 m.

Etomology: This species name, *magnasigma* (Latin), refers to the large size of the sigma in this species.

Remarks: The plumose skeleton with thick choanosomal fibres forming radiating tracts places this species in *Lissodendoryx (Acanthodoryx)* rather than *Lissodendoryx* (*Lissodendoryx*) in which the fibres form a distinct reticulation (Hooper and van Soest, 2002). There is only one species of *Lissodendoryx (Acanthodoryx)* from shallow water in the *Philippines Lissodendoryx (Acanthodoryx) fibrosa* (Lévi, 1961). This species has a radiating choanosomal skeleton made up of thick bundles of acanthostyles (150-170 µm), tylote ectosomal spicules (200-240 µm), and no sigmas, compared to the smooth choanosomal styles, ectosomal strongyles and three categories of sigmas seen in this species. There are 13 species of *Lissodendoryx (Lissodendoryx)* known from the N. Atlantic. It is distinguishable from most other *Lissodendoryx (Lissodendoryx)* of the North Atlantic, aside from the distinctly different skeletal structure, due to the extremely large size of its largest category of sigmas. These are well over 100 µm longer than the sigmas of *Lissodendoryx (Lissodendoryx) polymorpha* (Topsent, 1892) which has the second biggest (50 µm). Its two categories of chela and its large megascleres are also distinctive. *Lissodendoryx (Lissodendoryx) fertilior* Topsent, 1904, has ectosomal spicules that can reach the same size and larger than this species but lacks the two categories of chela and the two larger categories of sigma.

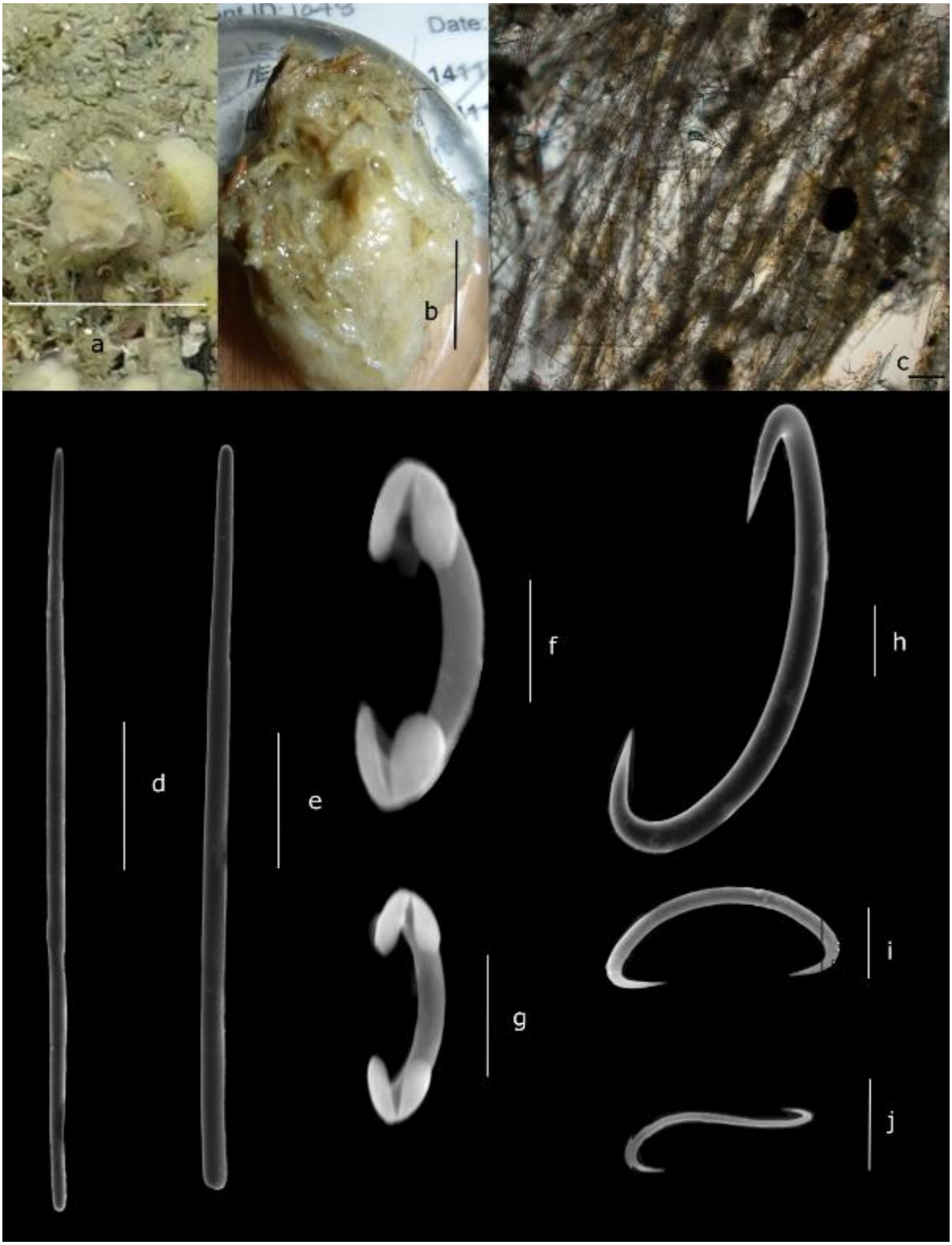

Figure 3-6. *Lissodendoryx (Acanthodoryx) magnasigma sp. nov.* a) *In situ* appearance specimen DY081 1411 scale bar 5 cm; b) Appearance specimen DY081 1411, scale bar 2 cm; c) Skeleton DY081 1411, ectosome to top, scale bar 200 µm; spicules DY081 1411 d) ectosomal tornote, scale bar 100

µm, e) style, scale bar 100 µm, f) arcuate isochela 1, scale bar 10 µm, g) arcuate isochela 2, scale bar 10 µm, h) sigma 1, scale bar 25 µm, i) sigma 2, scale bar 25 µm, j) sigma 3, scale bar 10 µm.

Family Dendoricellidae Hentschel, 1923

Genus *Fibulia* Carter, 1886

***Fibulia textilitesta* sp. nov.**

(Figure 3-7; Table II)

Type material: **Holotype:** Sample in 95% ethanol, tissue section, and spicule preparation on slides. DY081 241. Station 5, Orphan Knoll (50°2.879'N, 45°22.581'W); depth 3462 m; collected 8th July 2017.

Diagnosis: Erect, ovate, white *Fibulia*. Megascleres centrotylote oxea; microscleres arcuate isochelae.

Description: Erect, ovate or club-shaped, 2 cm long 1 cm wide with a parchment-like surface. Colour white.

Skeleton: Ectosome; tightly inter-crossing tangential mass of oxea forming a felted crust. Choanosome; irregular plumose bundles of oxea with many loose oxea and chelae.

Spicules:

1. **Oxea ,** 757-(900)-1318 x 14-(20)-24 µm, very slightly curved smooth shafts, tips sharply pointed. Most are centrotylote. Some have a swelling at their centre, in others, the swelling is nearer their tip, a minority have no swelling at all.
2. **Arcuate isochelae 1**, 31-37 µm long, thick shaft with three wide flattened alae one-fifth of total length, central tooth shorter by 40%, shaft slightly curved.

Distribution: Recorded from Orphan Knoll seamount off the coast of Newfoundland, Canada in the Labrador Sea, recorded depth 3461m.

Etymology: This species name, derives from *textilis* (Latin) meaning woven and *testa* (Latin) meaning earthenware jar, and refers to the appearance of the felted crust.

Remarks: We assign this specimen to *Fibulia* based on its possession of a single size class of oxea (Hooper, 2002).

Worldwide there are currently ten species of *Fibulia* considered valid (van Soest *et al.*, 2021). None of these possess centrotylote oxea; however, this can be an unreliable characteristic as it can vary with silica concentrations in the water (Maldonado *et al.*, 1999). Most of the species of *Fibulia* have much small oxea in comparison to this species; these include *F. anchorata* (Carter, 1881) (300 µm), *F. carnosa* Carter, 1886 (155-245 µm), *F. conulissima* (Whitelegge, 1906) (170 µm), *F. cribriporosa* (Burton, 1929) (480 µm), *F. hispidosa* (Whitelegge, 1906) (180-200 µm), *F. intermedia* (Dendy, 1896) (250 µm), *F. myxillioides* (Burton, 1932) (248-333 µm), and *F. novaezealandiae* (Brøndsted, 1924) (350 µm). Two more have smaller oxea with a size range only just outside the range seen in this species *F. maeandrina* (Kirkpatrick, 1907) (579 µm), and *F. ramosa* (Ridley and Dendy, 1886) (600 µm), although neither has centrotylote oxea. They also both have C-shaped, strongly curved chela compared to the almost flat chela in this species, *F. maendrina* has chelae with long central alae with two lateral bifurcated alae and *F. ramosa* has chelae with sharply pointed alae. This distinguishes them both from the chela seen in this species.

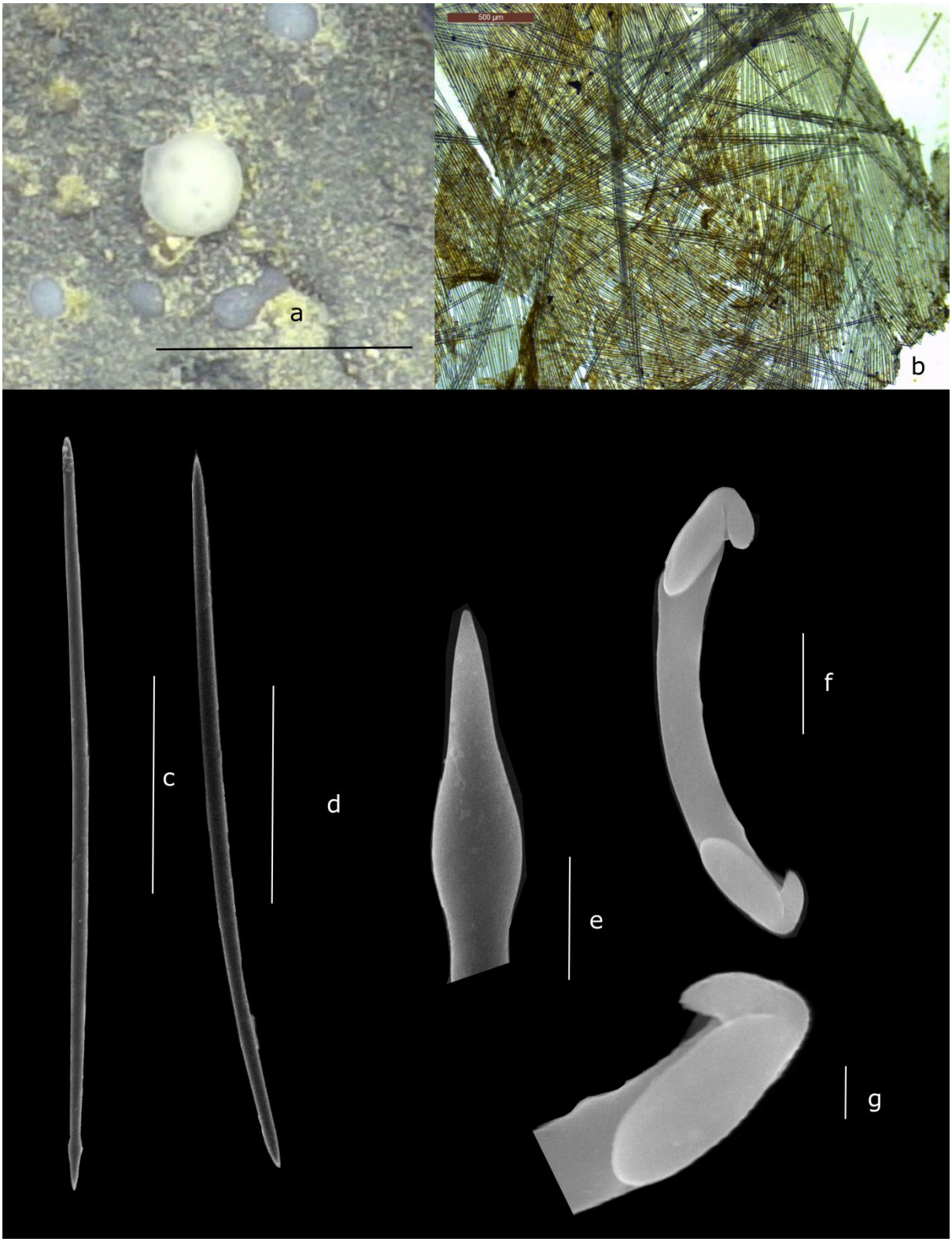

Figure 3-7. *Fibulia textilitesta* sp. nov. a) *In situ* appearance specimen DY081 241, scale bar 5 cm; b) Skeleton DY081 241, scale bar 500 µm; spicules DY081 241, c) centrotylote oxea, scale bar 250 µm, d) oxea, scale bar 250 µm, e) head of centrotylote oxea, scale bar 20 µm, g) arcuate isochela, scale bar 10 µm. g) head of arcuate isochela, scale bar 2.5 µm.

Family Hymedesmiisae Topsent, 1928

Genus *Hymedesmia* Bowerbank, 1864

Subgenus *Hymedesmia (Hymedesmia)* Bowerbank, 1864

***Hymedesmia (Hymedesmia) caerulea* sp. nov.**

(Figure 3-8; Table II)

Type material: **Holotype:** Sample in 95% ethanol, tissue section, and spicule preparation on slides. DY081 959. Station 36, Nuuk (63°19.987'N, 52°45.836'W); depth 1052 m; collected 22nd July 2017.

Diagnosis: Striking Blue, encrusting *Hymedesmia*. Megascleres acanthostyles and polytylote strongyles; microscleres anchorate isochelae 53-(65)-74 µm.

Description: Thinly encrusting, hispid, with the thickest example having a slightly lumpy felt like texture with circular pore sieves. Colour in life a striking royal blue, visible from a considerable distance, brown in alcohol. Sponge encrusting on rocks, in patches on bedrock, or completely covering cobbles, patch size 5-15 cm thickness 2-5 mm.

Skeleton: Basal Layer of acanthostyles standing erect on substrate with columns of 11-20 strongyles ascending to the surface. There is a very thick layer of chelae in the ectosome.

Spicules:

1. **Acanthostyles 1,** 315-(315)-415 x 8-(10)-14 µm, entirely spined with dense, large, hooked spines on the head and smaller and sparser spines at tip, head slightly tylote.
2. **Acanthostyle 2,** 165-(182)-210 x 3-(4)-5 µm, completely spined, head not tylote.
3. **Polytylote strongyles,** 419-(445)-531 x 4-(5)-7 µm.
4. **Anchorate isochelae,** 53-(65)-74 µm, strongly curved with small slightly recurved alae and asmooth and slightly oval shaft.

Distribution: Recorded from the shelf off the coast of Greenland in the Labrador Sea, from both the shelf off Nuuk and the Southern tip of Greenland, recorded depths 691-1051 m.

Etymology: This species name derives from, *caerulea* (Latin), meaning blue, and refers to the colour of this species.

Remarks: A relatively small group of species in the genus *Hymedesmia (Hymedesmia)* have polytylote strongyles as ectosomal spicules, one category of arcuate chelae, and two categories of

acanthostyles, the larger of which are completely spined. These include *H. (H.) gibbosa* Goodwin et al., 2011*, H. (H.) rugosa* Lundbeck, 1910, *H. (H.) helgae* Stephens, 1920*,* and *H. (H.) serrulata* Vacelet, 1969. *H. (H.) gibbosa* and *H. (H.) rugosa* may be distinguished by the lack of tylote head on the smaller acanthostyles and differing chelae morphologies. This species lacks the central hump on the stem seen in *H. (H.) gibbosa* and has a continuous C-shaped curve on the stem unlike the winged curve of *H. (H.) rugosa*. In addition, *H. (H.) gibbosa* has much longer primary acanthostyles (387-572 µm), and *H. rugosa* has much shorter strongyles (310-417 µm). *H. (H.) helgae* has the most similar size ranges of spicules but has shorter secondary acanthostyles (125-150 µm) and considerably smaller chela (35-40 µm) than those seen in this species. There are seven species that have the same combination of chelae and acanthostyles as seen here with strongyles are not polytylote. These are *H. (H.) gaussiana* Hentschel, 1914*, H. (H.) minuta* Alander, 1935*, H. (H.) splenium* Lundbeck, 1910*, H. (H.) laptikhovskyi* Goodwin et al., 2016 *, H. (H.) rowi* van Soest, 2017 and *H. (H.) croftsae* Goodwin et al., 2016. These need to be considered as the polytylote trait can be variable depending on silica levels in the seawater (Maldonado *et al.*, 1999). However, all of these species have considerably smaller chelae with *H. (H.) splenium* having the largest at 41-47 µm.

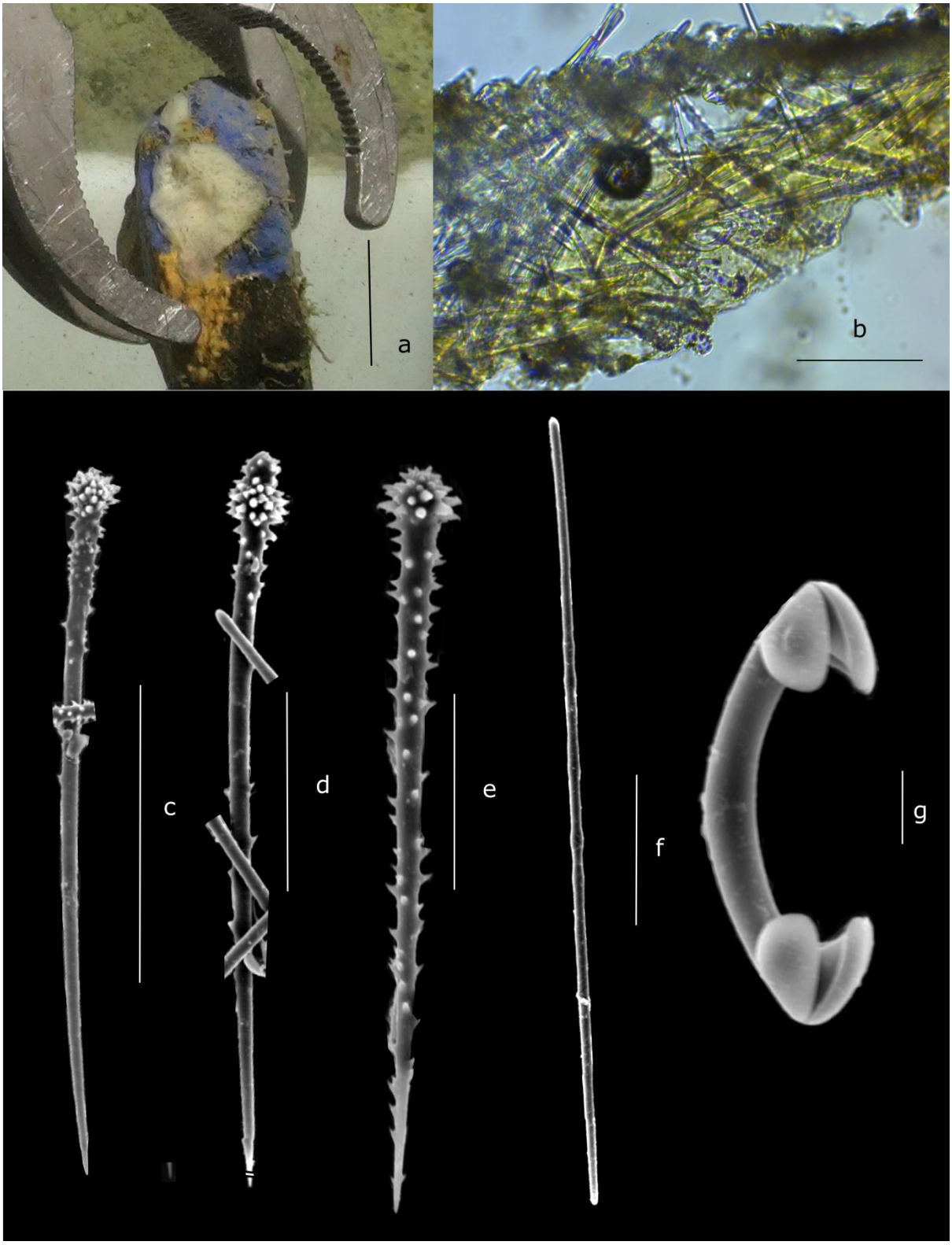

Figure 3-8. *Hymedesmia (Hymedesmia) caerulea* sp. nov. a) specimen appearance during collection DY081 959, scale bar 10 cm; b) Extosomal crust DY081 959, scale bar 200 µm; spicules DY081 959 c) acanthostyle 1, scale bar 200 µm, d) acanthostyle 1, scale bar 100 µm, e) acanthostyle 2, scale bar 50µm, f) polytylote strongyle, scale bar 100 µm, g) anchorate isochelae, scale bar 10 µm.

***Hymedesmia (Hymedesmia) alba* sp. nov.**

(Figure 3-9; Table II)

Type material: **Holotype:** Sample in 95% ethanol, tissue section, and spicule preparation on slides. DY081 991. Station 36, Nuuk (63°19.9870, 52°45.8360'W); depth 1052 m; collected 22nd July 2017.

Diagnosis: Lumpy, white, Encrusting *Hymedesmia*. Megascleres acanthostyles and oxea; microscleres anchorate isochelae 57-61-71 µm.

Description: Encrusting, hispid, lumpy uneven surface with circular pore sieve, Colour yellow-white, in life and alcohol. Sponge encrusting on rocks, in a patch 5 by 10 cm.

Skeleton: Basal Layer of acanthostyles standing erect on the substrate with ascending columns 5-10 oxea leading to a mesh of ectosomal spicules at the surface. Chelae present thought the tissue with a very thick layer of chelae in the ectosome

Spicules:

1. **Acanthostyles 1,** tylote 350-(378)-401 x 14-(16)-18 µm, Strongly spined at the head with reduced small spines along the remaining two-thirds of their length and the tip smooth, head slightly tylote.
2. **Acanthostyle 2,** 198-(205)-213 x 8-(10)-11 µm, completely spined, with a slightly tylote head.
3. **Ectosomal oxea,** 220-(341)-398 x 6-(10)-15 µm, smooth, slightly bend in middle.
4. **Anchorate isochelae,** 57-(64)-71 µm, thin shaft with small alae.

Distribution: Type specimen recorded from the shelf off the coast of Nuuk in the Labrador Sea, recorded depth 1052 m.

Etymology: This species name derives from *alba* (Latin), meaning white, and refers to the colour of this species.

Remarks: Twenty-three *Hymedesmia (Hymedesmia)* species have two categories of acanthostyles, tornotes or oxea as ectosomal spicules and one category of chelae as microscleres. This species is distinguishable from these due to the large size of its chelae. In this group, only *H. (H.) nummulus* Lundbeck, 1910, and *H.(H) clavigera* Lundbeck, 1910, have chelae greater than 40 µm in length, and these are still significantly smaller, being 28-54 and 41-52 µm respectively. *H. (H.) nummulus* has much larger acanthostyles (510-950 µm) and ectosomal spicules which are longer (350-460 µm) and strongyles tending to tornotes rather than oxea. *H.(H) clavigera* is has much shorter large acanthostyles (250-298 µm) and oxea (95-120 µm).

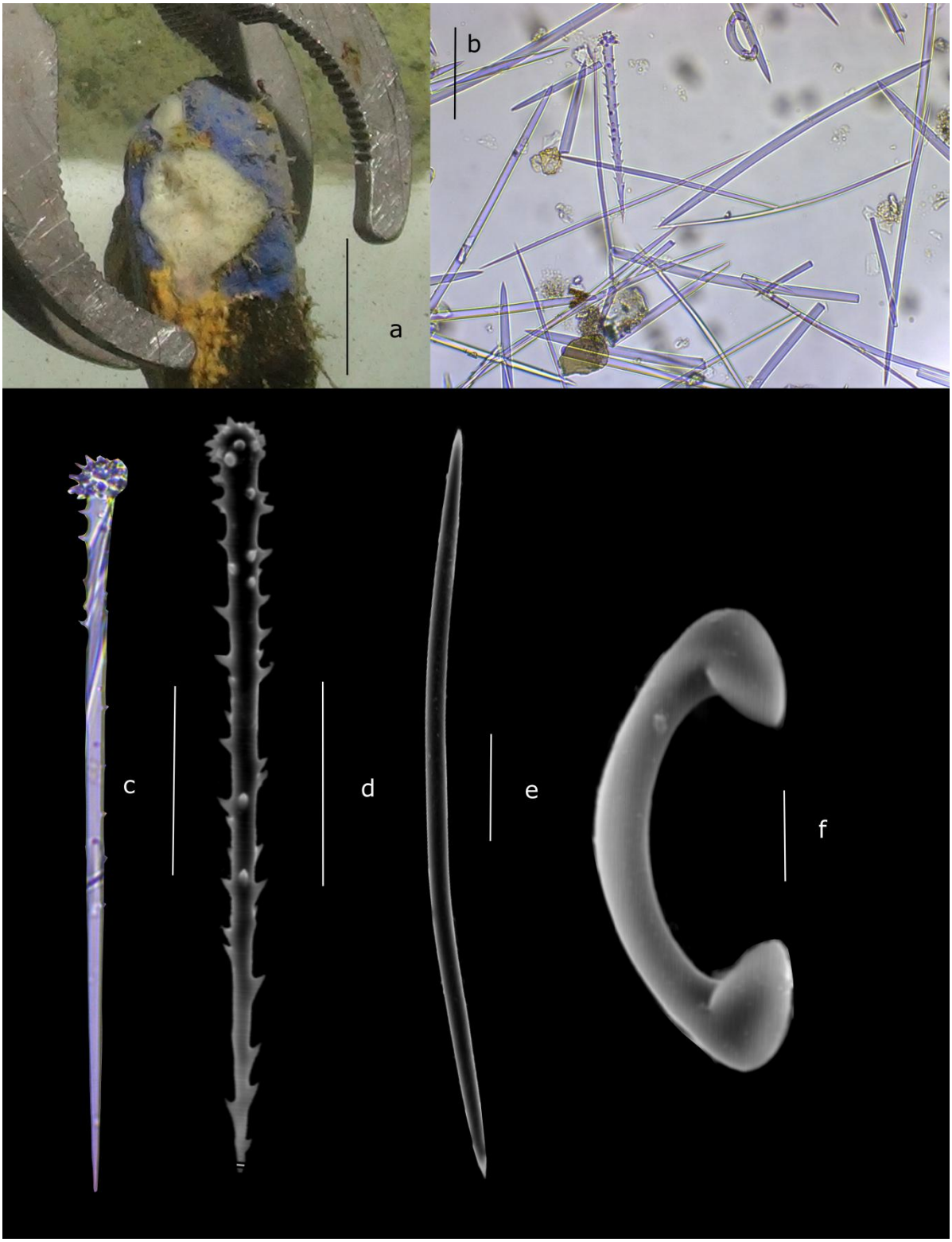

Figure 3-9. *Hymedesmia (Hymedesmia) alba* sp. nov. a) specimen appearance during collection DY081 991, marked with Arrow, scale bar 10 cm; spicules DY081 991, b) acanthostyle 2, ecosomal oxea and anchorate isochelae under light microscopy, scale bar 100 µm, c) acanthostyle 1, scale bar 100 µm, c) acanthostyle 2, scale bar 50 µm, d) ectosomal oxea, scale bar 50 µm, e) anchorate isochelae, scale bar 10 µm.

Hymedesmia (Hymedesmia) crux (Schmidt, 1875)

(Figure 3-10; Table II)

Material: Sample in 95% ethanol, tissue section, and spicule preparation on slides. DY081 1138. Station 36, Nuuk (63°19.9870, 52°45.9890'W); depth 1160 m; collected 22nd July 2017.

Description: Thinly encrusting, hispid, Colour in life yellow-brown, brown in alcohol. Sponge encrusting on dead coral polyps.

Skeleton: Basal Layer of acanthostyles standing erect on the substrate with bundles of strongyles rising to the surface. Chelae present thoughout the tissue with a very dense layer at the surface.

Spicules:

1. **Acanthostyles 1 (larger category),** 300-(397)-463 x 17-(19)-21 µm, well spined at the head with smaller spines along length reducing in size towards the tip.
2. **Acanthostyles 2 (smaller category),** 174-(187)-207 x 8-(10)-12 µm, completely spined, with slightly tylote head.
3. **Strongyles,** 339-(395)-421 x 4-(5)-7 µm, smooth, rarely polytylote.
4. **Anchorate isochelae,** 38-(42)-49 µm, strongly curved with 3 large alae almost touching, substantial spines along the back of their shaft. The width of the alae is approximately equal to the total length of the chelae.

Distribution: Specimen recorded from the shelf off the coast of Nuuk in the Labrador Sea, recorded depth 1160 m.

Remarks: Hymedesmia (Hymedesmia) crux was originally described from Southern Norway and has subsequently been recorded from Celtic Seas (1331 m) (Stephens, 1920), The Faroe plateau (293-887 m)(Hentschel, 1929), and Iceland(539 m) (Lundbeck, 1910). This specimen corresponds relatively well to the original descriptions of *H. (H.) crux,* particularly the distinctive chelae shape. The larger acanthostyles (Acanthostyles I) from Lundbeck's specimen (380-400 x 20-30 µm) were smaller and slightly thicker than seen in ours, and the smaller acanthostryles (Acanthostyles II) in his specimen were slightly smaller (120-150 µm).The strongyles described by Lundbeck measure 270-380 x 6-8 µm, slightly smaller than in our specimen. The chelae measurements are very close to our specimen with a lot of overlap: those in Lundbeck's specimen measuring 31-43 µm. The shape of the chelae in both specimens is very similar and distinctive with the shape and overlapping sizes of the other spicules confirming this species.

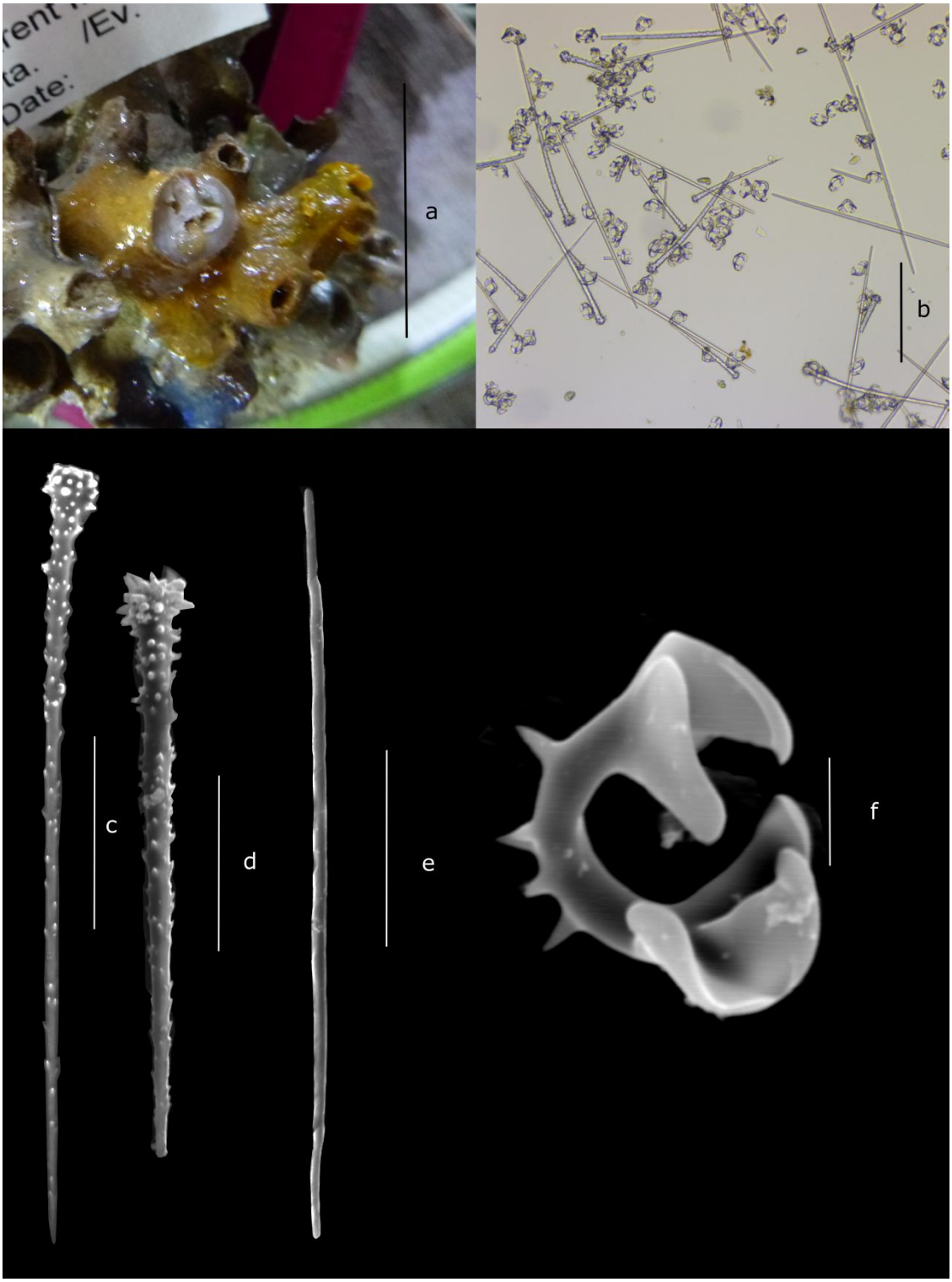

Figure 3-10. *Hymedesmia (Hymedesmia) crux* (Schmidt, 1875) a) Appearances specimen DY081 1138, scale bar 2cm; spicules DY081 1138 b) acanthostyle 1, acanthostyle 2, strongle and anchorate isochelae under light microscopy, scale bar 200 µm, c) acanthostyle 1, scale bar 100µm, d) acanthostyle 2, scale bar 50 µm, e) strongle, scale bar 100 µm, f) anchorate isochelae, scale bar 10 µm.

Family Latrunculliidae Topsent, 1922

Genus *Sceptrella* Schmidt, 1870

***Sceptrella matia* sp. nov.**

(Figure 3-11; Table II)

Type material: **Holotype:** Sample in 95% ethanol, tissue section, and spicule preparation on slides. DY081 1127. Station 50, Southwest Greenland (60°5.4100'N, 46°38.2310'W); depth 934 m; collected 28th July 2017.

Paratypes: Sample in 95% ethanol, tissue section, and spicule preparation on slides. DY081 1265. Station 50, Southwest Greenland (60°5.410'N, 46°38.231'W); depth 934 m; collected 28th July 2017.

Diagnosis: Erect, lobate to amorphous *Sceptrella* with areolate porefields. Megascleres styles; microscleres two sizes of isoconicodiscorhabds with furcate whorls of spines.

Description: Erect, lobate to amorphous *Sceptrella* 1-2 cm long. Surface even and non-hispid with areolate porefields. Colour in life and preservation rose-white to yellow-white with a hard incompressible ectosomal layer.

Skeleton: Choanosome: consists of columns of styles (9-12 spicules wide) rising to the ectosome.Isoconicodiscorhabds are scattered throughout the choanosome. Ectosome: a thick (300-1000 µm), dense layer of isoconicodiscorhabds with the ends of the choanosomal style columns extending halfway through the isoconicodiscorhabd crust.

Spicules:

1. **Polytylote styles,** 524-581 x 9-11 µm. straight, polytylote, fusiform, pointed (Holotype). 525-548 x 8-10 µm (Paratype).
2. **Isoconicodiscorhabds 1,** 80-134 µm long, shafts 9-25 µm wide. Stout shaft with each end surrounded by a ring of oblique smooth spines, and at equal distances along the shaft are two whorls of similar smooth spines. The apical whorl is oblique and arranged in a crown-like structure. Spicules are visible in development with simultaneous development of spined whorls (Holotype). 101-133 x 16-24 µm (Paratype).
3. **Isoconicodiscorhabds 2,** 30-57 µm long, shafts 6-11 µm wide. Stout shaft with each end surrounded by a ring of oblique smooth spines, and at equal distances along the shaft are two whorls of similar smooth spines. The apical whorl is oblique and arranged in a crown-

like structure. In some of the smallest examples, the two median whorls merge into the apical whorls, forming a dumbbell-like structure. Spicules are visible in development with simultaneous development of spined whorls (Holotype). 35-63 x 7-10 µm (Paratype).

Distribution: Type specimen recorded from the shelf off the coast of Southwest Greenland in the Labrador Sea, recorded depth 932 m.

Etymology: This species name, derives from matia (Latin) meaning ceremonial mace, and refers to the shape of the isoconicodiscorhabds.

Remarks: Worldwide, there are three species of *Sceptrella* considered valid (van Soest *et al.*, 2021). This species is easily distinguishable from *Sceptrella biannulata* (Topsent, 1892) and S*. insignis* (Topsent, 1890) by their megascleres*. S. biannulata* has perfectly smooth styles (300-400 µm), and *S. insignis* has subtylostyles with a single median swelling (325 µm) compared to the larger polytylote styles in this species. This species is closest to *S. regalis* Schmidt, 1870*,* which has smooth, centrally thickened, fusiform anisostyles (410 µm). However, these are missing the multiple median swellings seen in this species and are slightly smaller. The isoconicodiscorhabds in *S. regalis* come in three size classes (I=50 µm II=70 µm III=127 µm), and the projecting spines are covered with smaller secondary spines. In contrast, our species has two categories of isoconicodiscorhabds with entirely smooth projecting spines. *S. regalis* also has amphiclade sceptres, which are not seen in this species. The habit is also distinctly different between the two; S. *regalis*. is encrusting with oscular processes, whereas this species is lobate to amorphous with areolate porefields.

There are examples of isoconicodiscorhabds in development in this species which correspond almost exactly to the simultaneous development of the spines as seen in S. *regalis* (Samaai, Govender and Kelly, 2004). This ontology of the *Sceptrella* is in contrast to the asynchronous spine development of the *Cyclacanthia* and is a good confirmation of the correct genus (Samaai, Govender and Kelly, 2004).

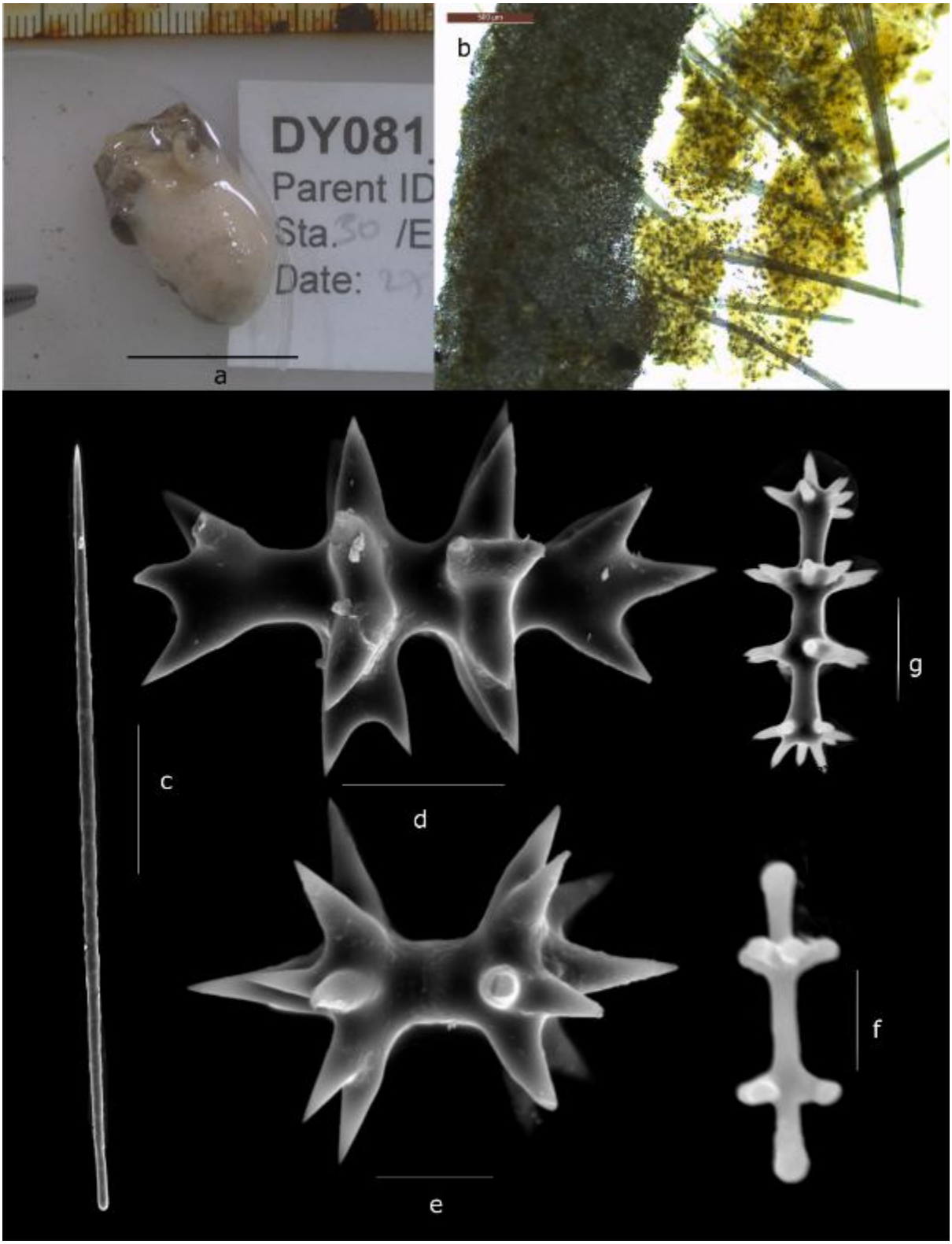

Figure 3-11. *Sceptrella matia* sp. nov. a) Appearance specimen DY081 1127, scale bar 2 cm; b) Skeleton DY081 1127, ectosome to top, scale bar 500 µm; spicules DY081 1127 c) Polytylote style, scale bar 100 µm, d) Isoconicodiscorhabd 1, scale bar 25 µm, e) Isoconicodiscorhabd 2, scale bar 10

µm, f) developmental Isoconicodiscorhabd, scale bar 10 µm. g) developmental Isoconicodiscorhabd, scale bar 25 µm.

Family Microcionidae Carter, 1875

Genus *Clathria* Schmidt, 1862

Subgenus *Clathria (Axosuberites)* Topsent, 1893b

***Clathria (Axosuberites) radix* sp. nov.**

(Figure 3-12; Table II)

Type material: **Holotype:** Sample in 95% ethanol, tissue section, and spicule preparation on slides. DY081 323. Station 50, Southwest Greenland (60°5.2502'N, 46°38.2920'W); depth 772 m; collected 28th July 2017.

Paratypes: Sample in 95% ethanol, tissue section, and spicule preparation on slides. DY081 316. Station 50, Southwest Greenland (60°5.3470'N, 46°38.1930'W); depth 809 m; collected 28th July 2017. Sample in 95% ethanol, tissue section, and spicule preparation on slides. DY081 874. Station 31, Nuuk (63°51.9170'N, 53°16.9250'W); depth 801 m; collected 20th July 2017.

Diagnosis: Dichotomous branching, fan-shaped, *Axosuberites*. Megascleres subtylostyles and styles; microscleres palmate isochelae 22-(26)-28 µm and toxa 95-(248)-355 µm.

Description: Sponge with regular dichotomous branching from a central stem. Branches are in one plane, forming a fan shape. Specimens can reach 16 cm high and 25 cm wide. Branches are approximately circular, hispid, 0.2-(0.3)-0.5 cm in diameter and slightly tapered at the tips. Colour in life and preservation slightly yellow, fading to white at branch ends. Texture hard and non-elastic. Sponge connected to substrate with a structure comprised of several short, clumped root-like processes which anchor it to the sediment.

Skeleton:

Axial skeleton reticulate. Formed of 40 µm thick multispicular tracts of the principal subtylostyles. Subectosomal radial extra-axial skeleton with ascending plumose columns of larger subectosomal auxilliary subtylostyles arising perpendicularly from the edges of the axial skeleton. Ectosome with

discrete plumose bundles of auxillary subtylostyles, arising from the ends of the extra-axial skeleton columns. Microscleres are abundant and scattered through the choanosome.

Spicules:

1. **Principal subtylostyles,** 174-(220)-348 x 9-(12)-14 µm, smooth, slightly curved, occasionally lightly acanthose (Holotype). 194-225 x 11-13 µm (DY081 316), 202-356 x 22-24 (DY081 874) (Paratypes).
2. **Subectosomal subtylostyles 1,** 1186-(1228)-1606 x 10-(13)-15 µm, smooth straight with swollen heads curved echinating subtylostyles (Holotype). 1190-1596 x 10-(13)-15 µm (DY081 316), 1359-1440 x 12-(13)-15 (DY081 874) (Paratypes).
3. **Subectosomal subtylostyles 2,** 609-(652)-855 x 5-8-10 µm, very straight close to tylostyle (Holotype). 560-782 x 5-(7)-8 µm (DY081 316), 610-800 x 5-(8)-10 (DY081 874) (Paratypes).
4. **Auxillary subtylostyles** 380-(500)-724 x 4-(5)-7 µm, larger onesoccasionally slightly curved (Holotype). 400-710 x 5-7 µm (DY081 316), 390-720 x 4-8 (DY081 874) (Paratypes).
5. **Toxa**, 94-(225)-388 µm, large, winged with a distinct narrow and deep central flexure (Holotype). 97-355 µm (DY081 316), 103-287 (DY081 874) (Paratypes).
6. **Palmate isochelae**, 22-(26)-28 µm long, with alae approximately 1/3 of total length (Holotype). 24-26 µm (DY081 316), 22-28 (DY081 874) (Paratypes).

Distribution: Recorded from the shelf off the coast of Greenland in the Labrador Sea, from both the shelf off Nuuk and the Southern tip of Greenland, recorded depth 770-862 m.

Etymology: This species name, derives from *radix* (Latin), meaning root, and refers to the shape of the branching morphology

Remarks: This is the first recorded species of *Clathria (Axosuberites)* from the North Atlantic. There are 23 species currently considered valid (van Soest *et al.*, 2021) reviewed in Annunziata et al., 2019 with two species described subsequently by Fernandez et al., 2020. All but one of these have been described from the southern hemisphere, with only *C. (A.) lambei* (Koltun, 1955)reported from the Pacific Arctic (Koltun, 1955). This species is distinct from *C. (A.) lambei* as *C. (A.) lambei* lacks toxa and has two types of acanthostyles (lightly spined 36-218 µm, heavily spined 166-384 µm). The single category of toxa in this species have a similar size range to the toxa of *C. (A.) canaliculata* (Whitelegge, 1906) (18-(220)-550 µm), *C. (A.) georgianensis* Hooper, 1996 (30-540 µm), and *C. (A.) ramea* (Koltun, 1964). However, the bend in the centre of toxa of *C. (A.) canaliculata* and *C. (A.) georgianensis* as far less exaggerated than seen in this species. In addition, *C. (A.) canaliculata* has smaller subtylostyles (80-(114)-165 µm) as well as an additional smaller category of chelae (I=4-(4.6)-8 µm II=14-(17.5)-22 µm). *(A.) georgianensis* as well as differing toxa has no subtylostyles and smaller chelae (9-15 µm). *C. (A.) ramea* is easily distinguished by the lack of chelae and much larger styles (700-1500 µm).

The toxa of *C. (A.) fromontae* Hooper, 1996 (I=275-(377)-470 II= 40-(46)-55 µm), *C. (A.) macrotoxa* (Bergquist and Fromont, 1988) (I=275-(377)-470 µm II= 42-(48)-53 µm), *C. (A.) multitoxaformis* (Bergquist and Fromont, 1988) (I=150-(178)-220 µm II= 170-(174)-180 µm III= 33-(39)-43 µm), and *C. (A.) rosita* Goodwin et al., 2012 (I=51-327 µm II=15-34 µm), all fall into the same size range seen in this species. However, this species has only one type of toxa, whereas the other species have several forms of toxa. *C. (A.) fromontae* has long and thin toxa with slight central flexure and a fine toxa with a wide central flexure. The toxa of *C. (A.) macrotoxa,* and *C. (A.) multitoxaformis* a have a wide central flexure. *C. (A.) rosita* does not have chelae aand has much smaller subtylostyles.

All other deepwater species either lack toxa (*C. (A.) riosae* van Soest, 2017*,* and *C. (A.) aurantia* Annunziata et al., 2019*,* or the size range of the toxa is outside of the range seen here (*C. (A.) cylindrica*(Ridley and Dendy, 1886) (45-86-130 µm), *C. (A.) marplatensis* (Cuartas, 1992) (I=560-1000 µm II=235-400 µm), *C. (A.) nidificata* (Kirkpatrick, 1907) (638 µm), *C.(A.) pachyaxia* (Lévi, 1960) (50-80 µm), and *C. (A.) thetidis* (Hallmann, 1920) (I=175-(774)-1280 µm II=22-(104)-168 µm).

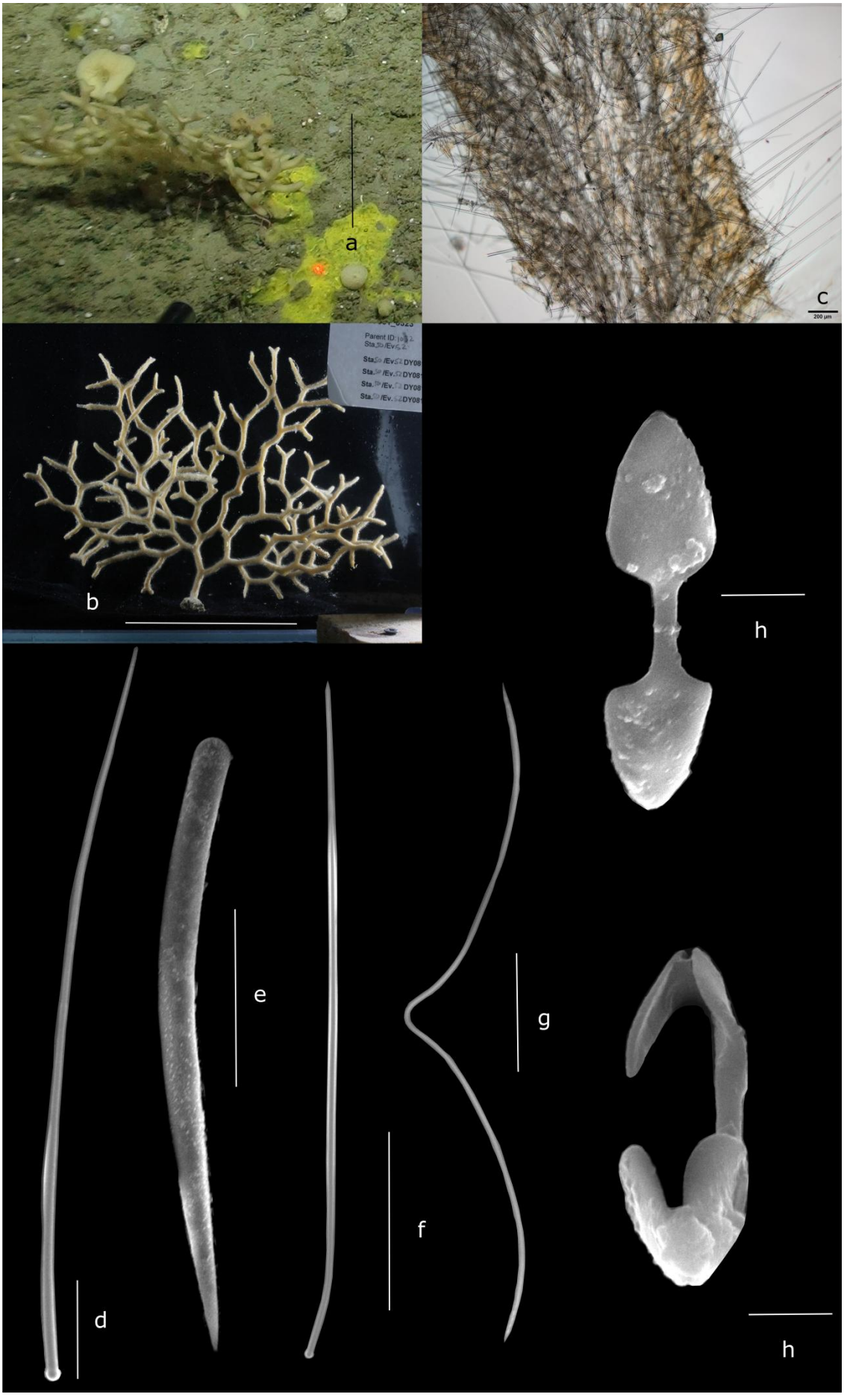
a
c
200 µm
b
h
e
g
f
d
h

Figure 3-12. *Clathria (Axosuberites) radix* sp. nov. a) *In situ* appearance specimen DY081 323, scale bar 10 cm; b) appearance specimen DY081 323, scale bar 10 cm; c) Skeleton DY081 323, extremity to top, scale bar 200 µm; spicules DY081 323 d) auxillary subtylostyle, scale bar 50 µm, e) principal subtylostyle, scale bar 100 µm, f) subectosomal subtylostyle, scale bar 250 µm, g) toxa, scale bar 50 µm, h) palmate isochelae, scale bar 5 µm.

Family Myxillidae Dendy, 1922

Genus *Stelodoryx* Topsent, 1904

***Stelodoryx groenlandica* sp. nov.**

(Figure 3-13; Table II, V)

Type material: **Holotype:** Sample in 95% ethanol, tissue section and spicule preparation on slides. DY081 1231. Station 50, Southwest Greenland (60°5.3740'N, 46°**'W); depth 973 m; collected 27th July 2017.

Diagnosis: Small, irregular encrusting *Stelodoryx* with a finely hispid surface. Megascleres tornotes and styles; microscleres two categories of arcuate isochela.

Description: Irregularly encrusting and with no visible oscula. Sponge 2 cm in diameter 1 cm in thickness. Encrusting around the base of a dead bivalve, in irregular tufts. Colour in life white to yellow, white in alcohol. When broken it appears to be made up of hair-like strands connected together.

Skeleton: Choanosome: Styles forming multispicular strands and plumoreticulate tracts, microscleres throughout. Ectosome: vertical brushes of tornotes and microscleres.

Spicules: (Table V.)

1. **Styles,** 361-1073 x 14-(18)-24 µm, smooth along length, head slightly tylote in some cases.
2. **Tornotes,** 360-400 µm long 4-(6)-7 µm wide, conical points straight smooth shafts.
3. **Arcuate isochelae 1**, 66-(69)-74 µm long, four to six long needle like alae 40% of total length, slightly curved shaft.
4. **Arcuate isochelae 2**, 43-(47)-49 µm long, four to six long needle like alae 45% of total length with small gap between opposite alae, slightly curved shaft.

Distribution: Recorded from the shelf off the coast of the Southern tip of Greenland in the Labrador Sea, recorded depth 972 m.

Etymology : This species is named after Greenland, referring to the type location.

Remarks: Five species of *Stelodoryx* are currently known from the North Atlantic and Arctic (van Soest *et al.*, 2021). *S. flabellata* Koltun, 1959 and *S. pectinata* (Topsent, 1890) can be distinguished as their choanosomal skeleton is formed of acanthostyles rather than styles. Several other species can be distinguished from *S. groenlandica* by their possession of ornamented tornotes in contrast to smooth conical points: *S. pluridentata* (Lundbeck, 1905) has tornotes with acanthose ends, in *S. procera* Topsent, 1904, and *S. toporoki* Koltun, 1958, the tornote heads are microspined. Aside from the tornotes, *S. pluridentata* has very large, long-toothed chela (71-115 µm) compared to the largest category of chela in this species and lacks the second category of smaller chela. *S. toporoki* has a funnel-shaped morphology, much bigger long-toothed chela (119-157 µm) and a second category of short toothed chela. *S. procera*, possesses two categories of styles (I=350-400 µm II=620-700 µm), the large toothed chelae are slightly smaller with outward splayed alae (35-55 µm) and is an erect, lobate leaf shape.

Stelodoryx groenlandica can be distinguished from *Stelodoryx rictus* by a number of features. *S. groenlandica* has a small category of chela with 4-6 very long alae which almost meet, compared with the three very short alae seen in *S. ora*. *S. groenlandica* only has one category of tornotes lacking the curved, larger and thicker tornotes (414-(520)-622/14-(18)-24 µm) of the two categories seen in *S. ora*. The styles seen in *S. groenlandica* are straight with slightly tylote heads in some cases compared to the slightly curved and shorter styles (581-(650)-725 µm) of *S. rictus* with no slightly tylote individuals seen. The overall morphology is also very different with *S. groenlandica* being encrusting compared with the erect leaf shape of *S. ora.*

Worldwide there are 18 species of *Stelodoryx* considered valid (Table V.) (van Soest *et al.*, 2021) However, of those not from the North Atlantic or Arctic, seven have tylotes with microspined heads, and two more do not have ectosomal styles, *S. dubia* (Burton, 1928) has two categories of acanthostyles (I=280 µm II=70 µm) and *S. strongyloxeata* Lehnert & Stone, 2020, has strongyleoxea (245-290-318 µm). The remaining species is distinguished by having smaller styles than this species in combination with other spicule variations. *S. multidentata* (Boury-Esnault and Van Beveren, 1982) has polytylote tornotes (255-312 µm), two categories of chela, with the first having 5-12 alae (I=32-58 II=15-17), and smaller styles (455-520 µm). *S. argentinae* Bertolino et al., 2007, has two

categories of small styles (I=287-(351)-412 II=188-(220)-260) and anisostrongyles with spined ends (209-(240)-262 µm). *S. siphofuscus* Lehnert & Stone, 2015, has two categories of styles (I=328-412 II=228-335), the smaller having an apical tooth but no tornotes. Finally, *S. lissostyla* (Koltun, 1959) has styles(332-421 µm), tornotes (260-332 µm), and chela (I=26-30 µm II=13-17 µm), which are considerably smaller.

Table V. Spicule dimensions of global *Stelodoryx* Species.

Stelodoryx Species	**Choanosomal styles µm**	**Ectosomal tornotes µm**	**isochela µm**	**other µm**
***S. flabellata* Koltun,1959**	microspined stles and stongles 322-425 x 12-20	smooth 250-312 x 4-6	polydentate 56-72	none
***S. pectinata* (Topsent, 1890) (measurements from Topsent, 1892)**	acanthostyles 465 x 16	smooth 415 x 5	two categoriess, 10 alae i= 60, ii=20	none
***S. pluridentata* (Lundbeck,1905) (measurements from Koltun, 1958)**	smooth 320-520 x 9-23	microspined ends 176-320 x 5-11	71-115	none
***S. procera* Topsent, 1904**	two catagories of smooth styles i=350-400 x 12 ii= 620-700 x 12	smooth 235-300	splayed, wide flat alae 45	none
***S. toporoki* Koltun, 1958**	smooth, rarely microspined 509-1140 x 21-31	microspined ends 218-300 x 8-10	two categories, 4-5 alae i=119-157, ii=31-40	none
***S. argentinae* Bertolino, 2007**	two catagories of smooth styles i= 287-412 x 10-15 ii= 118-260 x 2	anisostrongles with microspined ends 209-262 x 5-10	spatuliferous, 5 alae 40-65	none
***S. chlorophylla* Lévi, 1993**	mucronate base 650-780	tylostyles microspined ends 450	three categories i= 55-60, ii=30-35, iii=13-14	none
***S. cribrigera* (Ridley & Dendy, 1886)**	smooth 650 x 25	tylotes with microspined ends 300 x 8	three alae 80	none
***S.dubia* (Burton,1928)**	two catagories of acanthostyles i= 280 x 20 ii= 70 x 11	end shape variable (oval, hastate, mucronate or globular) 140 x 4	5 splayed thin alae 11	sigmata 42
***S. jamesorri* Lehnert & Stone, 2020**	styles to stronglyloxeas, 325-657 x 33-45	tylotes microspined ends 212-315 x 8-12	two categories i=82-135, ii=27-32	none
***S. lissostyla* (Koltun,1959)**	smooth rarely microspined 332-421 x 11-13	smooth 260-332 x 5-6	two categories i=26-30, ii=13-17	none
***S. mucosa* Lehnert & Stone, 2015**	acanothostyles 395-452 x 11-29	microspined ends 205-252 x 8-10	45-67	fine sigmas, 13-18
***S. multidentata* (Boury-Esnault & van Beveren, 1982)**	smooth 455-520	polytylotes 255-312	two catagories i (5-12 alae) = 32-58, ii (3 alae) = 15-17	none
***S. oxeata* Lehnert, 2006**	oxeas microspined heads 517-558 x 20-30	microspined ends 230-270 x 9-11	three catagories i=54-110, ii=23-32, iii=9-13	centrotylote sigmas,8-12
***S. phyllomorpha* Lévi, 1993**	smooth 700-750	styles with microspinned ends 450-530	three catagories i (3 alae) = 45-55, ii (3 alae)= 30, iii (7 alae) = 18-25	sigmas 20
***S. siphofuscus* Lehnert & Stone, 2015**	smooth styles 328-412 x 13-20	styles somtimes with an apical tooth 228-335 x 8-10	two catagories i= 72-91, ii= 28-45	none
***S. strongyloxeata* Lehnert & Stone, 2020**	stongyloxeas 245-318 x 15-35	style like tornotes 142-205 x 4-10	two catagories i= 67-96, ii=23-40	none
***S. vitiazi* (Koltun, 1955)**	acanthostyles 436-520	microspined ends 190-291	26-46	none
***S. groenlandica sp.nov*. DY081 - 1231 (Holotype)**	smooth rarely slightly tylote 361-1073 x 14-24	smooth 360-400 x 4-7	two catagories 4-6 alae i= 66-69-74, ii = 43-47-49	none
***S. rictus sp.nov*. DY081 - 42(Holotype)**	smooth 581-(650)-725 x 16-(24)-32	two catagories i = 414-(520)-622 x 14-(18)-24, ii = 371-(400)-414 x 3-7-9	two catagories i (5 alae) = 49-(52)-61, ii (3 alae) = 56-57	none
S. rictus sp.nov. DY081 - 243 (Paratype)	smooth 639-715	two catagories i= 420-433 x 15-18, ii = 402-415 x 5-7	two catagories i (5 alae) = 49-59, ii (3 alae) = 56-58	none
S. rictus sp.nov. DY081 - 82(Paratype)	smooth 620-650-694	two catagories i =577-(650)-702 x 15-(17)-24, ii = 383-(400)-445 x 3-6-10	two catagories i (5 alae) = 48-(60)-81, ii (3 alae) = 54-(56) -60	none

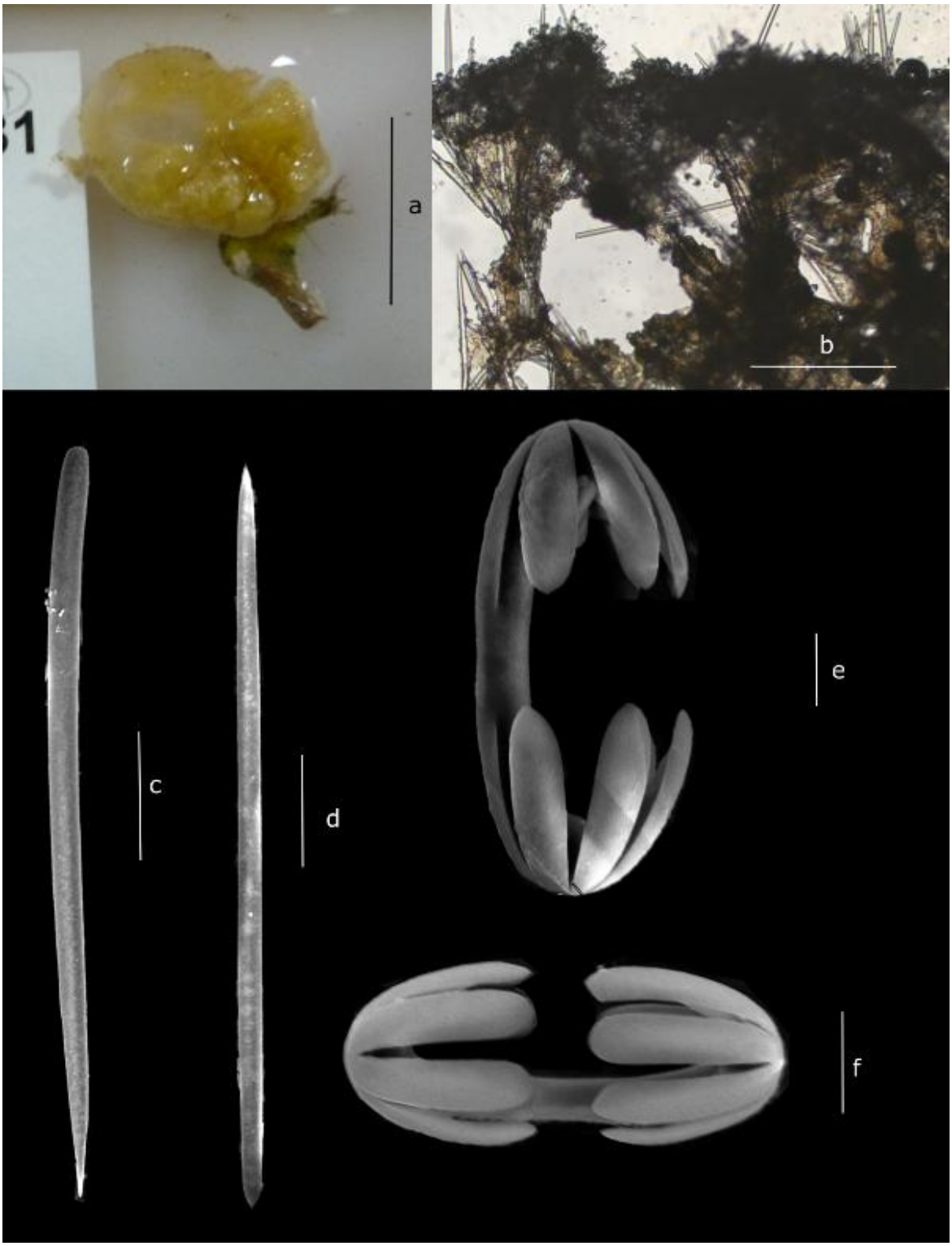

Figure 3-13. *Stelodoryx groenlandica* sp. nov. a) *A*ppearance specimen DY081 1231, scale bar 2 cm; b) Skeleton DY081 1231, ectosome to top, scale bar 500 µm; spicules DY081 1231 c) style, scale bar 25 µm, d) tornote, scale bar 25 µm, e) arcuate isochela 1, scale bar 10 µm, f) arcuate isochela 2, scale bar 10 µm.

***Stelodoryx rictus* sp. nov**

(Figure 3-14; Table II, V)

Type material: **Holotype:** Sample in 95% ethanol, tissue section and spicule preparation on slides. DY081 42. Station 5, Orphan Knoll (50°2.9080'N, 45°22.5430'W); depth 3450 m; collected 8th July 2017.

Paratypes: Sample in 95% ethanol, tissue section and spicule preparation on slides. DY081 243. Station 5, Orphan Knoll (50°2.9170'N, 45°22.5540'W); depth 934 m; collected 8th July 2017.

Diagnosis: Erect foliaceous *Stelodoryx* with lobate margin and a short peduncle. Megascleres styles and two categories of tornotes; microscleres three categories of arcuate isochelae.

Description: Erect, lobate leaf shape with a short stem, plumoreticulate skeletal tracts clearly visible. Specimen 8cm long 2.5 cm wide, 2 mm thick. Colour in life yellow-brown at edges, darkening toward centre, with dark brown veins.

Skeleton: Choanosome: Styles and tornotes forming thick plumoreticulate multispicular tracts, which get thinner towards the periphery. Microscleres abundant throughout. Ectosome: vertical brushes of tornotes and microscleres.

Spicules: (Table V.)

1. **Styles,** 581-(650)-725 x 16-(24)-32 µm, smooth, curved.
2. **Tornotes 1,** 414-(520)-622 x 14-(18)-24 µm, conical points, curved smooth shafts.
3. **Tornotes 2**, 371-(400)-414 x 3-(7)-9 µm, thinner, conical points, straight smooth shafts.
4. **Arcuate isochelae 1**, 49-(52)-61 µm long, five long rounded alae 45% of total length with small gap between opposite alae, shaft very slightly curved.
5. **Arcuate isochelae 2**, 56-57 µm long, curved shaft three sharp alae fifth of total length.

Distribution: Recorded from the Orphan Knoll seamount in the Labrador Sea, off the coast of Newfoundland, Canada. Recorded depth 3449-3450 m.

Etymology : The name of this species, *rictus* (Latin), refers to the shape of the large arcuate isochelae

Remarks:

Five species of *Stelodoryx* are currently known from the North Atlantic and Arctic (van Soest *et al.*, 2021). *Stelodoryx flabellata* (Koltun, 1959) and *S. pectinata* (Topsent, 1890) can be distinguished from this species as their choanosomal skeleton is formed of acanthostyles rather than styles.Several other species can be distinguished from *Stelodoryx* sp. nov. by the possession of ornamented

tornotes, which are in contrast to the smooth conical points of the tornotes in this species: *S. pluridentata* (Lundbeck, 1905) has tornotes with acanthose ends, *S. procera* Topsent, 1904 and *S. toporoki* Koltun, 1958, the tornote heads are microspined. Aside from the tornotes, *S. pluridentata* has very large, long-toothed chelae (71-115 µm) compared to this species and lacks the second category of short-toothed chelae. *S. toporoki* has a funnel-shaped morphology and much bigger long-toothed chelae (119-157 µm) The morphology of this species is probably closest to *S. procera*, however *S. procera* possesses two categories of styles (I=350-400 µm II=620-700 µm), and the large toothed chelae are slightly smaller with outward splayed alae (35-55 µm).

Stelodoryx rictus can be distinguished from *Stelodoryx groenlandica* by a number of features, as discussed above.

Worldwide there are 18 species of *Stelodoryx* considered valid (Table V.) (van Soest *et al.*, 2021) However, of those not from the North Atlantic or Arctic, seven have tylotes with microspined heads, and two more do not have ectosomal styles, *S. dubia* (Burton, 1928) has two categories of acanthostyles (I=280 µm II=70 µm) and *S. strongyloxeata* Lehnert & Stone, 2020 has strongyleoxea (245-290-318 µm). The remaining species are distinguishable by having smaller styles than this species, combined with other spicule variations. *S. multidentata* (Boury-Esnault and Van Beveren, 1982) has polytylote tornotes (255-312 µm), two categories of chela, with the first having 5-12 alae (I=32-58 II=15-17) and slightly smaller styles (455-520 µm). *S. argentinae* Bertolino et al., 2007 has two categories of small styles(I=287-(351)-412, II=188-(220)-260) and anisostrongyles with spined ends (209-(240)-262 µm). *S. siphofuscus* Lehnert & Stone, 2015 has two categories of styles (I=328-412, II=228-335), the smaller having an apical tooth but has no tornotes. Finally *S. lissostyla* (Koltun, 1959) probably has the closest spicule compliment to this species; however, the styles (332-421 µm), tornotes (260-332 µm) and chela (I=26-30 µm II=13-17 µm) are all considerably smaller.

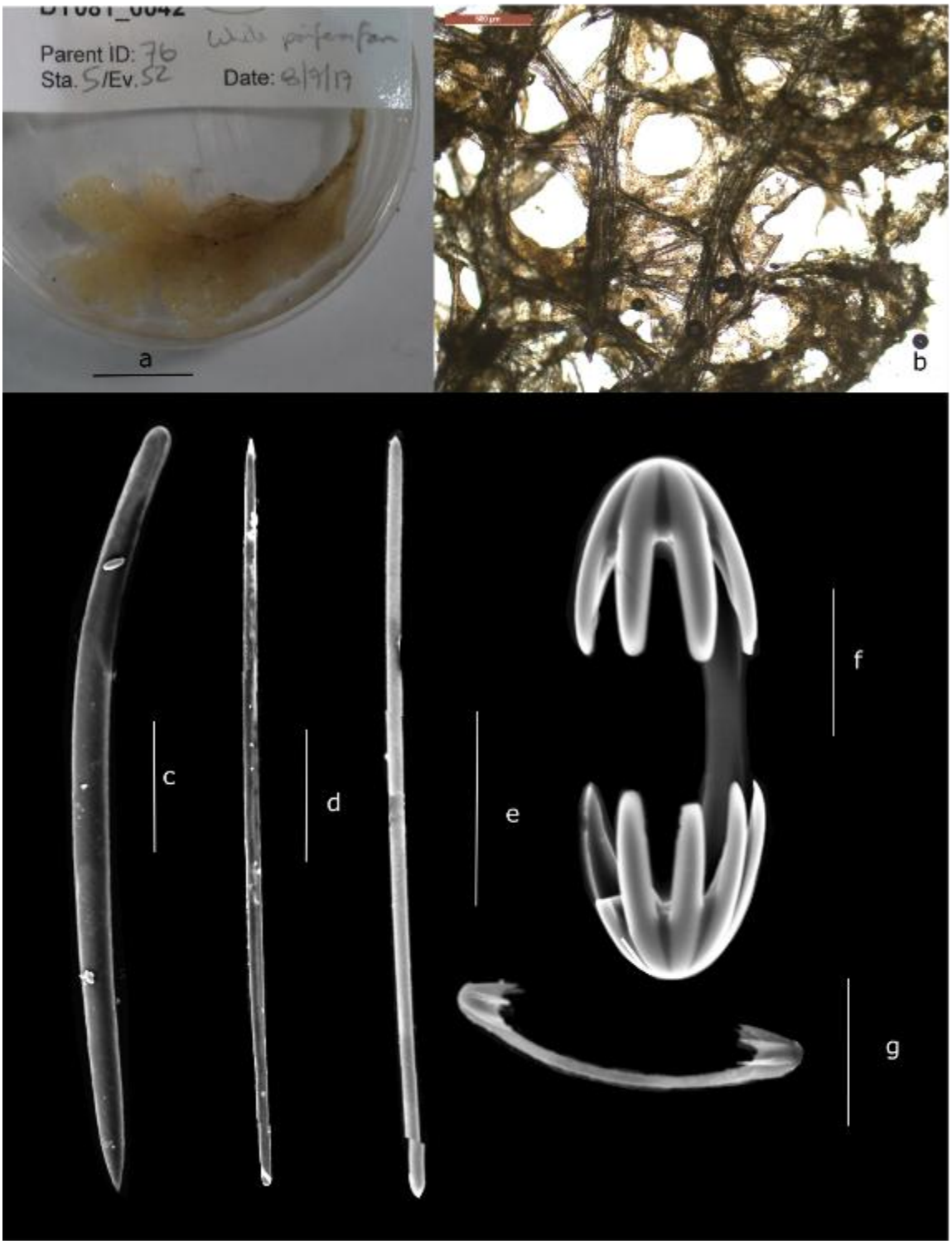

Figure 3-14. *Stelodoryx rictus* sp. nov. a) *A*ppearance specimen DY081 42, scale bar 2cm; b) Skeleton DY081 42, scale bar 500µm; spicules DY081 42 c) style, scale bar 100µm, d) tornote 1, scale bar 100 µm, e) tornote 2, scale bar 100 µm, f) arcuate isochela 1, scale bar 10µm, g) arcuate isochela 2, scale bar 10 µm.

Class Homoscleromorpha Bergquist, 1978

Order Homosclerophorida Dendy, 1905

Family Plakinidae Schulze, 1880

Genus *Plakina* Schulze, 1880

***Plakina jactus* sp. nov.**

(Figure 3-15; Table II)

Type material: **Holotype:** Sample in 95% ethanol, tissue section and spicule preparation on slides. DY081 1159. Station 50, Southwest Greenland (60°5.4100'N, 46°38.2310'W); depth 934 m; collected 28th July 2017.

Diagnosis: Globular, massively encrusting *Plakina*. Single category of tetralophose calthrops.

Description: massively encrusting forming elongated globular structure with a flattened base. Surface hard and smooth, subectosomal cavities visible through the ectosome in places. Sponge 4.1 cm by 2 cm wide with a thickness of 0.9 cm. Colour in life off white, white in alcohol.

Skeleton: Choanosome: unstructured, loosely arranged tetralophose calthrops. Ectosome: Densely packed tetralophose calthrops forming crust 200 µm thick.

Spicules:

1. **Tetralophose calthrop 1,** 39-(47)-67 µm diameter, actines 15-(18)-24 µm long. Showing ramification pattern '1m' with all actines branching into two or three midway along. There are rare examples where one actine is not branched.
2. **Tetralophose calthrop 2,** 37-(45)-66 µm diameter, actines 16-(18)-23 µm long. Showing general ramification pattern '1m' for three of the actines branching into three midways along. The fourth actine has a ramification pattern of '1m, ts' the secondary ramification at the tips forming two to four rounded buds. There are small, rounded budding along the actins between the two ramifications, however, these do not constitute a true additional ramification.

Distribution: Recorded from the shelf off the Sothern tip of Greenland in the Labrador Sea, recorded depth 934 m.

Etymology: The name of this species derives from *jactus* (Latin), meaning to throw, and refers to the shape of the tetraplophose calthrops, which resembes a throwing jack, these derive their name from this root.

Remarks: There are currently three species of *Plakina* in the North Atlantic (van Soest *et al.*, 2021). All three have a mixture microcathrops and lophocathrops with at least one category with severely reduced actines. *P. monolopha* Schulze, 1880, and *P. trilopha* Schulze, 1880, are both Mediterranean species but have been recorded in the Eastern Atlantic, with *P. brachylopha* Topsent, 1927 described from the Azores. The lophose calthrops of *P. brachylopha* are distinct from those seen here. They have only one actine showing a ramification pattern usually with two rounds of ramification and one or two other actines commonly being missing or reduced. *P. brachylopha* also has a category of irregular almost sinuous microcathrops which are not present here. *P. trilopha* has 9 categories of spicules ranging from diods, triodes cathrops to trilophose cathrops, distinctly different to the two categories of tetralophose calthrops seen here. The trilophose calthrops of *P. trilopha* (17-(21)-24 µm) look similar to the unadorned category of tetralophose calthrops seen here, however they are considerably smaller. *P. monolopha* again has diods triodes and calthrops that have no ramification. The lophose calthrops of *P. monolopha* have an initial median ramification and a secondary ramification at the tip of a single actine, unlike the ramification on all of the actines of both categories of tetralophose calthrops recorded in this species. This species is distinct from the other *Plankina* restricted to the Mediterranean as they all lack branching calthrops and the lophose calthrops are all smaller than those measured here (Lage *et al.*, 2018).

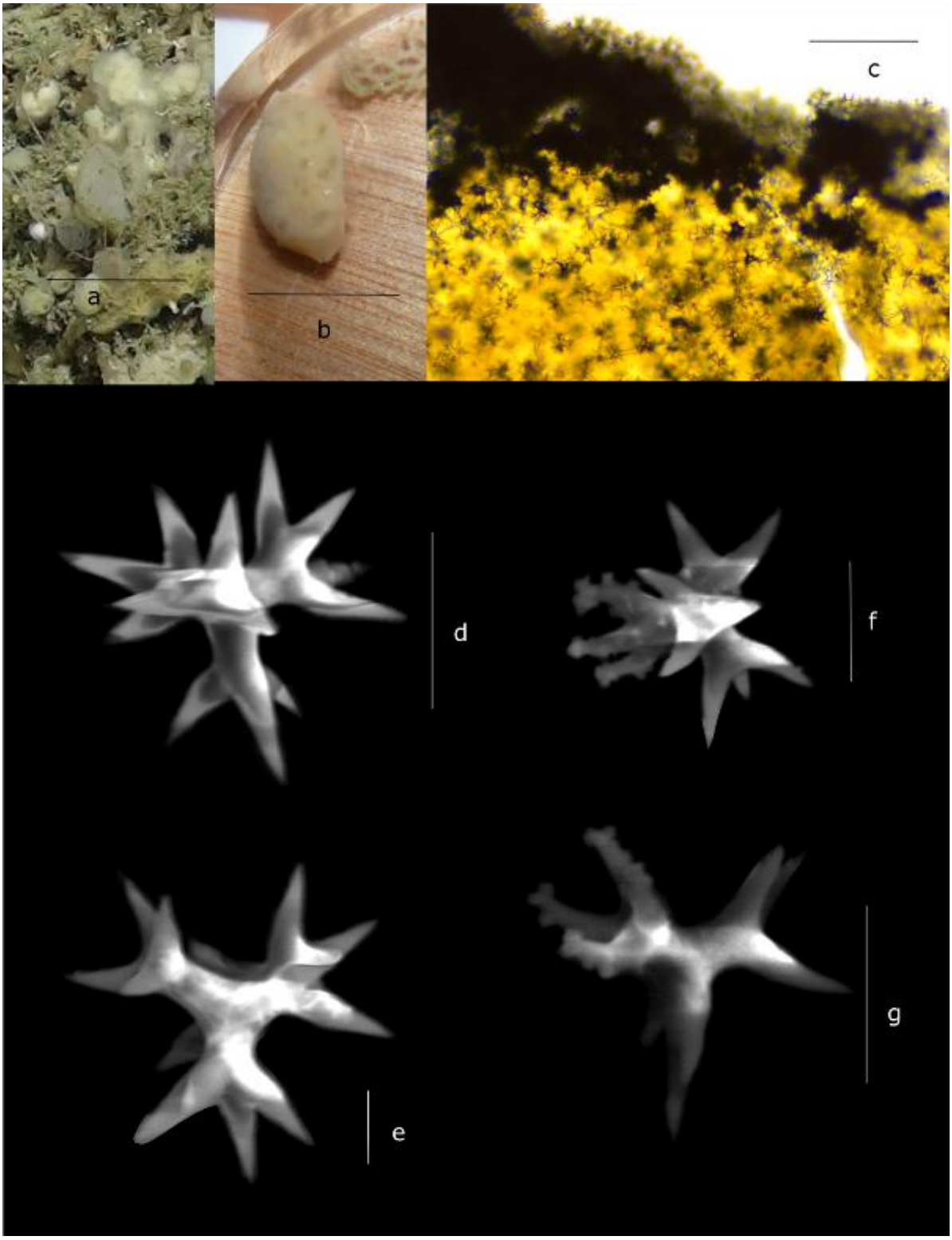

Figure 3-15. *Plakina jactus* sp. nov. a) *In situ* appearance specimen DY081 1159 scale bar 5 cm; b) Appearance of specimen DY081 1159 post collection, c) Skeleton DY081 1159, ectosome to top, scale bar 200 µm; spicules DY081 1159 d) tetralophose calthrop 1, scale bar 25 µm, e) tetralophose calthrop 1 , scale bar 10 µm, f) tetralophose calthrop 2, scale bar 20 µm, g) tetralophose calthrop 2, scale bar 25 µm.

3.5. Discussion

Of the 67 species recorded in this study, 13 are new to science, and 13 are new records from the Labrador Sea and West Atlantic (Table 2). All the species new to science, and the majority of those which are new records for the area, are either encrusting, very small (< 5cm), or fragile. These morphologies of sponges are unlikely to have been sampled effectively before, as most of the sampling in the area has been done using remote sampling methods such as trawling and dredging (Vacelet and Perez, 1998). Using these sampling techniques would – in all likelihood – have lost or destroyed these new species. The use of an ROV enabled the collection of delicate and encrusting species. In particular, the suction apparatus on the ROV allowed the collection of thinly encrusting and very small species that would usually be impossibly to sample even with a standard ROV robotic arm. It also enabled the effective sampling of steep bedrock habitats where the highest sponge occurrences are found (Willenz *et al.*, 2009). It is impossible to effectively sample these using dredging and trawling due to the risk of gear entanglement and the ineffective nature of sampling gear on this substrate. Therefore, sampling using the ROV has enabled us to capture a more complete picture of species diversity and provides *in situ* observations of the species recorded. This information is of great value to field surveyors, and to studies looking at the wider ecological distribution of species in the area as, having been confirmed with specimens, it may be possible to identify many of these from imagery in the future. This lack of information about encrusting species is a common problem even in well-studied localities such as the waters around the United Kingdom (Picton and Goodwin, 2007b; Goodwin and Picton, 2009; Willenz *et al.*, 2009).

The species assemblages recorded in this study most closely resemble that of the Faroese sponge grounds and more broadly the general boreal sponge grounds of the North East Atlantic (Klitgaard and Tendal, 2004). However, there are still fewer species described here than recorded from the Eastern Atlantic at a similar latitude (van Soest *et al.*, 2012; 2021). recent work has significantly increased the number of species recorded from the Western Atlantic (Hestetun, Tompkins-Macdonald and Rapp, 2017b; Baker *et al.*, 2018; Dinn and Leys, 2018; Murillo *et al.*, 2018; Dinn, Edinger and Leys, 2019; Dinn *et al.*, 2020), suggesting that this low species diversity may be down to a sampling bias. This study supports this theory given the high numbers of species previously not recorded in the Labrador Sea.

The Labrador Sea, particularly the west coast of Greenland off Nuuk, appears to have a very high sponge species diversity. At each sampling locality, we recorded a high number of distinct species: 31 off Orphan knoll, 41 off Nuuk Greenland, and 16 off Southwest Greenland (SWGL). The lower

number of sponge species off SWGL is probably due to the lower number of collection stations and therefore samples collected. Only *Geodia barretti* Bowerbank, 1858, and *Stryphnus fortis* (Vosmaer, 1885) are present across all three localities, with 15 species present at two localities. Nuuk and SWGL have the greatest overlap of species, with 14 species present at both localities compared with four shared between SWGL and Orphan Knoll, and only three between Nuuk and Orphan knoll. This overlap between the two Greenland localities is probably due to similarities in environmental conditions.

The sampling stations off Nuuk and SWGL are influenced by two water masses: the Subpolar Mode Water (SPMW) and the arctic derived South Greenland Coastal Waters (CW) with melt water runoff from the Greenland Ice sheets. These waters masses are gradually modified as they move further North, until they encounter the Baffin Bay Polar Water (Talley and McCartney, 1982; Lavender, Davis and Owens, 2000; Yeager and Jochum, 2009; Rysgaard *et al.*, 2020). The SPMW has temperature of 4-6 °C and Salinity of 34- 35 with the CW having temperatures of 0 °C and salinity 33 (Talley and McCartney, 1982; Lavender, Davis and Owens, 2000; Yeager and Jochum, 2009; Talley *et al.*, 2011; Rysgaard *et al.*, 2020). All specimens collected were deep enough to be primary within the SPMW (**Chapter 1.** Figure 1-8, 1-9, 1-10, 1-11). In contrast, Orphan knoll sits in the fluctuation zone between the Labrador Sea Water (LSW) and the North Atlantic Deep water (NADW) (Talley and McCartney, 1982; Lavender, Davis and Owens, 2000; Yeager and Jochum, 2009; Talley *et al.*, 2011). The LSW and NADW have similar temperature and salinity profiles. The LSW having temperatures of 4 °C and salinity 35, with NADW temperatures of 3 °C and salinity 35 (Talley and McCartney, 1982; Lavender, Davis and Owens, 2000; Yeager and Jochum, 2009; Talley *et al.*, 2011; Rysgaard *et al.*, 2020) however, there is a significant difference in oxygen levels with oxygen concentrations of LSW around 290 Mm/L and NADW at 270 Mm/L (Talley and McCartney, 1982; Lavender, Davis and Owens, 2000; Yeager and Jochum, 2009; Talley *et al.*, 2011)These different water masses interact to produce very different ocean conditions at each site and may explain the variability between the three sites (Howell *et al.*, 2016). The effect of these water masses can be seen in the species at Orphan Knoll, which appear to have a mix of boreal and arctic species due to the presence of both the Arctic Labrador Sea Water and the more southerly North Atlantic Deep Water (Murillo *et al.*, 2012, 2018). We see this mixing of species in the *Geodia* Lamarck, 1815; the Orphan Knoll site has both typically Arctic (*Geodia parva* Hansen, 1885) and boreal species (*Geodia barretti* Bowerbank, 1858, *Geodia macandrewii* Bowerbank, 1858, *Geodia phlegraei* Sollas, 1880) together (Cárdenas, Rapp, Klitgaard, *et al.*, 2013). This pattern has been observed in the *Geodia* Lamarck, 1815 present at Flemish Cap, Flemish Pass and the Grand Banks of Newfoundland (Cárdenas, Rapp, Klitgaard, *et al.*, 2013). However, there are more Arctic species present at Orphan knoll than Flemish Cap, Flemish Pass, and

the Grand Banks of Newfoundland (Murillo *et al.*, 2012), potentially due to the increased influence of the Labrador Sea Water at Orphan Knoll. The Greenland assemblages have a higher occurrence of more typical Arctic species, although they differ considerably from the assemblages seen further north in Baffin Bay (Murillo *et al.*, 2018; Dinn *et al.*, 2020). This is probably due to the very cold saline Baffin Bay Polar Water mass not extending as far south as either Nuuk or SWGL. Interestingly there were very few *Geodia* Lamarck, 1815, present at both Greenland sites and all belonged to one species (*Geodia barretti* Bowerbank, 1858). The lack of *Geodia* Lamarck, 1815, diversity is not what would be expected for the region (Cárdenas, Rapp, Klitgaard, *et al.*, 2013; Knudby, Kenchington and Murillo, 2013; Howell *et al.*, 2016), and may be due to the unique interaction of the local water masses. Further work looking at the environmental variables and drivers of distribution of these species would be valuable, particularly looking at how the changing climate will affect this ecosystem.

The observations in this study of high abundance and biodiversity of sponges at all the sampling sites both off Eastern Canada and off the west coast of Greenland has potential implications for the marine policy in the area. Particularly the presence of VME indicator species, both those forming deep sea sponge aggregations (*Geodia* Lamarck, 1815, *Stelletta* Schmidt, 1862) and hard-bottom sponge garden forming species (*Mycale (Mycale) lingua* (Bowerbank, 1866), *Polymastia* Bowerbank, 1862, *Axinella* Schmidt, 1862, *Craniella cranum* (Müller, 1776), etc) off Greenland. Identification of these 'sponge grounds' (Klitgaard and Tendal, 2004; Hogg, Tendal and Conway, 2010; Wei *et al.*, 2020) and the additional taxonomic information should help to improve more comprehensive distribution models of these VME in the Labrador Sea. Hopefully, this will lead to increased protection – or at least an increase in monitoring – of the ecological health of the West Greenland sponge grounds.

3.6. Acknowledgments

This research was funded by the European Research Council (ERC Starting Grant 678371 ICY-LAB). We would like to thank Paco Cardenas, Alexander Plotkin, Joana Xavier and Toufiek Samaai for their helpful discussion and assistance regarding aspects of sponge taxonomy. The organizers of the 5th International Workshop on Taxonomy of Atlanto-Mediterranean Deep Sea and Cave Sponges, Marseille, for the introducing TC to sponge taxonomy. Michelle Taylor who was responsible for the biological collection on the DY081 Cruise. Emily Rayfield and Jeremy Philips for their advice and

general discussion. Finally, many thanks to the Master and crew of the RRS discovery with a particular thanks to the ROV pilots David Turner, Allan Davies, David Edge, Russell Locke, Ella Richards, Josue Viera Rivero and Andrew Webb

4. Chapter 4. Sponge Biogeography within the Southern Labrador Sea

Author contributions and declaration:

T.Culwick, conceived the study. T.Culwick carried out the study. T.Culwick interpreted and processed the data with the help of K.R.Hendry and C.Goodwin.

4.1. Abstract

Deep-sea sponges are an important part of marine benthic ecosystems, providing habitats for other organisms and supporting areas of high biodiversity. They are vulnerable to bottom-contact fishing and rapid oceanic changes resulting from climate change. This study uses principal component analysis on sponge species data and *in situ* environmental data to identify sponge assemblages and investigates the drivers of their distribution. We show that there are two distinct assemblages defined by the physical oceanographic conditions they inhabit within the sponge specimens assessed in this study. We suggest that these parameters, notably temperature, depth, and oxygen concentration, are the primary controlling factors for sponge distribution in the Labrador Sea. We suggest that this is ultimately a water mass controlled system of distribution and explore the implication of this. Within these sponge assemblages we show there is a strong secondary grouping based on local ocean nutrient concentrations, which have not been considered in previous studies due to the unavailability of data at suitable granularity. We discuss the implications of these findings for modeling the distribution of sponges in the Labrador Sea, as well as new insights into the vulnerability of these assemblages to climate change relevant for conservation strategies.

4.2. Introduction

Identifying the drivers behind sponge distribution is fundamental for fully understanding their distribution, importance, and function within the global ocean. Sponges are an overlooked component of the benthic marine ecosystem, although they are known to perform important functional roles with the ocean. Their most important role is as a habitat-building organism in both shallow water and deep-sea environments (Miller *et al.*, 2012; Knudby, Kenchington and Murillo, 2013; Roberts *et al.*, 2018). These sponge habitats actively support areas of high biodiversity (Klitgaard and Tendal, 2004; Murillo *et al.*, 2012; Hawkes *et al.*, 2019), act as nurseries for many fish species (Klitgaard, 1995; Freese and Wing, 2003), and can influence primary production by controlling nutrient availability (Bell, 2008; Maldonado, Ribes and van Duyl, 2012; Murillo *et al.*, 2012; Kutti, Bannister and Fosså, 2013; Maldonado, 2016). Understanding the environmental factors that influence the distribution of the sponge species and assemblages both increases our understanding of the organisms themselves and gives us parameters to predict their total distribution and function. This understanding will ultimately feed into marine protection strategies or at least highlight the risks posed to – and potential impacts on – sponge grounds and habitats. Deep-sea sponge aggregations are at risk from bottom-contact fishing methods due to their sedentary nature and slow growth rates (Lindholm, Auster and Valentine, 2004; Howell, 2010; Kenchington, Murillo-Perez, *et al.*, 2011; Bell, McGrath, *et al.*, 2015; Grant *et al.*, 2018, 2019; Culwick *et al.*, 2020) and are recognized by the Oslo and Paris Conventions (OSPAR) (OSPAR commission, 2008, 2010).

OSPAR defines sponge aggregations as occuring “on both soft and hard substrates and are principally composed of Hexactinellids and Demosponges. Hexactinellids have been reported at densities of 4-5m2 and ‘massive’ growth forms of demosponges have been reported at densities of 0.5-1/m2" (OSPAR commission, 2008, 2010). The FAO in defining the Vulnerable marine ecosystem habitat of ‘Deep-sea sponge aggregations’ (FAO, 2009) splits this down further into: " Other sponge aggregations" primarily Geodiidae, Ancorindiae, Pachastrellidae , " Hard-bottom sponge gardens" Containing Axinellidae, Mycalidae, Polymastiidae, Tetillidae, and "Glass sponge communities". In the current literature, sponge grounds (Hogg et al. 2010; Murillo et al. 2016, 2018 and sponge aggregations (OSPAR, 2010) are used interchangeably. We will be using these definitions; "Sponge Aggregations" are habitats with a high numbers of sponges present, encompass sponge gardens and sponge grounds (FAO, 2009). "Sponge grounds" are habitats where sponges dominate. In the North

Atlantic typically astrophorids are the most common species and can constitute up to 90% of the biomass (Hogg et al. 2010; Murillo et al. 2016, 2018).

In the North Atlantic, patterns of sponge species distribution and the extent of sponge aggregations have been attributed to several factors in other biogeographic studies. The most prevalent drivers are thought to be silicic acid concentration (Beazley *et al.*, 2015; Howell *et al.*, 2016) temperature, depth (Rice, Thurston and New, 1990; Bett, 2001; Murillo *et al.*, 2012) and particulate carbon availability (Barthel, Tendal and Thiel, 1996; Howell *et al.*, 2016) as well as flow conditions around the sponges effected by internal waves, topography and bottom currents (Klitgaard and Tendal, 2004; Kutti, Bannister and Fosså, 2013; Howell *et al.*, 2016; Culwick *et al.*, 2020). Recent Studies looking at the distribution of sponges in the North Atlantic have used trawl data (Kenchington, Link, *et al.*, 2011; Murillo *et al.*, 2012, 2018; Knudby, Kenchington and Murillo, 2013), Remotely Operated Vehicle (ROV) footage, towed camera video (Beazley *et al.*, 2015; McIntyre *et al.*, 2016), a combination of ROV footage and trawls and grabs (Dinn *et al.*, 2020), and samples collected directly from an ROV (**Chapter 3**).

On top of these studies looking directly at distribution, there have been efforts to predict the distribution of dense sponge grounds, based on environmental parameters (Knudby, Kenchington and Murillo, 2013; Murillo *et al.*, 2016). These studies used basin-scale environmental datasets based on availability and a general notion of relevance derived from large-scale studies of the area, and were narrowed down based on coverage and the removal of correlated variables (Knudby, Kenchington and Murillo, 2013). These studies then use a presence/absence/abundance of species to construct models of distribution by comparison to relevant environmental parameters. There have been questions regarding the reliability of these models, as they rely on a very basic understanding of ecology in the area and the environmental drivers of species distribution (Howell *et al.*, 2016) and appear to have poor performance when extrapolating to area of simular enviromental conditions, potentially due to differences in watermass structure (Knudby, Kenchington and Murillo, 2013; Murillo *et al.*, 2016).

Water masses have been linked to the geographic and bathymetric structure of benthic faunas within ocean basins across a number of regions and taxonomic groups (Howell, Billett and Tyler, 2002; Bauer *et al.*, 2018; Busch *et al.*, 2020; Eerkes-Medrano *et al.*, 2020). There is a large amount of literature written on cold water corals linking their biogeographic distribution to water masses (Dullo, Flögel and Rüggeberg, 2008; Rüggeberg *et al.*, 2011; Kenchington *et al.*, 2017). For sponges, there appears to be direct links between water mass and current structure and some taxonomic groups, particularly those in the genus *Geodia* Lamarck, 1815, (Hogg, Tendal and Conway, 2010;

Maldonado *et al.*, 2017). Roberts et al., (2021) mapped *Geodia* species in the North Atlantic and Nordic Sea tracking water masses based on potential temperature and salinity curves. They demonstrated sponges were particularly associated with the turning points of these curves. They were also able to show links between Arctic *Geodia* (*Geodia parva* Hansen, 1885*, Geodia hentscheli* Cárdenas *et al.*, 2010) and Arctic intermediate and lower water masses in the Nordic sea and dense overflows in the North Atlantic. These were separate and different to boreal *Geodia* (*Geodia barretti* Bowerbank, 1858, *Geodia macandrewii* Bowerbank, 1858, *Geodia phlegraei* Sollas, 1880), which were associated with upper and intermediate waters in the Northeast Atlantic and upper Atlantic derived water in the Nordic sea. The exact mechanisms behind these links were not looked at in this study. However, they suggest that physical constrains of the water masses impact on larval distribution and evolved tolerances of the sponges. Water column stratification may also benefit sponges filtering feeding due to associated phenomena for example density current neopholoid layers and internal waves. The link between sponge distribution and water masses has been suggested previously by Klitgaard & Tendal (2004), with observations of hydrological conditions in the Northeast Atlantic pointing to specific water masses as well as sponge grounds appearing to follow branches of the North Atlantic Drift. This idea was explored further for *Geodia* species in the North Atlantic, a study found that typically boreal and arctic sponges occurred together in areas of potential mixing between water masses (Cárdenas, Rapp, Klitgaard, *et al.*, 2013). Water masses have also been attributed to the distribution of *Geodia* in the Sackville Spur off Newfoundland (Beazley *et al.,* 2015).

In this study, we aim to increase the understanding of the environmental drivers of distribution for sponges in the Labrador Sea and to identify areas where we would expect sponge assemblages and the species they contain to occur in the area. We use a taxonomic data set combined with environmental variables collected alongside the sponge samples and conduct a principal component analysis to draw out the key drivers of distribution. We intend this localized environmental data set to provide a much more accurate view of the conditions around the sponges at these localities. We discuss the implications and possible explanations of our results and their impacts on our understanding of sponge distribution in the areas and how this distribution may be impacted into the future.

4.3. Methods

4.3.1. Study sites

Samples and environmental variables were collected on RRS Discovery cruise DY081 as part of the Isotope CYcling in the Labrador Sea (ICY-LAB) project. The aim was to capture the whole biogeochemical system within the Labrador Sea with sites chosen due to their differing water mass interactions and coastal proximity. Sponge sampling was part of the investigation of the biogeography of siliceous organisms in the Labrador Sea.

Samples and Oceanographic datasets were collected from three study sites located at Orphan Knoll seamount, off the coast of Nuuk, and off South West Greenland. Each study site was contained several sampling stations (**Chapter 3**: Figure 3-1. Table I).

4.3.2. Sponge species identification

Samples were collected using the UK National Marine Facilities Remotely Operated Vehicle (ROV), *Isis*. Samples were collected with the manipulator arm or suction system. Time, depth, location, broad description, and *in situ*photographs were collected for each sample collection. Taxonomic identification was done using a combination of optical and scanning electron microscopy (**Chapter 3: 3.3. Material and methods**).

4.3.3. Physical oceanography

Physical oceanographic variables were collected alongside sample collection using the ROV which was mounted with six 1.7L Niskins bottles and a Sea-Bird SBE 49 CTD. The CTD recorded data throughout the dive, and these raw data were processed by Particle Swarm Optimization using standard Sea-Bird data processing software. The ROV mounted Niskin bottles were fired at points of particular interest along the ROV track approximately evenly throughout the dive's duration.

The collection event was matched to the corresponding ROV mounted CTD measurement for depth, temperature, and conductivity using the time of the collection event for each sample. Salinity was calculated from these measurements. Each sample collection event was matched to the nearest ROV mounted Niskin water sample measurements for inorganic macronutrient concentrations (nitrite, nitrate, silicic acid, and phosphate). Samples of water were frozen at -20°C, and macronutrients were analyzed at the Plymouth Marine Laboratory ashore. Analysis was performed using a SEAL analytical AAIII segmented flow colorimetric auto-analyser using classical analytical techniques for nitrate, nitrite, silicic acid (or DSi), and phosphate, as described in Woodward & Rees, (2001). The uncertainties for the analytical results were between 2-3%, and the limits of detection for nitrate

and phosphate were 0.02 µM, 0.01 µM for nitrite, and silicic acid did not ever approach the limits of detection (Hendry *et al.*, 2019) .

When Niskin water samples were not available, data from the closest Niskin water sample from the shipboard CTD rosette cast were used.

Sensors mounted on the nearest CTD rosette cast were used to collect measurements of turbidity, oxygen concentration, and fluorescence. The measurements from the depths corresponding to collection event were matched to each sample.

Measurements of highly correlated or duplicate variables were removed from the data set. For duplicate measurements, those taken closest to the sample location were used. For highly correlated variables, only one was used to prevent the principal component analysis from overemphasizing its importance. These variables included; beam transmission and turbulence which are highly correlated in this data (R=-0.95), conductivity and salinity, where conductivity is used to calculate salinity, and pressure and depth.

4.3.4. Principal component analysis

Principal component analysis (PCA) was used as a data reduction technique as it keeps the variance while minimizing the mean square approximate errors. This enables us to obtain lower-dimensional data while keeping as much of the data variance as possible. It also enables the identification of the dominant mode of data (Fung and LeDrew 1987). PCA converts the data into smaller uncorrelated variables that are easier to interpret but still capture most of the variation within the original dataset (Dunteman 1989). The principal components are produced from the original data so that the first principal component accounts for the largest proportion of the variance and each subsequent component accounts for the largest proportion of the remaining variance (Fung and LeDrew 1987).

The PCA study was performed using prcomp function from 'stats', a statistic package run in RStudio.

4.4. Results

The results from the PCA analysis show the first three principal components account for 79.3% of the cumulative percentage variation (Figure 4-2), with the 4th accounting for only 8%. The first principal component (PC1) accounts for 41.3% of the total variance. The variables that make up PC1 are temperature, depth, oxygen concentration, silicic acid concentration, and nitrite concentration (Figure 4-3), with temperature, depth, and oxygen concentration having a slightly higher percentage

contribution (approximately 17.5%) than silicic acid and nitrite concentrations (approximately 12.5%). Principal component two (PC2) accounts for 23.5% of the total variance and is mostly accounted for by nitrate and phosphate concentrations (Figure 4-4). PC1 and PC2 make up the majority (64.8%) of the variance seen with principal component three (PC3) accounting for only 14.5% of the total variance and could be discounted. However, PC3 has a significant proportion of its variance explained by salinity, depth, temperature and florescence (Figure 4-5), which may help identify water mass effects. The correlation and p values for each variable was significantly greater than expected from a random distribution, with temperature showing particularly high correlation and very low p values.

The PCA biplot of PC1 and PC2 show clear separation in the community of sponges as well as slight spreading of these communities along PC1 (Figure 4-1). There is strong grouping by locality and station, with the Orphan Knoll sponges distinctly separated from the Greenland sponges along PC1. The Orphan Knoll sponges from station 5 (STA5) are separated into two groups along PC2 driven by low nitrate phosphate in the shallower sponges. The Orphan Knoll sponges from station 13 (STA13) plot closest to the Greenland sponges, although there is no overlap between the localities. There is a large cluster comprising the sponges from the Greenland localities, with Nuuk sponges clustering with – and slightly overlapping – the South West Greenland (SWGL), suggesting very similar conditions. However, within this larger group, the sponges in each locality cluster together, and each stations clusters together with the locality. The edges of these groupings overlap, suggesting each station has unique local environmental conditions but grades into the others in the region. The Nuuk group from station 37 (STA37) is an exception, being separated from the other Greenland sponges along PC1 driven mostly by the higher nitrite measurement. The nitrite concentrations associated with two of the sponges from this station are particularly high (0.23 µM).

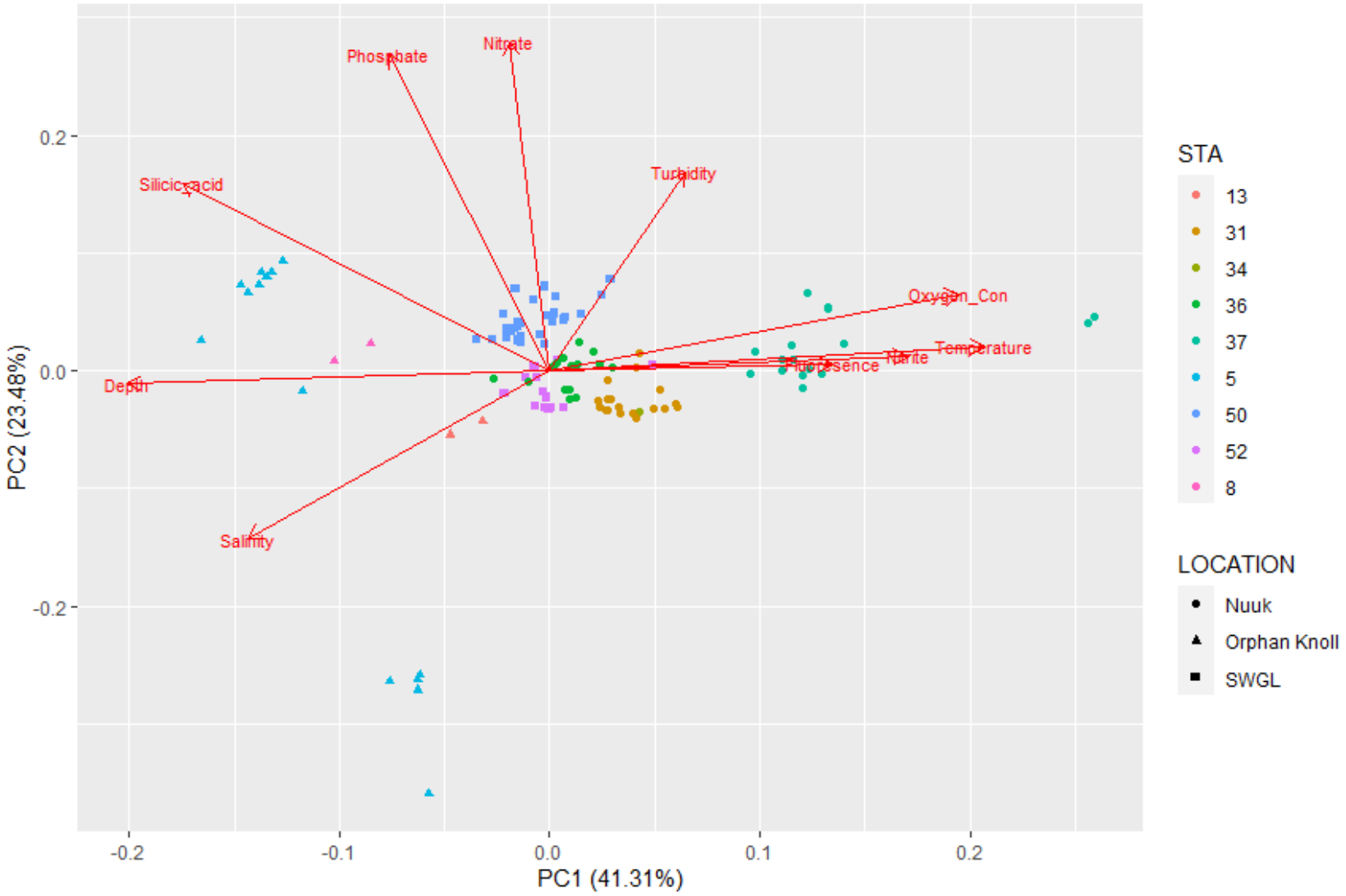

Figure 4-1. Principal Component Analysis biplot. Samples are labeled by location and colored by sampling station.

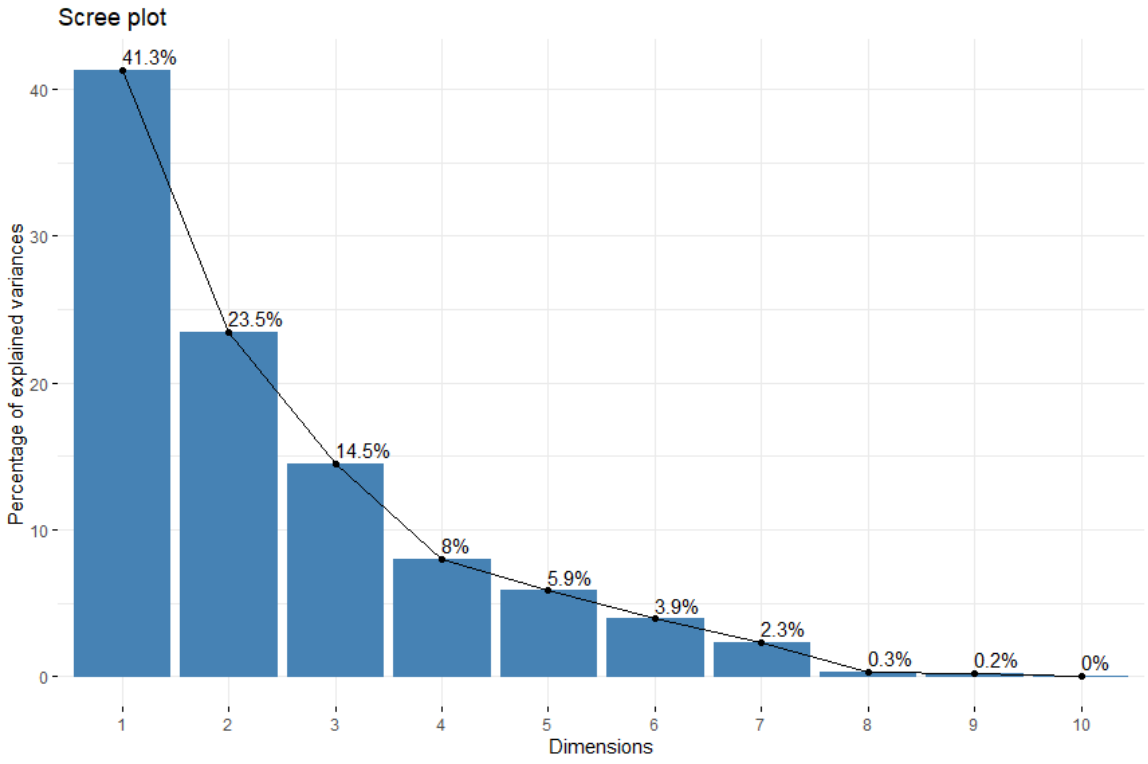

Figure 4-2. Principal Component Analysis Scree plot of the first 10 principal components of the environment variable for sponges from Orphan Knoll, Nuuk, and Greenland.

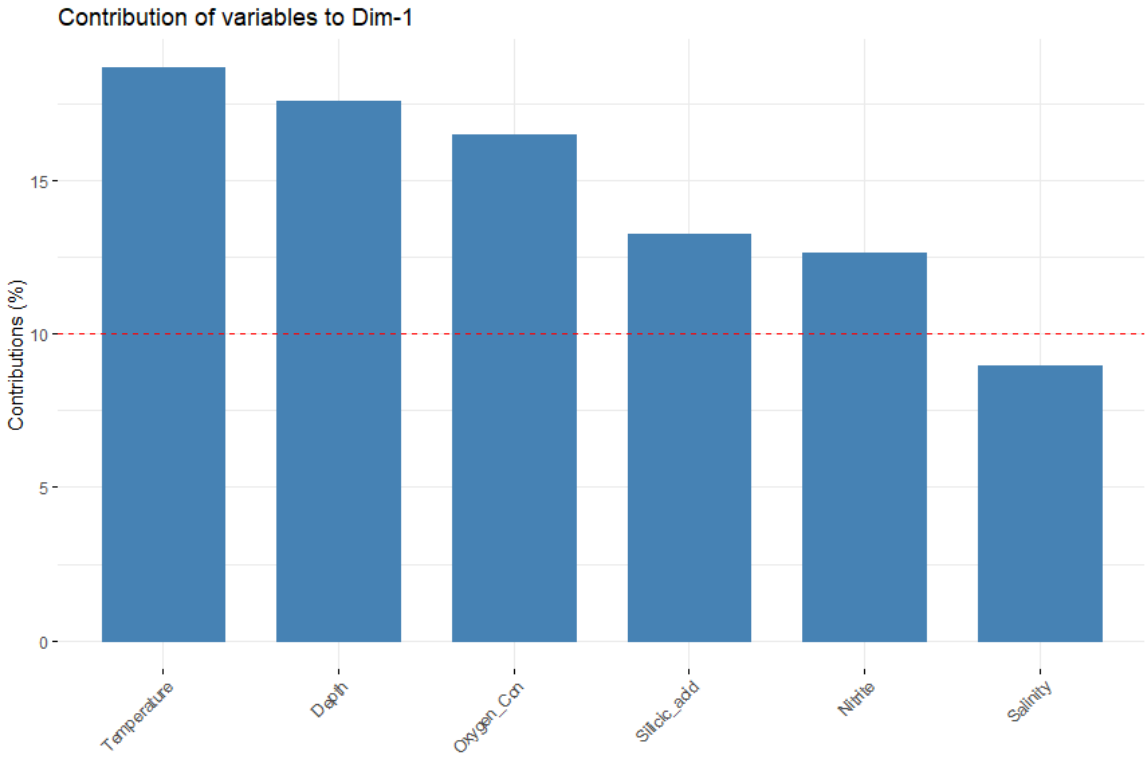

Figure 4-3. Principal Component Analysis Scree plot showing percentage contributions of the first 5 variables making up Principal component 1.

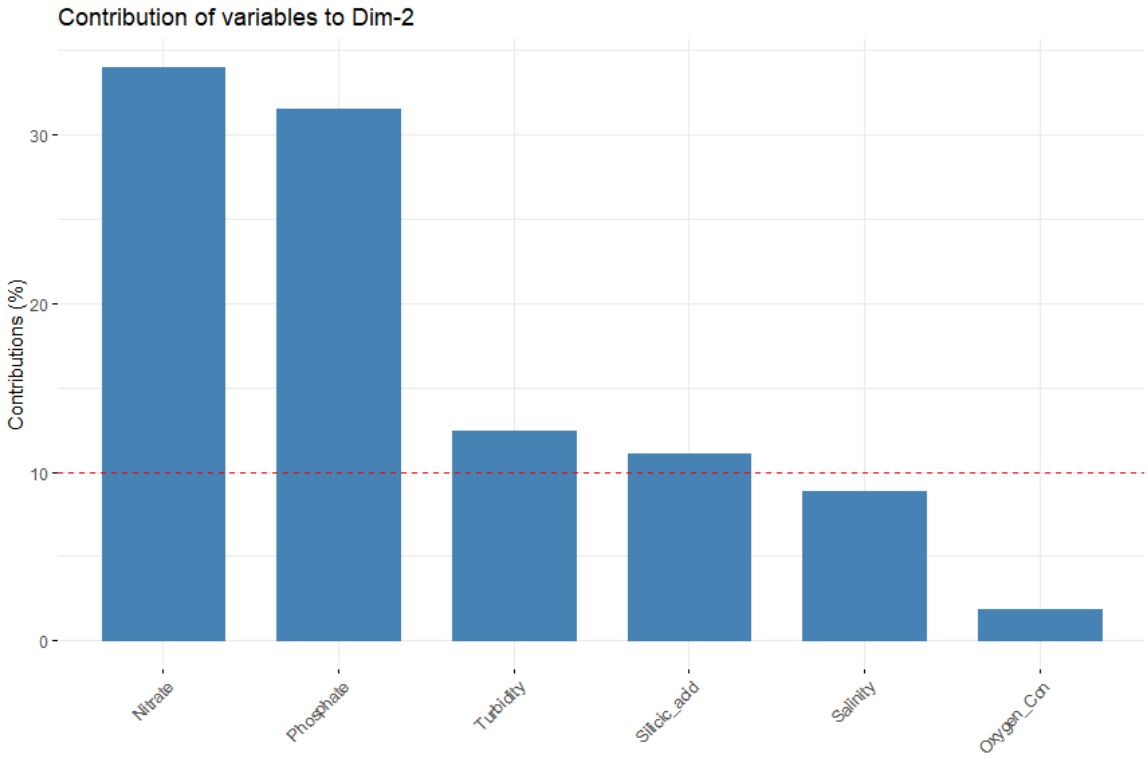

Figure 4-4. Principal Component Analysis Scree plot showing percentage contributions of the first 5 variables making up Principal component 2.

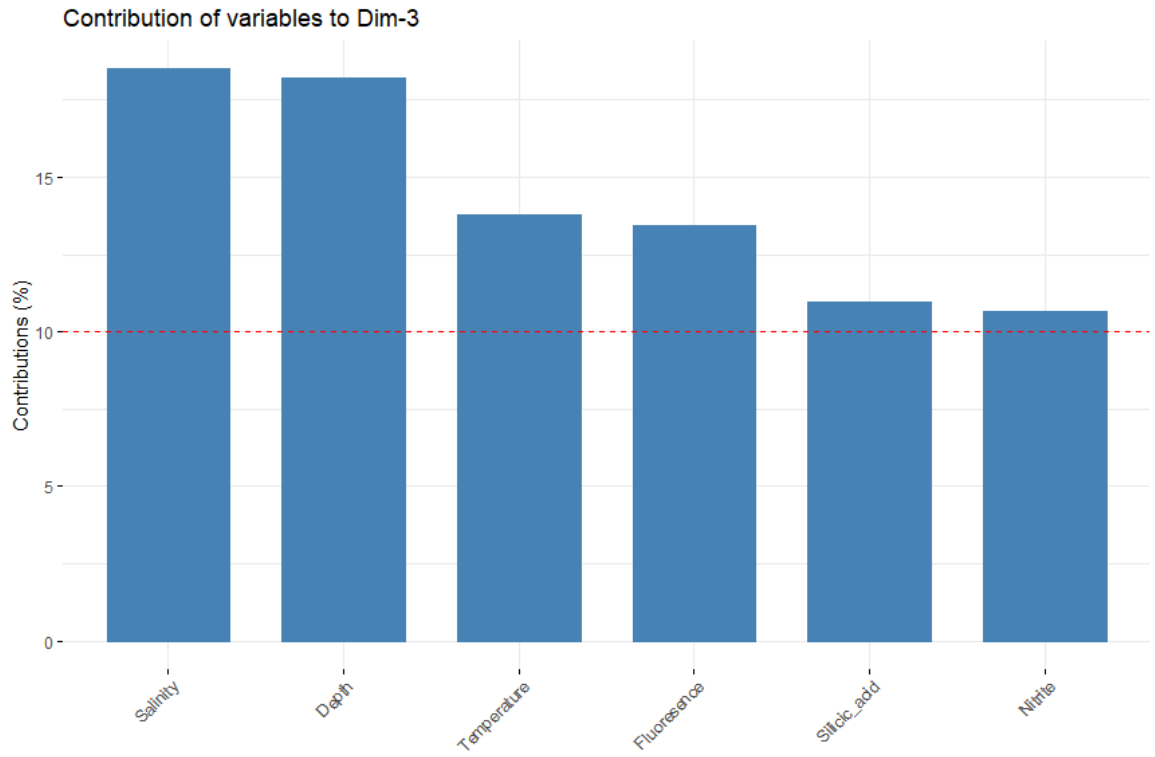

Figure 4-5. Principal Component Analysis Scree plot showing percentage contributions of the first 5 variables making up Principal component 3.

4.5. Discussion

This study provides an increased insight into the driving factors behind the distribution of sponge assemblages and sponge species within the Labrador Sea. There are at least two separate sponge groups within the Labrador Sea, located on Orphan Knoll and the Greenland shelf. These two groups are separated by PC1, which primarily reflects physical parameters suggesting that oceanic forcing has a role in separating or dictating the composition of these different sponge communities. The differing oceanographic condition in the study sites are driven by the interplay of the dominant water masses in the two areas: The upper Subpolar Mode Water (uSPMW), deep Subpolar Mode Water (dSPMW) and South Greenland Coastal Waters (CW) influencing the South West Greenland shelf, whereas Orphan Knoll sits in between Labrador Sea Water (LSW) and North Atlantic Deep Water (NADW) (**Chapter 1**. Figure 1-6,1-7,-8,1-9,1-10,1-11) (Talley and McCartney, 1982; Lavender, Davis and Owens, 2000; Yeager and Jochum, 2009; Talley *et al.*, 2011; Rysgaard *et al.*, 2020).

These two grouping of sponges from the PCA based on environmental parameters in this study are also separated taxonomically as differing sponge assemblages. There is very little overlap of species between the Orphan Knoll sponges and those of the Greenland shelf (**Chapter 3**: Table II). In comparison, the overlap in species found at the sites on the Greenland shelf is quite considerable (**Chapter 3**: Table II).

The dominance of the physical parameters as predictors of distribution for these assemblages was expected. Given that other studies looking at drivers of species distribution in the areas have identified depth, bottom salinity (Knudby, Kenchington and Murillo, 2013) bottom temperature, and primary production (Murillo *et al.*, 2018), in addition to silicic acid concentration (Beazley *et al.*, 2015; Howell *et al.*, 2016), as key parameters. In addition to directly linking physical parameters to sponge assemblage distribution, it has been demonstrated that there are direct links between water mass, current structure, which these parameters can be proxies for, and the distribution of some taxonomic groups of sponge, particularly those of genus *Geodia* Lamarck, 1815, (Hogg, Tendal and Conway, 2010; Maldonado *et al.*, 2017; Roberts *et al.*, 2021). Disentangling the importance of environmental parameters as opposed to the constraints and structuring due to water masses is difficult and beyond this study. However, we are able to look more closely at the relative importance of some of the mechanisms compared to others. To do this we need to understand how each environmental parameters affects sponge physiology and ecology so we can attempt to disregard correlated but unimportant parameters.

Temperature has the greatest contribution to PC1 (Figure 4-1 , 4-2) and therefore also to the separation of the sponge groupings in this study. This is in line with other studies (Murillo *et al.*, 2018; Busch *et al.*, 2020; Roberts *et al.*, 2021) and is one of the potential mechanisms linking water masses to sponge distribution (Klitgaard and Tendal, 2004; Hogg, Tendal and Conway, 2010; Cárdenas, Rapp, Best, *et al.*, 2013; Beazley *et al.*, 2015; Maldonado *et al.*, 2017; Roberts *et al.*, 2021). Temperature has been suggested to play a role in the efficiency of cell function based on the rate of regeneration and reaggregation at various temperatures in shallow water sponges (Runzel, 2016). For cellular function, there is a balance between low temperatures resulting in low molecular activity and high temperatures resulting in protein denaturing, and this optimum temperature varies dependent adaptive traits of individual species. Gene expression is known to change depending on temperatures both in shallow and deep water sponges (Guzman and Conaco, 2016; González-Aravena *et al.*, 2019), with short term stress resulting in the expression of genes involved in signal transduction and immunity pathways as well as the production of heat shock proteins and antioxidants. Long exposure to stress affects the expression of genes responsible for repair signaling and apaptosis (Guzman and Conaco, 2016). This change in gene expression may let sponges adapt to local changes in the environment. However, the shallow water species from the Philippines, looked at in this study, are normaly exposed to variable temperatures and therefore you would expect they would have evolved a more robust way of coping with temperature fluctuations than those of the deep sea. This worry is compounded when looking the gene expression in response to temperature changes in cold water Antarctic sponges. Where a similar response is seen with a rise of 1 degree and no change in response with increase temperatures suggesting a limited temperature rise would case stress at the limit of the organism capability to cope with (González-Aravena *et al.*, 2019). Temperature is also a factor in the ability of glass sponges to propagate electrical signals due to these use of calcium/potassium impulses which are very temperature sensitive and one of the reasons they are restricted to deep, colder waters (Leys, 2003; Leys, Mackie and Reiswig, 2007; Leys and Meech, 2011). The distribution of species based on temperature is probably due to geophysical adaption or evolved tolerances to specific temperature ranges for specific sponge species. This adaption is not limited to the sponges themselves but also to the symbiotic bacteria that are associated with them, which also appear species-specific (Pita *et al.*, 2013, 2018; Easson and Thacker, 2014; Thomas *et al.*, 2016; Steinert *et al.*, 2017, 2020; Cárdenas *et al.*, 2019). In some shallow water sponges, we know these symbionts have temperature thresholds different to that of the host sponge and can be lost (Webster, Cobb and Negri, 2008) or undergo rapid uncontrolled growth (Rützler, 1988), both of which negatively affect the host sponges. Although in others, the bacterial communities appear relatively stable even through relatively large temperature changes

(Cárdenas *et al.*, 2019). Bottom water temperatures in the Labrador Sea (Figure 4-6) are relatively uniform along the South West Greenland shelf until north of Nuuk. They differ substantially to the seamount at Orphan Knoll, which is up to 4^{o}C warmer. However, the sponge aggregations at Orphan Knoll are at greater depths than those of Greenland, so the local conditions are colder, potentially explaining the higher number of glass sponges at Orphan Knoll.

If we use temperature to map the extent of these sponge assemblages, it would predict the South Western Greenland assemblage could extend up towards the southern end of Baffin Bay, before disappearing as the influx of the BBPW increases (Rysgaard *et al.*, 2020). There is very little overlap between the species present off Nuuk and SWGL and those described in Baffin Bay and the northwest Labrador Sea close to Baffin Island (Murillo *et al.*, 2018; Dinn *et al.*, 2020), confirming this prediction. Further predictions based on these variables would also suggest that the East coast of Canada, north of Newfoundland, should look similar to those off the Greenland shelf. Interestingly in the Murrillo *et al.* (2018) study – focusing on *Geodia* Lamarck, 1815, off the Canadian east coast –a gap in *Geodia* Lamarck, 1815, presence was described in the region where we would expect to see the Greenland sponge assemblage. This gap may correspond to the extension of our Greenland sponge assemblage into this area. We found the Greenland assemblage to contain very low numbers and low diversity of *Geodia* Lamarck, 1815, (only one species of *Geodia* Lamarck, 1815, was identified). However, this prediction would require ground-truthing, given that it is based on comparison to the assemblages and conditions at Orphan Knoll, and given the differences in the water masses and environmental conditions (e.g. silicic acid concentrations) between the Eastern Canadian shelf and West Greenland Shelf (Figure 4-7).

This leads on to the second largest component of PC1: depth (Figure 4-1 , 4-2). There is probably no direct mechanistic link outside the photic zone between depth and sponge distribution although it appears to be a factor in the distribution of sponge grounds (Howell, Billett and Tyler, 2002; Howell, 2010; Howell *et al.*, 2016; Roberts *et al.*, 2021), with the most directly linked mechanistic pathway being through pressure (Leys and Hill, 2012). We know control over the flow through sponges is necessary to prevent the destruction of canals due to uneven pressures between incurrent and excurrent systems, partially when considering adaption to damage (Leys and Hill, 2012). Therefore sponges must have a mechanism for detecting fine changes in pressure (Leys and Hill, 2012). How capable a species is of adapting to pressure differences, may explain why there are depth ranges for particular species. However, depth is probably most likely to be a proxy for unmeasured correlated factors, including current speed, water mass structure, food availability, and sediment type (Howell, Billett and Tyler, 2002; Howell, 2010; Howell *et al.*, 2016; Roberts *et al.*, 2021). The high contribution

of depth combined with that of temperature and oxygen concentrations, (the third largest component of PC1 (Figure 4-1 , 4-2) all of which are major proxy for separating water masses within the Labrador Sea, suggest that they may be the true driving force behind distribution.

The mechanisms behind sponge distribution based on water mass are not clear cut and probably result from a set of cumulative factors. One of the considerations is the supply of food and larval recruitment from enhanced currents (Genin *et al.*, 1986; Rice, Thurston and New, 1990; White *et al.*, 2010). Nepheloid layer are layers of water above the ocean floor that contain significant concentrations of resuspended matter, which are possible sources of food and larvae. The nepheloid layers are formed by internal waves and tide at the continental slope or shelf edge (McCave, 1986; Thorpe and White, 1988). In particular, intermediate nepheloid layers are known to transport larvae (Ryan *et al.*, 2014). These layers are usually associated with the edges of water masses (McCave, 1986; Thorpe and White, 1988). Interestingly a number of sponges at Orphan Knoll cluster at the boundary of the LSW and NADW, this boundary is highlighted by the rapid change in water oxygen concentrations (**Chapter 1.** Figure 1-7). This suggest that nepheloid layers may play a part in the particular distribution of these species.

The presence of both the Arctic influenced LSW, and the Atlantic derived NADW at Orphan knoll (Talley and McCartney, 1982; Lavender, Davis and Owens, 2000; Yeager and Jochum, 2009; Talley *et al.*, 2011) is reflected in the species present (Chapter 3). We see a combination of more southern species observed previously described from the Mid-Atlantic Ridge, Flemish Cap, and Celtic Sea areas (Cárdenas, Rapp, Best, *et al.*, 2013; Cárdenas and Rapp, 2015; Howell *et al.*, 2016), with the majority of these sponges located well within NADW (**Chapter 1.** Figure 1-6,1-7). This observation suggests that these deeper Orphan Knoll sponges experience conditions usually associated with more southern waters, potentially explaining some of the species found. The small number of sponges located at the boundary between the NADW and the LSW (**Chapter 1.** Figure 1-6 1-7), corresponding to stations 8 and 13, which cluster closer to the Greenland sponges in the PCA (Figure 4-1) suggesting some level of influence from the LSW on the local conditions at these stations. The combination of both Arctic and Atlantic faunas results in a much higher level of biodiversity than recorded off the Flemish Cap, Flemish Pass, and Grand Banks of Newfoundland (Murillo *et al.*, 2012). However, the higher biodiversity could also be partly due to lack of smaller and encrusting species in the Murillo *et al.* (2012) study, which may be due to their sample collection methods (**Chapter 3**). The combination of distinct oceanographic conditions and combination of boreal and Arctic species suggest that Orphan Knoll is a distinct sponge assemblage within the Labrador Sea.

The relative importance of silicic acid concentration for the grouping of the different sponge assemblages (Figure 4-1 , 4-2) was expected, as it is a known driver of sponge distribution in the North Atlantic (Howell *et al.*, 2016). The Greenland sponges, particularly STA37, show very low levels of ambient silicic acid concentration compared to the Orphan Knoll sponges. Looking at the bottom water silicic acid concentrations in the Labrador Sea, we can see variable very low concentrations on the South West Greenland Shelf (4 μmol/kg) with higher values at Orphan Knoll (15 μmol/kg) (Figure 4-7). This distribution may explain the smaller sizes of the sponges species found of the South West Greenland Shelf, where the sponges may lack sufficient ambient silicic acid to produce substantial spicule frameworks (Maldonado *et al.*, 2011).

Within the two main Orphan Knoll and Greenland assemblages, the variation between the stations is driven by other nutrient variables aside from silicic acid. The clusters are primarily separated by PC2, with high loadings from nitrate and phosphate concentrations, but also PC1, with high loading from nitrite, particularly for the STA37 (Figure 4-1). STA37 sits very close to the end of a large trench cutting into the Greenland shelf and – unlike the rest of the sponge samples – plots off the CTD temperature profile (Figure 4-8), suggesting that this topographic feature may be impacting the oceanographic conditions around it. An outflow of more nutrient-rich subsurface waters may explain the higher level of nitrite, nitrate and phosphate seen at STA37. The bottom water phosphate concentrations along the South West Greenland shelf are generally low (< 1.2 μM) with a high background variability (Figure 4-8). This variable pattern is also seen in the bottom water nitrate concentrations (Figure 4-9), but it has a slightly more consistent reduction in concentration moving from the southwest point of Greenland up to Nuuk. Due to the mixing of water masses and influx of meltwater there is probably a large amount of local variability occurring on the shelf edge. Our expectation based on this analysis is that there is no strong distinction between Orphan Knoll and the South West Greenland shelf in terms of phosphate and nitrate concentrations, which is confirmed by bottom water observations (**Chapter 1**. Figure 1-9, 1-10). Although nitrate and phosphate are not taken up directly by the sponges, there is evidence that the bacteria with the sponges do, and that sponges will facilitate the internal conditions necessary for nitrate uptake (Osinga *et al.*, 2001; Hoffmann *et al.*, 2009; Rooks *et al.*, 2020). They are also potential proxies for primary production, the other proxy in this study would be fluorescence which has a low importance on grouping, but this is unsurprising due to the sponges collected being below the photic zone. Average surface chlorophyll concentrations is a better proxy (Figure 4-10), this has slightly higher levels near Greenland than around Orphan Knoll. Primary production in the surface ocean plays a role in the availability of food for filter feeds at the seafloor and may be a factor in separating these

two aggregations. Including direct measurement of POC in further studies would be a much better way of assessing the importance of food availability to sponge distribution.

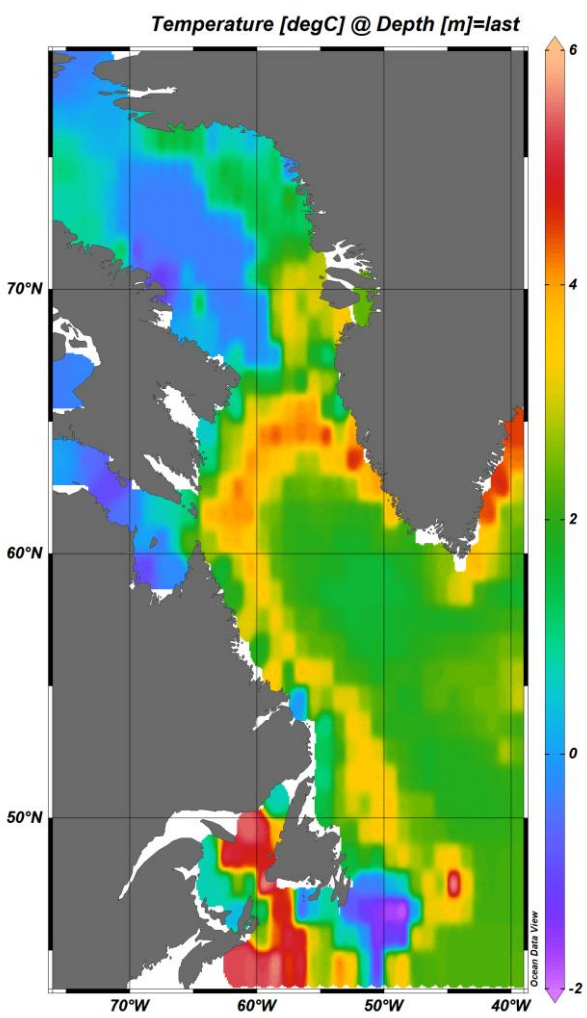

Figure 4-6. Map of bottom water temperature for the Labrador Sea Maps generated using Ocean Data View using the WOA18 database.

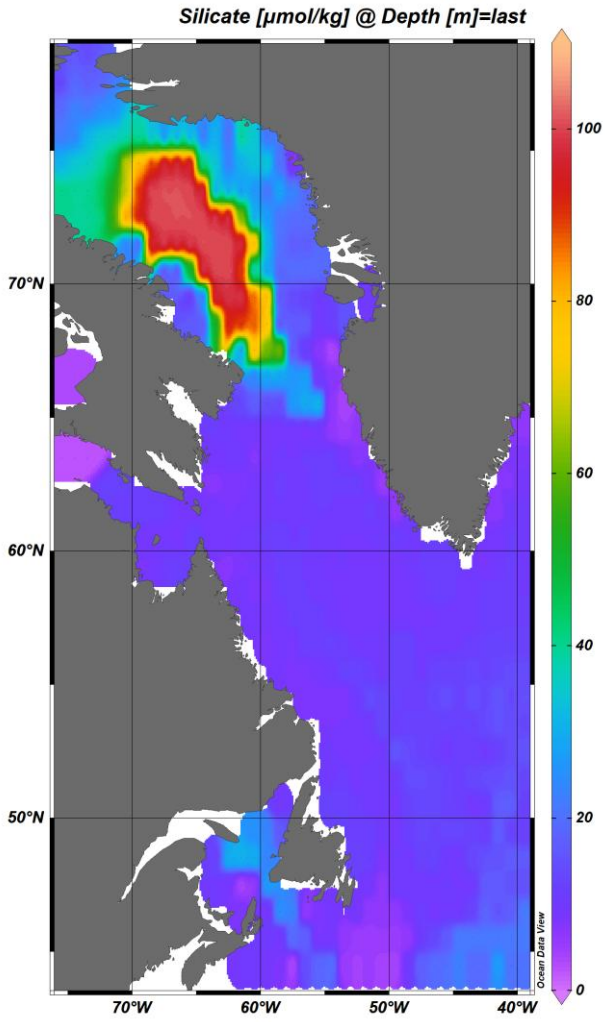

Figure 4-7. Map of bottom water silicate concentration for the Labrador Sea. Maps generated using Ocean Data View using the WOA18 database.

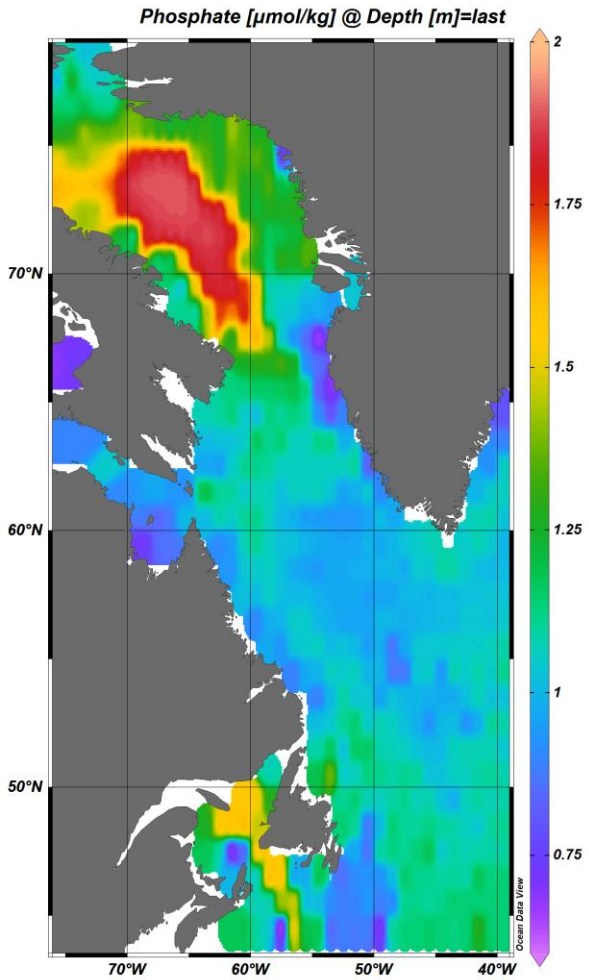

Figure 4-8. Map of bottom water phosphate concentration for the Labrador Sea. Maps generated using Ocean Data View using the WOA18 database.

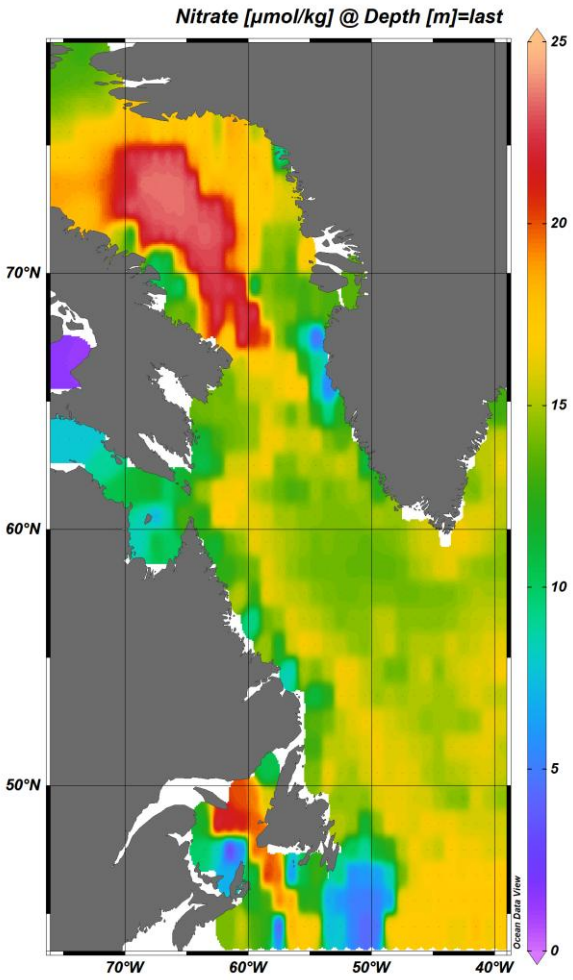

Figure 4-9. Map of bottom water nitrate concentration for the Labrador Sea. Maps generated using Ocean Data View using the WOA18 database.

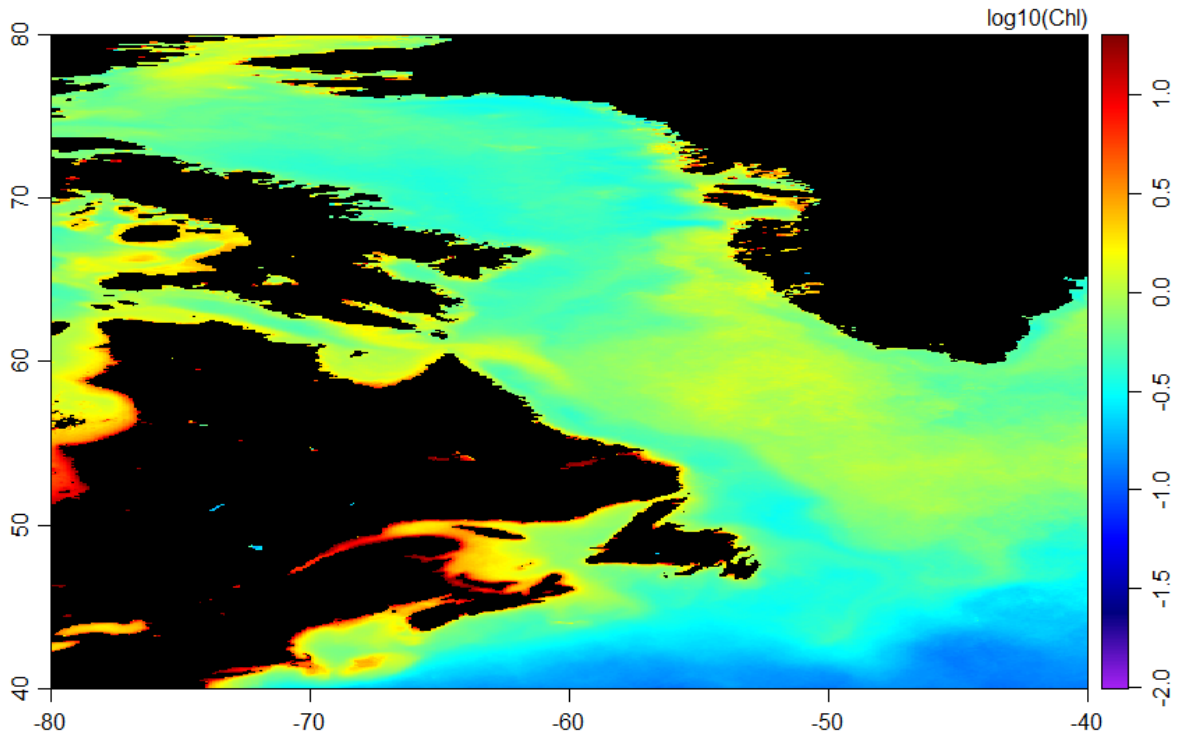

Figure 4-10. Map of summer (2002-2021) seasonal climatology, chlorophyll concentration (MODIS-aqua) for the Labrador Sea. Map generated using R using NASA Sea-viewing Wide Field-of-view Sensor (SeaWiFS) Ocean Color Data, NASA

The comparative regional homogeneity of nitrate, phosphate, and nitrite concentrations, when put next to other physical parameters in large-scale studies may explain the low importance for species distribution allocated in other studies (Knudby, Kenchington and Murillo, 2013; Murillo *et al.*, 2016). This low importance given to nitrate, phosphate, and nitrite concentrations may also be due to the lack of good regional data relating to these variables. For example, none of these variables are included in the Knudby *et al.* (2013) study, potentially for this reason. However, by using coarse regional data, previous studies have missed the importance of this variability for local species distribution that we were able to observe in this study using *in situ* environmental observations. However, small-scale distribution of species within an assemblage is far less important than large-scale distribution of those assemblages, particularly when looking at the vulnerability and necessary protections of these habitats. The functional roles that sponge grounds perform relate to them as a whole habitat building assemblages, rather than any specific species being critical to the habitats function impact (Knudby, Kenchington and Murillo, 2013; Kenchington *et al.*, 2015; Howell *et al.*, 2016). The focus on variables readily available at these large spatial scales may result in overlooking important – but difficult to obtain – variables, driving small-scale sponge distribution. This, in turn, means we may be missing potential local risks to these habitats. The pattern of clustering driven by nitrate, nitrite, and phosphate within the two main assemblages shows the value of obtaining *in situ* local environment data when collecting sponge specimens to study distribution within sponge grounds.

The uniqueness in the Labrador Sea of the environmental conditions associated with the sponge assemblage at Orphan Knoll is worrying, given predicted changes in the climate. We have shown here that the physical parameters in the ocean play an important role in the distribution of these sponges. Therefore we would expect as conditions within the ocean change that the locations that these sponges can inhabit would also shift. For models of temperature change within the Labrador Sea, we see an average increase in temperature and a large increase in variability (Lavoie, Lambert and Gilbert, 2017) (Chapter 5. Figure 5-1). The increase in temperature may not be a problem for the Greenland assemblages as the more gradual change in oceanographic condition along the Greenland coast would potentially facilitate a gradual move north as the ocean warms. These changing conditions are still worrying for this assemblage as their slow growth rates and sessile nature mean that sponges are unlikely to cope with rapid changes in climate. Unfortunately this is compounded for the sponges assemblage at Orphan Knoll as there is not another area with similar conditions close by, potentially resulting in the loss of this unique mixed sponge habitat. The increase in temperature variation is more worrying than the increase in temperature, given the stability of water temperature in the deep sea, the ability of deep-sea sponges to cope with high temperature

variability is unknown. More worrying is the potential changes to the water masses structure in the Labrador Sea with an increasing influx of fresh water and changes in deep water formation (Zantopp *et al.*, 2017; Garcia-Quintana *et al.*, 2019; Holliday *et al.*, 2020). Given that the environmental condition within the Labrador Sea are primarily driven by these water masses, changes in how these would result in massive differences in local environmental condition far beyond any average temperature changes for the region(Rahmstorf, 2000, 2003; Clark *et al.*, 2002) . These changes in water mass structure have the potential to be very rapid and potentially catastrophic for sessile benthic organisms reliant on specific environmental conditions, as seen here. Further work looking at sponges density and species association within these sponge aggregations would enable a greater understanding of how variation in environmental condition effect sponge density rather than just there distribution. This would need a systematic sample collection survey or a combination of gridded ROV tracts and sample collections. Perhaps more valuable to furthering this study would be the creation of a larger data set, including more regions within the Labrador Sea, particularly more sites on the Greenland shelf.

4.6. Conclusions

We have shown the presence of at least two separate sponge assemblages within the Labrador Sea, and that physical parameters on the ocean floor act as the primary differentiators between the two.

The West Greenland shelf assemblage is influenced by the SPMW and is characterized by low *Geodia* Lamarck, 1815, diversity. The conditions in which the West Greenland shelf assemblages occur extend along the West Greenland coast up to the latitude of Baffin Island and up the east coast of Canada at similar latitudes. We would consequently expect this species assemblage to extend into these areas. This assemblage is potentially less vulnerable to climate variability as species may be able to shift north with changes in climate. However, they are still very vulnerable to changes in ocean circulation and water mass structure.

In contrast, the Orphan Knoll assemblage is influenced by both LSW and NADW water masses and consequently has high biodiversity. Ambient conditions found here are unique to this seamount, making its fauna vulnerable to changes in water mass structure and temperature fluctuation associated with anthropogenic climate change.

Expanding the number of sites included in the study to cover more areas of the Greenland and Canadian shelf would be a good next step for this study. A more systematic density and distribution study of species on the Greenland shelf would also be invaluable for understanding the species grouping and better weighting the importance of various environmental parameters for specific species.

5. Chapter 5. Concluding Remarks

5.1. Overview

The aim of this thesis was to increase our ability to predict and model the distribution and density of sponge species and sponge grounds within the Labrador Sea. This was motivated by the need for better constraints on the ecological and biogeochemical role these organisms perform. I have presented three studies each taking differing approaches to this problem. A mathematical modeling study aiming to constrain the role of fluid forcing in distribution alongside a clustering analysis, a taxonomic study expanding our knowledge of sponge biodiversity and a biogeographic study looking at environmental divers of distribution. I have described 12 new sponge species and identified parameters driving distribution at various scales. These new species have probably been missed from previous studies as they are all small, delicate or encrusting and required the ROV to collect. The ROV also enabled the detailed *in situ* measurements of environmental variables, which have been utilized in the final biogeographical study. Each study has increased our understanding of these organisms and help build a better picture of their distribution and density within the Labrador Sea. However, the more pertinent conclusions of all of the study are around how they demonstrate both how little we understand of these organisms and how vulnerable they are to anthropogenic damage.

5.2. Sponge ground identification

Each of the studies show significant differences between the sponge grounds located in the three study locations sampled by the DY081 discovery cruise. This observation in itself is a new and interesting find, although not unexpected given that the sampling locations were chosen based on areas with differing dominate water masses (Talley and McCartney, 1982; Lavender, Davis and Owens, 2000; Yeager and Jochum, 2009; Hendry, 2017). The lack of research into sponges in the Labrador Sea particularly the shelf of West Greenland, with the last taxonomic study in this area being from 1933 (Brøndsted, 1933a), means that any observation or information considerable increases our understanding of the region.

The clustering analysis enabled a robust investigation into the patterns of distribution between the sites, allowing statistical testing of the observational hypothesis. Each of the sites showed clustering patterns with the Hexactinellida dominated site at Orphan knoll showing the strongest clustering pattern. The separation of sponges into distinct types of sponge grounds at the three localities is corroborated when looking at the species data. There is very little overlap between each of the localities particularly between the West Greenland localities and Orphan knoll as only 7 out of the 67 species occur on both side of the Labrador Sea. However, unlike the clustering study where the *Geodia* Lamarck, 1815, dominated site at Orphan knoll and the South West Greenland site are most similar, the biodiversity study has the two Greenland localities most closely associated with 14 species common between them. This is probably as a result of the limited ability to scale up the clustering analysis due to the limited dimensions of the study. The distinct species assemblages present at each of the localities provides us with our primary explanation for the clustering pattern differences when this information is combined with the observations and conclusions of the fluid dynamics modeling. Each of the sponge species has different morphologies and sizes which in turn will affect how they interact with the flow around them. Having observed that at all of the localities the sponges are creating a boundary layer, then it follows that – for each separate assemblages – the exact arrangement of the sponges is based on which species are present. This leads on to the question: what is driving the species differentiation between the three localities? The results from the principle component analysis performed on the *in situ* environmental data alongside the biodiversity data reinforces the distinction between the Orphan Knoll sponges and those from the shelf of West Greenland. The primary component separating these two assemblages is made up of physical parameters: temperature, depth and conductivity having the highest percentage contribution with oxygen and silicic acid concentrations making up the remainder. This finding provides weight to the conclusion that the lack of overlap between species in these two regions is due to environmental conditions. Interestingly there is grouping within the West Greenland region groups that does not align as expected with locality. This grouping is driven by the second principle component made up of nutrient parameters showing an overlap between the two Greenland localities. The nutrients (nitrate, phosphate, silicic acid) are fairly homogenous with fluctuating small scale local variability along the western shelf of Greenland.

Overall there appear to be two levels of sponge distribution patterns at different scales that we can see within the Southern Labrador Sea. At regional scales there is strong evidence of two separate habits in the Southern Labrador Sea, distinguished by different species and environmental conditions: the 'Orphan Knoll type' assemblage, and the 'West Greenland type' assemblage. At a

smaller scale within these assemblages there are species grouping based on nutrient parameters and local flow conditions.

5.3. Risks of anthropogenic damage to sponge grounds

A recurring theme when looking at the findings of these studies is the vulnerability of sponge grounds to anthropogenic damage. This risks for sponges are thought to be higher than many other organisms as they are sessile, slow growing and long lived (Lindholm, Auster and Valentine, 2004; Howell, 2010; Kenchington, Murillo-Perez, *et al.*, 2011; Bell, McGrath, *et al.*, 2015; Grant *et al.*, 2018, 2019). The first and most obvious risk is the destruction as a result of bottom contact fishing methods (Ewing and Kilpatrick, 2013; Clark *et al.*, 2016). The severity of this risk is highlighted with the observation of the slowed boundary layer formed by the sponge structures **(Chapter 2).** The consistency of the boundary layer occurrence at all the study sites suggests an ecological advance to it presence for the sponges. The removal of the sponge structures as is seen in the wake of fishing using bottom contact fishing methods (e.g. trawling) would result in the reduction of this boundary layer effect. If this boundary feature is beneficial then its loss would have implications for future recruitment of larvae, recovery of the sponges and the sponge ground habitat itself. Combining these effects with the slow growth rates potentially results in the inability of sponge grounds to recover once damaged in this way.

The presence of Vulnerable Marine Ecosystems (VMEs) at threat from fishing on the east Canadian shelf is well document (Hogg, Tendal and Conway, 2010; Kenchington *et al.*, 2015; ICES, 2009) with specific habitats and indicator species described for the region (Hogg, Tendal and Conway, 2010; Kenchington *et al.*, 2015; ICES, 2009). This identification has led to some efforts to manage fishing in the area to try and mitigate damaged caused. However, this is not true off the West Greenland shelf, with no recorded VME or presence of VME indicator species to date (ICES, 2021). I have described the presence of vulnerable marine ecosystem indicator species (Hogg, Tendal and Conway, 2010; Kenchington *et al.*, 2015) (ICES, 2009) at all sites in this study **(Chapter 3)** including those off Greenland. This suggests that the protected areas in the Labrador Sea should be far more widespread than they are now. Having collected and filmed these sponge grounds off Greenland using an ROV and positively identified VME indicator species I would suggest these localities should be considered VMEs (ICES,2009), particularly given the current fishing practices and planned sea floor exploitation off Greenland (Ewing and Kilpatrick, 2013; Clark *et al.*, 2016; Long and Jones,

2021). Looking at the drivers of distribution indicated by the biogeography study and mapping these condition in the Labrador Sea, it is likely that these vulnerable sponge grounds may extent most of the way up the West Greenland shelf – an area with very little if any fisheries protection for sponges (Long and Jones, 2021). Given that we identified 12 new species within these are locations in a single study, there is likely a current underestimation of diversity and, so, the lack of protection is very concerning.

Beyond this very direct threat, the greater worry comes from anthropogenic driven climate change. The findings that physical ocean parameters govern the location and species within the sponge assemblages paint a worrying picture as we know that these parameters are likely to change in the area with average increase in sea temperature and a greater levels of fluctuation as well as decreased levels of dissolved oxygen present (Figure 5.1,5.2). This appears to be particularly pertinent for the Orphan Knoll assemblage as the environmental condition it inhabits are unique in the Labrador Sea. This means that any potential of species migration to adapt to a change climate seems reduced, potentially resulting in the total loss of this habitat. There is potentially a better outlook for the West Greenland assemblage as the more gradual changes up the coast of Greenland may enable species migration over time. However, due to the slow growth rates, long life spans and sessile nature if the changes are too rapid they may still be overwhelmed. The speed of the changes in this area may be exceptionally rapid due to the influx of melt water from the Greenland icecap to this particularly area of the Labrador Sea changing the water mass properties and potentially there circulation.

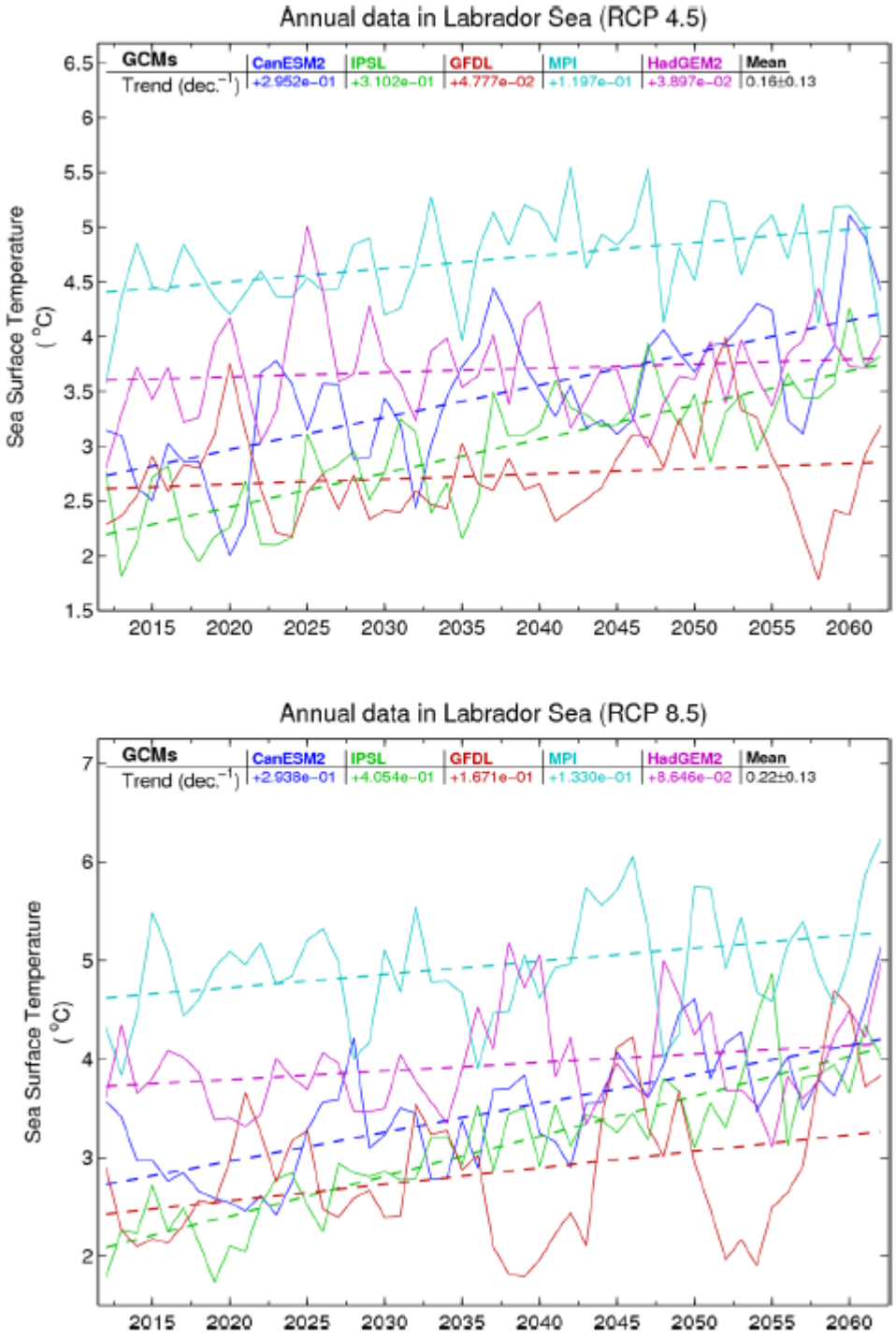

Figure 5-1. Future sea surface temperature trends (°C/decade) in the Labrador Sea for the 2012-2062 period for RCPs 4.5 and 8.5. Figure 39. from " Projections of Future Physical and Biogeochemical Conditions in the Northwest Atlantic from CMIP5 Global Climate Models" (Lavoie, Lambert and Gilbert, 2017).

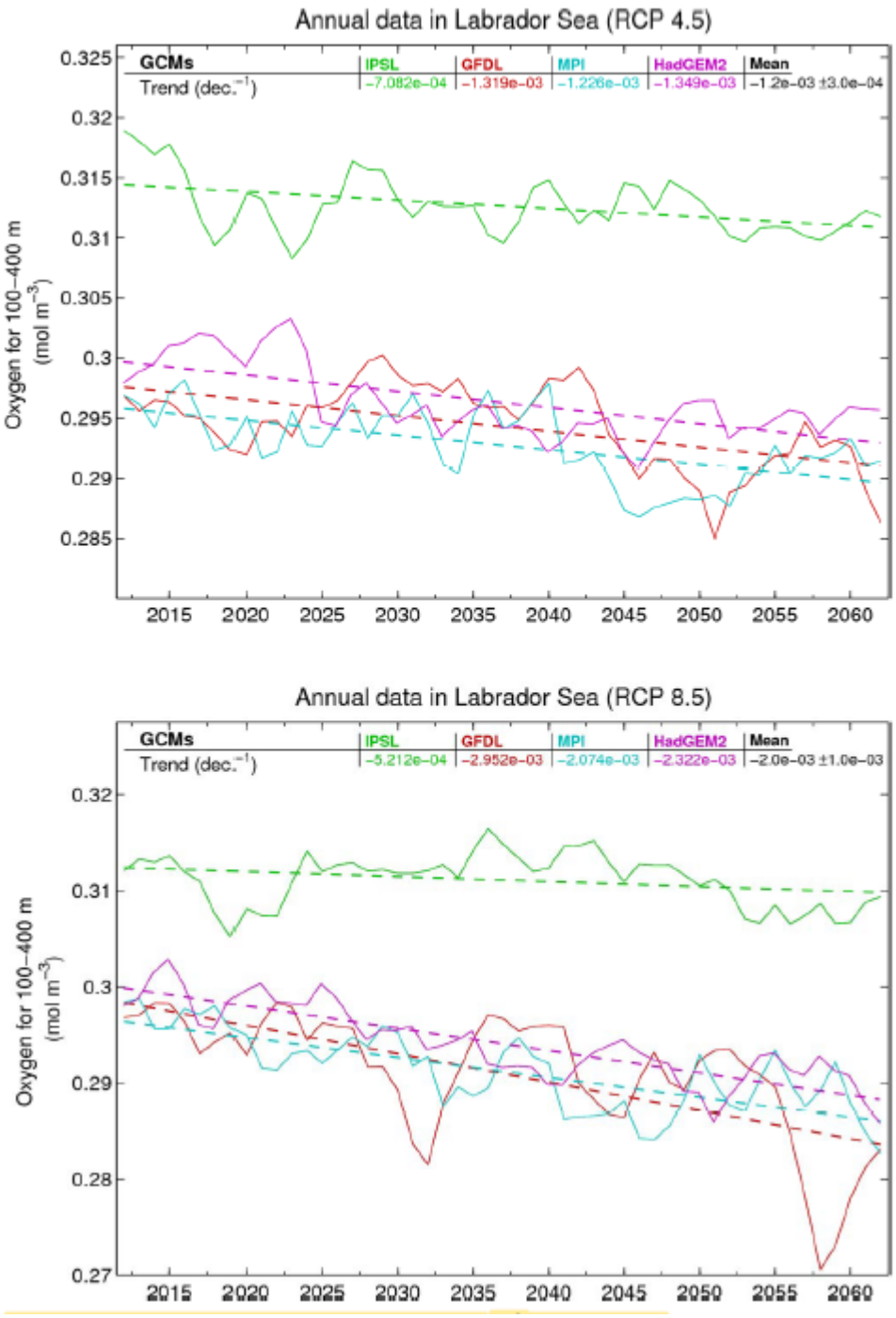

Figure 5-2. Future oxygen concentration trends (mol m^{-3}/decade) at 100-400 m in the Labrador Sea for the 2012-2062 period for RCPs 4.5 and 8.5. Figure 50. from " Projections of Future Physical and Biogeochemical Conditions in the Northwest Atlantic from CMIP5 Global Climate Models" (Lavoie, Lambert and Gilbert, 2017).

These findings, coupled with how understudied sponges are historically, leads to the tragic conclusions that in all likelihood many sponge species and habitats in the Labrador Sea will disappear due to anthropogenic influence without ever having being observed.

5.4. Further work

This thesis has barely scratched the surface of potential work needed in this area to understand how sponge grounds work and the drivers of their distribution and density. Each of the studies have follow on work that would enhance our understanding of theses assemblages and sponge distribution in general.

5.4.1. Flow modeling

The effect of topography on the local distribution patterns of sponges in an area would be an interesting and logical next application of the fluid modeling technique. Given at a small scale we see this boundary layer created by the sponge structure slowing the flow around them. Does this also extend to clustering around topographic structures which also effect flow rates on the sea floor? This would require both a detailed topography map of the sea floor at a very high resolution and an accurate way to assess sponge occurrences in the area. Both of these could be obtained from a systematic ROV image survey and a digital surface model created using the same methodology used here. I would hypothesize that they would cluster in areas of slower flow, for example on the leeward side of boulders, potentially explaining patterns of higher sponge density within a sponge ground. The effect of topographic features such as boulders and hollows, could also be initially estimated using the current model using idealized structural models to calculating he wake effect. From these flow models we could hypothesis the expected clustering pattern of sponges around these features and compare these predictions to insitu observations. This proposed study would be most informative if it were possible to obtain detailed current data for the areas, particularly average current velocity, maximum velocity, tidal variability and in an ideal world, measurements from within the boundary layer.

If we had maximum velocity data within an area we could begin to put constraints on particular species if we were able to understand more about the mechanical properties of sponge structures.

One of the major limitations I had with these models was the lack of any information about the deformation and failure properties of sponges in general. It would be invaluable for the extension of these type of studies to do destructive testing on a number of commonly found sponge species. It would enable the modeling the stress strain forcing given variable flow condition in an area as well as identification of the point of failure. which in turn would enable the prediction of maximum flow velocity possible in a locality for each of these sponges to exist.

Increasing the complexity and realism of the sponge shapes within the model would also be an interesting avenue for further study. I particularly would be interested in the effect of spines and other extensions to the sponges' general morphology. To do this I would initially try and create a hyperrealist 3d model of a sponge using images from a CT scan of a sponge sample. Based on the flow fields created I would potentially expand this to look at the interaction of multiple individuals and specific species morphology. To achieve this I would have to improve the method of 3D model creation and change the meshing tools used in this study, as the current method of photogrametry and inbuilt Comsol Mesher would not be able to cope with the increased model resolution. This would also be key problem to solve to expanding the area of sea floor included within the model.

Another general improvement of the model would be including the outflow from the sponges. This extra element to the flow field will certainly have an effect on the boundary layer and may give us a better understanding of what the advantages and disadvantages this layer of slowed flow has for the individual sponge.

5.4.2. Biodiversity

The biodiversity study conducted in this thesis did not include the 25 hexactinellid samples that were collected on the DY081 cruise and were only identified to class. Identifying these sample to species level would be the obvious first extension to this study. The difficulty lies in the cryptic nature of many species within this class, making identification from taxonomy alone challenging, with specimens more usually identified using genetic sequencing. Conducting these analyses would give a much more complete picture of sponge biodiversity in the three localities particularly as we know that the deeper areas of the Orphan Knoll locality are dominated by these sponges. Genetic sequencing the new species as well as those with extended extent into the Labrador Sea would be another avenue to pursue. In particular it would be interesting to see if the sequences for *Phakellia*

cf .*robusta* (Bowerbank, 1866) matched that of *P. robusta*. The sequences for the new species would be also be a good way to confirm the genus in which they have been placed.

There is also work needing to be done on the genus *Iophon* (Gray, 1867) in the North Atlantic, particularly as the unspecified *Iophon* species in the biodiversity study is probably a species new to science. I was unable to describe it in this study as the species delineation of the rest of the genus is very poorly constrained, with contradictory and overlapping descriptions of spicule measurements and shape. A full review of the genus is needed probably with genetic sequencing of all known North Atlantic species to definitively sort out the species groupings.

Further biodiversity studies conducted using an ROV with the Labrador Sea would be invaluable. Having demonstrated the value of this collection method for capturing a greater proportion of the biodiversity in an area, as it is able to capture small, delicate and encrusting sponges that would usually be lost. I would expect that using this collection method at previously studies sites would yield a greater number and diversity of species present.

5.4.3. Biogeography

The conclusions of the biogeography study would be made much clearer and its predictions would be more specific, if an idea of how the physical condition of the Labrador Sea might change over time. Physical parameters such as ocean temperatures have been key variables in many climate modeling studies. It would be interesting to obtain the results from climate models of bottom waters temperatures over a range of climate scenarios, for the Labrador Sea. These results would hopefully give us a clear picture of how changes in the climate would manifest in this region.

Further work to test the prediction we have made on sponge assemblage distribution would also be worth pursuing. To look at the prediction that the Eastern Canadian shelf North of Newfoundland and south of Baffin Island would be similar to the West Greenland shelf assemblage could be initially tested by comparison of our assemblage to the current survey data of the area. Although it would be worth keeping in mind that most of these data are derived from trawl collections (Baker *et al.*, 2018; Murillo *et al.*, 2018) and so will be missing the smaller and more delicate species we were able to collect using the ROV. For the assemblage on the West Greenland shelf this would potentially involve further sponge sample collection using an ROV to in able the collection of *in situ* environmental variables.

6. Bibliography

Abelson, A. and Denny, M. (1997) 'Settlement of marine organisms in flow', *Annual Review of Ecology and Systematics*, 28(1), pp. 317–339. doi: 10.1146/annurev.ecolsys.28.1.317.

Achlatis, M. *et al.* (2019) 'Photosynthesis by symbiotic sponges enhances their ability to erode calcium carbonate', *Journal of Experimental Marine Biology and Ecology*, 516, pp. 140–149.

Ackers, R. *et al.* (2007) 'Sponges of the British Isles—a colour guide and working document'. Marine Conservation Society.

Alander, H. (1935) 'Additions to the Swedish sponge fauna.', *Arkiv för Zoologi*, 28B(5), pp. 1–6.

Alander, H. (1942) 'Sponges from the Swedish west-coast and adjacent waters. ', *Ph.D. Thesis. (University of Lund, H. Struves: Gøteborg)*. Available at: http://www.marinespecies.org/porifera/porifera.php?p=sourcedetails&id=7036.

Althaus, F. *et al.* (2009) 'Impacts of bottom trawling on deep-coral ecosystems of seamounts are long-lasting', *Marine Ecology Progress Series*, 397, pp. 279–294. Available at: https://www.int-res.com/abstracts/meps/v397/p279-294/ (Accessed: 12 December 2019).

Anjum, K. *et al.* (2016) 'Marine sponges as a drug treasure', *Biomolecules and Therapeutics*. Korean Society of Applied Pharmacology, pp. 347–362. doi: 10.4062/biomolther.2016.067.

Annunziata, B. B. *et al.* (2019) 'Two new Clathria (Axosuberites) Topsent, 1893 (Demospongiae: Poecilosclerida) from Northeastern Brazil', *Zootaxa*, 4671(4), pp. 500–510. doi: 10.11646/zootaxa.4671.4.2.

Archambault, P. *et al.* (2010) 'From sea to sea: Canada's three oceans of biodiversity', *PLoS ONE*, p. e12182. doi: 10.1371/journal.pone.0012182.

Baddeley, A. *et al.* (2014) *On tests of spatial pattern based on simulation envelopes*, *Ecological Monographs*.

Baker, E. L. *et al.* (2018) *Epibenthic Megafauna of the Disko Fan Conservation Area in the Davis Strait (Eastern Arctic) Identified from In Situ Benthic Image Transects Ocean and Ecosystem Sciences Division Fisheries and Oceans Canada Canadian Technical Report of Fisheries and Aqu*, *Canadian Technical Report of Fisheries and Aquatic Sciences*. Available at: http://www.vliz.be/imisdocs/publications/319250.pdf (Accessed: 20 April 2021).

Bamber, J. L. *et al.* (2018) 'The land ice contribution to sea level during the satellite era', *Environmental Research Letters*, 13(6), p. 063008. doi: 10.1088/1748-9326/AAC2F0.

Barrio Froján, C. R. S. *et al.* (2012) 'An evaluation of benthic community structure in and around the Sackville Spur closed area (Northwest Atlantic) in relation to the protection of vulnerable marine ecosystems', *ICES Journal of Marine Science*, 69(2), pp. 213–222. doi: 10.1093/ICESJMS/FSS004.

Barthel, D., Tendal, O. S. and Thiel, H. (1996) 'A Wandering Population of the Hexactinellid Sponge Pheronema carpenteri on the Continental Slope off Morocco, Northwest Africa', *Marine Ecology*, 17(4), pp. 603–616. doi: 10.1111/j.1439-0485.1996.tb00420.x.

Bauer, S. L. M. *et al.* (2018) 'Water masses and depth structure prokaryotic and T4-like viral communities around hydrothermal systems of the Nordic Seas', *Frontiers in Microbiology*, 9(MAY), p. 1002. doi: 10.3389/FMICB.2018.01002/BIBTEX.

Baums, I. B. *et al.* (2020) 'Evidence of Vent-Adaptation in Sponges Living at the Periphery of Hydrothermal Vent Environments: Ecological and Evolutionary Implications Vent-Adaptation in Peripheral Sponges', *Frontiers in Microbiology | www.frontiersin.org*, 1. doi: 10.3389/fmicb.2020.01636.

Beazley, L. *et al.* (2013) 'Deep-sea sponge grounds enhance diversity and abundance of epibenthic megafauna in the Northwest Atlantic', *ICES Journal of Marine Science*, 70(7), pp. 1471–1490. doi: 10.1093/icesjms/fst124.

Beazley, L. *et al.* (2015) 'Drivers of epibenthic megafaunal composition in the sponge grounds of the Sackville Spur, northwest Atlantic', *Deep-Sea Research Part I: Oceanographic Research Papers*, 98, pp. 102–114. doi: 10.1016/j.dsr.2014.11.016.

Bell, J. J. (2008) 'The functional roles of marine sponges', *Estuarine, Coastal and Shelf Science*, 79(3), pp. 341–353. doi: 10.1016/J.ECSS.2008.05.002.

Bell, J. J., Mcgrath, E., *et al.* (2015) 'Global conservation status of sponges', *Conservation Biology*. Blackwell Publishing Inc., pp. 42–53. doi: 10.1111/cobi.12447.

Bell, J. J., McGrath, E., *et al.* (2015) 'Sediment impacts on marine sponges', *Marine Pollution Bulletin*, 94(1–2), pp. 5–13. doi: 10.1016/J.MARPOLBUL.2015.03.030.

Bell, J. J. *et al.* (2018) 'Climate change alterations to ecosystem dominance: how might sponge-dominated reefs function?', *Ecology*, 99(9), pp. 1920–1931. doi: 10.1002/ecy.2446.

Bell, J. J. and Barnes, D. K. A. (2000a) 'The distribution and prevalence of sponges in relation to environmental gradients within a temperate sea lough: Inclined cliff surfaces', *Diversity and Distributions*, 6(6), pp. 305–323. doi: 10.1046/j.1472-4642.2000.00092.x.

Bell, J. J. and Barnes, D. K. A. (2000b) 'The influences of bathymetry and flow regime upon the morphology of sublittoral sponge communities', *Journal of the Marine Biological Association of the United Kingdom*, (80), pp. 707–718. Available at: https://www.cambridge.org/core/services/aop-cambridge-core/content/view/897C6F9DD55CDAE38D63CC286268C1E7/S0025315400002538a.pdf/influences_of_bathymetry_and_flow_regime_upon_the_morphology_of_sublittoral_sponge_communities.pdf (Accessed: 3 April 2018).

Berg, C. (1899) 'Substitución de nombres genéricos. III', *Communicaciones del Museo Nacional de Buenos Aires*, 1(3), pp. 77–80. Available at: https://www.marinespecies.org/aphia.php?p=sourcedetails&id=7110.

Bergquist, P. R. (1978) 'Sponges', *Hutchinson: London, University of California Press, Berkeley & Los Angeles*, pp. 1–268. Available at: http://www.marinespecies.org/porifera/porifera.php?p=sourcedetails&id=7119.

Bergquist, P. R. and Fromont, P. J. (1988) 'The Marine Fauna of New Zealand: Porifera, Demospongiae, Part 4 Poecilosclerida. ', *New Zealand Oceanographic Institute Memoir*, 96, pp. 1–197. Available at: http://www.marinespecies.org/porifera/porifera.php?p=sourcedetails&id=7124.

Berman, J. *et al.* (2013) 'Testing the suitability of a morphological monitoring approach for identifying temporal variability in a temperate sponge assemblage', *Journal for Nature Conservation*,

21(3), pp. 173–182. doi: 10.1016/J.JNC.2012.12.003.

Bertolino, M. *et al.* (2007) 'Sponges from a submarine canyon of the Argentine Sea. *In*: Custódio MR, Lôbo-Hajdu G, Hajdu E, Muricy G (eds) Porifera Research. Biodiversity, Innovation and Sustainability. Livros de Museu Nacional 28, Rio de Janeiro', in, pp. 189–201. Available at: http://www.marinespecies.org/porifera/porifera.php?p=sourcedetails&id=44006.

Bett, B. J. (2001) 'UK Atlantic Margin Environmental Survey: Introduction and overview of bathyal benthic ecology', *Continental Shelf Research*, 21(8–10), pp. 917–956. doi: 10.1016/S0278-4343(00)00119-9.

Bett, B. J. and Rice, A. L. (1992) 'The influence of hexactinellid sponge (Pheronema carpenteri) spicules on the patchy distribution of macrobenthos in the porcupine seabight (Bathyal ne atlantic)', *Ophelia*, 36(3), pp. 217–226. doi: 10.1080/00785326.1992.10430372.

Bhatia, M. P. *et al.* (2013) 'Erratum: Greenland meltwater as a significant and potentially bioavailable source of iron to the ocean', *Nature Geoscience 2013 6:6*, 6(6), pp. 503–503. doi: 10.1038/ngeo1833.

Bluhm, H. (2001) 'Re-establishment of an abyssal megabenthic community after experimental physical disturbance of the seafloor', *Deep Sea Research Part II: Topical Studies in Oceanography*, 48(17–18), pp. 3841–3868. doi: 10.1016/S0967-0645(01)00070-4.

Bo, M. *et al.* (2014) 'Fishing impact on deep Mediterranean rocky habitats as revealed by ROV investigation', *Biological Conservation*, 171, pp. 167–176. doi: 10.1016/J.BIOCON.2014.01.011.

Bourgeois, S. *et al.* (2016) 'Glacier inputs influence organic matter composition and prokaryotic distribution in a high Arctic fjord (Kongsfjorden, Svalbard)', *Journal of Marine Systems*, 164, pp. 112–127. doi: 10.1016/J.JMARSYS.2016.08.009.

Boury-Esnault, N. and Van Beveren, M. (1982) 'Les Démosponges du plateau continental de Kerguelen-Heard', *Comité national français des recherches antarctiques*, 52, pp. 1–175. Available at: http://www.marinespecies.org/porifera/porifera.php?p=sourcedetails&id=7198.

Bowerbank, J. S. (1858) 'On the Anatomy and Physiology of the Spongiadae. Part I. On the Spicula.', *Philosophical Transactions of the Royal Society*. Available at: http://www.marinespecies.org/porifera/porifera.php?p=sourcedetails&id=7202.

Bowerbank, J. S. (1862) 'On the Anatomy and Physiology of the Spongiadae. Part III On the Generic Characters, the Specific Characters, and on the Method of Examination. ', *Philosophical Transactions of the Royal Society*. Available at: http://www.marinespecies.org/porifera/porifera.php?p=sourcedetails&id=7205.

Bowerbank, J. S. (1864) 'A Monograph of the British Spongiadae.Volume 1. (Ray Society: London): i-xx, 1-290, pls I-XXXVII.', in. Available at: https://biodiversitylibrary.org/page/1883085.

Bowerbank, J. S. (1866) 'A Monograph of the British Spongiadae. Volume 2. (Ray Society: London): i-xx, 1-388.', in, pp. 1–388. Available at: https://biodiversitylibrary.org/page/1905089.

Bradshaw, C. *et al.* (2012) 'Bottom trawling resuspends sediment and releases bioavailable contaminants in a polluted fjord', *Environmental Pollution*, 170, pp. 232–241. doi: 10.1016/j.envpol.2012.06.019.

Broad, E. (2019) *A molecular and morphological redescription of the demosponge Phakellia (Bowerbank, 1862) provides evidence of cryptic speciation in the North East Atlantic*. Zoological Society of London.

Brøndsted, H. V (1924) 'Papers from Dr. Th. Mortensen's Pacific Expedition 1914-16. XXIII. Sponges from New Zealand. Part I. ', *Videnskabelige Meddelelser fra Dansk naturhistorisk Forening i Kjøbenhavn*, 77, pp. 435-483. Available at: http://www.marinespecies.org/porifera/porifera.php?p=sourcedetails&id=7251.

Brøndsted, H. V (1933a) 'The Godthaab Expedition 1928. Porifera', *Meddelelser om Grønland*, 79(51–25), p. (5):1-25. Available at: http://www.marinespecies.org/porifera/porifera.php?p=sourcedetails&id=7256.

Brøndsted, H. V (1933b) 'The Scoresby Sound Committee's 2nd East Greenland Expedition in 1932 to King Christian IX's Land. Porifera. ', *Meddelelser om Grønland*, 104(12), pp. 1–10. Available at: http://www.marinespecies.org/porifera/porifera.php?p=sourcedetails&id=132517.

Brusca, R. C. and Brusca, G. J. (2003) *Invertebrates*. Basingstoke.

Buhl-Mortensen, L. *et al.* (2010) 'Biological structures as a source of habitat heterogeneity and biodiversity on the deep ocean margins', *Marine Ecology*, 31(1), pp. 21–50. doi: 10.1111/j.1439-0485.2010.00359.x.

Burton, M. (1928) 'Report on some Deep-Sea Sponges from the Indian Museum collected by R.I.M.S. "Investigator''. Part II. Tetraxonida (concluded) and Euceratosa"', *Records of the Indian Museum*, 30(1), pp. 109–138. Available at: http://www.marinespecies.org/porifera/porifera.php?p=sourcedetails&id=7261.

Burton, M. (1929) 'Porifera. Part II. Antarctic sponges. ', *British Antarctic ('Terra Nova') Expedition, 1910. Natural History Report, London, Zoology*. Available at: http://www.marinespecies.org/porifera/porifera.php?p=sourcedetails&id=7263.

Burton, M. (1932) 'Sponges', *Discovery Reports*. Available at: http://www.marinespecies.org/porifera/porifera.php?p=sourcedetails&id=7275.

Busch, K. *et al.* (2020) 'On giant shoulders: How a seamount affects the microbial community composition of seawater and sponges', *Biogeosciences*, 17(13), pp. 3471–3486. doi: 10.5194/BG-17-3471-2020.

Camillo, C. G. Di *et al.* (2013) 'Sponge disease in the Adriatic Sea', *Marine Ecology*, 34(1), pp. 62–71. doi: 10.1111/J.1439-0485.2012.00525.X.

Cape, M. R. *et al.* (2018) 'Nutrient release to oceans from buoyancy-driven upwelling at Greenland tidewater glaciers', *Nature Geoscience 2018 12:1*, 12(1), pp. 34–39. doi: 10.1038/s41561-018-0268-4.

Cárdenas, C. A. *et al.* (2019) 'Temporal Stability of Bacterial Communities in Antarctic Sponges', *Frontiers in microbiology*, 10. doi: 10.3389/FMICB.2019.02699.

Cárdenas, P. *et al.* (2010) 'Molecular taxonomy and phylogeny of the Geodiidae (Porifera,Demospongiae, Astrophorida) - combining phylogenetic and Linnaean classification', *Zoologica Scripta*, 39(1), pp. 89–106. doi: 10.1111/j.1463-6409.2009.00402.x.

Cárdenas, P. *et al.* (2011) 'Molecular Phylogeny of the Astrophorida (Porifera, Demospongiaep) Reveals an Unexpected High Level of Spicule Homoplasy', *PLoS ONE*. Edited by D. Steinke, 6(4), p. e18318. doi: 10.1371/journal.pone.0018318.

Cárdenas, P., Rapp, H. T., Best, M., *et al.* (2013) 'A revision of boreo-arctic Atlantic Tetillidae (Demospongiae, Spirophorina): new records and new species', in *9th World Sponge Conference*

2013. Vol 4.

Cárdenas, P., Rapp, H. T., Klitgaard, A. B., *et al.* (2013) 'Taxonomy, biogeography and DNA barcodes of Geodia species (Porifera, Demospongiae, Tetractinellida) in the Atlantic boreo-arctic region', *Zoological Journal of the Linnean Society*, 169(2), pp. 251–311. doi: 10.1111/zoj.12056.

Cárdenas, P. and Rapp, H. T. (2015) 'Demosponges from the Northern Mid-Atlantic Ridge shed more light on the diversity and biogeography of North Atlantic deep-sea sponges', *Journal of the Marine Biological Association of the United Kingdom*, 95(7). doi: 10.1017/S0025315415000983.

Carter, H. J. (1875) 'Notes introductory to the study and classification of the Spongida. Part II. Proposed classification of the Spongida', *Annals and Magazine of Natural History*, 4(16), pp. 126–145. Available at: http://www.marinespecies.org/porifera/porifera.php?p=sourcedetails&id=162891.

Carter, H. J. (1876) 'Descriptions and Figures of Deep-Sea Sponges and their Spicules, from the Atlantic Ocean, dredged up on board H.M.S."Porcupine'', chiefly in 1869 (concluded)"', *Annals and Magazine of Natural History*. Available at: http://www.marinespecies.org/porifera/porifera.php?p=sourcedetails&id=7325.

Carter, H. J. (1881) ' XXXVI.— Supplementary report on specimens dredged up from the Gulf Manaar, together with others from the sea in the vicinity of the Basse Rocks and from Bass's Straits respectively, presented to the Liverpool Free Museum by Capt. H. Cawne Warren ', *Annals and Magazine of Natural History*, 7(41), pp. 361–385. doi: 10.1080/00222938109459534.

Carter, H. J. (1882) 'Some Sponges from the West Indies and Acapulco in the Liverpool Free Museum described, with general and classificatory Remarks.', *Annals and Magazine of Natural History*. Available at: https://www.biodiversitylibrary.org/page/26194801#page/360/mode/1up.

Carter, H. J. (1886) 'Descriptions of Sponges from the Neighbourhood of Port Phillip Heads, South Australia, continued', *Annals and Magazine of Natural History*. Available at: http://www.marinespecies.org/porifera/porifera.php?p=sourcedetails&id=7356.

Cathalot, C. *et al.* (2015) 'Cold-water coral reefs and adjacent sponge grounds: hotspots of benthic respiration and organic carbon cycling in the deep sea', *Frontiers in Marine Science*, 2, p. 37. doi: 10.3389/fmars.2015.00037.

Cebrian, E. *et al.* (2011) 'Sponge Mass Mortalities in a Warming Mediterranean Sea: Are Cyanobacteria-Harboring Species Worse Off?', *PLOS ONE*, 6(6), p. e20211. doi: 10.1371/JOURNAL.PONE.0020211.

Cerrano, C. *et al.* (2000) 'A catastrophic mass-mortality episode of gorgonians and other organisms in the Ligurian Sea (North-western Mediterranean), summer 1999', *Ecology Letters*, 3(4), pp. 284–293. doi: 10.1046/J.1461-0248.2000.00152.X.

Chindapol, N. *et al.* (2013) 'Modelling Growth and Form of the Scleractinian Coral Pocillopora verrucosa and the Influence of Hydrodynamics', *PLoS Computational Biology*. Edited by E. J. Crampin, 9(1), p. e1002849. doi: 10.1371/journal.pcbi.1002849.

Chu, J. W. F. and Leys, S. P. (2010) 'High resolution mapping of community structure in three glass sponge reefs (Porifera, Hexactinellida)', *Marine Ecology Progress Series*, 417, pp. 97–113. doi: 10.3354/meps08794.

Clark, M. R. *et al.* (2009) 'The Ecology of Seamounts: Structure, Function, and Human Impacts', *http://dx.doi.org/10.1146/annurev-marine-120308-081109*, 2(1), pp. 253–278. doi:

10.1146/ANNUREV-MARINE-120308-081109.

Clark, M. R. *et al.* (2016) 'The impacts of deep-sea fisheries on benthic communities: a review', *ICES Journal of Marine Science: Journal du Conseil*, 73(suppl 1), pp. i51–i69. doi: 10.1093/icesjms/fsv123.

Clark, M. R. *et al.* (2019) 'Little Evidence of Benthic Community Resilience to Bottom Trawling on Seamounts After 15 Years', *Frontiers in Marine Science*, 6(FEB), p. 63. doi: 10.3389/FMARS.2019.00063.

Clark, P. U. *et al.* (2002) 'The role of the thermohaline circulation in abrupt climate change', *Nature 2002 415:6874*, 415(6874), pp. 863–869. doi: 10.1038/415863a.

Coad, B. and Reist, J. (2019) 'Marine fishes of Arctic Canada'. University of Toronto Press.

Collins, M. *et al.* (2019) 'Extremes, Abrupt Changes and Managing Risk', in Pörtner, H. O. et al. (eds) *IPCC Special Report on the Ocean and Cryosphere in a Changing Climate*.

Conway, K. W. *et al.* (2017) 'Sponge Reefs of the British Columbia, Canada Coast: Impacts of Climate Change and Ocean Acidification', in *Climate Change, Ocean Acidification and Sponges*. Cham: Springer International Publishing, pp. 429–445. doi: 10.1007/978-3-319-59008-0_10.

Cook, S. E. and Conway, K. W. (2008) 'Status of the glass sponge reefs in the Georgia Basin', *Marine Environmental Research*, 66, pp. S80–S86. doi: 10.1016/J.MARENVRES.2008.09.002.

Cresswell, A. K. *et al.* (2017) 'A functional-structural coral model', in *MODSIM2017: 22nd International Congress on Modelling and Simulation*. Modelling and Simulation Society of Australia and New Zealand Inc., pp. 237–243. Available at: https://www.mssanz.org.au/modsim2017/B2/cresswell.pdf (Accessed: 6 July 2018).

Cuartas, E. I. (1992) 'Poríferos intermareales de San Antonio Oeste, Provincia de Río Negro, Argentina (Porifera: Demospongiae). ', *Neotropica*, 38, pp. 111–118. Available at: http://www.marinespecies.org/porifera/porifera.php?p=sourcedetails&id=39068.

Culwick, T. *et al.* (2020) 'Sponge Density and Distribution Constrained by Fluid Forcing in the Deep Sea', *Frontiers in Marine Science*, 7, p. 395. doi: 10.3389/fmars.2020.00395.

D'Onghia, G. *et al.* (2015) 'Macro- and megafauna recorded in the submarine Bari Canyon (southern Adriatic, Mediterranean Sea) using different tools', *Mediterranean Marine Science*, 16(1), pp. 180–196. doi: 10.12681/mms.1082.

Darnis, G. *et al.* (2012) 'Current state and trends in Canadian Arctic marine ecosystems: II. Heterotrophic food web, pelagic-benthic coupling, and biodiversity', *Climatic Change*, 115(1), pp. 179–205. doi: 10.1007/s10584-012-0483-8.

Dayton, P. K. *et al.* (1974) 'Biological Accommodation in the Benthic Community at McMurdo Sound, Antarctica', *Ecological Monographs*, 44(1), pp. 105–128. doi: 10.2307/1942321.

Dendy, A. (1896) 'Catalogue of Non-Calcareous Sponges collected by J. Bracebridge Wilson, Esq., M.A., in the neighbourhood of Port Phillip Heads. Part II.', *Proceedings of the Royal Society of Victoria (New Series)*, 8, pp. 14–51. Available at: http://www.marinespecies.org/porifera/porifera.php?p=sourcedetails&id=7400.

Dendy, A. (1905) 'Report on the sponges collected by Professor Herdman,at Ceylon, in 1902. ', in *In: Herdman, W.A. (Ed.), Report to the Government of Ceylon on the Pearl Oyster Fisheries of the Gulf of Manaar. 3 (Supplement 18). (Royal Society: London).* Available at:

http://www.marinespecies.org/porifera/porifera.php?p=sourcedetails&id=7402.

Dendy, A. (1922) 'Report on the Sigmatotetraxonida collected by H.M.S."Sealark'' in the Indian Ocean. *In*: Reports of the Percy Sladen Trust Expedition to the Indian Ocean in 1905, Vol. 7"', *Transactions of the Linnean Society of London*. Available at: http://www.marinespecies.org/porifera/porifera.php?p=sourcedetails&id=7412.

Dendy, A. (1924) 'Porifera. Part I. Non-Antarctic sponges. Natural History Report.', *British Antarctic (Terra Nova) Expedition, 1910 (Zoology)*. Available at: http://www.marinespecies.org/porifera/porifera.php?p=sourcedetails&id=7413.

Dinn, C. *et al.* (2020) 'Sponge communities in the eastern Canadian Arctic: species richness, diversity and density determined using targeted benthic sampling and underwater video analysis', *Polar Biology*. doi: 10.1007/s00300-020-02709-z.

Dinn, C., Edinger, E. and Leys, S. P. (2019) 'Sponge (Porifera) fauna of Frobisher Bay, Baffin Island, Canada with the description of an Iophon rich sponge garden', *Zootaxa*, 4576(2), pp. 301–325. doi: 10.11646/zootaxa.4576.2.5.

Dinn, C. and Leys, S. (2018) 'Field guide to sponges of the Eastern Canadian Arctic'. Department of Biological Sciences, Education and Resource Archive, University of Alberta.

Downey, R. V. *et al.* (2012) 'Diversity and distribution patterns in high Southern latitude sponges', *PLoS ONE*, 7(7), p. e41672. doi: 10.1371/journal.pone.0041672.

Downey, R. V., Fuchs, M. and Janussen, D. (2018) 'Unusually diverse, abundant and endemic deep–sea sponge fauna revealed in the Sea of Okhotsk (NW Pacific Ocean)', *Deep-Sea Research Part II: Topical Studies in Oceanography*, 154, pp. 47–58. doi: 10.1016/j.dsr2.2018.02.005.

Duchassaing de Fonbressin, P. and Michelotti, G. (1864) 'Spongiaires de la mer Caraibe', *Natuurkundige verhandelingen van de Hollandsche maatschappij der wetenschappen te Haarlem* . Available at: https://www.marinespecies.org/aphia.php?p=sourcedetails&id=7448.

Dullo, W. C., Flögel, S. and Rüggeberg, A. (2008) 'Cold-water coral growth in relation to the hydrography of the Celtic and Nordic European continental margin', *Marine Ecology Progress Series*, 371, pp. 165–176. doi: 10.3354/MEPS07623.

Durán Muñoz, P. *et al.* (2020) 'Cold-water corals and deep-sea sponges by-catch mitigation: Dealing with groundfish survey data in the management of the northwest Atlantic Ocean high seas fisheries', *Marine Policy*, 116, p. 103712. doi: 10.1016/J.MARPOL.2019.103712.

Durrieu De Madron, X. *et al.* (2005) 'Trawling-induced resuspension and dispersal of muddy sediments and dissolved elements in the Gulf of Lion (NW Mediterranean)', *Continental Shelf Research*, 25(19–20), pp. 2387–2409. doi: 10.1016/J.CSR.2005.08.002.

Easson, C. G. and Thacker, R. W. (2014) 'Phylogenetic signal in the community structure of host-specific microbiomes of tropical marine sponges', *Frontiers in Microbiology*, 5(OCT), p. 532. doi: 10.3389/FMICB.2014.00532/ABSTRACT.

Eerkes-Medrano, D. *et al.* (2020) 'A community assessment of the demersal fish and benthic invertebrates of the Rosemary Bank Seamount marine protected area (NE Atlantic)', *Deep-Sea Research Part I: Oceanographic Research Papers*, 156. doi: 10.1016/J.DSR.2019.103180.

Eriksson, B. K. *et al.* (2010) 'Major changes in the ecology of the wadden sea: Human impacts, ecosystem engineering and sediment dynamics', *Ecosystems*, 13(5), pp. 752–764. doi:

10.1007/s10021-010-9352-3.

Ewing, G. P. and Kilpatrick, R. (2013) 'Estimating the gear footprint of demersal trawl and longline fishing gears used in the Heard Island and McDonald Islands fisheries .', in Welsford, D. C. et al. (eds) *Demersal fishing interactions with marine benthos in the Australian EEZ of the Southern Ocean: An assessment of the vulnerability of benthic habitats to impact by demersal gears*. Australian Antarctic Division, p. 265.

Fallon, S. J. *et al.* (2010) 'A simple radiocarbon dating method for determining the age and growth rate of deep-sea sponges', *Nuclear Instruments and Methods in Physics Research Section B: Beam Interactions with Materials and Atoms*, 268(7–8), pp. 1241–1243. doi: 10.1016/J.NIMB.2009.10.143.

FAO (2009) *International Guidelines For The Managment of Deep-Sea Fisheries In The High Seas*. Rome.

Fernandez, J. C. *et al.* (2020) 'Sponges from Doumer Island, Antarctic Peninsula, with description of new species of Clathria (Axosuberites) Topsent, 1893 and Hymeniacidon Bowerbank, 1858, and a re-description of H. torquata Topsent, 1916', *Zootaxa*, 4728(1), pp. 77–109. doi: 10.11646/zootaxa.4728.1.4.

Fleming, J. (1828) 'A history of British animals, exhibiting the descriptive characters and systematical arrangement of the genera and species of quadrupeds, birds, reptiles, fishes, Mollusca, and Radiata of the United Kingdom; including the indigenous, extirpated, and extin', *Edinburgh, Bell & Bradfute / London, James Duncan*. doi: 10.5962/bhl.title.12859.

Freese, J. L. and WIng, B. L. (2003) 'Juvenile Red Rockfish, Sebastes sp., Associations with Sponges in the Gulf of Alaska', *Marine Fisheries Review*, 65(3), pp. 38–42.

Friedlingstein, P. *et al.* (2006) 'Climate–Carbon Cycle Feedback Analysis: Results from the C 4 MIP Model Intercomparison', *Journal of Climate*, 19(14), pp. 3337–3353. doi: 10.1175/JCLI3800.1.

Fristedt, K. (1887) 'Sponges from the Atlantic and Arctic Oceans and the Behring Sea', *Vega-Expeditionens Vetenskap. Iakttagelser (Nordenskiöld) 4*, pp. 22–31. Available at: http://www.marinespecies.org/aphia.php?p=sourcedetails&id=7480.

Fuller, S. (2011) *Diversity of Marine Sponges in the Northwest Atlantic*. Dalhousie University.

Fyfe, J. C., Gillett, N. P. and Zwiers, F. W. (2013) 'Overestimated global warming over the past 20 years', *Nature Climate Change 2013 3:9*, 3(9), pp. 767–769. doi: 10.1038/nclimate1972.

Garcia-Quintana, Y. *et al.* (2019) 'Sensitivity of Labrador Sea Water Formation to Changes in Model Resolution, Atmospheric Forcing, and Freshwater Input', *Journal of Geophysical Research: Oceans*, 124(3), pp. 2126–2152. doi: 10.1029/2018JC014459.

Garrabou, J. *et al.* (2009) 'Mass mortality in Northwestern Mediterranean rocky benthic communities: Effects of the 2003 heat wave', *Global Change Biology*, 15(5), pp. 1090–1103. doi: 10.1111/j.1365-2486.2008.01823.x.

Genin, A. *et al.* (1986) 'Corals on seamount peaks provide evidence of current acceleration over deep-sea topography', *Nature 1986 322:6074*, 322(6074), pp. 59–61. doi: 10.1038/322059a0.

González-Aravena, M. *et al.* (2019) 'Warm temperatures, cool sponges: the effect of increased temperatures on the Antarctic sponge Isodictya sp.', *PeerJ*, 7(12). doi: 10.7717/PEERJ.8088.

Goodwin, C. E. *et al.* (2016) 'Sponge biodiversity of Beauchêne and the Sea Lion Islands and south-

east East Falkland, Falkland Islands, with a description of nine new species. In: Schönberg CHL, Fromont J, Hooper NA, Sorokin S, Zhang W, de Voogd N (eds) New Frontiers in Sponge', *Journal of the Marine Biological Association of the United Kingdom*, 96, pp. 263–290. doi: 10.1017/s0025315414001775.

Goodwin, C. E. *et al.* (2017) 'Carnivorous sponges (Porifera : Demospongiae : Poecilosclerida : Cladorhizidae) from the Drake Passage (Southern Ocean) with a description of eight new species and a review of the family Cladorhizidae in the Southern Ocean', *Invertebrate Systematics*, 31(1), p. 37. doi: 10.1071/IS16020.

Goodwin, C. E., Brewin, P. E. and Brickle, P. (2012) 'Sponge biodiversity of South Georgia island with descriptions of fifteen new species', *Zootaxa*, 3542, pp. 1–48. Available at: http://www.mapress.com/zootaxa/2012/f/z03542p048f.pdf.

Goodwin, C. E. and Picton, B. (2009) 'Demosponges of the genus Hymedesmia (Poecilosclerida: Hymedesmidae) from Rathlin Island, Northern Ireland, with a description of six new species', *Zoological Journal of the Linnean Society*, 156(4), pp. 896–912. doi: 10.1111/j.1096-3642.2008.00498.x.

Goodwin, C. E., Picton, B. and Van Soest, R. W. M. (2011) 'Hymedesmia (Porifera: Demospongiae: Poecilosclerida) from Irish and Scottish cold-water coral reefs, with a description of five new species.', *Journal of the Marine Biological Association of the United Kingdom*, 91(5), pp. 979–997. Available at: http://www.marinespecies.org/porifera/porifera.php?p=sourcedetails&id=151861.

Goosse, H. *et al.* (2018) 'Quantifying climate feedbacks in polar regions', *Nature Communications*, 9(1). doi: 10.1038/S41467-018-04173-0.

Grant, N. *et al.* (2018) 'Suspended sediment causes feeding current arrests in situ in the glass sponge Aphrocallistes vastus', *Marine Environmental Research*, 137, pp. 111–120. doi: 10.1016/j.marenvres.2018.02.020.

Grant, N. *et al.* (2019) 'Effect of suspended sediments on the pumping rates of three species of glass sponge in situ', *Marine Ecology Progress Series*, 615, pp. 79–101. doi: 10.3354/meps12939.

Grant, R. E. (1836) 'Animal Kingdom. Pp. 107-118', in *In: Todd, R.B. (Ed.),The Cyclopaedia of Anatomy and Physiology. Volume 1*. Available at: http://www.marinespecies.org/porifera/porifera.php?p=sourcedetails&id=7516.

Gray, J. E. (1867) 'Notes on the Arrangement of Sponges, with the Descriptions of some New Genera', *Proceedings of the Zoological Society of London*. Available at: http://www.marinespecies.org/porifera/porifera.php?p=sourcedetails&id=7530.

Gray, J. E. (1870) 'Notes on Anchoring Sponges (in a letter to Mr. Moore)', *Annals and Magazine of Natural History*. Available at: https://www.marinespecies.org/aphia.php?p=sourcedetails&id=7540.

Greenan, B. J. W. *et al.* (2010) 'Interdisciplinary oceanographic observations of Orphan Knoll', *NAFO Scientific Council Meeting*, 10/19(June).

Greenwood, J. E., Truesdale, V. W. and Rendell, A. R. (2001) 'Biogenic silica dissolution in seawater — in vitro chemical kinetics', *Progress in Oceanography*, 48(1), pp. 1–23. doi: 10.1016/S0079-6611(00)00046-X.

Guillas, K. C. *et al.* (2019) 'Settlement of juvenile glass sponges and other invertebrate cryptofauna on the Hecate Strait glass sponge reefs', *Invertebrate Biology*, 138(4). doi: 10.1111/ivb.12266.

Guzman, C. and Conaco, C. (2016) 'Gene Expression Dynamics Accompanying the Sponge Thermal Stress Response', *PLOS ONE*, 11(10), p. e0165368. doi: 10.1371/JOURNAL.PONE.0165368.

Hajdu, E. *et al.* (2017) 'Deep-sea dives reveal an unexpected hexactinellid sponge garden on the Rio Grande Rise (SW Atlantic). A mimicking habitat?', *Deep-Sea Research Part II: Topical Studies in Oceanography*, 146, pp. 93–100. doi: 10.1016/j.dsr2.2017.11.009.

Hallmann, E. F. (1916) 'A revision of the genera with microscleres included, or provisionally included, in the family Axinellidae; with descriptions of some Australian species. Part I. ', *Proceedings of the Linnean Society of New South Wales*. Available at: http://www.marinespecies.org/porifera/porifera.php?p=sourcedetails&id=7576.

Hallmann, E. F. (1920) 'New Genera of Monaxonid Sponges related to the Genus *Clathria*.', *Proceedings of the Linnean Society of New South Wales*. Available at: http://www.marinespecies.org/porifera/porifera.php?p=sourcedetails&id=7577.

HallSpencer, J., Allain, V. and Foss, J. H. (2002) 'Trawling damage to Northeast Atlantic ancient coral reefs', *Proceedings of the Royal Society of London. Series B: Biological Sciences*, 269(1490), pp. 507–511. doi: 10.1098/RSPB.2001.1910.

Hanjalić, K. and Launder, B. E. (1972) 'A Reynolds stress model of turbulence and its application to thin shear flows', *Journal of Fluid Mechanics*, 52(4), pp. 609–638. doi: 10.1017/S002211207200268X.

Hansen, G. A. (1885) 'Spongiadae. The Norwegian North-Atlantic Expedition 1876-1878', *Zoology*. Available at: http://www.marinespecies.org/porifera/porifera.php?p=sourcedetails&id=7585.

Hawkes, N. *et al.* (2019) 'Glass sponge grounds on the Scotian Shelf and their associated biodiversity', *Marine Ecology Progress Series*, 614. doi: 10.3354/meps12903.

Hawkings, J. R. *et al.* (2014) 'Ice sheets as a significant source of highly reactive nanoparticulate iron to the oceans', *Nature Communications 2014 5:1*, 5(1), pp. 1–8. doi: 10.1038/ncomms4929.

Hawkings, J. R. *et al.* (2017) 'Ice sheets as a missing source of silica to the polar oceans', *Nature Communications 2017 8:1*, 8(1), pp. 1–10. doi: 10.1038/ncomms14198.

Hendry, K. (2017) *RRS Discovery DY081 - cruise summary report*. Available at: https://www.bodc.ac.uk/resources/inventories/cruise_inventory/report/16378/ (Accessed: 9 April 2018).

Hendry, K. R. *et al.* (2019) 'The biogeochemical impact of glacial meltwater from Southwest Greenland', *Progress in Oceanography*, 176. doi: 10.1016/j.pocean.2019.102126.

Henry, L.-A. and Hart, M. (2005) 'Regeneration from Injury and Resource Allocation in Sponges and Corals – a Review', *International Review of Hydrobiology*, 90(2), pp. 125–158. doi: 10.1002/IROH.200410759.

Henry, L. A. and Roberts, J. M. (2014a) 'Applying the OSPAR habitat definition of deep-sea sponge aggregations to verify suspected records of the habitat in UK waters', *JNCC Report*, 508. Available at: www.jncc.defra.gov.uk (Accessed: 12 December 2019).

Henry, L. A. and Roberts, J. M. (2014b) 'Recommendations for best practice in deep-sea habitat classification: Bullimore et al. as a case study', *ICES Journal of Marine Science*. Oxford University Press, pp. 895–898. doi: 10.1093/icesjms/fst175.

Hentschel, E. (1914) 'Monaxone Kieselschwämme und Hornschwämme der Deutschen Südpolar-

Expedition 1901-1903.', *Deutsche Südpolar-Expedition*. Available at: http://www.marinespecies.org/porifera/porifera.php?p=sourcedetails&id=7614.

Hentschel, E. (1923) 'Erste Unterabteilung der Metazoa: Parazoa, Porifera-Schwämme. Pp. 307-418, fig. 288-377.', in *In: Kükenthal, W. &Krumbach, T. (Eds), Handbuch der Zoologie. Eine Naturgeschichteder Stämme des Tierreiches. Vol. 1, Protozoa, Porifera, Coelenterata,Mesozoa. (Walter de Gruyter und Co: Berlin and Leipzig)*. Available at: http://www.marinespecies.org/porifera/porifera.php?p=sourcedetails&id=7616.

Hentschel, E. (1929) 'Die Kiesel- und Hornschwämme des Nördlichen Eismeers. Pp. 857-1042, pls XII-XIV', in In*: Römer, F., Schaudinn, F., Brauer, A. & Arndt, W. (Eds), Fauna Arctica. Eine Zusammenstellung der arktischen Tierformen mit besonderer Berücksichtigung des Spitzbergen-Gebietes auf Grund der Ergebnisse der Deutschen Expedition in das Nördliche E*. Available at: http://www.marinespecies.org/porifera/porifera.php?p=sourcedetails&id=7617.

Hentschel, U. *et al.* (2002) 'Molecular evidence for a uniform microbial community in sponges from different oceans', *Applied and Environmental Microbiology*, 68(9), pp. 4431–4440. doi: 10.1128/AEM.68.9.4431-4440.2002.

Hestetun, J. T. *et al.* (2015) 'Cladorhizidae (Porifera, Demospongiae, Poecilosclerida) of the deep Atlantic collected during Ifremer cruises, with a biogeographic overview of the Atlantic species', *Journal of the Marine Biological Association of the United Kingdom*. Cambridge University Press, pp. 1311–1342. doi: 10.1017/S0025315413001100.

Hestetun, J. T. *et al.* (2016) 'The systematics of carnivorous sponges', *Molecular Phylogenetics and Evolution*, 94. doi: 10.1016/j.ympev.2015.08.022.

Hestetun, J. T., Rapp, H. T. and Pomponi, S. (2019) 'Deep-Sea Carnivorous Sponges From the Mariana Islands', *Frontiers in Marine Science*, 6(JUL), p. 371. doi: 10.3389/FMARS.2019.00371.

Hestetun, J. T., Tompkins-Macdonald, G. and Rapp, H. T. (2017a) 'A review of carnivorous sponges (Porifera: Cladorhizidae) from the Boreal North Atlantic and Arctic', *Zoological Journal of the Linnean Society*, 181(1), pp. 1–69. doi: 10.1093/zoolinnean/zlw022.

Hestetun, J. T., Tompkins-Macdonald, G. and Rapp, H. T. (2017b) 'A review of carnivorous sponges (Porifera: Cladorhizidae) from the Boreal North Atlantic and Arctic', *Zoological Journal of the Linnean Society*, 181(1), pp. 1–69. doi: 10.1093/zoolinnean/zlw022.

Hewitt, J. E. and Thrush, S. F. (2010) 'Empirical evidence of an approaching alternate state produced by intrinsic community dynamics, climatic variability and management actions', *Marine Ecology Progress Series*, 413, pp. 267–276. doi: 10.3354/meps08626.

Higgin, T. (1877) 'Description of some Sponges obtained during a Cruise of the Steam-Yacht "Argo'' in the Caribbean and neighbouring Seas. "', *Annals and Magazine of Natural History*. Available at: http://www.marinespecies.org/porifera/porifera.php?p=sourcedetails&id=7625.

Hirschmüller, H. (2005) 'Accurate and efficient stereo processing by semi-global matching and mutua information', in *Proceedings - 2005 IEEE Computer Society Conference on Computer Vision and Pattern Recognition, CVPR 2005*. IEEE Computer Society, pp. 807–814. doi: 10.1109/CVPR.2005.56.

Hoffmann, F. *et al.* (2009) 'Complex nitrogen cycling in the sponge Geodia barretti', *Environmental microbiology*, 11(9), pp. 2228–2243. doi: 10.1111/J.1462-2920.2009.01944.X.

Hogg, M., Tendal, O. and Conway, K. (2010) 'Deep-sea sponge grounds: reservoirs of biodiversity'. UNEP-WCMC Biodiversity Series No. 32.

Holliday, N. P. *et al.* (2020) 'Ocean circulation causes the largest freshening event for 120 years in eastern subpolar North Atlantic', *Nature Communications 2020 11:1*, 11(1), pp. 1–15. doi: 10.1038/s41467-020-14474-y.

Holtmeier, F. and Broll, G. (2017) 'Feedback effects of clonal groups and tree clusters on site conditions at the treeline: implications for treeline dynamics', *Climate Research*, 73(1–2), pp. 85–96. doi: 10.3354/cr01431.

Hooper, J. N. A. (1996) 'Revision of Microcionidae (Porifera: Poecilosclerida: Demospongiae), with description of Australian species', *Memoirs of the Queensland Museum*, 40, pp. 1–626. Available at: https://www.biodiversitylibrary.org/page/40092950.

Hooper, J. N. A. and van Soest, R. W. M. (2002) *Systema Porifera. A Guide to the Classification of Sponges*, *Systema Porifera*. doi: 10.1007/978-1-4615-0747-5_1.

Hopwood, M. J. *et al.* (2018) 'Non-linear response of summertime marine productivity to increased meltwater discharge around Greenland', *Nature Communications 2018 9:1*, 9(1), pp. 1–9. doi: 10.1038/s41467-018-05488-8.

Howell, K. L. (2010) 'A benthic classification system to aid in the implementation of marine protected area networks in the deep/high seas of the NE Atlantic', *Biological Conservation*, pp. 1041–1056. doi: 10.1016/j.biocon.2010.02.001.

Howell, K. L. *et al.* (2016) 'The distribution of deep-sea sponge aggregations in the North Atlantic and implications for their effective spatial management', *Deep-Sea Research Part I: Oceanographic Research Papers*, 115, pp. 203–220. doi: 10.1016/j.dsr.2016.07.005.

Howell, K. L., Billett, D. S. M. and Tyler, P. A. (2002) 'Depth-related distribution and abundance of seastars (Echinodermata: Asteroidea) in the Porcupine Seabight and Porcupine Abyssal Plain, N.E. Atlantic', *Deep-Sea Research Part I: Oceanographic Research Papers*, 49(10), pp. 1901–1920. doi: 10.1016/S0967-0637(02)00090-0.

Howell, K. L., Bullimore, R. D. and Foster, N. L. (2014) 'Quality assurance in the identification of deep-sea taxa from video and image analysis: Response to Henry and Roberts', *ICES Journal of Marine Science*, pp. 899–906. doi: 10.1093/icesjms/fsu052.

ICES (2009) *Report of the ICES Advisory Committee, 2009, Book 6 North Sea*. International Council for the Exploration of the Sea.

Juul-Pedersen, T. *et al.* (2015) 'Seasonal and interannual phytoplankton production in a sub-Arctic tidewater outlet glacier fjord, SW Greenland', *Marine Ecology Progress Series*, 524, pp. 27–38. doi: 10.3354/MEPS11174.

Kahn, A. S. *et al.* (2015) 'Benthic grazing and carbon sequestration by deep-water glass sponge reefs', *Limnology and Oceanography*, 60(1), pp. 78–88. doi: 10.1002/lno.10002.

Kahn, A. S., Chu, J. W. F. and Leys, S. P. (2018) 'Trophic ecology of glass sponge reefs in the Strait of Georgia, British Columbia', *Scientific Reports*. doi: 10.1038/s41598-017-19107-x.

Kamatani, A. (1971) 'Physical and chemical characteristics of biogenous silica', *Marine Biology*, 8(2), pp. 89–95. doi: 10.1007/BF00350922.

Kanna, N. *et al.* (2018) 'Upwelling of Macronutrients and Dissolved Inorganic Carbon by a Subglacial Freshwater Driven Plume in Bowdoin Fjord, Northwestern Greenland', *Journal of Geophysical Research: Biogeosciences*, 123(5), pp. 1666–1682. doi: 10.1029/2017JG004248.

Kazanidis, G. *et al.* (2019) 'Distribution of Deep-Sea Sponge Aggregations in an Area of Multisectoral Activities and Changing Oceanic Conditions', *Frontiers in Marine Science*, 6. doi: 10.3389/fmars.2019.00163.

Keller, C. (1880) 'Neue Coelenteraten aus dem Golf von Neapel', *Archiv für mikroskopische Anatomie und Entwicklungsmechanik*, pp. 18:271-280. Available at: https://www.marinespecies.org/aphia.php?p=sourcedetails&id=7696.

Kelly, M. and Vacelet, J. (2011) 'Three new remarkable carnivorous sponges (Porifera, Cladorhizidae) from deep New Zealand and Australian (Macquarie Island) waters', *Zootaxa*, 2976, pp. 55–68. Available at: http://www.marinespecies.org/porifera/porifera.php?p=sourcedetails&id=152401.

Kenchington, E. *et al.* (2017) 'Water mass characteristics and associated fauna of a recently discovered Lophelia pertusa (Scleractinia: Anthozoa) reef in Greenlandic waters', *Polar Biology*, 40(2), pp. 321–337. doi: 10.1007/S00300-016-1957-3/TABLES/1.

Kenchington, E. L. *et al.* (2010) 'Delineating Coral and Sponge Concetrations in the Biogeographic Regions of the East Coast of Canada Using Spatial Analyses', *DFO Can Sci Advis Sec Res Doc*, 3848, p. 208. Available at: http://publications.gc.ca/site/eng/394440/publication.html (Accessed: 21 April 2021).

Kenchington, E. L., Murillo-Perez, F. J., *et al.* (2011) *Development of Encounter Portocols and Assessment of Significant Adverse Impact by Bottom Trawling for Sponge Grounds and Sea Pen Fields in the NAFO Regulatory Area*, *NAFO SCR Doc*. Available at: http://archive.nafo.int/open/sc/2011/scr11-075.pdf (Accessed: 21 April 2021).

Kenchington, E. L., Link, H., *et al.* (2011) 'Identification of Mega- and Macrobenthic Ecologically and Biologically Significant Areas (EBSAs) in the Hudson Bay Complex, the Western and Eastern Canadian Arctic', *DFO Canadian Science Advisory Secretariat Research Document*, 2011/071(January 2011), p. vi+52 p.

Kenchington, E. L. *et al.* (2014) 'Kernel density surface modelling as a means to identify significant concentrations of vulnerable marine ecosystem indicators', *PLoS ONE*. Edited by S. Thrush, 9(10), p. e109365. doi: 10.1371/journal.pone.0109365.

Kenchington, E. L. *et al.* (2015) 'Coral, sponge, and other vulnerable marine ecosystem indicator identification guide, NAFO area', *NAFO Scientific Council Studies*, 2015(47), pp. 1–74. doi: 10.2960/S.v47.m1.

Kenchington, E. L., Power, D. and Koen-Alonso, M. (2013) 'Associations of demersal fish with sponge grounds on the continental slopes of the northwest Atlantic', *Marine Ecology Progress Series*, 477, pp. 217–230. doi: 10.3354/meps10127.

King, B., Zhang, H. P. and Swinney, H. L. (2010) 'Tidal flow over three-dimensional topography generates out-of-forcing-plane harmonics', *Geophysical Research Letters*, 37(14), p. 14606. doi: 10.1029/2010GL043221.

King, M. D. *et al.* (2018) 'Seasonal to decadal variability in ice discharge from the Greenland Ice Sheet', *Cryosphere*, 12(12), pp. 3813–3825. doi: 10.5194/TC-12-3813-2018.

Kirkpatrick, R. (1907) ' XXXIX.— Preliminary report on the Monaxonellida of the National Antarctic expedition ', *Annals and Magazine of Natural History*, 20(117), pp. 271–291. doi: 10.1080/00222930709487333.

Klitgaard, A. B. (1995) 'The fauna associated with outer shelf and upper slope sponges (porifera,

demospongiae) at the faroe islands, northeastern Atlantic', *Sarsia*, 80(1), pp. 1–22. doi: 10.1080/00364827.1995.10413574.

Klitgaard, A. B. and Tendal, O. S. (2004) 'Distribution and species composition of mass occurrences of large-sized sponges in the northeast Atlantic', *Progress in Oceanography*, 61(1), pp. 57–98. doi: 10.1016/j.pocean.2004.06.002.

Knudby, A., Kenchington, E. and Murillo, F. J. (2013) 'Modeling the distribution of Geodia sponges and sponge grounds in the Northwest Atlantic', *PLoS ONE*. Edited by R. Pronzato, 8(12), p. e82306. doi: 10.1371/journal.pone.0082306.

Koltun, V. M. (1955) 'Sponges. Atlas of the Invertebrate Fauna of the Far-Eastern Seas of the USSR. ', *Akademiya Nauk SSSR*. Available at: http://www.marinespecies.org/porifera/porifera.php?p=sourcedetails&id=131343.

Koltun, V. M. (1958) '[Cornacuspongia of sea waters washing the South Sakhalin and the South Kurile Island region.]', *Issledovaniya dal'nevostochnÿkh morei SSR*. Available at: http://www.marinespecies.org/porifera/porifera.php?p=sourcedetails&id=7746.

Koltun, V. M. (1959) '[Siliceous horny sponges of the northern and fareastern seas of the U.S.S.R.] [In Russian]', *Opredeliteli po faune SSR, izdavaemye Zoologicheskim muzeem Akademii nauk*, 67, pp. 1-236. Available at: http://www.marinespecies.org/porifera/porifera.php?p=sourcedetails&id=7747.

Koltun, V. M. (1964) 'Sponges of the Antarctic. 1 Tetraxonida and Cornacuspongida. Pp. 6-133, 443-448.', in *In: Pavlovskii, E.P., Andriyashev,A.P. & Ushakov, P.V. (Eds), Biological Reports of the Soviet Antarctic Expedition (1955-1958)*. Available at: http://www.marinespecies.org/porifera/porifera.php?p=sourcedetails&id=7750.

Koopmans, M., Martens, D. and Wijffels, R. H. (2009) 'Towards commercial production of sponge medicines', *Marine Drugs*, 7(4), pp. 787–802. doi: 10.3390/md7040787.

Koslow, J. A. *et al.* (2001) 'Seamount benthic macrofauna off southern Tasmania: community structure and impacts of trawling', *Marine Ecology Progress Series*, 213, pp. 111–125. doi: 10.3354/MEPS213111.

Kostov, Y., Armour, K. C. and Marshall, J. (2014) 'Impact of the Atlantic meridional overturning circulation on ocean heat storage and transient climate change', *Geophysical Research Letters*, 41(6), pp. 2108–2116. doi: 10.1002/2013GL058998.

Krause, J. W. *et al.* (2018) 'Biogenic silica production and diatom dynamics in the Svalbard region during spring', *Biogeosciences*, 15(21), pp. 6503–6517. doi: 10.5194/BG-15-6503-2018.

Krause, J. W. *et al.* (2019) 'Silicic acid limitation drives bloom termination and potential carbon sequestration in an Arctic bloom', *Scientific Reports 2019 9:1*, 9(1), pp. 1–11. doi: 10.1038/s41598-019-44587-4.

Kutti, T., Bannister, R. J. and Fosså, J. H. (2013) 'Community structure and ecological function of deep-water sponge grounds in the Traenadypet MPA-Northern Norwegian continental shelf', *Continental Shelf Research*, 69, pp. 21–30. doi: 10.1016/j.csr.2013.09.011.

Lage, A. *et al.* (2018) 'A new cave-dwelling species of *Plakina* (Porifera: Homoscleromorpha) from Crete, Greece (South Aegean Sea). *in* Deep Sea and Cave sponges, Klautau, M., Pérez, T., Cárdenas, P. & De Voogd, N. (eds)', *Zootaxa*, 4466(1), pp. 39–48. doi: 10.11646/zootaxa.4466.1.5.

Lamarck, J.-B. de (1815) 'Suite des polypiers empâtés', *Mémoires du Muséum d'Histoire naturelle,*

Paris. Available at: http://www.marinespecies.org/porifera/porifera.php?p=sourcedetails&id=7764.

Lambe, L. (1900) 'Sponges from the coasts of Northeastern Canada and Greenland', *Trans R Soc Canada*, 6, pp. 19–49.

Lavender, K. L., Davis, R. E. and Owens, W. B. (2000) 'Mid-depth recirculation observed in the interior Labrador and Irminger seas by direct velocity measurements', *Nature*, 407(6800), pp. 66–69. doi: 10.1038/35024048.

Lavoie, D., Lambert, N. and Gilbert, D. (2017) 'Projections of Future Trends in Biogeochemical Conditions in the Northwest Atlantic Using CMIP5 Earth System Models', *https://doi.org/10.1080/07055900.2017.1401973*, 57(1), pp. 18–40. doi: 10.1080/07055900.2017.1401973.

Lee, W. L. *et al.* (2012) 'An extraordinary new carnivorous sponge, *Chondrocladia lyra*, in the new subgenus *Symmetrocladia* (Demospongiae, Cladorhizidae), from off of northern California, USA', *Invertebrate Biology*, 131(4), pp. 259–284. doi: 10.1111/ivb.12001.

Lehnert, H. and Stone, R. P. (2015) 'New species of sponges (Porifera, Demospongiae) from the Aleutian Islands and Gulf of Alaska', *Zootaxa*, 4033(4), pp. 451–483. doi: 10.11646/zootaxa.4033.4.1.

Lehnert, H. and Stone, R. P. (2016) 'A comprehensive inventory of the Gulf of Alaska sponge fauna with the description of two new species and geographic range extensions', *Zootaxa*, 4144(3), pp. 365–382. doi: 10.11646/zootaxa.4144.3.5.

Lehnert, H. and Stone, R. P. (2020) 'Three new species of Poecilosclerida (Porifera, Demospongiae, Heteroscleromorpha) from the Aleutian Islands, Alaska', *Zootaxa*, 4851(1), pp. 137–150. doi: 10.11646/zootaxa.4851.1.5.

Leidy, J. (1868) '"Description of a new sponge: *Pheronema annae*"', *Proceedings of the Academy of Natural Sciences of Philadelphia 1868(6) Biological and Microscopical department of the Academy of Natural Sciences*, pp. 9–10. Available at: https://www.marinespecies.org/aphia.php?p=sourcedetails&id=7810.

Lendenfeld, R. von (1898) 'Die Clavulina der Adria. ', *Nova acta Academiae Caesareae Leopoldino Carolinae germanicae naturaecuriosorum*. Available at: http://www.marinespecies.org/porifera/porifera.php?p=sourcedetails&id=7827.

Lévi, C. (1960) 'Spongiaires des côtes occidentales africaines. ', *Bulletin de l'Institut français d'Afrique noire (A. Sciences naturelles)*, 22(3), pp. 743–769. Available at: http://www.marinespecies.org/porifera/porifera.php?p=sourcedetails&id=7850.

Lévi, C. (1961) 'Spongiaires des Iles Philippines, principalement récoltées au voisinage de Zamboanga', *Philippine Journal of Science.*, 88(4), pp. 509–533. Available at: http://www.marinespecies.org/porifera/porifera.php?p=sourcedetails&id=7853.

Leys, S. P. (2003) 'The significance of syncytial tissues for the position of the hexactinellida in the metazoa.', *Integrative and comparative biology*, 43(1), pp. 19–27. doi: 10.1093/icb/43.1.19.

Leys, S. P. *et al.* (2004) 'Patterns of glass sponge (Porifera, Hexactinellida) distribution in coastal waters of British Columbia, Canada', *Marine Ecology Progress Series*, 283, pp. 133–149. doi: 10.3354/meps283133.

Leys, S. P. *et al.* (2011) 'The Sponge Pump: The Role of Current Induced Flow in the Design of the Sponge Body Plan', *PLoS ONE*. Edited by P. Roopnarine, 6(12), p. e27787. doi:

10.1371/journal.pone.0027787.

Leys, S. P. and Hill, A. (2012) 'The Physiology and Molecular Biology of Sponge Tissues', *Advances in Marine Biology*, 62, pp. 1–56. doi: 10.1016/B978-0-12-394283-8.00001-1.

Leys, S. P. and Lauzon, N. R. J. (1998) 'Hexactinellid sponge ecology: growth rates and seasonality in deep water sponges', *Journal of Experimental Marine Biology and Ecology*, 230(1), pp. 111–129. doi: 10.1016/S0022-0981(98)00088-4.

Leys, S. P., Mackie, G. O. and Reiswig, H. M. (2007) 'The Biology of Glass Sponges', *Advances in Marine Biology*, 52, pp. 1–145. doi: 10.1016/S0065-2881(06)52001-2.

Leys, S. P. and Meech, R. W. (2011) 'Physiology of coordination in sponges', *https://doi.org/10.1139/z05-171*, 84(2), pp. 288–306. doi: 10.1139/Z05-171.

Leys, S. P. and Riesgo, A. (2012) 'Epithelia, an Evolutionary Novelty of Metazoans', *Journal of Experimental Zoology Part B: Molecular and Developmental Evolution*, 318(6), pp. 438–447. doi: 10.1002/JEZ.B.21442.

Lim, S. C., de Voogd, N. J. and Tan, K. S. (2012) 'Biodiversity of shallow-water sponges (Porifera) in Singapore and description of a new species of Forcepia (Poecilosclerida: Coelosphaeridae)', *Contributions to Zoology*, 81(1), pp. 55–71. doi: 10.1163/18759866-08101004.

Lindholm, J., Auster, P. and Valentine, P. (2004) 'Role of a large marine protected area for conserving landscape attributes of sand habitats on Georges Bank (NW Atlantic)', *Marine Ecology Progress Series*, 269, pp. 61–68. doi: 10.3354/meps269061.

Linnaeus, C. (1767) 'Systema naturae per regna tria naturae: secundum classes, ordines, genera, species, cum characteribus, differentiis, synonymis, locis. Ed. 12. 1., Regnum Animale. 1 & 2. ', *Holmiae [Stockholm], Laurentii Salvii*. Available at: http://www.biodiversitylibrary.org/item/83650#5.

Long, S. and Jones, P. J. S. (2021) 'Greenland's offshore Greenland halibut fishery and role of the Marine Stewardship Council certification: A governance case study', *Marine Policy*, 127, p. 104095. doi: 10.1016/J.MARPOL.2020.104095.

Lopes, D. A., Bravo, A. and Hajdu, E. (2011) 'New carnivorous sponges (Cladorhizidae:Poecilosclerida:Demospongiae) from off Diego Ramírez Archipelago (south Chile), with comments on taxonomy and biogeography of the family', *Invertebrate Systematics*, 25(5), p. 407. doi: 10.1071/IS11015.

Love, M. S. *et al.* (2013) 'Whole-body concentrations of elements in three fish species from offshore oil platforms and natural areas in the Southern California Bight, USA', *Bulletin of Marine Science*, 89(3), pp. 717–734. doi: 10.5343/bms.2012.1078.

Lowe, D. G. (2004) 'Distinctive image features from scale-invariant keypoints', *International Journal of Computer Vision*, 60(2), pp. 91–110. doi: 10.1023/B:VISI.0000029664.99615.94.

Ludeman, D. A., Reidenbach, M. A. and Leys, S. P. (2017) 'The energetic cost of filtration by demosponges and their behavioural response to ambient currents.', *The Journal of experimental biology*, 220(Pt 6), pp. 995–1007. doi: 10.1242/jeb.146076.

Lundbeck, W. (1902) 'Porifera. (Part I.) Homorrhaphidae and Heterorrhaphidae.', in *In: The Danish Ingolf-Expedition. 6(1). (Bianco Luno: Copenhagen)*. Available at: http://www.marinespecies.org/porifera/porifera.php?p=sourcedetails&id=7893.

Lundbeck, W. (1905) 'Porifera. (Part II.) Desmacidonidae', *The Danish Ingolf-Expedition*, 6(21–219), p. (2):1-219. Available at: http://www.marinespecies.org/porifera/porifera.php?p=sourcedetails&id=7894.

Lundbeck, W. (1909) 'The Porifera of East Greenland', *Meddelelser om Grønland*, 29, pp. 423–464. Available at: http://www.marinespecies.org/porifera/porifera.php?p=sourcedetails&id=7896.

Lundbeck, W. (1910) 'Porifera. (Part III.) Desmacidonidae ', *The Danish Ingolf-Expedition*, 6(3), pp. 1–124. Available at: http://www.marinespecies.org/porifera/porifera.php?p=sourcedetails&id=7897.

Lundsten, L., Reiswig, H. M. and Austin, W. C. (2014) 'Four new species of Cladorhizidae (Porifera, Demospongiae, Poecilosclerida) from the Northeast Pacific', *Zootaxa*, 3786(2), pp. 101–123. doi: 10.11646/zootaxa.3786.2.1.

Luo, H. *et al.* (2016) 'Oceanic transport of surface meltwater from the southern Greenland ice sheet', *Nature Geoscience 2016 9:7*, 9(7), pp. 528–532. doi: 10.1038/ngeo2708.

Lynch-Stieglitz, J. (2017) 'The Atlantic Meridional Overturning Circulation and Abrupt Climate Change', *http://dx.doi.org/10.1146/annurev-marine-010816-060415*, 9(1), pp. 83–104. doi: 10.1146/ANNUREV-MARINE-010816-060415.

Maldonado, M. (1992) 'Demosponges of the red coral bottoms from the Alboran Sea', *Journal of Natural History*, 26, pp. 1131–1161.

Maldonado, M. *et al.* (1999) 'Decline in Mesozoic reef-building sponges explained by silicon limitation', *Nature*, 401(6755), pp. 785–788. doi: 10.1038/44560.

Maldonado, M. *et al.* (2005) 'Siliceous sponges as a silicon sink: An overlooked aspect of benthopelagic coupling in the marine silicon cycle', *Limnology and Oceanography*, 50(3), pp. 799–809. doi: 10.4319/lo.2005.50.3.0799.

Maldonado, M. *et al.* (2011) 'Silicon uptake by sponges: A twist to understanding nutrient cycling on continental margins', *Scientific Reports*, 1(1), p. 30. doi: 10.1038/srep00030.

Maldonado, M. (2016) 'Sponge waste that fuels marine oligotrophic food webs: a re-assessment of its origin and nature', *Marine Ecology*, 37(3), pp. 477–491. doi: 10.1111/maec.12256.

Maldonado, M. *et al.* (2017) 'Sponge grounds as key marine habitats: A synthetic review of types, structure, functional roles, and conservation concerns', in *Marine Animal Forests: The Ecology of Benthic Biodiversity Hotspots*. Springer, pp. 145–183. doi: 10.1007/978-3-319-21012-4_24.

Maldonado, M., Ribes, M. and van Duyl, F. C. (2012) *Nutrient Fluxes Through Sponges. Biology, Budgets, and Ecological Implications*. 1st edn, *Advances in Marine Biology*. 1st edn. Elsevier Ltd. doi: 10.1016/B978-0-12-394283-8.00003-5.

Mariani, S. *et al.* (2006) 'International Association for Ecology Dispersal Strategies in Sponge Larvae: Integrating the Life History of Larvae and the Hydrologic Component', *Source: Oecologia*, 149(1), pp. 174–184. doi: 10.1007/s00442-006-0429-9.

Marshall, W. (1876) 'Ideen über die Verwandtschaftsverhältnisse der Hexactinelliden', *Zeitschrift für wissenschaftliche Zoologie*, 27(1), pp. 113–136. Available at: https://www.marinespecies.org/aphia.php?p=sourcedetails&id=7922.

Massaro, A. J. *et al.* (2012) 'Behavioral and morphological changes caused by thermal stress in the Great Barrier Reef sponge Rhopaloeides odorabile', *Journal of Experimental Marine Biology and*

Ecology, 416–417, pp. 55–60. doi: 10.1016/J.JEMBE.2012.02.008.

McCarthy, G. D. *et al.* (2015) 'Ocean impact on decadal Atlantic climate variability revealed by sea-level observations', *Nature 2015 521:7553*, 521(7553), pp. 508–510. doi: 10.1038/nature14491.

McCave, I. N. (1986) 'Local and global aspects of the bottom nepheloid layers in the world ocean', *Netherlands Journal of Sea Research*, 20(2–3), pp. 167–181. doi: 10.1016/0077-7579(86)90040-2.

McClintock, J. B. *et al.* (2005) 'Ecology of antarctic marine sponges: An overview', in *Integrative and Comparative Biology*. Integr Comp Biol, pp. 359–368. doi: 10.1093/icb/45.2.359.

McIntyre, F. D. *et al.* (2016) 'Distribution and diversity of deep-sea sponge grounds on the Rosemary Bank Seamount, NE Atlantic', *Marine Biology*, 163(6), pp. 1–11. doi: 10.1007/s00227-016-2913-z.

Mecklenburg, C. W., Møller, P. R. and Steinke, D. (2011) 'Biodiversity of arctic marine fishes: Taxonomy and zoogeography', *Marine Biodiversity*, pp. 109–140. doi: 10.1007/s12526-010-0070-z.

Meire, L. *et al.* (2016) 'High export of dissolved silica from the Greenland Ice Sheet', *Geophysical Research Letters*, 43(17), pp. 9173–9182. doi: 10.1002/2016GL070191.

Meire, L. *et al.* (2017) 'Marine-terminating glaciers sustain high productivity in Greenland fjords', *Global Change Biology*, 23(12), pp. 5344–5357. doi: 10.1111/GCB.13801.

Meredith, M. *et al.* (2019) 'Polar Regions', in Pörtner, H. O. et al. (eds) *IPCC Special Report on the Ocean and Cryosphere in a Changing Climate*.

Miller, R. J. *et al.* (2012) 'Structure-Forming Corals and Sponges and Their Use as Fish Habitat in Bering Sea Submarine Canyons', *PLoS ONE*. Edited by J. M. Roberts, 7(3), p. e33885. doi: 10.1371/journal.pone.0033885.

Morozov, G., Sabirov, R. M. and Anisimova, N. (2018) 'New data on sponges from Svalbard Archipelago with a description of a new species of Halicnemia', *Journal of Natural History*, 52(7–8), pp. 491–507. doi: 10.1080/00222933.2018.1440020.

Morrow, C. *et al.* (2012) 'Congruence between nuclear and mitochondrial genes in Demospongiae: A new hypothesis for relationships within the G4 clade (Porifera: Demospongiae)', *Molecular Phylogenetics and Evolution*, 62(1), pp. 174–190. doi: 10.1016/j.ympev.2011.09.016.

Morrow, C. *et al.* (2019) 'Integrating morphological and molecular taxonomy with the revised concept of Stelligeridae (Porifera: Demospongiae)', *Zoological Journal of the Linnean Society*, 187(1), pp. 31–81. doi: 10.1093/zoolinnean/zlz017.

Morrow, C. and Cárdenas, P. (2015) 'Proposal for a revised classification of the Demospongiae (Porifera)', *Frontiers in Zoology*, 12(1), pp. 1–27. doi: 10.1186/s12983-015-0099-8.

Müller, O. F. (1776) 'Zoologiæ Danicæ Prodromus, seu Animalium Daniæ et Norvegiæ indigenarum characteres, nomina, et synonyma imprimis popularium. Havniæ [Copenhagen]: Hallageri', *Zoologiae Danicae prodromus, seu animalium Daniae et Norvegiae indigenarum characteres, nomina, et synonymy imprimis popularium.* doi: 10.5962/bhl.title.13268.

Murillo, F. J. *et al.* (2012) 'Deep-sea sponge grounds of the Flemish Cap, Flemish Pass and the Grand Banks of Newfoundland (Northwest Atlantic Ocean): Distribution and species composition', *Marine Biology Research*, 8(9), pp. 842–854. doi: 10.1080/17451000.2012.682583.

Murillo, F. J. *et al.* (2016) 'Ancient deep-sea sponge grounds on the Flemish Cap and Grand Bank, northwest Atlantic', *Marine Biology*, 163(3), pp. 1–11. doi: 10.1007/s00227-016-2839-5.

Murillo, F. J. *et al.* (2018) 'Sponge assemblages and predicted archetypes in the eastern Canadian Arctic', 597, pp. 115–135. doi: 10.3354/meps12589.

Najafi, M. R., Zwiers, F. W. and Gillett, N. P. (2015) 'Attribution of Arctic temperature change to greenhouse-gas and aerosol influences', *Nature Climate Change 2014 5:3*, 5(3), pp. 246–249. doi: 10.1038/nclimate2524.

Nelson, D. M. and Dortch, Q. (1996) 'Silicic acid depletion and silicon limitation in the plume of the Mississippi River: evidence from kinetic studies in spring and summer', 136, pp. 163–178. Available at: http://www.int-res.com/articles/meps/136/m136p163.pdf (Accessed: 9 April 2018).

Nita, B. G. and Allaire, R. (2017) 'On the Three Dimensional Interaction between Flexible Fibers and Fluid Flow', *Fluids 2017, Vol. 2, Page 4*, 2(1), p. 4. doi: 10.3390/FLUIDS2010004.

Notz, D. and Stroeve, J. (2016) 'Observed Arctic sea-ice loss directly follows anthropogenic CO2 emission', *Science*, 354(6313), pp. 747–750. doi: 10.1126/SCIENCE.AAG2345.

Orejas, C. *et al.* (2009) 'Cold-water corals in the Cap de Creus canyon, northwestern Mediterranean: spatial distribution, density and anthropogenic impact', *Marine Ecology Progress Series*, 397, pp. 37–51. doi: 10.3354/MEPS08314.

Osinga, R. *et al.* (2001) 'Sponge–microbe associations and their importance for sponge bioprocess engineering', *Hydrobiologia 2001 461:1*, 461(1), pp. 55–62. doi: 10.1023/A:1012717200362.

OSPAR commission (2008) *OSPAR List of Threatened and/or Declining Species and Habitats. (Reference number: 2008-6).*

OSPAR commission (2010) *Background Document for Deep-Sea sponge aggregations (485)*.

Overland, J. *et al.* (2019) 'The urgency of Arctic change', *Polar Science*, 21, pp. 6–13. doi: 10.1016/J.POLAR.2018.11.008.

Owen, R. (1841) 'Description of a New Genus and Species of Sponge (*Euplectella aspergillum*)', *Proceedings of the Zoological Society of London*, 9, pp. 3–5. Available at: http://www.marinespecies.org/porifera/porifera.php?p=sourcedetails&id=7998.

Palanques, A., Guillén, J. and Puig, P. (2001) 'Impact of bottom trawling on water turbidity and muddy sediment of an unfished continental shelf', *Limnology and Oceanography*, 46(5), pp. 1100–1110. doi: 10.4319/LO.2001.46.5.1100.

Palter, J. *et al.* (2017) 'Climate, ocean circulation, and sea level changes under stabilization and overshoot pathways to 1.5 K warming', *Earth System Dynamics Discussions*, pp. 1–19. doi: 10.5194/ESD-2017-105.

Palumbi, S. R. (1986) 'How Body Plans Limit Acclimation: Responses of a Demosponge to Wave Force', *Ecology*, 67(1), pp. 208–214. doi: 10.2307/1938520.

Pedulli, M. *et al.* (2014) 'Estimates of potential new production (PNP) for the waters off the western Antarctic Peninsula (WAP) region', *Continental Shelf Research*, 84, pp. 54–69. doi: 10.1016/J.CSR.2014.05.011.

Picton, B. and Goodwin, C. E. (2007a) 'Article in Journal of the Marine Biological Association of the UK ·'. doi: 10.1017/S0025315407058122.

Picton, B. and Goodwin, C. E. (2007b) 'Sponge biodiversity of Rathlin Island, Northern Ireland', *Journal of the Marine Biological Association of the United Kingdom*, 87(6), pp. 1441–1458. doi:

10.1017/S0025315407058122.

Piepenburg, D. *et al.* (2011) 'Towards a pan-Arctic inventory of the species diversity of the macro- and megabenthic fauna of the Arctic shelf seas', *Marine Biodiversity*, pp. 51–70. doi: 10.1007/s12526-010-0059-7.

Pineda, M. C., Duckworth, A. and Webster, N. (2016) 'Appearance matters: sedimentation effects on different sponge morphologies', *Journal of the Marine Biological Association of the United Kingdom*, 96(02), pp. 481–492. doi: 10.1017/S0025315414001787.

Pita, L. *et al.* (2013) 'Host rules: spatial stability of bacterial communities associated with marine sponges (Ircinia spp.) in the Western Mediterranean Sea', *FEMS Microbiology Ecology*, 86(2), pp. 268–276. doi: 10.1111/1574-6941.12159.

Pita, L. *et al.* (2018) 'The sponge holobiont in a changing ocean: from microbes to ecosystems', *Microbiome*, 6(1), p. 46. doi: 10.1186/s40168-018-0428-1.

Pithan, F. and Mauritsen, T. (2014) 'Arctic amplification dominated by temperature feedbacks in contemporary climate models', *Nature Geoscience*, 7(3), pp. 181–184. doi: 10.1038/NGEO2071.

Plotkin, A., Gerasimova, E. and Rapp, H. T. (2018) 'Polymastiidae (Porifera: Demospongiae) of the Nordic and Siberian Seas', *Journal of the Marine Biological Association of the United Kingdom*, 98(6), pp. 1273–1335. doi: 10.1017/S0025315417000285.

Prado, E. *et al.* (2021) 'In situ Growth Rate Assessment of the Hexactinellid Sponge Asconema setubalense Using 3D Photogrammetric Reconstruction', *Frontiers in Marine Science*, 8, p. 26. doi: 10.3389/FMARS.2021.612613.

Pusceddu, A. *et al.* (2014) 'Chronic and intensive bottom trawling impairs deep-sea biodiversity and ecosystem functioning', *Proceedings of the National Academy of Sciences of the United States of America*, 111(24), pp. 8861–8866. doi: 10.1073/pnas.1405454111.

Rahmstorf, S. (2000) 'The Thermohaline Ocean Circulation: A System with Dangerous Thresholds?', *Climatic Change 2000 46:3*, 46(3), pp. 247–256. doi: 10.1023/A:1005648404783.

Rahmstorf, S. (2003) 'Thermohaline circulation: The current climate', *Nature 2003 421:6924*, 421(6924), pp. 699–699. doi: 10.1038/421699a.

Rapp, H. T., Janussen, D. and Tendal, O. S. (2011) 'Calcareous sponges from abyssal and bathyal depths in the Weddell Sea, Antarctica.', *Deep-Sea Research II*, 58, pp. 58–67. Available at: http://www.marinespecies.org/porifera/porifera.php?p=sourcedetails&id=149706.

Rice, A. L., Thurston, M. H. and New, A. L. (1990) 'Dense aggregations of a hexactinellid sponge, Pheronema carpenteri, in the Porcupine Seabight (northeast Atlantic Ocean), and possible causes', *Progress in Oceanography*, 24(1–4), pp. 179–196. doi: 10.1016/0079-6611(90)90029-2.

Rickert, D., Schlüter, M. and Wallmann, K. (2002) 'Dissolution kinetics of biogenic silica from the water column to the sediments', *Geochimica et Cosmochimica Acta*, 66(3), pp. 439–455. doi: 10.1016/S0016-7037(01)00757-8.

Ridley, S. O. and Dendy, A. (1886) 'Preliminary report on the Monaxonida collected by H.M.S. Challenger. Part I.', *Annals and Magazine of Natural History*, 18, pp. 470-493. Available at: http://www.marinespecies.org/porifera/porifera.php?p=sourcedetails&id=8095.

Ríos, P. *et al.* (2021) 'Increasing Knowledge of Biodiversity on the Orphan Seamount: A New Species

of Tedania (Tedaniopsis) Dendy, 1924', *Frontiers in Marine Science*, 8. doi: 10.3389/fmars.2021.612857.

Ripley, B. D. (1976) 'The second-order analysis of stationary point processes', *Journal of Applied Probability*, 13(2), pp. 255–266. doi: 10.2307/3212829.

Ripley, B. D. (1977) 'Modelling Spatial Patterns', *Journal of the Royal Statistical Society. Series B (Methodological)*, 39(2), pp. 172–212. Available at: http://www.jstor.org/stable/2984796.

Ripley, B. D. (1981) *Spatial Statistics*. Hoboken, NJ, USA: John Wiley & Sons, Inc. (Wiley Series in Probability and Statistics). doi: 10.1002/0471725218.

Roberts, D. E. and Davis, A. R. (1996) 'Patterns in sponge (Porifera) assemblages on temperate coastal reefs off Sydney, Australia', *Marine and Freshwater Research*, 47(7), pp. 897–906. doi: 10.1071/MF9960897.

Roberts, E. M. *et al.* (2021) 'Water masses constrain the distribution of deep-sea sponges in the North Atlantic Ocean and Nordic Seas', *Marine Ecology Progress Series*, 659, pp. 75–96. doi: 10.3354/meps13570.

Roberts, E. M. M. *et al.* (2018) 'Oceanographic setting and short-timescale environmental variability at an Arctic seamount sponge ground', 138, pp. 98–113. Available at: https://www.sciencedirect.com/science/article/pii/S0967063718300256 (Accessed: 14 May 2019).

Robertson, L. M., Hamel, J.-F. and Mercier, A. (2017) 'Feeding in deep-sea demosponges: Influence of abiotic and biotic factors', *Deep Sea Research Part I: Oceanographic Research Papers*, 127, pp. 49–56. doi: 10.1016/J.DSR.2017.07.006.

Rolinski, S., Segschneider, J. and Sündermann, J. (2001) 'Long-term propagation of tailings from deep-sea mining under variable conditions by means of numerical simulations', *Deep Sea Research Part II: Topical Studies in Oceanography*, 48(17–18), pp. 3469–3485. doi: 10.1016/S0967-0645(01)00053-4.

Romanou, A. *et al.* (2017) 'Role of the ocean's AMOC in setting the uptake efficiency of transient tracers', *Geophysical Research Letters*, 44(11), pp. 5590–5598. doi: 10.1002/2017GL072972.

Rooks, C. *et al.* (2020) 'Deep-sea sponge grounds as nutrient sinks: Denitrification is common in boreo-Arctic sponges', *Biogeosciences*, 17(5), pp. 1231–1245. doi: 10.5194/bg-17-1231-2020.

Rooper, C. N. *et al.* (2011) 'Modeling the impacts of bottom trawling and the subsequent recovery rates of sponges and corals in the Aleutian Islands, Alaska', *Continental Shelf Research*, 31(17), pp. 1827–1834. doi: 10.1016/J.CSR.2011.08.003.

Roy, V., Iken, K. and Archambault, P. (2015) 'Regional variability of megabenthic community structure across the canadian arctic', *Arctic*, 68(2), pp. 180–192. doi: 10.14430/arctic4486.

Rubio-Portillo, E. *et al.* (2016) 'Effects of the 2015 heat wave on benthic invertebrates in the Tabarca Marine Protected Area (southeast Spain)', *Marine Environmental Research*, 122, pp. 135–142. doi: 10.1016/J.MARENVRES.2016.10.004.

Rüggeberg, A. *et al.* (2011) 'Water mass characteristics and sill dynamics in a subpolar cold-water coral reef setting at Stjernsund, northern Norway', *Marine Geology*, 282(1–2), pp. 5–12. doi: 10.1016/J.MARGEO.2010.05.009.

Runzel, C. C. (2016) 'Sponge physiology: the effects of temperature on the regeneration and

reaggregation of sponges (Haliclona reniera)', *Peer Preprints - University of California*. doi: 10.7287/PEERJ.PREPRINTS.2654V1.

Rützler, K. (1988) 'Mangrove sponge disease induced by cyanobacterial symbionts: failure of a primitive immune system?', *Diseases of aquatic organisms* , 5, pp. 143–149. Available at: https://repository.si.edu/handle/10088/7696?show=full (Accessed: 10 April 2022).

Rützler, K. and Macintyre, I. G. (1978) 'Siliceous sponge spicules in coral reef sediments', *Marine Biology*, 49(2), pp. 147–159. doi: 10.1007/BF00387114.

Rützler, K., Macintyre, V. V. and Smith, K. T. (1990) *New perspectives in sponge biology : papers contributed to the Third International Conference on the Biology of Sponges, convened by Willard D. Hartman and Klaus Rützler, Woods Hole, Massachusetts, 17-23 November 1985*. Smithsonian Institution Press. Available at: http://agris.fao.org/agris-search/search.do?recordID=US201300715022 (Accessed: 1 February 2018).

Ryan, J. P. *et al.* (2014) 'Distributions of invertebrate larvae and phytoplankton in a coastal upwelling system retention zone and peripheral front', *Journal of Experimental Marine Biology and Ecology*, 459, pp. 51–60. doi: 10.1016/J.JEMBE.2014.05.017.

Rysgaard, S. *et al.* (2020) 'An Updated View on Water Masses on the pan-West Greenland Continental Shelf and Their Link to Proglacial Fjords', *Journal of Geophysical Research: Oceans*, 125(2), p. e2019JC015564. doi: 10.1029/2019JC015564.

Samaai, T., Govender, V. and Kelly, M. (2004) '*Cyclacanthia* n. g. (Demospongiae : Poecilosclerida : Latrunculiidae incertae sedis), a new genus of marine sponges from South African waters, and description of two new species.', *Zootaxa*, 725, pp. 1–18. Available at: http://www.marinespecies.org/porifera/porifera.php?p=sourcedetails&id=9856.

Sampaio, Í. *et al.* (2012) 'Cold-water corals landed by bottom longline fisheries in the Azores (north-eastern Atlantic)', *Journal of the Marine Biological Association of the United Kingdom*, 92(7), pp. 1547–1555. doi: 10.1017/S0025315412000045.

Sandberg Sørensen, L. *et al.* (2018) '25 years of elevation changes of the Greenland Ice Sheet from ERS, Envisat, and CryoSat-2 radar altimetry', *Earth and Planetary Science Letters*, 495, pp. 234–241. doi: 10.1016/J.EPSL.2018.05.015.

Sarà, M. *et al.* (1992) 'Biogeographic traits and checklist of Antarctic demosponges', *Polar Biology*, 12(6–7), pp. 559–585. doi: 10.1007/BF00236980.

Sars, G. O. (1872) 'On some remarkable forms of animal life from the great deeps off the Norwegian coast. Part 1, partly from posthumous manuscripts of the late prof. Mich. Sars. University Program for the 1rs half-year 1869', *Brøgger & Christie, Christiania viii*, 82, pp. 1–6. Available at: http://biodiversitylibrary.org/page/11677777.

Schmidt, O. (1862) 'Die Spongien des adriatischen Meeres', *Leipzig 1862*. Available at: http://www.marinespecies.org/porifera/porifera.php?p=sourcedetails&id=8175.

Schmidt, O. (1870) 'Grundzüge einer Spongien-Fauna des atlantischen Gebietes.', in. Available at: http://www.marinespecies.org/porifera/porifera.php?p=sourcedetails&id=8180.

Schmidt, O. (1875) 'Spongien. Die Expedition zur physikalisch-chemischen und biologischen Untersuchung der Nordsee im Sommer 1872. ', *Jahresbericht der Commission zur Wissenschaftlichen Untersuchung der Deutschen Meere in Kiel*. Available at: http://www.marinespecies.org/porifera/porifera.php?p=sourcedetails&id=8183.

Schmidt, O. (1880) ‘Die Spongien des Meerbusen von Mexico (Und des caraibischen Meeres). Heft II. Abtheilung II. Hexactinelliden. Abtheilung III. Tetractinelliden. Monactinelliden und Anhang. Nachträge zu Abtheilung I (Lithistiden). Pp. 33-90, pls V-X. *In*: Reports on ’, in. Available at: https://www.marinespecies.org/aphia.php?p=sourcedetails&id=8186.

Schönberg, C. H. L. (2016) ‘Happy relationships between marine sponges and sediments – a review and some observations from Australia’, *Journal of the Marine Biological Association of the United Kingdom*, 96(02), pp. 493–514. doi: 10.1017/S0025315415001411.

Schrama, E. J. O., Wouters, B. and Rietbroek, R. (2014) ‘A mascon approach to assess ice sheet and glacier mass balances and their uncertainties from GRACE data’, *Journal of Geophysical Research: Solid Earth*, 119(7), pp. 6048–6066. doi: 10.1002/2013JB010923.

Schulze, F. E. (1878) ‘Untersuchungen über den Bau und die Entwicklung der Spongien. Vierte Mittheilung. Die Familie der Aplysinidae’, *Zeitschrift für wissenschaftliche Zoologie*, 30, pp. 379–420. Available at: https://www.marinespecies.org/aphia.php?p=sourcedetails&id=8201.

Schulze, F. E. (1880) ‘Untersuchungen über den Bau und die Entwicklung der Spongien. Neunte Mittheilung. Die Plakiniden’, *Zeitschrift für wissenschaftliche Zoologie*, 34(2), pp. 407–451. Available at: http://www.marinespecies.org/porifera/porifera.php?p=sourcedetails&id=8204.

Schulze, F. E. (1886) ‘Über den Bau und das System der Hexactinelliden’, *Abhandlungen der Königlichen Akademie der Wissenschaften zu Berlin (Physikalisch-Mathematische Classe)*, pp. 1–97. Available at: https://www.marinespecies.org/aphia.php?p=sourcedetails&id=8206.

Schuster, A. *et al.* (2021) ‘Systematics of “lithistid” tetractinellid demosponges from the Tropical Western Atlantic—implications for phylodiversity and bathymetric distribution’, *PeerJ*, 9. doi: 10.7717/peerj.10775.

Serreze, M. C., Barrett, A. P. and Stroeve, J. (2012) ‘Recent changes in tropospheric water vapor over the Arctic as assessed from radiosondes and atmospheric reanalyses’, *Journal of Geophysical Research Atmospheres*, 117(10). doi: 10.1029/2011JD017421.

Shamloo, H., Rajaratnam, N. and Katopodis, C. (2001) ‘Hydraulics of simple habitat structures’, *Journal of Hydraulic Research*, 39(4), pp. 351–366. doi: 10.1080/00221680109499840.

Shepherd, A. *et al.* (2012) ‘A Reconciled Estimate of Ice-Sheet Mass Balance’, *Science*, 338(6111), pp. 1183–1189. doi: 10.1126/SCIENCE.1228102.

van Soest, R. W. M. *et al.* (2012) ‘Global diversity of sponges (Porifera)’, *PLoS ONE*, p. e35105. doi: 10.1371/journal.pone.0035105.

van Soest, R. W. M. (2017) ‘Sponges of the Guyana Shelf’, *Zootaxa*, 4217(1). doi: 10.11646/zootaxa.4217.1.1.

van Soest, R. W. M. *et al.* (2021) *World Porifera Database*, *World Porifera Database*. doi: 10.14284/359.

Sollas, W. J. (1880) ‘The sponge-fauna of Norway; a Report on the Rev. A.M. Norman’s Collection of Sponges from the Norwegian Coast.’, *Annals and Magazine of Natural History*. Available at: http://www.marinespecies.org/porifera/porifera.php?p=sourcedetails&id=8243.

Sollas, W. J. (1885) ‘A Classification of the Sponges. ’, *Annals and Magazine of Natural History*. Available at: http://www.marinespecies.org/porifera/porifera.php?p=sourcedetails&id=8247.

Sollas, W. J. (1886) ‘Preliminary account of the Tetractinellid sponges Dredged by H.M.S. “Challenger’’ 1872-76. Part I. The Choristida.”’, *Scientific Proceedings of the Royal Dublin Society (new series)*, 5, pp. 177–199. Available at: https://www.marinespecies.org/aphia.php?p=sourcedetails&id=8249.

Steinert, G. *et al.* (2017) ‘Host-specific assembly of sponge-associated prokaryotes at high taxonomic ranks’, *Scientific Reports 2017 7:1*, 7(1), pp. 1–9. doi: 10.1038/s41598-017-02656-6.

Steinert, G. *et al.* (2020) ‘Compositional and Quantitative Insights Into Bacterial and Archaeal Communities of South Pacific Deep-Sea Sponges (Demospongiae and Hexactinellida)’, *Frontiers in Microbiology*, 11, p. 716. doi: 10.3389/FMICB.2020.00716/BIBTEX.

Stephens, J. (1920) ‘The freshwater sponges of Ireland.’, *Proceedings of the Royal Irish Academy*, 35, pp. 205-254. Available at: http://www.marinespecies.org/porifera/porifera.php?p=sourcedetails&id=172651.

Strehlow, B. W. *et al.* (2017) ‘Sediment tolerance mechanisms identified in sponges using advanced imaging techniques’, *PEER Journal*, 5, pp. 1–26. doi: 10.7717/peerj.3904.

Stuecker, M. F. *et al.* (2018) ‘Polar amplification dominated by local forcing and feedbacks’, *Nature Climate Change 2018 8:12*, 8(12), pp. 1076–1081. doi: 10.1038/s41558-018-0339-y.

Taboada, S. *et al.* (2022) ‘Genetic diversity, gene flow and hybridization in fan-shaped sponges (Phakellia spp.) in the North-East Atlantic deep sea’, *Deep Sea Research Part I: Oceanographic Research Papers*, 181, p. 103685. doi: 10.1016/J.DSR.2021.103685.

Talley, L. D. *et al.* (2011) ‘Descriptive physical oceanography: An introduction: Sixth edition’, *Descriptive Physical Oceanography: An Introduction: Sixth Edition*, pp. 1–555. doi: 10.1016/C2009-0-24322-4.

Talley, L. D. and McCartney, M. S. (1982) ‘Distribution and Circulation of Labrador Sea Water’, *Journal of Physical Oceanography*, 12(11), pp. 1189–1205. doi: 10.1175/1520-0485(1982)012<1189:dacols>2.0.co;2.

Tendal, O. S. (1973) ‘Sponges collected by the Swedish Deep Sea Expedition’, *Zoologica Scripta*, 2, pp. 33–38. Available at: http://www.marinespecies.org/porifera/porifera.php?p=sourcedetails&id=42387.

Thamatrakoln, K. and Hildebrand, M. (2008) ‘Silicon uptake in diatoms revisited: a model for saturable and nonsaturable uptake kinetics and the role of silicon transporters.’, *Plant physiology*, 146(3), pp. 1397–407. doi: 10.1104/pp.107.107094.

Thomas, T. *et al.* (2016) ‘Diversity, structure and convergent evolution of the global sponge microbiome’, *Nature Communications*, 7. doi: 10.1038/ncomms11870.

Thomson, C. W. (1869) ‘On *Holtenia*, a Genus of Vitreus Sponges.’, *Proceedings of the Royal Society of London*, 18, pp. 32–35. Available at: https://www.marinespecies.org/aphia.php?p=sourcedetails&id=8314.

Thomson, C. W. (1873) ‘The Depths of the Sea. Macmillan and Co.: London, 527 pp’, in. Available at: https://www.biodiversitylibrary.org/page/16330317.

Thorpe, S. A. and White, M. (1988) ‘A deep intermediate nepheloid layer’, *Deep Sea Research Part A. Oceanographic Research Papers*, 35(9), pp. 1665–1671. doi: 10.1016/0198-0149(88)90109-4.

Tompkins-Macdonald, G. J. and Leys, S. P. (2008) 'Glass sponges arrest pumping in response to sediment: Implications for the physiology of the hexactinellid conduction system', *Marine Biology*, 154(6), pp. 973–984. doi: 10.1007/S00227-008-0987-Y/FIGURES/8.

Tompkins, G. *et al.* (2017) *Sponges from the 2010-2014 Paamiut Multispecies Trawl Surveys, Eastern Arctic and Subarctic: Class Demospongiae, Subclass Heteroscleromorpha, Order Poecilosclerida, Family Coelosphaeridae, Genera Forcepia and Lissodendoryx*, *Canadian Technical Report of Fisheries and Aquatic Sciences*.

Topsent, E. (1890) 'Notice préliminaire sur les spongiaires recueillis durant les campagnes de l'Hirondelle', *Bulletin de la Société zoologique de France*, 15, pp. 65-71. Available at: http://www.marinespecies.org/porifera/porifera.php?p=sourcedetails&id=8321.

Topsent, E. (1892) 'Contribution à l'étude des Spongiaires de l'Atlantique Nord (Golfe de Gascogne, Terre-Neuve, Açores)', *Résultats des campagnes scientifiques accomplies par le Prince Albert I. Monaco*. Available at: http://www.marinespecies.org/porifera/porifera.php?p=sourcedetails&id=8326.

Topsent, E. (1893a) 'Note sur la faune des Spongillides de France.', *Bulletin de la Société Zoologique de France*, 18. Available at: http://www.marinespecies.org/porifera/porifera.php?p=sourcedetails&id=132678.

Topsent, E. (1893b) 'Note sur quelques éponges du Golfe de Tadjoura recueillies par M. le Dr. L. Faurot. ', *Bulletin de la Société zoologique de France*, 18, pp. 177-182. Available at: http://www.marinespecies.org/porifera/porifera.php?p=sourcedetails&id=8330.

Topsent, E. (1893c) 'Nouvelle série de diagnoses d'éponges de Roscoff et de Banyuls. ', *Archives de Zoologie expérimentale et générale*. Available at: http://www.marinespecies.org/porifera/porifera.php?p=sourcedetails&id=8332.

Topsent, E. (1901a) 'Les Spongiaires de l'expédition antarctique belge et la bipolarité des faunes', *Comptes Rendus hebdomadaires des Scéances de l'Académie des Sciences, Paris*, 132, pp. 168–169. Available at: http://www.marinespecies.org/porifera/porifera.php?p=sourcedetails&id=365559.

Topsent, E. (1901b) 'Spongiaires. Résultats du voyage du S.Y. 'Belgica'en 1897-99 sous le commandement de A. de Gerlache de Gomery. ', *Expédition antarctique belge. Zoologie*. Available at: http://www.marinespecies.org/porifera/porifera.php?p=sourcedetails&id=8350.

Topsent, E. (1904) 'Spongiaires des Açores', *Résultats des campagnes scientifiques accomplies par le Prince Albert I. Monaco*. Available at: https://biodiversitylibrary.org/page/40603003.

Topsent, E. (1922) 'Les mégasclères polytylotes des Monaxonides et la parenté des Latrunculiines.', *Bulletin de l'Institut océanographique Monaco*, 415, pp. 1-8. Available at: http://www.marinespecies.org/porifera/porifera.php?p=sourcedetails&id=8382.

Topsent, E. (1925) 'Etude des Spongiaires du Golfe de Naples.', *Archives de Zoologie expérimentale et générale*. Available at: http://www.marinespecies.org/porifera/porifera.php?p=sourcedetails&id=8387.

Topsent, E. (1927) 'Diagnoses d'Éponges nouvelles recueillies par le Prince Albert ler de Monaco', *Bulletin de l'Institut océanographique Monaco*, (502), pp. 1–19. Available at: http://www.marinespecies.org/porifera/porifera.php?p=sourcedetails&id=8389.

Topsent, E. (1928) 'Spongiaires de l'Atlantique et de la Méditerranée provenant des croisières du Prince Albert ler de Monaco', *Résultats des campagnes scientifiques accomplies par le Prince Albert I.*

Monaco, pp. 74:1-376,. Available at: http://www.marinespecies.org/porifera/porifera.php?p=sourcedetails&id=8393.

Tréguer, P. J. *et al.* (2017) 'Influence of diatom diversity on the ocean biological carbon pump', *Nature Geoscience 2017 11:1*, 11(1), pp. 27–37. doi: 10.1038/s41561-017-0028-x.

Tréguer, P. J. and De La Rocha, C. L. (2013) 'The World Ocean Silica Cycle', *Annual Review of Marine Science*, 5(1), pp. 477–501. doi: 10.1146/annurev-marine-121211-172346.

Vacelet, J. (1969) 'Eponges de la Roche du Large et de l'étage bathyal de Méditerranée (Récoltes de la soucoupe plongeante Cousteau et dragages). Mémoires du Muséum national d'Histoire naturelle', *Mémoires du Muséum national d'Histoire naturelle (A, Zoologie)*. Available at: http://www.marinespecies.org/porifera/porifera.php?p=sourcedetails&id=8446.

Vacelet, J., Boury-Esnault, N. and Harmelin, J.-G. (1994) 'Hexactinellid Cave, a unique deep-sea habitat in the scuba zone', *Deep Sea Research I*, 41, pp. 965–973. Available at: http://www.marinespecies.org/porifera/porifera.php?p=sourcedetails&id=172934.

Vacelet, J. and Perez, T. (1998) 'Two new genera and species of sponges (Porifera, Demospongiae) without skeleton from a Mediterranean cave', *Zoosystema*, 20(1), pp. 5–22.

Vad, J. *et al.* (2018) 'Potential Impacts of Offshore Oil and Gas Activities on Deep-Sea Sponges and the Habitats They Form', in, pp. 33–60. doi: 10.1016/bs.amb.2018.01.001.

Velicogna, I., Sutterley, T. C. and Broeke, M. R. van den (2014) 'Regional acceleration in ice mass loss from Greenland and Antarctica using GRACE time-variable gravity data', *Geophysical Research Letters*, 41(22), pp. 8130–8137. doi: 10.1002/2014GL061052.

Vicente, V. P. (1990) 'Response of sponges with autotrophic endosymbionts during the coral-bleaching episode in Puerto Rico', *Coral Reefs 1990 8:4*, 8(4), pp. 199–202. doi: 10.1007/BF00265011.

Victorero, L. *et al.* (2018) 'Out of Sight, But Within Reach: A Global History of Bottom-Trawled Deep-Sea Fisheries From >400 m Depth', *Frontiers in Marine Science*, 5. doi: 10.3389/fmars.2018.00098.

Vosmaer, G. C. J. (1885) 'The Sponges of the "Willem Barents'' Expedition 1880 and 1881. "', *Bijdragen tot de Dierkunde*. Available at: http://www.marinespecies.org/porifera/porifera.php?p=sourcedetails&id=8538.

Wassenberg, T. J., Dews, G. and Cook, S. D. (2002) 'The impact of fish trawls on megabenthos (sponges) on the north-west shelf of Australia', *Fisheries Research*, 58(2), pp. 141–151. doi: 10.1016/S0165-7836(01)00382-4.

Webster, N. S., Cobb, R. E. and Negri, A. P. (2008) 'Temperature thresholds for bacterial symbiosis with a sponge', *The ISME Journal 2008 2:8*, 2(8), pp. 830–842. doi: 10.1038/ismej.2008.42.

Wei, C. *et al.* (2020) 'Seafloor biodiversity of Canada's three oceans: Patterns, hotspots and potential drivers', *Diversity and Distributions*. Edited by K. C. Burns, 26(2), pp. 226–241. doi: 10.1111/ddi.13013.

Westoby, M. J. *et al.* (2012) '"Structure-from-Motion" photogrammetry: A low-cost, effective tool for geoscience applications', *Geomorphology*, 179, pp. 300–314. doi: 10.1016/j.geomorph.2012.08.021.

White, J. W. *et al.* (2010) 'Population persistence in marine reserve networks: incorporating spatial heterogeneities in larval dispersal', *Marine Ecology Progress Series*, 398, pp. 49–67. doi: 10.3354/MEPS08327.

Whitelegge, T. (1906) 'Sponges. Part 1. Monaxonida, Ridley and Dendy. *In*: Scientific Results of the Trawling Expedition of H.M.C.S. "Thetis'' off the Coast of New South Wales in February and March, 1898"', *Memoirs of the Australian Museum*. Available at: http://www.marinespecies.org/porifera/porifera.php?p=sourcedetails&id=8582.

Wilkinson, C. R. and Cheshire, A. C. (1989) *Coral Reefs Patterns in the distribution of sponge populations across the central Great Barrier Reef**, *Coral Reefs*.

Wilkinson, C. R. and Evans, E. (1989) 'Sponge distribution across Davies Reef, Great Barrier Reef, relative to location, depth, and water movement', *Coral Reefs*, 8(1), pp. 1–7. doi: 10.1007/BF00304685.

Willenz, P. *et al.* (2009) 'Class Demospongiae', in Häussermann, V. and Försterra, G. (eds) *Marine Benthic Fauna of Chilean Patagonia*. Nature in Focus, Puerto Montt, pp. 94–170.

Woodward, E. M. S. and Rees, A. P. (2001) 'Nutrient distributions in an anticyclonic eddy in the northeast Atlantic Ocean, with reference to nanomolar ammonium concentrations', *Deep Sea Research Part II: Topical Studies in Oceanography*, 48(4–5), pp. 775–793. doi: 10.1016/S0967-0645(00)00097-7.

Wu, C.-S., Wu, D.-Y. and Wang, S.-S. (2019) 'Bio-based polymer nanofiber with siliceous sponge spicules prepared by electrospinning: Preparation, characterisation, and functionalisation', *Materials Science and Engineering: C*, p. 110506. doi: 10.1016/j.msec.2019.110506.

Wudrick, A. *et al.* (2020) *A Pictorial Guide to the Epibenthic Megafauna of Orphan Knoll (northwest Atlantic) Identified from In Situ Benthic Video Footage Ocean and Ecosystem Sciences Division Fisheries and Oceans Canada Canadian Technical Report of Fisheries and Aquatic Science*, *Canadian Technical Report of Fisheries and Aquatic Sciences*. doi: 10.5281/ZENODO.3835865.

Xavier, J. R. *et al.* (2010) 'Molecular evidence of cryptic speciation in the ''cosmopolitan" excavating sponge *Cliona celata* (Porifera, Clionaidae)', *Molecular Phylogenetics and Evolution*, 56, pp. 13–20. Available at: http://www.marinespecies.org/porifera/porifera.php?p=sourcedetails&id=387361.

Xavier, J. R. and van Soest, R. W. M. (2012) 'Diversity patterns and zoogeography of the Northeast Atlantic and Mediterranean shallow-water sponge fauna', *Hydrobiologia*, 687(1), pp. 107–125. doi: 10.1007/s10750-011-0880-4.

Xavier, J. R., Tojeira, I. and Van Soest, R. W. M. (2015) 'On a hexactinellid sponge aggregation at the Great Meteor seamount (North-east Atlantic)', *Journal of the Marine Biological Association of the United Kingdom*, 95(7), pp. 1389–1394. doi: 10.1017/s0025315415000685.

Yang, Q. *et al.* (2016) 'Recent increases in Arctic freshwater flux affects Labrador Sea convection and Atlantic overturning circulation', *Nature Communications 2016 7:1*, 7(1), pp. 1–8. doi: 10.1038/ncomms10525.

Yeager, S. G. and Jochum, M. (2009) 'The connection between Labrador Sea buoyancy loss, deep western boundary current strength, and Gulf Stream path in an ocean circulation model', *Ocean Modelling*, 30(2–3), pp. 207–224. doi: 10.1016/j.ocemod.2009.06.014.

Zantopp, R. *et al.* (2017) 'From interannual to decadal: 17 years of boundary current transports at the exit of the Labrador Sea', *Journal of Geophysical Research: Oceans*, 122(3), pp. 1724–1748. doi:

10.1002/2016JC012271.

Zumberge, J. A. *et al.* (2018) 'Demosponge steroid biomarker 26-methylstigmastane provides evidence for Neoproterozoic animals', *Nature Ecology and Evolution*, 2(11), pp. 1709–1714. doi: 10.1038/s41559-018-0676-2.

7. Appendices

7.1. Appendix A

frontiers in Marine Science

ORIGINAL RESEARCH
published: 16 February 2021
doi: 10.3389/fmars.2021.612857

Increasing Knowledge of Biodiversity on the Orphan Seamount: A New Species of *Tedania* (*Tedaniopsis*) Dendy, 1924

Pilar Ríos[1], Javier Cristobo[1], Emily Baker[2], Lindsay Beazley[2], Timothy Culwick[3] and Ellen Kenchington[2]*

[1] *Centro Oceanográfico de Gijón, Instituto Español de Oceanografía, Madrid, Spain,* [2] *Department of Fisheries and Oceans, Bedford Institute of Oceanography, Dartmouth, NS, Canada,* [3] *School of Earth Science, University of Bristol, Bristol, United Kingdom*

OPEN ACCESS

Edited by:
Daphne Cuvelier, Center for Marine and Environmental Sciences (MARE), Portugal

Reviewed by:
Merrick Ekins, Queensland Museum, Australia
Jose Cruz-Barraza, National Autonomous University of Mexico, Mexico

***Correspondence:**
Pilar Ríos
pilar.rios.lopez@gmail.com; pilar.rios@ieo.es

Specialty section:
This article was submitted to Deep-Sea Environments and Ecology, a section of the journal Frontiers in Marine Science

Received: *30 September 2020*
Accepted: *14 January 2021*
Published: *16 February 2021*

Citation:
Ríos P, Cristobo J, Baker E, Beazley L, Culwick T and Kenchington E (2021) Increasing Knowledge of Biodiversity on the Orphan Seamount: A New Species of Tedania (Tedaniopsis) Dendy, 1924. Front. Mar. Sci. 8:612857. doi: 10.3389/fmars.2021.612857

A new *Tedania* species (Porifera) was collect using remotely operated vehicles during the Canadian mission HUD2010-029 and the British RRS Discovery Cruise DY081, on the Orphan Seamount near the Orphan Knoll, northwest Atlantic, between 2999.88 and 3450.4 m depth. Orphan Knoll is an isolated, drowned continental fragment 550 km northeast Newfoundland in the Labrador Sea. This region is biologically rich and complex and in 2007, the regional fisheries management organization operating in the area regulated that no vessel shall engage in bottom-contact fishing activities until reviewed in 2020 with a review slated at the end of this year. Members of the genus *Tedania* are uncommon in the temperate northern hemisphere with only six species known previously: *Tedania* (*Tedania*) *anhelans*; *Tedania* (*Tedania*) *pilarriosae*; *Tedania* (*Tedania*) *suctoria*; *Tedania* (*Tedania*) *urgorrii*; *Tedania* (*Tedaniopsis*) *gurjanovae*; and *Tedania* (*Tedaniopsis*) *phacellina*. The particular features of the new sponge we describe are the very peculiar external morphology which is tree-like with dichotomous branching—a morphology not previously described in this subgenus; and the combination of spicules found: long styles, the typical tornotes of the subgenus and two sizes of onychaetes. Additional information is provided on other species of *Tedaniopsis* described from the Atlantic Ocean. Based on the characteristics reported, we propose a new species, *Tedania* (*Tedaniopsis*) *rappi* sp. nov. in honor of Prof. Hans Tore Rapp (1972–2020), University of Bergen, Norway, a renowned sponge taxonomist and coordinator of the Horizon 2020 SponGES project. The holotype of *T.* (*T.*) *phacellina* Topsent, 1912 from the Azores, the only other northern Atlantic species in the subgenus *Tedaniopsis*, was reviewed for comparison.

Keywords: sponges, VMEs, taxonomy, new species, *Tedania (Tedaniopsis) rappi*

INTRODUCTION

Orphan Knoll is an isolated, drowned continental fragment 550 km northeast of Newfoundland in the Labrador Sea (NW Atlantic) (Meredyk et al., 2020). The top of Orphan Knoll stands at 1,800–2,000 m and is marked by a series of protruding mounds at depths of between 1,800 and 2,300 m. The Orphan Seamount is located 9 km northeast of the southern-most extension of Orphan Knoll and is a volcanic seamount (Meredyk, 2017). Physical properties indicate that

mid-depth waters above Orphan Knoll are in a boundary region between outflow from the Labrador Sea (subpolar gyre) and northward flow of the North Atlantic Current (subtropical gyre). Near-bottom current measurements provide evidence for anti-cyclonic (clockwise) circulation around the knoll (Greenan et al., 2010) that could have impacts on the benthic communities. The Orphan Basin-Orphan Knoll region is biologically rich and complex (Wudrick et al., 2020), and strongly influenced by local processes and advection.

By the Northwest Atlantic Fisheries Organization (NAFO) to protect coral, sponges and other vulnerable marine ecosystems from impact by bottom contact fishing gear. Orphan Knoll is also considered an Ecologically or Biologically Significant Area (EBSA) by the Convention on Biological Diversity (2015).

In 2010, Fisheries and Oceans Canada (DFO) in collaboration with academic partners conducted a multidisciplinary oceanographic survey of Flemish Cap and Orphan Knoll onboard the CCGS *Hudson* in support of the identification and characterization of vulnerable marine ecosystems as part of Canada's contribution to the NEREIDA program (NAFO, 2016).

On Orphan Knoll and its associated seamount (Orphan Seamount), the remotely operated vehicle (ROV) ROPOS was used to collect high-resolution continuous video and digital still images of Orphan Knoll's diverse benthic communities and geological landscape. Specimen samples were collected using the manipulator arm of ROPOS to serve as taxonomic voucher specimens. We augment data collected during this survey with samples collected during the Isotope CYcling in the LABrador Sea (ICY-LAB) mission onboard RRS *Discovery* in 2017. The overall aim of that mission was to understand nutrient and isotope cycling regions of the Labrador Sea and Greenland fjords (Hendry et al., 2019).

During dive number 1340 by ROV ROPOS at Orphan Seamount, the holotype of the new species was collected. The transect took place between depths of 1,862 and 3,004 m, with an average of 2,455 m and a distance traveled of 11,515 m (Wudrick et al., 2020). This new species of the genus *Tedania* Gray, 1867, was collected close to 3,000 m in depth, inside the NAFO closed area and CBD EBSA, where the substrate were rocks of volcanic origin (Meredyk et al., 2020).

The genus *Tedania* is cosmopolitan and comprises 83 species, with 29 of them distributed in the northern hemisphere (Van Soest et al., 2021). *Tedania* is characterized by having diactinal ectosomal tornotes, or tylotes, usually provided with spines on the tyles, or smooth oxea-like spicules with mucronate apices. Choanosomal megascleres are styles with smooth or microspined bases and the microscleres are onychaetes that characterize the Family Tedaniidae Ridley and Dendy, 1886. The choanosomal megascleres (styles) are arranged in plumose, reticulate, plumo-reticulate or dendritic columns in the genus *Tedania* and the ectosomal skeleton is tangential or paratangential.

The genus *Tedania* had been subdivided into different subgenera. Desqueyroux-Faúndez and Van Soest (1996) followed by Van Soest (2002) created a subgeneric classification of *Tedania* with three subgenera: *Tedania*, *Tedaniopsis*, and *Trachytedania*. The last one is considered currently to be a valid genus (Cristobo and Urgorri, 2001; Van Soest, 2017) and is characterized by species having acanthostyles as choanosomal megascleres. Recently, a third subgenus was recognized, *Stylotedania* Van Soest, 2017 and nowadays the World Porifera Database (Van Soest et al., 2021) consider again three valid subgenera: *Tedania* Gray, 1867, *Tedaniopsis* Dendy, 1924, and *Stylotedania* Van Soest, 2017. The first one, differentiates those species of genus *Tedania* with ectosomal diactinal spicules with smooth or microspined heads, choanosomal monactinal or diactinal spicules and onychaetes. The second differentiates those where the ectosomal diactinal spicules have smooth heads, the choanosomal spicules are monactinal or diactinal and the typical onychaetes are present. The third differentiates those in which the ectosomal and choanosomal spicules are monactinal, diactinal spicules being absent and also have onychaetes (Van Soest, 2017; Aguilar-Camacho et al., 2018).

MATERIALS AND METHODS

Sampling was carried out on board the CCGS *Hudson* using the remotely operated vehicle ROPOS, in July 2010 during mission HUD2010-029 and on the RRS *Discovery* Cruise DY081 with the ROV *ISIS*, in July 2017. During the Hudson mission, a single specimen was collected using the manipulator arm of ROPOS at 2999.88 m depth from Orphan Seamount (**Figure 1**) and stored in its "biobox" until the ROV surfaced. A Seabird 49 CTD attached to this ROV provided temperature (2.1°C) and salinity (34.89‰) data at the time of collection. During the RRS *Discovery* cruise, sponges were collected either using the manipulator arms, or using a suction system. Upon recovery of the ROV to the surface, samples were transferred to buckets and taken into a wet lab for processing. Then, each sponge sample was labeled, measured and photographed.

The specimen from ROPOS was immediately preserved in 70% ethanol upon surfacing. The sample from ROV ISIS was carried in pre-chilled seawater into the cold room (4°C) to commence sampling triage and was preserved in 95% ethanol.

Details of the specimens examined are deposited in PANGAEA® Data Publisher[1] under the digital object identifier (DOI): https://doi.pangaea.de/10.1594/PANGAEA.924814

For the study of dissociated spicules, the organic matter was digested in sodium hypochlorite following the methods of Rapp (2006) and Cárdenas and Rapp (2012) and digested in nitric acid for SEM, following methods described in Cristobo et al. (1993). Spicules and skeleton were coated with gold-palladium using an Emscope Sputter coater SC 500 and examined with a Hitachi S570 SME at Station Marine d'Endoume (France) and a JEOL-JSM-6610 LV of the Oviedo University. The data for spicule sizes are based on 25 measurements for each spicule category, comprising minimum, maximum and average lengths in micrometers (μm). A light microscope (Nikon Eclipse 50i with a Nikon DS-Fi1 camera) was used. The skeleton was also photographed with the same camera system and stacking performed using the Helicon Focus program (129 images).

[1] www.pangaea.de

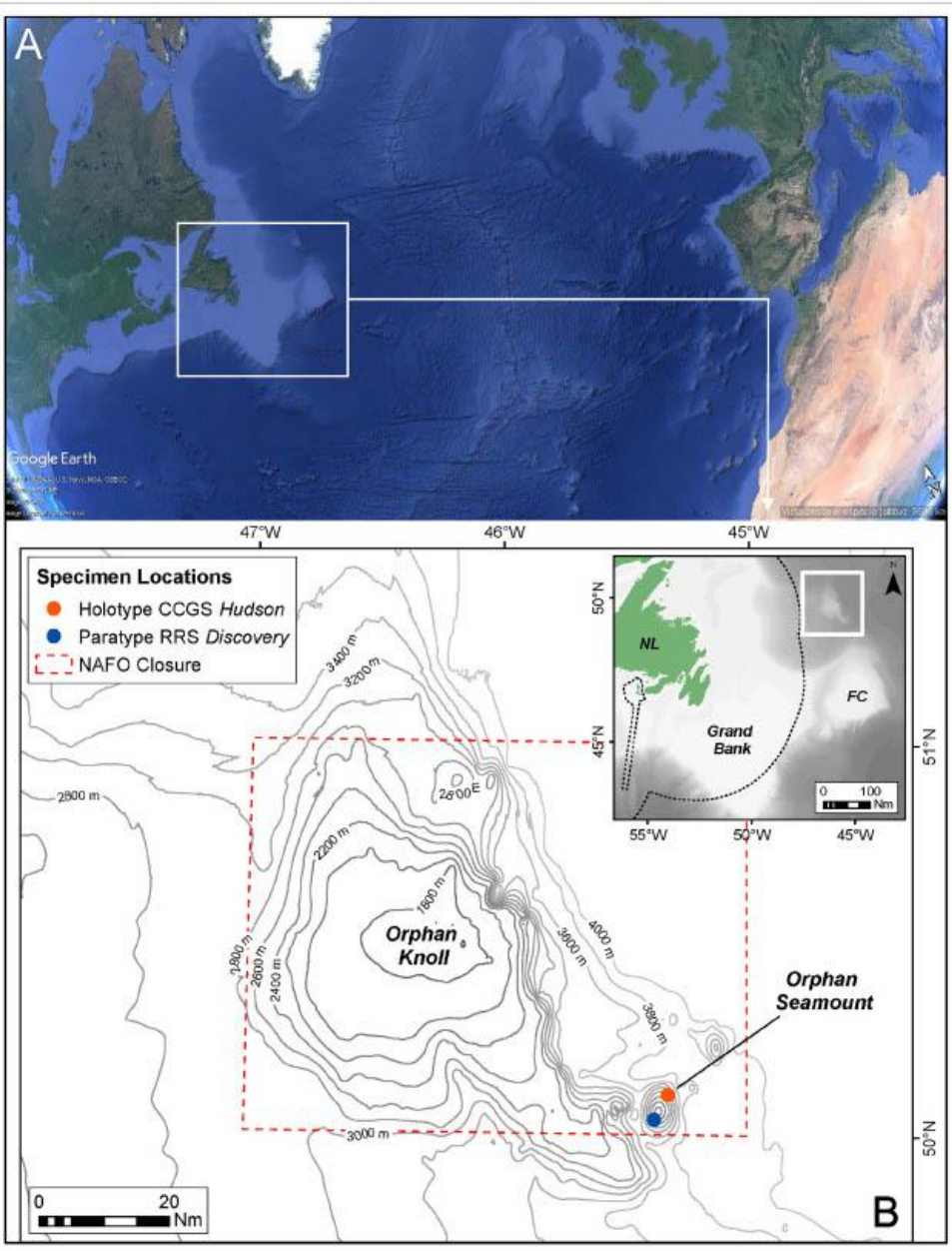

FIGURE 1 | Location of sampling sites of new species. **(A)** Situation of Orphan Knoll in the North Atlantic (from Google Earth). **(B)** Positions of specimens locations (Holotype and Paratype) on Orphan Seamount.

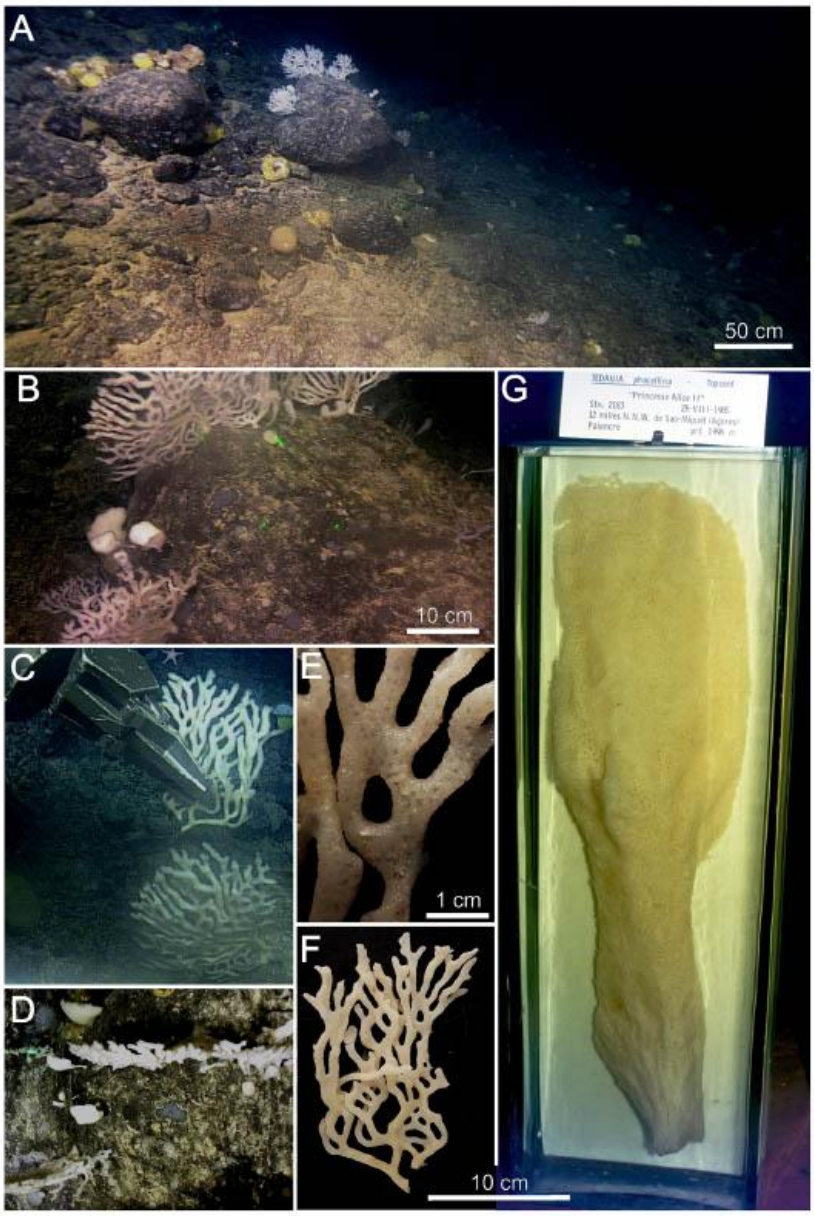

FIGURE 2 | *Tedania* (*Tedaniopsis*) *rappi* sp. nov. **(A,B)** Environment of holotype. **(C)** *In situ* collection of holotype. **(D)** View of two specimens from the downward facing camera. **(E)** Detail of the surface of the holotype on which the oscula are seen. **(F)** Holotype. **(G)** *Tedania* (*Tedaniopsis*) *phacelina*, Topsent's holotype located in the display cases of the Oceanographic Museum of Monaco. Note that figures **(F,G)** are on the same scale to compare the proportions and shapes of both species.

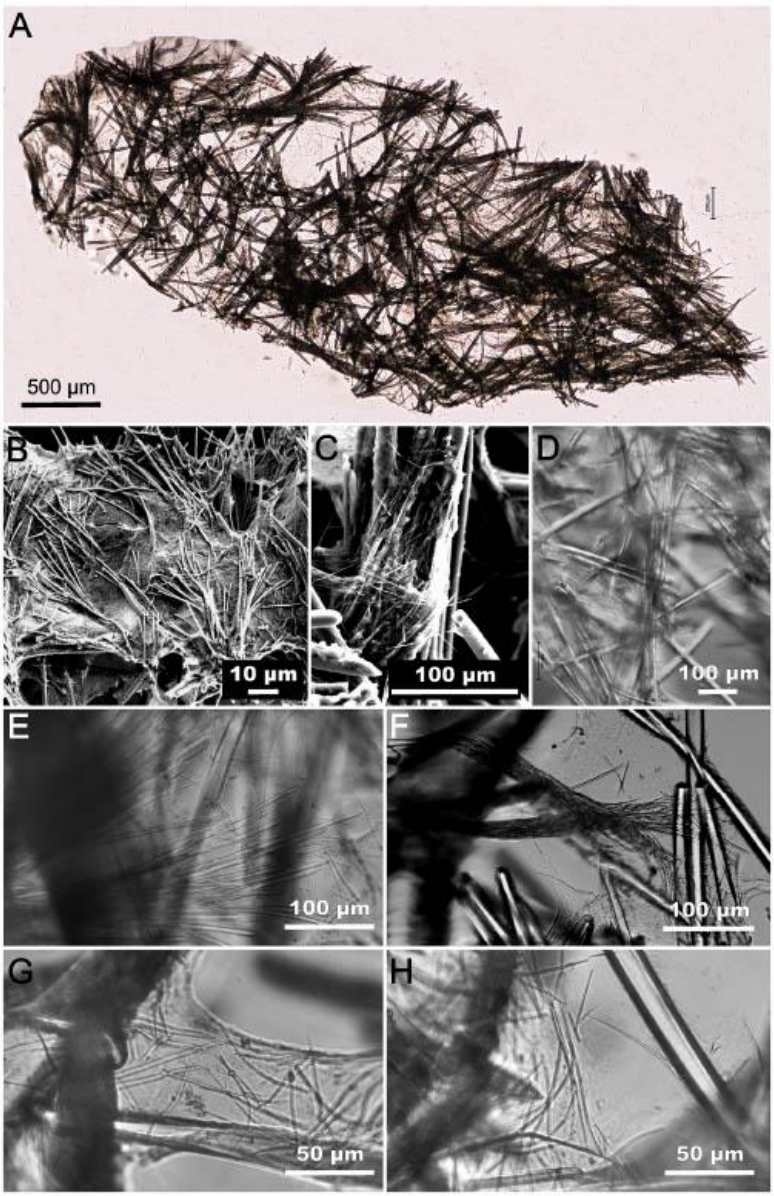

FIGURE 3 | *Tedania (Tedaniopsis) rappi* sp. nov. **(A)** Transversal section of a branch of holotype (light microscope, LM). **(B)** Scanning Electron Microscope (SEM) picture of the surface of sponge ectosomal tornotes protruding. **(C)** Detailed picture of group of onychaetes in choanosome (SEM). **(D)** Bundle of styles in choanosome (LM). **(E)** Bundles of tornotes projected in bouquets in the ectosome (LM). **(F)** Two trichodragmata in the ectosome (LM). **(G)** Onychaetes within a spongin fiber (LM). **(H)** Onychaetes in the choanosome (LM).

DNA was extracted from the holotype using a Qiagen DNeasy Blood and Tissue Kit (QIAgen) following an adapted version of the protocol provided by the manufacturer (overnight incubation in lysis buffer and proteinase K). We selected two molecular markers to amplify, *18S rDNA* (*18S*) and *28S rDNA* (*28S*). The complete 18S (1,766 bp) was amplified in three legs using the primers 1F-5R, 4F-7R, and a.20-9R (Giribet and Wheeler, 2001), and a fragment of 589 bp of 28S (D6 – D8 region) was amplified using the primers CMPOR1490F and CMPOR2170R (Morrow et al., 2012). D6 – D8 region was selected because these where the most successful PCRs regarding 28S. All 18S fragments were amplified using the PCR protocol 94°C, 5 min; (94°C, 1 min, 52°C, 1 min, 72°C, 1 min) × 38 cycles; 72°C, 10 min. We used a different protocol for 28S of 94°C, 5 min; (94°C, 1 min, 55°C, 1 min, 72°C, 1 min) × 38 cycles; 72°C, 10 min. All DNA markers were amplified in 12.5 μL reactions using 10.5 μL of VWR Red Taq DNA Polymerase 1.1× Master Mix (VWR International bvba/sprl, Belgium), 0.5 μL of the forward and reverse primers, and 1 μL of DNA template. PCR products, stained with GelRed® (Biotium, United States), were visualized in a 2.5% agarose gel electrophoresis, run at 90 V for 30 min. Sequencing was conducted on an ABI 3730XL DNA Analyser (Applied Biosystems, United States) at the Molecular Core Labs (Sequencing Facility) of the NHMUK, using the forward and reverse primers mentioned above. The DNA was degraded and the results were negative, probably because the genomic DNA loses quality in depth water samples (Kersken et al., 2018).

The electronic version of this article in PorTable Document Format (PDF) will represent a published work according to the International Commission on Zoological Nomenclature (ICZN), and hence the new names contained in the electronic version are effectively published under that Code from the electronic edition alone. This published work and the nomenclatural acts it contains have been registered in ZooBank, the online registration system for the ICZN. The ZooBank Life Science Identifiers (LSIDs) can be resolved and the associated information viewed through any standard web browser by appending the LSID to the prefix http://zoobank.org/. The LSID for this

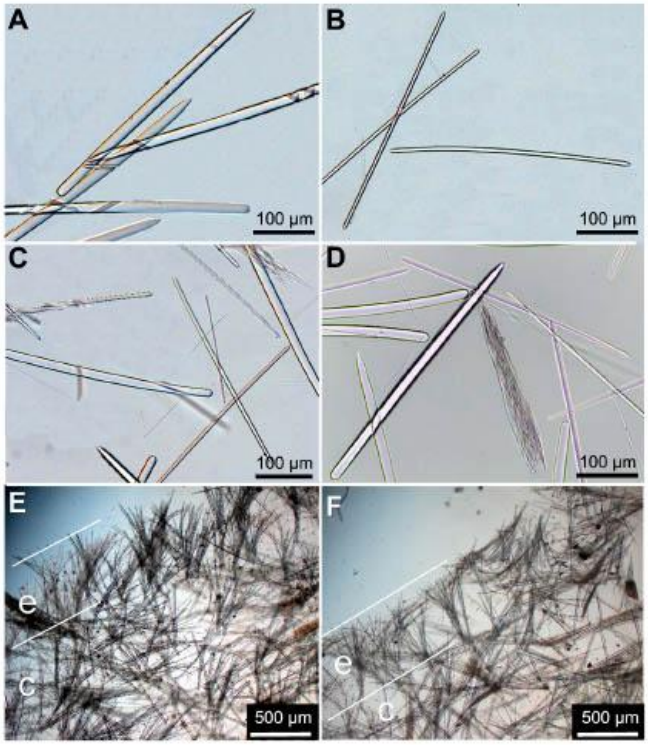

FIGURE 4 | Spicules of *Tedania* (*Tedaniopsis*) *rappi* sp. nov. (Paratype) as seen with a light microscope. **(A)** Styles. **(B)** Tornotes. **(C)** Different kinds of spicules. **(D)** Group of onychaetes in tricodragmata formation. **(E,F)** Skeleton with marked differentiation between ectosome (e) and choanosome (c).

publication is: urn:lsid:zoobank.org:pub:687D7886-46D4-461A-8799-2B76BB446D0C.

Global subgenus maps were derived from data provided by the World Porifera Database (Van Soest et al., 2021).

RESULTS

In this study we analyzed a new species of the *Tedaniopsis* subgenus collected in Orphan Seamount and re-examined *Tedania* (*Tedaniopsis*) *phacellina* Topsent, 1912 from Azores for comparison. This material is described and illustrated. The new species described here has the taxonomic authority restricted to Ríos, Cristobo, and Kenchington.

Systematics follow the SystemaPorifera (Hooper and Van Soest, 2002) chapter on Family Tedaniidae (Van Soest, 2002) and Morrow and Cárdenas (2015).

Phylum PORIFERA Grant, 1836
Class DEMOSPONGIAE Sollas, 1885
SubClass HETEROSCLEROMORPHA Cárdenas et al., 2012
Order POECILOSCLERIDA Topsent, 1928
Family TEDANIIDAE Ridley and Dendy, 1886
Genus *Tedania* Gray, 1867

Definition: Tedaniidae with differentiated ectosomal and choanosomal megascleres Van Soest (2002).

Subgenus *Tedaniopsis* Dendy, 1924

Diagnosis: *Tedania* with relatively long thick, smooth styles, occasionally modified to anisostrongyles or anisoxeas, as structural megascleres. Ectosomal megascleres are mucronate or tylostrongylote tornotes occasionally with one or more vestigial spines (Desqueyroux-Faúndez and Van Soest, 1996).

Tedania (*Tedaniopsis*) *rappi* Ríos, Cristobo and Kenchington sp. nov.

Type material: Holotype: TBD Orphan Seamount (NW Atlantic), 50.1119; −45.3199. Depth 2999.88 m, Coll. CCGS *Hudson*, 19.07.2010, 1 specimen. Rock substrate. In 70% Ethanol Canadian Museum of Nature number CMNI 2020-0004. Paratype: Atlantic Reference Centre (ARC) Museum (ARC 81604) Orphan Seamount (NW Atlantic), 50.0484; -45.3757, 3,450 m depth, Coll. RRS *Discovery*, 08.07.2017, 1 specimen. Rock substrate. In 100% Ethanol.

Holotype of *Tedania (Tedaniopsis) phacellina* Topsent, 1912, was revised. Museé Oceanographique Monaco; Collection of S.A.S. Le Prince de Monaco Station 2183, 28th August 1905, 1,998 m in depth. A small fragment (Schizotype) was analyzed by SEM.

Derivatio nominis: In honor of Prof. Hans Tore Rapp (1972–2020), University of Bergen, Norway, a renowned sponge taxonomist and dear colleague, who described 50 new species of sponges for science. Prof. Rapp was also coordinator and leader of the EU Horizon 2020 SponGES project which focused much needed attention on deep-sea sponges and their habitats.

Description

The *habitus* of the new species is arborescent, erect, branching, tree-like in appearance, flat, fan-shaped, it grows in one plane (bidimensional structure, **Figure 2D**). Size: 25 cm (width) × 15 cm (height). Attached to the substrate by a short and single peduncle [1 cm (width) × 2 cm height] from which it branches mainly in dichotomous arrangement; often, the branches anastomose between them (**Figures 2B,E**). The ends of each branch are rounded (**Figure 2**). The holotype (half of the whole specimen) measures 19 cm long and 12 cm wide (Paratype 6.5 × 6 cm). Each branch is elliptical in section from 5 to 9 mm. Slightly velvety surface with pores (oscules <1 mm diameter) arranged in regular distribution along branches. Consistency flexible and elastic. Color in life and in preservation white.

Skeleton

The choanosomal skeleton is a loose reticulation of bundles of 2–5 styles (paucispicular) with weaker interconnections of 1–2 spicules cemented with spongin (**Figures 3A,B,D**). The ectosomal skeleton consists of bundles of tornotes that are projected in bouquets to the surface (**Figure 3E**). Onychaetes, of two sizes, are scattered in the choanosome and within spongin fibers (**Figures 3G,H**). Both size classes of onychaetes can be placed among the tornotes of the ectosomal skeleton and frequently in tricodragmata (**Figure 3F**).

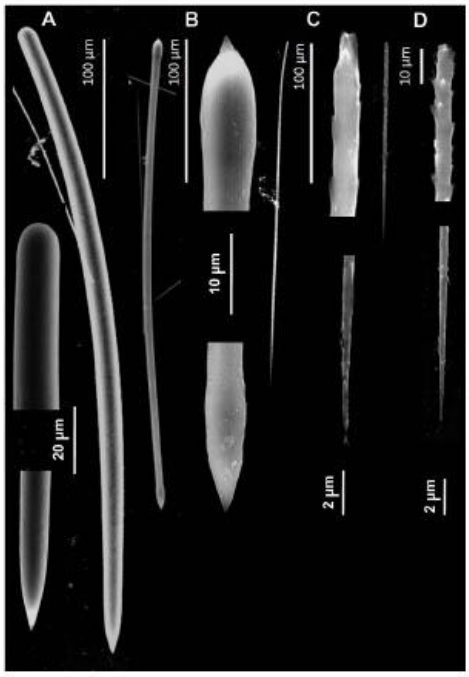

FIGURE 5 | Spicules of *Tedania (Tedaniopsis) rappi* sp. nov. (Holotype) as seen with a Scanning Electron Microscope. **(A)** Styles. **(B)** Tornotes. **(C)** Onychaetes I. **(D)** Onychaetes II.

Spicules Styles, Tornotes, and Onychaetes

Styles (**Figures 4A,B, 5A**). Straight or slightly curved near the basal end with a sharp point in the apical end. Uniform in length and thickness: 457.94 (505) 554.64 × 11.41 (14.05) 17.41 μm (Holotype). 406 (459) 504 × 14 (15.3) 17 μm (Paratype).

Tornotes (**Figures 4A–C, 5B**) Anisotornotes, with slightly inflated and lanceolate ends one of them more mucronate than the other. Measurements: 363.13 (408.68) 440.400 × 5.79 (6.58) 7.42 μm (Holotype). 379 (399.8) 422 × 6 (7.2) 8.6 μm (Paratype).

Onychaetes of two sizes. The largest (I) are 203.3 (234.40) 268.02 μm long (Holotype) 240 (268.3) 307 μm long (Paratype) (**Figures 4C, 5C**). The smallest (II) are 67.85 (76.19) 86.28 μm long (Holotype) 68 (79.8) 82 μm long (Paratype) (**Figures 3F–H, 4C,D, 5C,D**). The largest have uneven ends, one pointed and the other more or less rounded. The smaller ones have one end pointed and the other straight with 3–4 spines. We have observed the largest onychaetes grouped in trichodragmata (**Figures 3, 4**).

Distribution and Ecology

Orphan Seamount, where this new species was collected, is in a transition area between the Arctic and the Temperate Northern Atlantic ecoregions (Spalding et al., 2007). Specimens of the new species were seen in the slopes NE and SW of Orphan Seamount (Labrador Sea, NW Atlantic) attached to rocks of volcanic origin at 2,999–3,450 m; the mean bottom temperature was of 2.39 ± 0.03°C.

On the rock where the holotype specimen was sampled, there were at least 10 specimens of the same species and 39 in the whole transect (ROV dive number 1340, 11,515 m in total distance on bottom). The most characteristic fauna associated with the habitat are other Porifera mainly belonging to genus *Geodia* which represents the highest biomass and the highest number of specimens of the sponge grounds, mainly due to *G. phlegraei* (Sollas, 1880), and also *G. megastrella* Carter, 1876, *G. barretti* Bowerbank, 1858, *G. atlantica* (Stephens, 1915), *G. macandrewii* Bowerbank, 1858, and *G. hentscheli* Cárdenas et al., 2010. Other frequent Porifera are *Lissodendoryx (Lissodendoryx) complicata* (Hansen, 1885), *Hexadella detritifera* Topsent, 1913, *Stryphnus fortis* (Vosmaer, 1885), and *Polymastia corticata* Ridley and Dendy, 1886. Also hexactinellids such as *Farrea herdendorfi* Duplessis and Reiswig, 2004, cup-like species such as *Asconema fristedti* Tabachnick and Menshenina, 2007, *Chenolasma* sp. and cylindrical species such as *Dictyaulus romani* Murillo et al., 2013 or representatives of the families Euplectellidae or Rosellidae were present. Other invertebrates included Cnidarians such as *Bathypathes* sp., representatives of the family Clavulariidae, Chrysogorgiidae, several species of Scleractinia, *Anthomastus* sp., Echinoderms and fishes. The total number of individuals of each taxon/morphotype, abundance by transect and a pictorial guide of megafauna can be seen in Wudrick et al. (2020).

Remarks

The most notable difference from other species of subgenus *Tedaniopsis* is the erect, tree-like appearance of this species, which has never been recorded before in this subgenus. Goodwin et al. (2012) and Aguilar-Camacho et al. (2018) compiled the data from the majority of species of this subgenus from the Antarctic and South Atlantic and worldwide respectively, and none have any features like the new species, being mostly massives, such as *Tedania* (*Tedaniopsis*) *charcoti* Topsent, 1907; *T.* (*T.*) *armata*

TABLE 1 | Spicule characteristics of *Tedania* (*Tedaniopsis*) species from the northern hemisphere.

Specie	Megascleres (μm)		Microscleres (μm)		Habitus	Depth (m)	Distribution
	Choanosomal	Ectosomal	Onychaetas				
T. (T.) phacellina	Style	Tornote	Largest (I)	Smaller (II)			
Topsent, 1912	515–550 × 20–23	440–470 × 7	290–330 × 1.7	70–80	Erect blade	1,998	Azores
Topsent, 1912 re-measured (this study)	Styles I: 384.64 (471.65) 519.53 × 9.55 (16.78) 26.67 *N* = 25 Styles II: 438 (467.90) 511.04 × 5.7 (7.55) 11.58 *N* = 7	348.61 (379.23) 408 × 5.79 (7.20) 9.27 *N* = 25	180.08 (252.15) 285.26 *N* = 25	49.48 (64.93) 85.89 *N* = 25	Erect blade	1,998	Azores
T. (T.) gujarnovae							
Koltun, 1958	280–343 × 8–14	202–280 × 4–8	197–312 × 2	77–157 × 3–4	Cushion-shaped	60–100	E Tatar Strait, off Sakhalin, USSR
Bakus, 1964	296–373 × 9–13	204–252 × 4–7	142–265 × 1.5–1.6	40–91 × 2.2–3.5	Amorphous encrusting sponge	73–198	President Channel and San Juan Channel, San Juan Archipelago
T. (T.) rappi sp. nov.							
Holotype	457.94 (505) 554.64 × 11.41 (14.05) 17.41 *N* = 25	363.13 (408.68) 440.44 × 5.79 (6.58) 7.42 *N* = 25	229.93 (257.49) 277.22 *N* = 25	67.85 (76.19) 86.28 *N* = 25	Tree-like	2,999	Orphan Seamount
Paratype	406 (459) 504 × 14(15.3)17 *N* = 25	379 (399.8) 422 × 6(7.2)8.6 *N* = 25	240 (268.3) 307 × 1(1.2)2 *N* = 25	68 (79.8) 82 *N* = 20	Tree-like	3,450	Orphan Seamount

Sarà, 1978; *T. (T.) corticata* Sarà, 1978; *T. (T.) laminariae* Sarà, 1978; *T. (T.) cristagalli* Dendy, 1924; *T. (T.) gracilis* Hentschel, 1914; *T. (T.) massa* Ridley and Dendy, 1886; *T. (T.) sarai* Bertolino et al., 2007; *T. (T.) tenuicapitata* Ridley, 1881; *T. (T.) vanhoeffeni* Hentschel, 1914; globular such as *T. (T.) gracilis* Hentschel, 1914; *T. (T.) lanceta* Koltun, 1964; cup shaped such as *T. (T.) turbinata* (Dendy, 1924); *T. (T.) infundibuliformis* Ridley and Dendy, 1886; *T. (T.) tantula* (Kirkpatrick, 1907) or crust such as *T. (T.) aurantiaca* Goodwin et al., 2012 and *T. (T.) wellsae* Goodwin et al., 2012. The differences with respect to the two species from the northern hemisphere are also *habitus*, the spicule morphology and their ecology (**Table 1**). Topsent (1912) described *Tedania* (*Tedaniopsis*) *phacellina* from the NW São Miguel Island, in the Azores at 1,998 m in depth. Only one specimen was found and it has not been seen since, but it is a shallower species than the new one. Its shape is clearly different: *T. (T.) phacellina*, above its attachment, first rolls up into a cone, then, almost immediately, reopens to take the form of a vertical blade, flat and without branches. The blade is divided into two parts: the lower, narrow, in a fairly deep gutter; the upper one, longer, wider and slightly concave. It has the appearance of an oar paddle. *T. (T.) rappi*, as described above is branched, arborescent, and tree-like in appearance. Regarding the size, *T. (T.) phacellina*, is a large and robust sponge (47 cm high) (**Figure 2**).

Table 1 presents a comparison of the *Tedania* (*Tedaniopsis*) species from the northern hemisphere. *Habitus* is very different among them: Arborescent in the new species, cushion-shaped in *T. (T.) gujarnovae* and lamellate or cup-shaped in *T. (T.) phacellina*. Although they present a similar composition of the spicular types, differences between the three species can be appreciated. The styles of *T. (T.) gujarnovae* are clearly shorter (260–373 μm) than in the new species (406–554.6 μm). Those of *T. (T.) phacellina*, (384–550 × 9.5–26 μm) similar in length to *T. (T.) rappi*, however, they are much thicker (11.4–17.4 μm in the new) This is a remarkable difference. Also a second category of styles was found in the analysis of the holotype (**Figures 6, 7**); these are slightly thinner (5.7–11.5 μm) and scarce. The ectosomal tornotes are shorter in *T. (T.) gujarnovae* (202–280 μm) than in *T. (T.) phacellina* (348.6–470 μm) and in *T. (T.) rappi* (363–440.4 μm). In *T (T.) rappi* tornotes are mucronate in one end while *T. (T.) phacellina* have a short end (conical). In *T. (T.) phacellina* the ends are slightly more swollen than in *T. (T.) rappi*; tornotes do not have lanceolate ends in *T. (T.) gujarnovae*. The largest onychaetes in *T. (T.) gujarnovae* (142–312 μm) are also slightly smaller than in the other two species: *T. (T.) rappi* (229.9–307 μm), *T. (T.) phacellina* (180–330 μm). However, the small onychaetes (40–157 μm) are larger than in the other two species: *T. (T.) rappi* (67.8–86.2 μm), *T. (T.) phacellina* (49.4–85.8 μm).

In the three species, the bathymetric distribution is quite different: in shallower waters from the South Sakhalin and the South Kurile Island region, *T. (T.) gujarnovae* (60–190 m), *T. (T.) phacellina* from the Azores (1998 m) and the one that has been found deeper is *T. (T.) rappi* (2999–3450 m) from Orphan Seamount, in the North Western Atlantic.

A comparative table of all *Tedania* (*Tedaniopsis*) described species worldwide can be seen in Goodwin et al. (2012) and Aguilar-Camacho et al. (2018). Therefore, the new species is characterized by the external appearance as tree-like with dichotomous branching, long styles, the typical tornotes of the subgenus with lanceolated ends and two sizes of onychaetes.

DISCUSSION

The principal reviews of the *Tedania* genus have been carried out by Bergquist and Fromont (1988); Desqueyroux-Faúndez and Van Soest (1996), Van Soest (2002), and Aguilar-Camacho et al. (2018). The genus *Tedania* actually contain 83 species (Van Soest et al., 2021), 60 of them are included in the *Tedania* subgenus, 21 in *Tedaniopsis*, 1 in *Stylotedania* and one more without a description—*Tedania rubra* Von Lendenfeld, 1888 synonymized with *Tedania anhelans* by Hooper and Wiedenmayer (1994) but it remains *incertae sedis* as the description of Lendenfeld is inadequate (added by Van Soest, 2010 in Van Soest et al., 2021).

Most species of the genus *Tedania* have been reported from the southern hemisphere (54). The subgenus

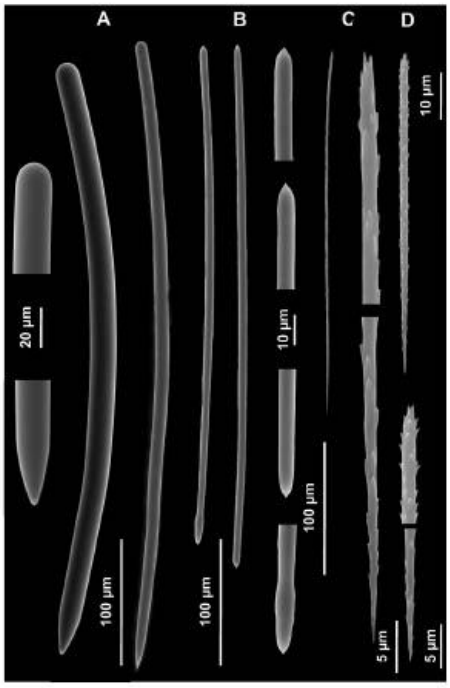

FIGURE 6 | Spicules of *Tedania (Tedaniopsis) phacellina*, Topsent, 1912. (Holotype) as seen with a Scanning Electron Microscope. **(A)** Styles. **(B)** Tornotes. **(C)** Onychaetes I. **(D)** Onychaetes II.

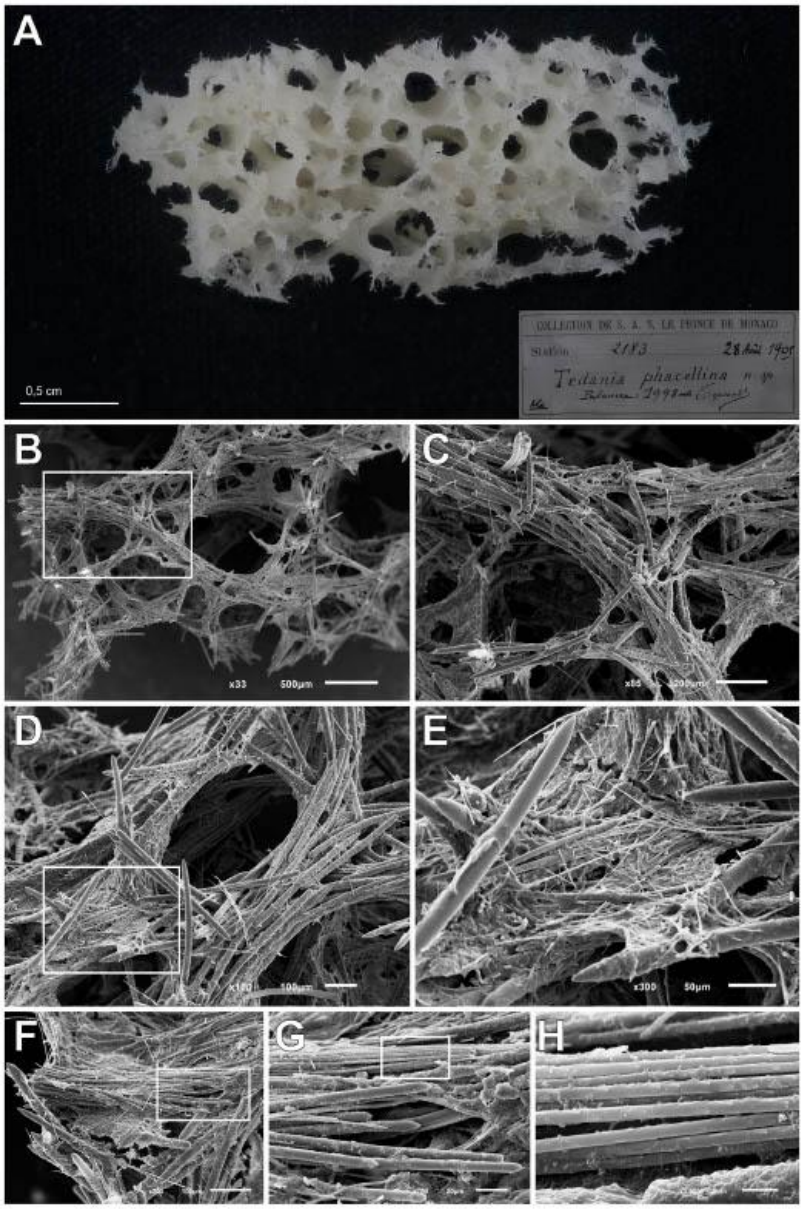

FIGURE 7 | *Tedania (Tedaniopsis) phacellina*, Topsent, 1912. **(A)** Schyzotype, the small fragment extract from the holotype used in this paper. **(B,C)** Section of choanosomal skeleton where the bundles of styles can be seen. **(D,E)** Skeleton around the aquiferous system composed of multispicular tracts and styles; onychaetes covering the tracts and imbibed in the spongin can be seen. **(F,G)** Bundles of ectosomal tornotes. **(H)** Onychaetes in trichodragmata.

Tedania is present in all oceans except Antarctica where the subgenus that predominates is *Tedaniopsis* (19 spp.). The distribution of *Tedania* (*Stylotedania*) *folium* Van Soest, 2017 is the tropical-Atlantic Guyana shelf (**Figures 8, 9**).

With respect to the northern hemisphere, the subgenus *Tedania* is represented by 26 species. The most abundant is *Tedania* (*Tedania*) *ignis* (Duchassaing de Fonbressin and Michelotti, 1864) frequent in both hemispheres, from the Bermudas in the north to Santa Catarina, southeast Brazil, Belize

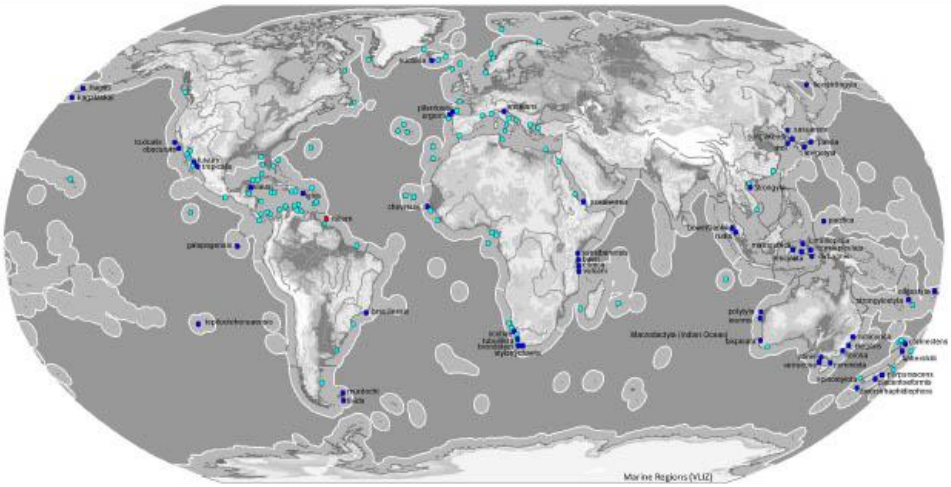

FIGURE 8 | Map of ecoregions (Spalding et al., 2007) showing the global diversity and distribution of the subgenus *Tedania* (blue marine dots for holotypes, light blue dots other records) and *Stylotedania* (red dot holotype) based on data derived from the World Porifera Database 2020.

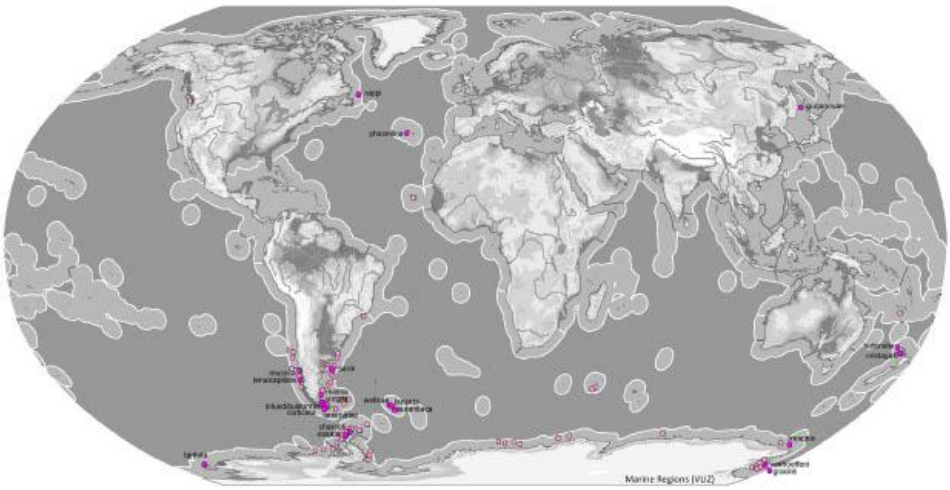

FIGURE 9 | Map of ecoregions (Spalding et al., 2007) showing the global diversity and distribution of the subgenus *Tedaniopsis* (purple dots for holotypes, pinks dots for other records) based on data derived from the World Porifera Database 2020 combined with the new data from the present study.

in the west and Fernando de Noronha, northeast of Brazil. The species was first noted in Hawaii in 1950 (Núñez-Pons et al., 2017). The occurrence of this species includes the Tropical Atlantic, Temperate South America and Eastern Indo-Pacific ecoregions (Spalding et al., 2007). *Tedania (Tedania) suctoria* Schmidt, 1870, has a wide distribution in both ecoregions and one more. From the Kola Fiord (Breitfuss, 1912) and Davis Strait (Murillo et al., 2018)in the Arctic to Cape Vert in the Tropical Atlantic ecoregion (Topsent, 1928) and the Azores (Topsent, 1904, 1928) in the Temperate North Atlantic ecoregion. *Tedania* (*Tedania*) *anhelans* (Vio G in Olivi,, 1792) is one of the most common species, distributed from the Celtic Seas in the north to the Gulf of Guinea in the south, the Azores in the west and the Levantine Sea in the east. Other species that live in the Temperate Northern Atlantic waters are *Tedania (Tedania) pilarriosae* Cristobo, 2002 and *Tedania (Tedania) urgorrii* Cristobo, 2002.

In the northern hemisphere the subgenus *Tedaniopsis* has been represented until now by two species: *Tedania (Tedaniopsis) phacellina* Topsent, 1912 in the Azores (Temperate Northern Atlantic) and *Tedania (Tedaniopsis) gurjanovae* Koltun, 1958 in Tatar Strait (Koltun, 1959) and San Juan Archipelago (Bakus, 1964) in the Temperate Northern Pacific ecoregion.

In summary, the main differences found between *T. (T.) rappi* (Tr) and *T. (T.) phacellina* (Tp) are the very different *habitus* –arborescent (Tr)/massive (Tp)—(**Figure 2**), coanosomal skeletal arrangement –paucispicular (Tr)/multispicular tracts (Tp)—(**Figures 3**, **4**, **7**); styles thickness –double in Tp–. Head terminations of tornotes –mucronate (Tr)/conical (Tp) with the ends somewhat swallowed in Tr–. The onychaetes have short spines (Tr) and the base is blunt (**Figures 5**, **6**).

In fact, the new *Tedania* (*Tedaniopsis*) *rappi* is the first species of this subgenus in the Arctic ecoregion as defined by Spalding et al. (2007). It was found not infrequently in an area closed to protect vulnerable marine ecosystems from the impacts of bottom contact fishing and in a CBD EBSA, the latter conferring enhanced motivation to identify and adopt appropriate measures for conservation and sustainable use by all industrial sectors. The identification of this unique species may warrant including the area in networks of marine protected areas in accordance with international law.

DATA AVAILABILITY STATEMENT

The datasets generated for this study can be found in the online repositories. The names of the repository/repositories and accession number(s) can be found below: ZooBank (urn:lsid:zoobank.org:act:4535FF69-E29C-4C2B-B47F-EC78117C8F2C).

AUTHOR CONTRIBUTIONS

EK and JC acquired the funding. LB and TC conducted the sampling. PR, EB, TC, and JC identified the fauna. JC and PR made the figures and tables with help from LB for **Figure 1**. All authors conceived and designed the study, reviewed drafts of the manuscript, and helped to write the manuscript.

FUNDING

This research has been performed in the scope of the SponGES project, which received funding from the European Union's Horizon 2020 Research and Innovation Programme under Grant Agreement No. 679849 and the European Research project ICY-LAB (ERC-2015-STG Grant Agreement No. 678371). Canadian field work was supported through Fisheries and Oceans Canada (DFO) International Governance Strategy (IGS) funded by EK and with DFO ship time allocated to EK.

ACKNOWLEDGMENTS

We would like to thank the captain and crew of CCGS Hudson and the Canadian Scientific Submersible Facility (CSSF) ROV team, for support during the Hudson 2010-029 mission. We would also like to thank the Principal Investigator Kate Hendry and Claire Goodwin, together with the captain, crew, and scientific party of the ICY-LAB expedition DY081. Also Camille Lirette (DFO, Canada) for send photos and frame grabs from ROPOS 2010 cruise dive 1340 and to Marieve Bouchard Marmen (DFO, Canada) for arranging the shipment of the holotype of *T. (T.) rappi* to be sent to the Canadian Museum of Nature (CMN) in Otawa. We thank J. M. Gagnon, CMN for his acceptance and rapid cataloging of that holotype. Technical assistance was obtained from our IEO colleagues Alejandra Calvo, from Marseille colleagues, Sandrine Chenesseau, and Jean Vacelet and Sergio Taboada from the Natural History Museum of London, who has worked in the DNA extraction and amplification of the holotype. We thank to Victor Vega (Universidad Oviedo) for his technical assistance during SEM image acquisition. Our most sincere thanks also, to Michelle Bruni of the Monaco Oceanographic Museum for her agile efforts and response for the revision of the holotype of *T. phacelina*. We are also grateful to the two reviewers for their valuable and constructive comments to previous version of this manuscript.

REFERENCES

Aguilar-Camacho, J. M., Carballo, J. L., and Cruz-Barraza, J. A. (2018). *Tedania* (*Porifera*: *Demospongiae*: *Poecilosclerida*) from the Mexican Pacific with the description of two new species. *J. Nat. Hist.* 52, 1311–1332.

Bakus, G. J. (1964). Morphogenesis of *Tedania gurjanovae* Koltun(*Porifera*). *Pacif. Sci.* 18, 58–63.

Bergquist, P. R., and Fromont, P. J. (1988). The marine fauna of New Zealand: *Porifera*, *Demospongiae*, Part 4 *Poecilosclerida*. New Zealand Ocean. *Inst. Mem.* 96, 1–197. doi: 10.1007/978-3-319-23534-9_1

Bertolino, M., Schejter, L., Calcinai, B., Cerrano, C., and Bremec, C. (2007). "Sponges from a submarine canyon of the Argentine sea," in *Porifera Research. Biodiversity, Innovation and Sustainability. Livros de Museu Nacional 28*, eds

M. R. Custódio, G. Lôbo-Hajdu, E. Hajdu, and G. Muricy (Rio de Janeiro), 189–201.
Bowerbank, J. S. (1858). On the anatomy and physiology of the spongiadae. part i. on the Spicula. *Philos. T. Roy. Soc.* 148, 279–332. doi: 10.1098/rstl.1858.0016
Breitfuss, L. L. (1912). Zur Kenntniss der Spongio-Fauna des Kola Fjords. *Trav. Soc. Imp. Nat. St. Pet. Sec. Zool.* 411–II, 61–80.
Cárdenas, P., Pérez, T., and Boury-Esnault, N. (2012). "Sponge systematics facing new challenges," in *Advances in Sponge Science: Phylogeny, Systematics, Ecology. Advances in Marine Biology*, Vol. 61, eds M. A. Becerro, M. J. Uriz, M. Maldonado, X. Turon. 79–209. doi: 10.1016/b978-0-12-387787-1.00010-6
Cárdenas, P., and Rapp, H. T. (2012). A review of Norwegian streptaster-bearing Astrophorida (*Porifera: Demospongiae: Tetractinellida*), new records and a new species. *Zootaxa* 52, 1–52. doi: 10.11646/zootaxa.3253.1.1
Cárdenas, P., Rapp, H. T., Schander, C., and Tendal, O. S. (2010). Molecular taxonomy and phylogeny of the Geodiidae (Porifera, Demospongiae, Astrophorida) - combining phylogenetic and Linnaean classification. *Zool. Scr.* 39, 89–106. doi: 10.1111/j.1463-6409.2009.00402.x
Carter, H. J. (1876). Descriptions and figures of deep-sea sponges and their spicules, from the atlantic ocean, dredged up on board H.M.S.'Porcupine', chiefly in 1869 (concluded). *Ann. Mag. Nat. Hist.* 18, 226–240. doi: 10.1080/00222937608682035
Convention on Biological Diversity (2015). *Ecologically or Biologically Significant Areas (EBSAs) Orphan Knoll.* Avaliable at: https://chm.cbd.int/database/record?documentID=204103 (accessed September 15, 2020).
Cristobo, F. J. (2002). The Genus *Tedania* (*Porifera, Demospongiae, Poecilosclerida*) in the waters of the iberian peninsula (Northeast Atlantic) with a description of two new Species. *Sarsia* 87, 362–377. doi: 10.1080/00364820210001558l5
Cristobo, F. J., and Urgorri, V. (2001). Revision of the genus Trachytedania (*Porifera: Poecilosclerida*) with a description of *Trachytedania ferrolensis* sp. nov. from the north-east Atlantic. *J. Mar. Biol. Ass.* 81, 569–579. doi: 10.1017/s0025315401004258
Cristobo, J., Urgorri, V., Solorzano, M. R., and Ríos, P. (1993). Métodos de recogida, estudio y conservación de las colecciones de poríferos. *Int. Symp. First World Cong. Preserv.Conserv. Nat. Hist. Coll.* 2, 277–287.
Dendy, A. (1924). Porifera. Part I. non-antarctic sponges. natural history report. british antarctic (Terra Nova) Expedition, 1910. *Zoology* 6, 269–392.
Desqueyroux-Faúndez, R., and Van Soest, R. W. M. (1996). A review of Iophonidae, *Myxillidae* and Tedaniidae occurring in the South East Pacific (*Porifera: Poecilosclerida*). *Rev. Suisse. Zool.* 103, 3–79. doi: 10.5962/bhl.part.79938
Duchassaing de Fonbressin, P., and Michelotti, G. (1864). Spongiaires de la mer Caraïbe. Natuurkundige verhandelingen van de Hollandsche maatschappij der wetenschappen te Haarlem. *Natuurkundige verhandelingen van de Hollandsche maatschappij der wetenschappen te Haarlem* 21, 1–124.
Duplessis, K., and Reiswig, H. M. (2004). Three new species and a new genus of Farreidae (*Porifera: Hexasterophora: Hexactinosida*). *Proc. Biol. Soc. Wash.* 117, 199–212.
Giribet, G., and Wheeler, W. C. (2001). Some unusual small-subunit ribosomal RNA sequences of metazoans. *Am. Museum Novit.* 3337, 1–16. doi: 10.1206/0003-00822001337<0001:SUSSRR<2.0.CO;2
Grant, R.E. (1836). "Animal kingdom," in *The Cyclopaedia of Anatomy and Physiology*, Vol. 1, ed. R. B. Todd (London: Sherwood, Gilbert, and Piper), 1–813.
Goodwin, C., Brewin, P. E., and Brickle, P. (2012). Sponge biodiversity of South Georgia island with descriptions of fifteen new species. *Zootaxa* 3542, 1–48. doi: 10.11646/zootaxa.3542.1.1
Gray, J. E. (1867). Notes on the arrangement of sponges, with the descriptions of some New Genera. *Proc. Zool. Soc. Lond.* 1867, 492–558.
Greenan, B. J. W., Yashayaev, I., Head, E. J. H., Harrison, W. G., Azetsu-Scott, K., Li, W. K. W., et al. (2010). *Interdisciplinary Oceanographic Observations of Orphan Knoll. NAFO SCR Doc. 10/19. Serial No. N5774.* Avaliable at: https://www.nafo.int/Portals/0/PDFs/sc/2010/scr10-019.pdf (accessed August 15, 2018).
Hansen, G. A. (1885). Spongiadae. the norwegian north-atlantic expedition 1876-1878. *Zoology* 13, 1–26. doi: 10.1080/00364827.1973.10411241
Hendry, K. R., Cassarino, L., Bates, S. L., Culwick, T., Frost, M., Goodwin, C., et al. (2019). Silicon isotopic systematics of deep-sea sponge grounds in the North Atlantic. *Quaternary Sci. Rev.* 210, 1–14. doi: 10.1016/j.quascirev.2019.02.017
Hentschel, E. (1914). Monaxone Kiesel schwämme und Hornschwämme der Deutschen Südpolar-Expedition 1901-1903. *Deutsche Südpolar-Expedition* 15, 35–141.
Hooper, J. N. A., and Van Soest, R. W. M. (eds) (2002). *Systema Porifera. A Guide to the Classification of Sponges.* New York, NY: Kluwer Academic, xix–xlviii. doi: 10.1007/978-1-4615-0747-5
Hooper, J. N. A., and Wiedenmayer, F. (1994). "*Porifera*," in *Zoological Catalogue of Australia*, ed. A. Wells (Melbourne: CSIRO), 12.
Kersken, D., Kocot, K., Janussen, D., Schell, T., Pfenninger, M., and Martínez Arbizu, P. (2018). First insights into the phylogeny of deep-sea glass sponges (*Hexactinellida*) from polymetallic nodule fields in the Clarion-Clipperton Fracture Zone (CCFZ), northeastern Pacific. *Hydrobiologia* 811, 283–293. doi: 10.1007/s10750-017-3498-3
Kirkpatrick, R. (1907). preliminary report on the monaxonellida of the national antarctic expedition. *Ann. Mag. Nat. Hist.* 7, 271–291. doi: 10.1080/00222930709487333
Koltun, V. M. (1958). [Cornacuspongia of sea waters washing the South Sakhalin and the South Kurile Island region.]. *Issledovaniya dal'nevostochnykh morei SSR SSR.* 5, 42–77.
Koltun, V. M. (1959). [Siliceous horny sponges of the northern and fareastern seas of the U.S.S.R.] [In Russian]. *Opredeliteli po faune SSR, izdavaemye Zoologicheskim muzeem Akademii nauk.* 67, 1–236.
Koltun, V. M. (1964). "Sponges of the Antarctic. 1Tetraxonida and Cornacuspongida," in *Biological Reports of the Soviet Antarctic Expedition (1955-1958). Akademya Nauk SSSR [English translation,1966, Israel Program for Scientific Translation]*, eds E. P. Pavlovskii, A. P. Andriyashev, and P. V. Ushakov 6–133,443–448.
Meredyk, S. P. (2017). *Physical Characterization and Benthic Megafauna Distribution and Species Composition on Orphan Knoll and Orphan Seamount, NW Atlantic.* Masters thesis, Memorial University of Newfoundland, St. John's, NL.
Meredyk, S. P., Edinger, E., Piper, D. J. W., Huvenne, V. A. I., Hoy, S., and Ruffman, A. (2020). Enigmatic deep-water mounds on the orphan knoll. Labrador Sea. *Front. Mar. Sci.* 6:744. doi: 10.3389/fmars.2019.00744
Morrow, C., and Cárdenas, P. (2015). Proposal for a revised classification of the *Demospongiae* (*Porifera*). *Front. Zool.* 12:7. doi: 10.1186/s12983-015-0099-8
Morrow, C. C., Picton, B. E., Erpenbeck, D., Boury-Esnault, N., Maggs, C. A., and Allcock, A. L. (2012). Congruence between nuclear and mitochondrial genes in *Demospongiae*: a new hypothesis for relationships within the G4 clade (*Porifera: Demospongiae*). *Mol. Phylogen. Evol.* 62, 174–190. doi: 10.1016/j.ympev.2011.09.016
Murillo, F. J., Kenchington, E., Tompkins, G., Beazley, L., Baker, E., Knudby, A., et al. (2018). Sponge assemblages and predicted archetypes in the eastern Canadian Arctic. *Mar. Ecol. Prog. Ser.* 597, 115–135. doi: 10.3354/meps12589
Murillo, F. J., Tabachnick, K. R., and Menshenina, L. L. (2013). Glass Sponges off the Newfoundland (Northwest Atlantic): Description of a New Species of *Dictyaulus* (Porifera: Hexactinellida: Euplectellidae). J. Mar. Biol. 2013:438485. doi: 10.1155/2013/438485
NAFO (2016). *Potential Vulnerable Marine Ecosystems Impacts of Deep-Sea Fisheries.* Avaliable at: https://www.nafo.int/Portals/0/PDFs/NEREIDA/diptico-nereida.pdf?ver=2016-08-09-104633-013 (accessed January 7, 2021).
Núñez-Pons, L., Calcinai, B., and Gates, R. D. (2017). Who's there? - First morphological and DNA barcoding catalogue of the shallow Hawaiian sponge fauna. *PLoS One* 12:e0189357. doi: 10.1371/journal.pone.0189357
Rapp, H. T. (2006). Calcareous sponges of the genera *Clathrina* and Guancha (*Calcinea, Calcarea, Porifera*) of Norway (north-east Atlantic) with the description of five new species. *Zool. J. Linn. Soc. Lon.* 147, 331–365. doi: 10.1111/j.1096-3642.2006.00221.x
Ridley, S. O., and Dendy, A. (1886). Preliminary report on the Monaxonida collected by H.M.S. *Challenger. Part I. Ann. Mag. Nat. Hist.* 18, 325–351. doi: 10.1080/00222938609459982
Ridley, S. O. (1881). "XI. Spongida. Horny and Siliceous Sponges of Magellan Straits, S.W. Chili, and Atlantic off SW Brazil," in *Account of the Zoological Collections made during the Survey of H.M.S. 'Alert' in the Straits of Magellan and on the Coast of Patagonia*, ed. A. Gunther (Proceedings of the Zoological Society of London), 107–141.

Sarà, M. (1978). Demospongie di acquesuperficialidella Terra del Fuoco (Spedizioni AMF Mares-GRSTS e SAI). *Boll. Mus. Ist. Biol. Univ. Genova.* 46, 7–117.

Schmidt, O. (1870). *Grundzüge Einer Spongien-Fauna des atlantischen Gebietes*, Vol. iii–iv. Leipzig: Wilhelm Engelmann, 1–88.

Sollas, W. J. (1880). The sponge-fauna of Norway; a report on the Rev. A.M. Norman's collection of sponges from the norwegian coast. *Ann. Mag. Nat. Hist.* 5, 130–144.

Sollas, W. J. (1885). A Classification of the Sponges. *Ann. Mag. Nat. His.* 16:395.

Spalding, M. D., Fox, H. E., Allen, G. R., Davidson, N., Ferdaña, Z. A., Finlayson, M., et al. (2007). Marine ecoregions of the world: a bioregionalization of coastal and shelf areas. *BioScience* 57, 573–583. doi: 10.1641/b570707

Stephens, J. (1915). Sponges of the coasts of Ireland. I.-the triaxonia and part of the Tetraxonida. *Fis. Ireland Sci. Invest.* 1914, 1–43.

Tabachnick, K. R., and Menshenina, L. L. (2007). Revision of the genus *Asconema* (Porifera: Hexactinellida: Rossellidae). *J. Mar. Biolog. Assoc. U.K.* 87, 1403–1429. doi: 10.1017/S0025315407058158

Topsent, E. (1904). Spongiaires des Açores. Résultats des campagnes scientifiques accomplies par le Prince Albert I. *Monaco* 25, 1–280.

Topsent, E. (1907). Poecilosclérides nouvelles recueillies par le Français dans l'Antarctique. *B. Mus. Natl. Hist. Nat. Paris* 13, 69–76.

Topsent, E. (1912). Sur une grande *Tedania* abyssale des Açores (*Tedania phacellina*, n. sp.). *Bulletin de l'Institut océanographique, Monaco.* 252, 1–7. doi: 10.1007/978-3-319-23534-9_1

Topsent, E. (1913). Spongiaires provenant des campagnes scientifiques de la 'Princesse Alice' dans les Mers du Nord (1898-1899 - 1906-1907). *Résultats des Campagnes Scientifiques Accomplies par le Prince Albert I de Monaco.* 45, 1–67.

Topsent, E. (1928). Spongiaires de l'Atlantique et de la Méditerranée provenant des croisières du Prince Albert Ier de Monaco. *Résultats des campagnes scientifiques accomplies par le Prince Albert I. Monaco* 74, 1–376.

Van Soest, R. W. M. (2002). "Family Tedaniidae Ridley & Dendy, 1886," in *Systema Porifera. A Guide to the Classification of Sponges. 1*, eds J. N. A. Hooper and R. W. M. Van Soest (New York, NY: Kluwer Academic), 625–632. doi: 10.1007/978-1-4615-0747-5_66

Van Soest, R. W. M. (2017). Sponges of the Guyana Shelf. *Zootaxa* 4217, 1–225. doi: 10.11646/zootaxa.4217.1.1

Van Soest, R. W. M., Boury-Esnault, N., Hooper, J. N. A., Rützler, K., de Voogd, N. J., Alvarez, B., et al. (2021). *World Porifera Database.* Accessed at http://www.marinespecies.org/porifera (accessed January 8, 2021).

Vio G in Olivi, , G. (1792). *Letter on sponges From the Gulf of Smyrna*, Chap. Bassano. Zoologia Adriatica, xi–xxxi.

Von Lendenfeld, R. (1888). *Descriptive Catalogue of the Sponges in the Australian Museum, Sidney*, Vol. i–xiv. London: Taylor & Francis, 1–260.

Vosmaer, G. C. J. (1885). The sponges of the 'willem Barents' expedition 1880 and 1881. *Bijdragen tot de Dierkunde* 12, 1–47.

Wudrick, A., Beazley, L., Culwick, T., Goodwin, C., Cárdenas, P., Xavier, J., et al. (2020). A pictorial guide to the epibenthic megafauna of orphan knoll (northwest Atlantic) identified from in situ benthic video footage. *Can. Tech. Rep. Fish. Aquat. Sci.* 3375:154.

Conflict of Interest: The authors declare that the research was conducted in the absence of any commercial or financial relationships that could be construed as a potential conflict of interest.

7.2. Appendix B

UNIQUE_ID	PARENT_ID	EVENT	STA	ROV_DIVE_NO	LOCATION	MAIN_PRESERV	GENETIC_MT	GENETIC_CG	Packing_location	Class or subclass	Order/suborder	Family	Genus	Species
860	575	6	31	333	Nuuk	E100		C192	SPON_BRIS_1	Demospongiae	Axinellida	Axinellidae	Axinella	artica
862	617	11	31	333	Nuuk	E100	C171	C172	SPON_BRIS_1	Demospongiae	Axinellida	Axinellidae	Axinella	artica
1413	1068	20	52	339	SWGL	E100			SPON_BRIS_3	Demospongiae	Axinellida	Axinellidae	Axinella	artica
1433	1082	44	52	339	SWGL	E100	A375	A376	SPON_BRIS_3	Demospongiae	Axinellida	Axinellidae	Axinella	artica
315	1014	32	50	338	SWGL	E100	C329	C330	SPON_BRIS_3	Demospongiae	Axinellida	Axinellidae	Phakellia	robusta
326	1018	34	50	338	SWGL	E100	C336	C337	SPON_BRIS_3	Demospongiae	Axinellida	Axinellidae	Phakellia	robusta
327	1028	39	50	338	SWGL	E100	C321	C322	SPON_BRIS_2	Demospongiae	Axinellida	Axinellidae	Phakellia	robusta
872	617	11	31	333	Nuuk	E100	C177	C178	SPON_BRIS_1	Demospongiae	Axinellida	Axinellidae	Phakellia	robusta
1133	1048	35	50	338	SWGL	E100		D280		Demospongiae	Axinellida	Axinellidae	Phakellia	robusta
1376	1034	26	50	338	SWGL	E100	C350	C351	SPON_BRIS_2	Demospongiae	Axinellida	Axinellidae	Phakellia	robusta
1378	1044	53	50	338	SWGL	E100	C357	C358	SPON_BRIS_2	Demospongiae	Axinellida	Axinellidae	Phakellia	robusta
1407	996	10	50	338	SWGL	E100	C367	C368	SPON_BRIS_2	Demospongiae	Axinellida	Axinellidae	Phakellia	robusta
1409	1048	35	50	338	SWGL	E100	A339	A340		Demospongiae	Axinellida	Axinellidae	Phakellia	robusta
1412	1068	20	52	339	SWGL	E100	C396	C397	SPON_BRIS_3	Demospongiae	Axinellida	Axinellidae	Phakellia	robusta
1109	1412	20	52	339	SWGL	E100		D283		Demospongiae	Axinellida	Stelligeridae	Halicnemia	flavospina
1218	1030	37	50	338	SWGL	E100		D270		Demospongiae	Axinellida	Stelligeridae	Halicnemia	flavospina
1230		6	50	338	SWGL	E100		D263		Demospongiae	Axinellida	Stelligeridae	Halicnemia	wagini

1269		6	50	338	SWGL	E100		D261		Demospongiae	Axinellida	Stelligeridae	Halicnemia	wagini
876	568	8	36	335	Nuuk	E100	C230	C231	SPON_BRIS_1	Demospongiae	Biemnida	Biemnidae	Biemna	dautzenberghi
1377	1080	41	50	338	SWGL	E100	A317	A318	SPON_BRIS_2	Demospongiae	Biemnida	Biemnidae	Biemna	variantia
1396	1020	32	52	339	SWGL	E100	C415	C416	SPON_BRIS_3	Demospongiae	Biemnida	Biemnidae	Biemna	variantia
797	591	42	31	333	Nuuk	E100				Demospongiae	Dendroceratida	Darwinellidae	Aplysilla	sp.7
865	595	36	36	335	Nuuk	E100	B69	B70	SPON_BRIS_1	Demospongiae	Hadromerida			
361	613	24	31	333	Nuuk	E100	C107	C108	SPON_BRIS_2	Demospongiae	Haplosclerida	Chalinidae	Haliclona (Gellius)	sp.1
846	1086	39	36	335	Nuuk	E100	B55	B56	SPON_BRIS_1	Demospongiae	Haplosclerida	Chalinidae	Haliclona (Gellius)	sp.1
857	1015	24	37	336	Nuuk	E100	C293	C294	SPON_BRIS_1	Demospongiae	Haplosclerida	Chalinidae	Haliclona (Haliclona)	urceolus
893	1001	10	37	336	Nuuk	E100	C315	C316		Demospongiae	Haplosclerida	Chalinidae	Haliclona (Haliclona)	urceolus
969	1011	22	36	335	Nuuk	E100	B57	B58	SPON_BRIS_2	Demospongiae	Haplosclerida	Chalinidae	Haliclona (Haliclona)	urceolus
1398	1050	10	52	339	SWGL	E100	C409	C410	SPON_BRIS_2	Demospongiae	Haplosclerida	Chalinidae	Haliclona (Haliclona)	urceolus
1403	1068	25	52	339	SWGL	E100	C394	C395	SPON_BRIS_3	Demospongiae	Haplosclerida	Chalinidae	Haliclona (Haliclona)	urceolus
861	1013	26	37	336	Nuuk	E100	C263	C264	SPON_BRIS_1	Demospongiae	Haplosclerida	Niphatida	Hemigellius	arcofer
314	1032	36	50	338	SWGL	-20	A294	A295		Demospongiae	Haplosclerida	Petrosiidae	Petrosia (Petrosia)	crassa
328	998	29	50	338	SWGL	E100		C327	SPON_BRIS_2	Demospongiae	Haplosclerida	Petrosiidae	Petrosia (Petrosia)	crassa
372	609	45	36	335	Nuuk	E100	B51	B52	SPON_BRIS_2	Demospongiae	Haplosclerida	Petrosiidae	Petrosia (Petrosia)	crassa
1399	1048	35	50	338	SWGL	E100	A341	A342	SPON_BRIS_2	Demospongiae	Haplosclerida	Petrosiidae	Petrosia (Petrosia)	crassa
1405	1078	11	50	338	SWGL	E100	C365	C366	SPON_BRIS_2	Demospongiae	Haplosclerida	Petrosiidae	Petrosia (Petrosia)	crassa
1410	1006	27	52	339	SWGL	E100	A350	A351	SPON_BRIS_3	Demospongiae	Haplosclerida	Petrosiidae	Petrosia (Petrosia)	crassa
1422	1004	28	52	339	SWGL	E100	A367	A368	SPON_BRIS_3	Demospongiae	Haplosclerida	Petrosiidae	Petrosia (Petrosia)	crassa
1423	1038	6	52	339	SWGL	-20	C440	C441		Demospo	Haplosclerida	Petrosiidae	Petrosia	crassa

										ngiae			(Petrosia)	
1432	1004	28	52	339	SWGL	E100	A365	A366	SPON_BRIS_3	Demospongiae	Haplosclerida	Petrosiidae	Petrosia (Petrosia)	crassa
90	89	31	5	327	Orphan Knoll	E100		A18		Demospongiae	Haplosclerida/Haplosclerina			
895	584	15	36	335	Nuuk	E100	C259	C236	SPON_BRIS_4_BAG5	Demospongiae	Haplosclerida/Haplosclerina			
852	618	15	31	333	Nuuk	E100	C169	C170	SPON_BRIS_1	Demospongiae	Haplosclerida/Petrosina	Petrosiidae	Petrosia (Petrosia)	crassa
1159	1048	35	50	338	SWGL	E100		A336		Demospongiae	Homosclerophorida	Plakinidae	Plakina	jactus
890	578	53	36	335	Nuuk	E100	B53	B54	SPON_BRIS_1	Demospongiae	Merliida	Hamacanthidae	Hamacantha (Vomerula)	papillata
1250	1030	37	50	338	SWGL	E100		D271		Demospongiae	Merliida	Hamacanthidae	Hamacantha (Vomerula)	papillata
569	604	7	31	333	Nuuk	E100		C127	SPON_BRIS_3	Demospongiae	Poecilosclerida	Acarnidae	Iophon	sp.2
843	1045	12	37	336	Nuuk	E100	C303	C304	SPON_BRIS_1	Demospongiae	Poecilosclerida	Acarnidae	Iophon	sp.2
847	1029	28	37	336	Nuuk	E100	C290	C291	SPON_BRIS_1	Demospongiae	Poecilosclerida	Acarnidae	Iophon	sp.2
877	1015	22	37	336	Nuuk	E100	C296	C297	SPON_BRIS_1	Demospongiae	Poecilosclerida	Acarnidae	Iophon	sp.2
1212	1015	24	37	336	Nuuk	E100		D244		Demospongiae	Poecilosclerida	Acarnidae	Iophon	sp.2
1375	1032	38	50	338	SWGL	E100	A302	A303	SPON_BRIS_3	Demospongiae	Poecilosclerida	Acarnidae	Iophon	sp.2
1402	1005	33	52	339	SWGL	E100	C398	C399	SPON_BRIS_3	Demospongiae	Poecilosclerida	Acarnidae	Iophon	sp.2
548	20	31	8	329	Orphan Knoll	E100		D78		Demospongiae	Poecilosclerida	Acarnidae		
855	309	54	36	335	Nuuk	E100	B67	B68	SPON_BRIS_1	Demospongiae	Poecilosclerida	Cladorhizidae	Asbestopluma (Asbestopluma)	frutex
695	573	22	31	333	Nuuk	E100		C112		Demospongiae	Poecilosclerida	Cladorhizidae	Asbestopluma (Asbestopluma)	pennatula
700	573	22	31	333	Nuuk	E100		C110		Demospongiae	Poecilosclerida	Cladorhizidae	Asbestopluma (Asbestopluma)	pennatula
727	573	22	31	333	Nuuk	E100		C113		Demospongiae	Poecilosclerida	Cladorhizidae	Asbestopluma (Asbestopluma)	pennatula
731	573	22	31	333	Nuuk	E100		C109		Demospongiae	Poecilosclerida	Cladorhizidae	Asbestopluma (Asbestopluma)	pennatula
732	573	22	31	333	Nuuk	E100		C111		Demospo	Poecilosclerida	Cladorhizidae	Asbestopluma	pennatula

										ngiae			(Asbestopluma)	
880	599	1	34	334	Nuuk		A218	A219	SPON_BRIS_2	Demospongiae	Poecilosclerida	Cladorhizidae	Asbestopluma (Asbestopluma)	pennatula
696	573	22	31	333	Nuuk	E100		C114		Demospongiae	Poecilosclerida	Cladorhizidae	Asbestopluma (Asbestopluma)	ruetzleri
432		35	31	333	Nuuk	E100		C198		Demospongiae	Poecilosclerida	Cladorhizidae	Cladorhiza	abyssicola
838	632	51	31	333	Nuuk	E100	A160	A161	SPON_BRIS_1	Demospongiae	Poecilosclerida	Cladorhizidae	Cladorhiza	abyssicola
325	1046	45	50	338	SWGL	E100	C332	C333	SPON_BRIS_3	Demospongiae	Poecilosclerida	Cladorhizidae	Cladorhiza	corticocancellata
332	5	8	5	327	Orphan Knoll	E100		C10	SPON_BRIS_4_BAG5	Demospongiae	Poecilosclerida	Cladorhizidae	Cladorhiza	gelida
44	75	62	5	327	Orphan Knoll	DRY		C27		Demospongiae	Poecilosclerida	Coelosphaeridae	Coelosphaera (Coelosphaera)	tubifex
81	65	13	5	327	Orphan Knoll	E100		D15		Demospongiae	Poecilosclerida	Coelosphaeridae	Coelosphaera (Coelosphaera)	tubifex
1106	946	44	36	335	Nuuk	E100		C260		Demospongiae	Poecilosclerida	Coelosphaeridae	Coelosphaera (Histiodermion)	dividuum
837	1029	25	37	336	Nuuk	E100	D229	D230	SPON_BRIS_1	Demospongiae	Poecilosclerida	Coelosphaeridae	Lissodendoryx (Ectyodoryx)	diversichela
1397	1048	35	50	338	SWGL	E100	A337	A338	SPON_BRIS_2	Demospongiae	Poecilosclerida	Coelosphaeridae	Lissodendoryx (Ectyodoryx)	loyningi
1411	1048	35	50	338	SWGL	E100			SPON_BRIS_2	Demospongiae	Poecilosclerida	Coelosphaeridae	Lissodendoryx (Acanthodoryx)	magnasigma
1181	1020	32	52	339	SWGL	DRY		D288		Demospongiae	Poecilosclerida	Coelosphaeridae	Lissodendoryx (Acanthodoryx)	magnasigma
904	1011	22	36	335	Nuuk	E100	B59	B60	SPON_BRIS_1	Demospongiae	Poecilosclerida	Dendoricellidae	Dendoricella	flabelliformis
1252	1002	61	50	338	SWGL	E100		D273		Demospongiae	Poecilosclerida	Dendoricellidae	Dendoricella	flabelliformis
317	1001	9	37	336	Nuuk	E100	C317	C318	SPON_BRIS_1	Demospongiae	Poecilosclerida	Esperiopsidae	Esperiopsis	villosa
1198		6	50	338	SWGL	E100		D262		Demospongiae	Poecilosclerida	Hymedesmiidae	Hymedesmia (Europhon)	sp.3
1138	946	44	36	335	Nuuk	E100		C262		Demospongiae	Poecilosclerida	Hymedesmiidae	Hymedesmia (Hymedesmia)	crux
842	591	49	31	333	Nuuk	E100	A183	A184	SPON_BRIS_1	Demospongiae	Poecilosclerida	Hymedesmiidae	Hymedesmia (Hymedesmia)	caerulea
959	294	59	36	335	Nuuk	E100		C253		Demospongiae	Poecilosclerida	Hymedesmiidae	Hymedesmia (Hymedesmia)	caerulea
1247	1032	50	50	338	SWGL		A300	A301	SPON_BRIS_2	Demospongiae	Poecilosclerida	Hymedesmiidae	Hymedesmia (Hymedesmia)	caerulea

991	294	59	36	335	Nuuk	E100		C254		Demospongiae	Poecilosclerida	Hymedesmiidae	Hymedesmia (Hymedesmia)	alba
1262		6	50	338	SWGL	E100		D264		Demospongiae	Poecilosclerida	Hymedesmiidae	Phorbas	sp.5
1194	1080	41	50	338	SWGL	E100		A316		Demospongiae	Poecilosclerida	Hymedesmiidae		
1127	1048	35	50	338	SWGL	E100		A335		Demospongiae	Poecilosclerida	Latrunculiidae	Septrella	matia
1265	1048	35	50	338	SWGL	E100	C392	D278		Demospongiae	Poecilosclerida	Latrunculiidae	Septrella	matia
316	1018	17	50	338	SWGL	E100	A291	A292	SPON_BRIS_2	Demospongiae	Poecilosclerida	Microcionidae (Microcioninae)	Clathria (Axosuberites)	radix
323	1032	52	50	338	SWGL	E100	C342	C343	SPON_BRIS_3	Demospongiae	Poecilosclerida	Microcionidae (Microcioninae)	Clathria (Axosuberites)	radix
874	589	58	31	333	Nuuk	E100	C155	C156	SPON_BRIS_1	Demospongiae	Poecilosclerida	Microcionidae (Microcioninae)	Clathria (Axosuberites)	radix
840	575	6	31	333	Nuuk	E100	C189	C190	SPON_BRIS_1	Demospongiae	Poecilosclerida	Microcionidae (Microcioninae)	Clathria (Clathria)	barleei
866	900	68	36	335	Nuuk	E100	A239	A240	SPON_BRIS_1	Demospongiae	Poecilosclerida	Microcionidae (Microcioninae)		
1240	1001	9	37	336	Nuuk	E100		D250		demospongiae	Poecilosclerida	Microcionidae(Ophlitaspongiinae)	Artemisina	arcigera
844	607	7	31	333	Nuuk	E100	C138	C139	SPON_BRIS_3	demospongiae	Poecilosclerida	Mycalidae	Mycale (Mycale)	lingua
859	1061	14	37	336	Nuuk	-20	C276	C277	SPON_BRIS_1	Demospongiae	Poecilosclerida	Mycalidae	Mycale (Mycale)	lingua
863	999	15	37	336	Nuuk	E100	C309	C310	SPON_BRIS_1	Demospongiae	Poecilosclerida	Mycalidae	Mycale (Mycale)	lingua
1234	999	15	37	336	Nuuk	E100		D248		demospongiae	Poecilosclerida	Mycalidae	Mycale (Mycale)	lingua
1395	1078	8	50	338	SWGL	E100	A330	A331	SPON_BRIS_2	Demospongiae	Poecilosclerida	Mycalidae	Mycale (Mycale)	lingua
894	591	43	31	333	Nuuk	-20	C162	C163	SPON_BRIS_4_BAG5	Demospongiae	Poecilosclerida	Myxillidae	Melonanchora	elliptica
1401	1052	18	52	339	SWGL	E100	C401	C393	SPON_BRIS_3	Demospongiae	Poecilosclerida	Myxillidae	Melonanchora	elliptica
321	68	66	5	327	Orphan Knoll	E100	C13	C14		Demospongiae	Poecilosclerida	Myxillidae	Myxilla (Myxilla)	sp.4
1263	996	10	50	338	SWGL	E100		D275		Demospongiae	Poecilosclerida	Myxillidae	Myxilla (Myxilla)	sp.4
1389	1034	46	50	338	SWGL	E100	A321	A322	SPON_BRIS_2	Demospongiae	Poecilosclerida	Myxillidae	Myxilla (Myxilla)	sp.4
42	76	58	5	327	Orphan	E100			SPON_BRIS_1	Demospo	Poecilosclerida	Myxillidae	Stelodoryx	ora

					Knoll					ngiae				
82	3	5	5	327	Orphan Knoll	E100			SPON_BRIS_2	Demospongiae	Poecilosclerida	Myxillidae	Stelodoryx	ora
242	5	7	5	327	Orphan Knoll	E100		C15		Demospongiae	Poecilosclerida	Myxillidae	Stelodoryx	ora
243	5	9	5	327	Orphan Knoll	E100		B6		Demospongiae	Poecilosclerida	Myxillidae	Stelodoryx	ora
1231	996	10	50	338	SWGL	E100		D274		Demospongiae	Poecilosclerida	Myxillidae	Stelodoryx	groenlandica
241	5	4	5	327	Orphan Knoll	E100		A12		Demospongiae	Poecilosclerida	Phellodermidae	Fibulia	textilitesta
322	5	7	5	327	Orphan Knoll	E100		B5	SPON_BRIS_1	Demospongiae	Poecilosclerida	Tedaniidae	Tedania (Tedaniopsis)	rappi
654	1061	16	37	336	Nuuk	E100		D221		Demospongiae	Polymastiida	Polymastiidae	Polymastia	andrica
879	1061	39	37	336	Nuuk	E100	C280	C308	SPON_BRIS_1	Demospongiae	Polymastiida	Polymastiidae	Polymastia	andrica
1088	1004	28	52	339	SWGL	E100		D293		Demospongiae	Polymastiida	Polymastiidae	Polymastia	thielei
1143	1036	11	52	339	SWGL	E100		D284		Demospongiae	Polymastiida	Polymastiidae	Polymastia	thielei
1384	1032	40	50	338	SWGL	E100	A298	A299	SPON_BRIS_2	Demospongiae	Polymastiida	Polymastiidae	Polymastia	thielei
869	1069	38	37	336	Nuuk	E100	C278	C279	SPON_BRIS_1	Demospongiae	Polymastiida	Polymastiidae	Polymastia	uberrima
871	1013	18	37	336	Nuuk	E100	C265	C266	SPON_BRIS_1	Demospongiae	Polymastiida	Polymastiidae	Polymastia	uberrima
1386	1034	25	50	338	SWGL	E100	A319	A320	SPON_BRIS_2	Demospongiae	Polymastiida	Polymastiidae	Polymastia	uberrima
1408	1054	29	52	339	SWGL	E100	C406	C407	SPON_BRIS_3	Demospongiae	Polymastiida	Polymastiidae	Polymastia	uberrima
29	21	58	8	329	Orphan Knoll	E100		C51		Demospongiae	Polymastiida	Polymastiidae	Spinularia	njordi
889	1029	20	37	336	Nuuk	E100	C288	C289	SPON_BRIS_4_BAG5	Demospongiae	Polymastiida	Polymastiidae	Weberella	bursa
368	621	24	13	331	Orphan Knoll	E100	C88	C89	SPON_BRIS_4_BAG3	Demospongiae	Suberitida	Halichondriidae	Halichondia (Halichondia)	sp.10
891	1013	18	37	336	Nuuk	E100	D208	D209	SPON_BRIS_1	Demospongiae	Suberitida	Halichondriidae	Halichondia (Halichondia)	sp.10
366	17	66	8	329	Orphan Knoll	-20	D74	D75		Demospongiae	Suberitida	Halichondriidae	Topsentia	sp.11
1083	1080	13	50	338	SWGL	E100		D265		Demospongiae	Suberitida	Stylocordylidae	Stylocordyla	borealis

1146	1050	12	52	339	SWGL	E100		D287		Demospongiae	Suberitida	Stylocordylidae	Stylocordyla	borealis
1225	1044	54	50	338	SWGL	E100		D268		Demospongiae	Suberitida	Stylocordylidae	Stylocordyla	borealis
1243	1015	23	37	336	Nuuk	E100		D243		Demospongiae	Suberitida	Stylocordylidae	Stylocordyla	borealis
318	1028	15	50	338	SWGL	E100	C323	C324	SPON_BRIS_2	Demospongiae	Suberitida	Suberitidae	Plicatellopsis	sp.8
1115	1050	7	52	339	SWGL	E100		A355		Demospongiae	Suberitida	Suberitidae	Rhizaxinella	sp.9
1227		6	50	338	SWGL	E100		D260		Demospongiae	Suberitida	Suberitidae	Rhizaxinella	sp.9
1264	1229	16	50	338	SWGL	E100		D276		Demospongiae	Suberitida	Suberitidae		
848	631	14	31	333	Nuuk	E100	C122	C123		Demospongiae	Tetractinellida			
885	594	13	36	335	Nuuk	-20	C247	C248		Demospongiae	Tetractinellida/Astrophorina	Acorinidae	Ancorina	sp.6
330	624	23	13	331	Orphan Knoll	E100		D127	SPON_BRIS_1	Demospongiae	Tetractinellida/Astrophorina	Ancorinidae	Paratimea	marionae
369	621	24	13	331	Orphan Knoll	E100	C91	C92	SPON_BRIS_4_BAG3	Demospongiae	Tetractinellida/Astrophorina	Ancorinidae	Paratimea	marionae
1394	1070	19	52	339	SWGL	-20	C418	C419		Demospongiae	Tetractinellida/Astrophorina	Ancorinidae	Paratimea	marionae
324	1032	42	50	338	SWGL	-20	A296	A297		Demospongiae	Tetractinellida/Astrophorina	Ancorinidae	Stryphnus	fortis
341	73	58	5	327	Orphan Knoll	E100	D39	D40	SPON_BRIS_4_BAG4	Demospongiae	Tetractinellida/Astrophorina	Ancorinidae	Stryphnus	fortis
875	285	14	36	335	Nuuk	-20	C241	C242		Demospongiae	Tetractinellida/Astrophorina	Ancorinidae	Stryphnus	fortis
1090	1020	32	52	339	SWGL	DRY		D289		Demospongiae	Tetractinellida/Astrophorina	Ancorinidae		
92	77	60	5	327	Orphan Knoll	E100		A20		Demospongiae	Tetractinellida/Astrophorina	Geodiidae	Geodia	barretti
273	113	6	5	327	Orphan Knoll	E100	D3	D4	SPON_BRIS_4_BAG1	Demospongiae	Tetractinellida/Astrophorina	Geodiidae	Geodia	barretti
275	113	6	5	327	Orphan Knoll	E100	C5	C6	SPON_BRIS_3	Demospongiae	Tetractinellida/Astrophorina	Geodiidae	Geodia	barretti
276	79	1	5	327	Orphan Knoll	E100	D5	D6	SPON_BRIS_4_BAG2	Demospongiae	Tetractinellida/Astrophorina	Geodiidae	Geodia	barretti
277	78	19	5	327	Orphan Knoll	E100	D17	D20	SPON_BRIS_4_BAG1	Demospongiae	Tetractinellida/Astrophorina	Geodiidae	Geodia	barretti
281	79	1	5	327	Orphan	E100	C7	C8	SPON_BRIS_4	Demospo	Tetractinellida/Astr	Geodiidae	Geodia	barretti

					Knoll				_BAG2	ngiae	ophorina			
282	79	1	5	327	Orphan Knoll	E100	D7	D8	SPON_BRIS_4_BAG4	Demospongiae	Tetractinellida/Astrophorina	Geodiidae	Geodia	barretti
283	79	5	5	327	Orphan Knoll	E100	D9	D10	SPON_BRIS_4_BAG4	Demospongiae	Tetractinellida/Astrophorina	Geodiidae	Geodia	barretti
284	79	12	5	327	Orphan Knoll	E100	D11	D12	SPON_BRIS_4_BAG2	Demospongiae	Tetractinellida/Astrophorina	Geodiidae	Geodia	barretti
289	1000	61	50	338	SWGL	-20	C360	C361		Demospongiae	Tetractinellida/Astrophorina	Geodiidae	Geodia	barretti
350	344	15	5	327	Orphan Knoll	E100	C23	C24	SPON_BRIS_1	Demospongiae	Tetractinellida/Astrophorina	Geodiidae	Geodia	barretti
352	3	31	5	327	Orphan Knoll	E100	C33	C34	SPON_BRIS_1	Demospongiae	Tetractinellida/Astrophorina	Geodiidae	Geodia	barretti
864	576	38	31	333	Nuuk	-20	C147	C148		Demospongiae	Tetractinellida/Astrophorina	Geodiidae	Geodia	barretti
886	577	33	36	335	Nuuk	E100	B63	B64	SPON_BRIS_1	Demospongiae	Tetractinellida/Astrophorina	Geodiidae	Geodia	barretti
278	74	64	5	327	Orphan Knoll	-20	D33	D34		Demospongiae	Tetractinellida/Astrophorina	Geodiidae	Geodia	macandrewii
345	74	58	5	327	Orphan Knoll	-20	D23	D24		Demospongiae	Tetractinellida/Astrophorina	Geodiidae	Geodia	macandrewii
348	77	59	5	327	Orphan Knoll	-20	D35	D35		Demospongiae	Tetractinellida/Astrophorina	Geodiidae	Geodia	macandrewii
293	67	30	5	327	Orphan Knoll	E100	C25	C26	SPON_BRIS_4_BAG3	Demospongiae	Tetractinellida/Astrophorina	Geodiidae	Geodia	parva
347	74	58	5	327	Orphan Knoll	-20	D31	D32	SPON_BRIS_4_BAG4	Demospongiae	Tetractinellida/Astrophorina	Geodiidae	Geodia	parva
334	78	31	5	327	Orphan Knoll	E100	C17	C18	SPON_BRIS_4_BAG1	Demospongiae	Tetractinellida/Astrophorina	Geodiidae	Geodia	phlegraei
342	3	31	5	327	Orphan Knoll	E100	C31	C32	SPON_BRIS_1	Demospongiae	Tetractinellida/Astrophorina	Geodiidae	Geodia	phlegraei
349	77	60	5	327	Orphan Knoll	E100	B3	B4	SPON_BRIS_1	Demospongiae	Tetractinellida/Astrophorina	Geodiidae	Geodia	phlegraei
371	633	12	31	333	Nuuk	E100	C116	C117	SPON_BRIS_1	Demospongiae	Tetractinellida/Astrophorina	Theneidae	Thenea	valdiviae
585	607	57	31	333	Nuuk	E100		C132	SPON_BRIS_1	Demospongiae	Tetractinellida/Astrophorina	Theneidae	Thenea	valdiviae
870	615	20	31	333	Nuuk	E100		C209	SPON_BRIS_1	Demospongiae	Tetractinellida/Astrophorina	Theneidae	Thenea	valdiviae
882	575	13	31	333	Nuuk	E100		C180	SPON_BRIS_1	Demospongiae	Tetractinellida/Astrophorina	Theneidae	Thenea	valdiviae
362	609	45	36	335	Nuuk	E100	C216	C217	SPON_BRIS_2	Demospongiae	Tetractinellida/Astrophorina			

892	634	17	31	333	Nuuk	E100	C187	C188	SPON_BRIS_4_BAG5	Demospongiae	Tetractinllida (Spirophorina)	Tetillidae	Craniella	cranium
868	607	21	31	333	Nuuk	E100	C128	C129	SPON_BRIS_1	Demospongiae	Tetractinllida (Spirophorina)	Tetillidae	Craniella	zetlandica
878	607	7	31	333	Nuuk	E100	C130	C131	SPON_BRIS_1	Demospongiae	Tetractinllida (Spirophorina)	Tetillidae	Craniella	zetlandica
91	77	60	5	327	Orphan Knoll	E100		A19		Demospongiae				
738	997	36	37	336	Nuuk	DRY		C271		Demospongiae				
1108	1020	21	52	339	SWGL	E100		A372		Demospongiae				
854	630	35	31	333	Nuuk	E100	C200	C201		Demospongiae/Keratosa				
1174	946	44	36	335	Nuuk	E100		C261		Demospongiae/Keratosa				
336	74	58	5	327	Orphan Knoll	E100	D25	D26	SPON_BRIS_1	Hexactinellida	Lyssacinosida	Rossellidae (Lanuginellinae)	Caulophacus	
313	1032	48	50	338	SWGL	E100	C340	C341	SPON_BRIS_4_BAG5	Hexactinellida	Lyssacinosida	Rossellidae (Rossellinae)	Nodastrella	ascoemaoida
359	636	9	31	333	Nuuk	E100	C103	C104	SPON_BRIS_1	Hexactinellida	Lyssacinosida	Rossellidae (Rossellinae)	Nodastrella	ascoemaoida
841	1008	25	36	335	Nuuk	E100	C251	C252	SPON_BRIS_2	Hexactinellida	Lyssacinosida	Rossellidae (Rossellinae)	Nodastrella	ascoemaoida
845	309	34	36	335	Nuuk	E100	C239	C240	SPON_BRIS_4_BAG5	Hexactinellida	Lyssacinosida	Rossellidae (Rossellinae)	Nodastrella	ascoemaoida
849	1061	7	37	336	Nuuk	E100	C274	C275	SPON_BRIS_1	Hexactinellida	Lyssacinosida	Rossellidae (Rossellinae)	Nodastrella	ascoemaoida
853	1045	7	37	336	Nuuk	E100	C305	C306	SPON_BRIS_1	Hexactinellida	Lyssacinosida	Rossellidae (Rossellinae)	Nodastrella	ascoemaoida
881	1013	28	37	336	Nuuk	E100	C267	C268	SPON_BRIS_1	Hexactinellida	Lyssacinosida	Rossellidae (Rossellinae)	Nodastrella	ascoemaoida
884	608	27	31	333	Nuuk	-20	C158	C159		Hexactinellida	Lyssacinosida	Rossellidae (Rossellinae)	Nodastrella	ascoemaoida
896	968	70	36	335	Nuuk	E100	C226			Hexactinellida	Lyssacinosida	Rossellidae (Rossellinae)	Nodastrella	ascoemaoida
896	995	18	36	335	Nuuk	E100	C233	C234	SPON_BRIS_1	Hexactinellida	Lyssacinosida	Rossellidae (Rossellinae)	Nodastrella	ascoemaoida
1309	1082	44	52	339	SWGL	E100		C435		Hexactinellida	Lyssacinosida	Rossellidae (Rossellinae)	Nodastrella	ascoemaoida
1385	1032	38	50	338	SWGL	-20	C346	C347		Hexactinellida	Lyssacinosida	Rossellidae (Rossellinae)	Nodastrella	ascoemaoida
1387	1080	10	50	338	SWGL	E100	C348	C349	SPON_BRIS_2	Hexactinellida	Lyssacinosida	Rossellidae (Rossellinae)	Nodastrella	ascoemaoida

1388	1078	6	50	338	SWGL	-20	C363	C364		Hexactinellida	Lyssacinosida	Rossellidae (Rossellinae)	Nodastrella	ascoemaoida
1404	1070	16	52	339	SWGL	E100	D291	D292	SPON_BRIS_3	Hexactinellida	Lyssacinosida	Rossellidae (Rossellinae)	Nodastrella	ascoemaoida
329	520	12	11	330	Orphan Knoll	E100	D80	D81	SPON_BRIS_1	Hexactinellida		Euplectellidae	Euplectella	
335	74	31	5	327	Orphan Knoll	STRUCT [-20]	D21	D22		Hexactinellida		Euplectellidae	Euplectella	
356	17	12	8	329	Orphan Knoll	STRUCT -20	C59	C60		Hexactinellida		Euplectellidae	Euplectella	
363	26	16	8	329	Orphan Knoll	STRUCT -20	C49	C63		Hexactinellida		Euplectellidae	Euplectella	
364	19	60	8	329	Orphan Knoll	STRUCT -20	C52	C53		Hexactinellida		Euplectellidae	Euplectella	
367	622	12	13	331	Orphan Knoll	DRY	C75	C76		Hexactinellida		Euplectellidae	Euplectella	
856	611	57	36	335	Nuuk	E100	C219	C220	SPON_BRIS_1	Hexactinellida		Euplectellidae	Euplectella	
319	66	17	5	327	Orphan Knoll	E100	C11	C12	SPON_BRIS_1	Hexactinellida				
331	68	66	5	327	Orphan Knoll	E100	C9	D16		Hexactinellida				
333	76	28	5	327	Orphan Knoll	E100	D1	D2	SPON_BRIS_4_BAG4	Hexactinellida				
337	77	31	5	327	Orphan Knoll	E100	D29	D30	SPON_BRIS_4_BAG4	Hexactinellida				
338	77	31	5	327	Orphan Knoll	E100	C19	C20	SPON_BRIS_1	Hexactinellida				
339	77	60	5	327	Orphan Knoll	E100	C21	C22	SPON_BRIS_1	Hexactinellida				
340	71	31	5	327	Orphan Knoll	E100	D37	D38	SPON_BRIS_1	Hexactinellida				
343	70	76	5	327	Orphan Knoll	E100	D13	D14	SPON_BRIS_1	Hexactinellida				
344	78	15	5	327	Orphan Knoll	E100	D17	D18	SPON_BRIS_4_BAG2	Hexactinellida				
346	74	65	5	327	Orphan Knoll	E100	D27	D28	SPON_BRIS_4_BAG2	Hexactinellida				
355	25	17	8	329	Orphan Knoll	E100	C56	C57	SPON_BRIS_1	Hexactinellida				
360	19	62	8	329	Orphan Knoll	-20	D76	D77		Hexactinellida				
365	25	17	8	329	Orphan	E100	D69	D70	SPON_BRIS_1	Hexactinel				

					Knoll					lida				
850	575	6	31	333	Nuuk	E100		C191	SPON_BRIS_1	Hexactinellida				
1400	1036	11	52	339	SWGL	E100	C402	C403	SPON_BRIS_3	Hexactinellida				
1406	1050	7	52	339	SWGL	E100	C411	C412	SPON_BRIS_2	Hexactinellida				